

New Insight into
Enzymatic Cross-linking of Globular Proteins:
From Nanostructure to Functionality

Yunus Sariçay

Thesis committee

Promotor

Prof. Dr. M.A. Cohen Stuart

Emeritus Professor of Physical Chemistry & Colloid Science

Wageningen University

Co-promotors

Dr. R.J. de Vries

Associate Professor, Laboratory of Physical Chemistry & Colloid Science

Wageningen University

Dr. P.A. Wierenga

Assistant Professor, Laboratory of Food Chemistry

Wageningen University

Other members

Prof. Dr. W.J.H. van Berkel, Wageningen University, The Netherlands.

Prof. Dr. U. Kulozik, Technical University of Munich, Germany.

Dr. P. Venema, Wageningen University, The Netherlands.

Dr. T. Huppertz, Nizo Food Research, The Netherlands.

This research was conducted under the auspices of the Graduate School VLAG (Advanced studies in Food Technology, Agrobiotechnology, Nutrition and Health Sciences).

New Insight into
Enzymatic Cross-linking of Globular Proteins:
From Nanostructure to Functionality

Yunus Sariçay

Thesis

submitted in fulfillment of the requirements for the degree of doctor
at Wageningen University,
by the authority of the Rector Magnificus
Prof. Dr. M.J. Kropff,
in the presence of the
Thesis Committee appointed by the Academic Board,
to be defended in public
on Wednesday 15th of October 2014
at 4 p.m. in the Aula.

Yunus Sariçay

New Insight into Enzymatic Cross-linking of Globular Proteins: From Nanostructure to
Functionality

218 pages

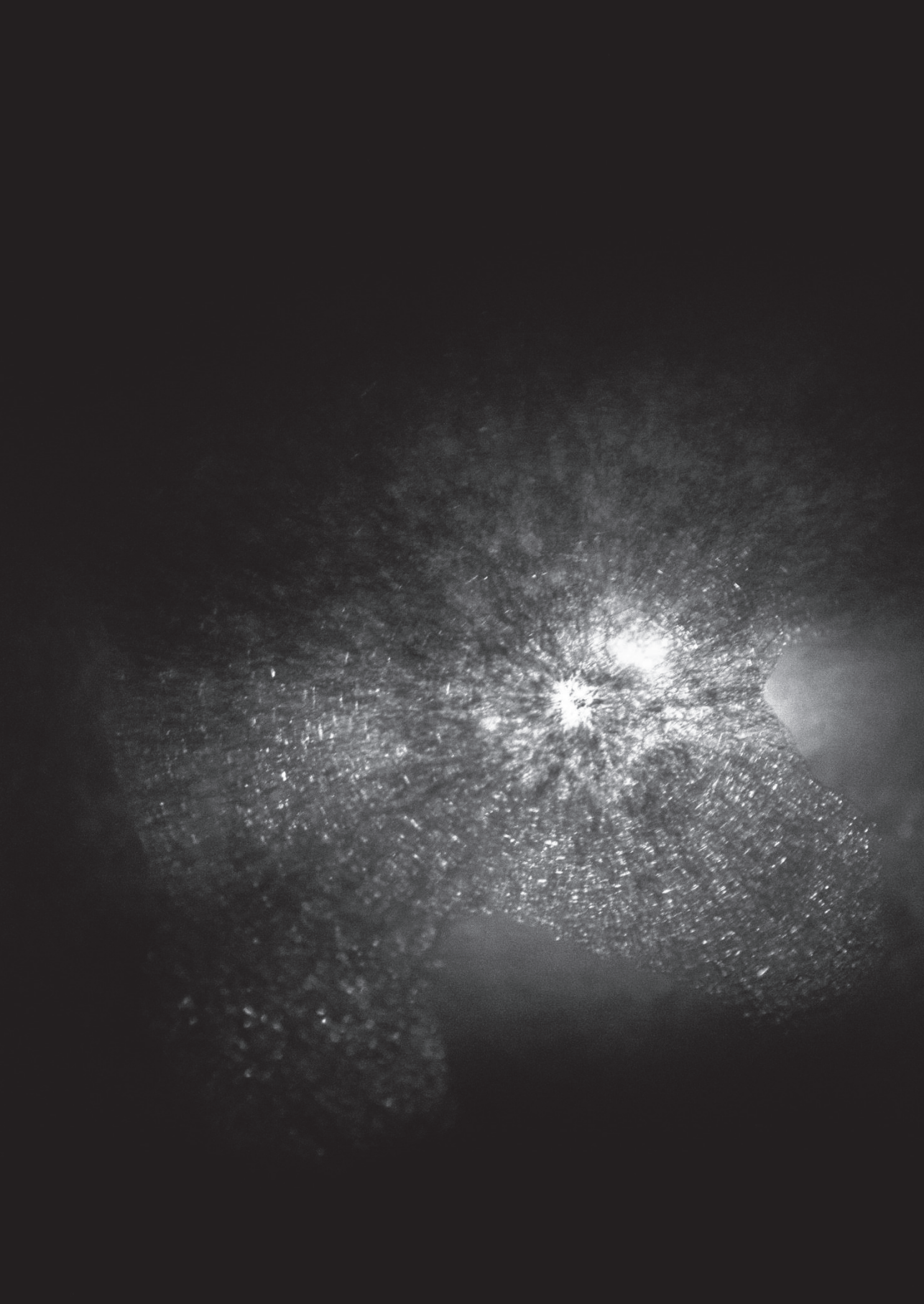
PhD thesis, Wageningen University, Wageningen, The Netherlands (2014) with references,
with summaries in English and Dutch.

ISBN: 978-94-6257-121-1

To my beloved parents

Table of contents

Chapter 1	General introduction	9
Part I. Peroxidase catalyzed cross-linking of apo-α-lactalbumin		
Chapter 2	Nanostructure development during peroxidase catalyzed cross-linking of apo- α -lactalbumin	33
Chapter 3	Changes in protein conformation and surface hydrophobicity upon peroxidase-catalyzed cross-linking of apo- α -lactalbumin	63
Chapter 4	Rheological properties of dispersions of enzymatically cross-linked apo- α -lactalbumin nanoparticles	87
Chapter 5	High stability of enzymatically cross-linked apo- α -lactalbumin nanoparticles against thermal aggregation	111
Part II. Comparison of peroxidase-, laccase- and tyrosinase-catalyzed cross-linking		
Chapter 6	Structural and physical properties of enzymatically cross-linked apo- α -lactalbumin nanoparticles: Laccase versus peroxidase	139
Chapter 7	General discussion	169
Summary		196
Samenvatting		199
List of publications		203
Acknowledgement		204
About the author		211
Overview of completed training activities		212



Chapter 1

General Introduction

The background of the page is a dark, abstract image. It features a bright, star-like point of light in the center, surrounded by a swirling, nebula-like pattern of dust and gas. The overall effect is a sense of cosmic depth and mystery.

Introduction

Proteins serve different functions in foods. They provide stability to foams and emulsions, can give rise to gelation when heated but of course are also important for their nutritional value (1). The ability of proteins to provide specific function in food system is often called “*protein functionality*”, and many protein functionalities (but not all) strongly relate to the physical properties of the proteins and their assemblies (2). This thesis deals with modifying the whey protein α -lactalbumin using cross-linking enzymes to improve its food functional properties. Whey proteins are widely used in foods and beverages for nutritional and functional purposes. Their functional properties can be altered by different types of protein modifications: physical, chemical and enzymatic (3). The main types of enzymatic protein modifications relevant for food technology are hydrolysis and cross-linking (4).

In the last two decades, the cross-linking enzyme microbial transglutaminase (mTG) has received a lot of attention since its action on food protein substrates can enhance protein functionality in many food applications (e.g. dairy and cereal applications, meat and fish processing) (5). A range of other cross-linking enzymes that could eventually prove to be alternative to mTG are still under investigation. Cross-linking enzymes that have potential for food applications are classified in two main categories (1) transferases (i.e. transglutaminase) (2) oxidoreductases (i.e. peroxidase, laccase, tyrosinase) (6). Enzymes in the two groups differ in their cross-linking mechanism and chemistry. Briefly, transglutaminase induces cross-linking of lysine to glutamine while oxidative enzymes catalyze oxidations, mainly of tyrosine residues, which can then lead to cross-linking in a number of ways (Table.1).

The functional impact of enzymatic protein cross-linking has been extensively studied for especially mTG (5, 7, 8). In contrast, the effect of cross-linking enzymes on the mesoscale physical properties of enzymatically cross-linked protein are poorly understood (Fig.1). Enzymatic protein cross-linking involves in covalently coupling of proteins into protein oligomers, followed by the further assembly of oligomers into large clusters, called “*protein nanoparticles*” in this thesis.

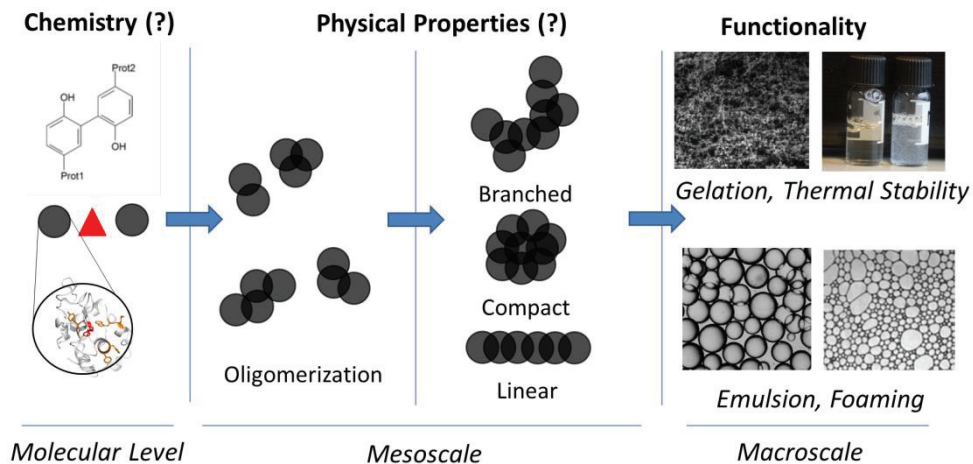


Figure.1. Enzymatic protein cross-linking at multiple length scales: (●) protein, (▲) enzyme.

Finally, if cross-linking can continue even further, protein networks are formed. To our knowledge, the effect of enzymatic protein cross-linking on properties of protein structures at multiple length scales (from the molecular level to the mesoscale, and then to the macroscale) has not been addressed so far. Therefore, the aim of this thesis is:

to elucidate effects of enzymatic cross-linking on the molecular and mesoscale properties of apo- α -lactalbumin, in order to explore and understand the possible food functional properties of enzymatically cross-linked protein nanoparticles in food formulations.

In this introductory chapter, we first briefly review research on the enzymatic cross-linking of food proteins, introducing among others the various oxidative enzymes that are used in this thesis. Next is some background information on the substrate protein that we have chosen: Calcium free, apo- α -lactalbumin. Our research focuses on cross-linking of food proteins into nanoparticles (as opposed to, for example, cross-linking into protein oligomers, or cross-linking into macroscopic networks) and a large section is devoted to uses and properties of protein nano- and micro-particles as an ingredient in food formulations.

Table.1. Overview of enzymes used for cross-linking proteins.

Enzyme	Target amino acids	Cross-linking Bonds	Reference
<i>Transferases</i> Transglutaminase	Glutamyl side chains of protein	Formation of glutamyl-lysyl isopeptide bonds	(9)
<i>Oxidoreductases</i> Peroxidase	Tyrosyl side chains of protein; phenolic compounds	Radical formation; radical couplings; (e.g. tyrosine-tyrosine)	(10)
Laccase	Tyrosyl side chains of protein; phenolic compounds	Radical formation; radical couplings; (e.g. tyrosine-tyrosine)	(11)
Tyrosinase	Tyrosyl side chains of protein; phenolic compounds	Radical formation; radical couplings; (e.g. tyrosine-tyrosine)	(12)

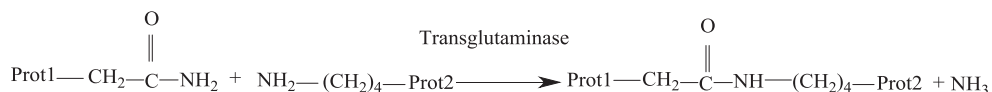
Enzymatic cross-linking of food proteins

Reaction mechanisms cross-linking catalyzed by different oxidative enzymes, differ in many relevant details, and this ultimately leads to the different effects on food protein functionality that are observed when different oxidative enzymes act on the same food protein substrate. This section gives provides an introduction to the mode of action of the various oxidative enzymes used in this study.

Transglutaminase

Transglutaminase catalyzes an acyl-transfer reaction in which the carboxamide groups of glutamine side chains (the acyl donors) are cross-linked to lysine side chains (acyl acceptors) (Fig.2) (13). The enzymatic reaction generates one mole of ammonia (NH₃) for

each cross-linking bond. Commercially available microbial transglutaminase (mTG) is used in the food industry for structuring foods in several food applications (i.e. dairy application, meat and fish processing) (7, 8). Transglutaminase has been found to induce the cross-linking of many proteins including gelatin, myofibrillar, milk, soy, fish and cereal proteins (14):



Prot= Protein

Figure.2. Transglutaminase-catalyzed cross-linking of lysine to glutamine

Peroxidase

Peroxidases are oxidoreductase enzymes that catalyze the oxidation of donor substrates (e.g. phenols) in the presence of hydrogen peroxide (H_2O_2) (15). The enzymatic oxidation results in the formation of radicals and that further react with other substrates. Peroxidase from horseradish has been found to catalyze reaction involving Tyr, Phe, Trp, His, and Cys residues with Tyr being the most reactive residue for enzymatic oxidation (16). Oxidative cross-linking of tyrosine upon peroxidase-catalysed cross-linking is illustrated in Fig.3.

Peroxidase (HRP C) has two metal-binding sites that connect to a single iron (III) (referred to 'heme group') and two calcium ions. Removal of calcium leads to a decreased enzyme activity and a decreased thermal stability (15). In the resting state, the iron heme group (Fe-III) in peroxidase reacts with H_2O_2 , generating a two-electron oxidized intermediate (Compound I) active state. Compound I catalyzes the oxidation of the donor substrate (AH), yielding a one-electron oxidized intermediate (Compound II) and a free radical. Subsequently, Compound II returns back to the resting state (to the form of native enzyme) by oxidizing another donor substrate (AH) (Fig.4).

PEROXIDASE-CATALYZED CROSS-LINKING

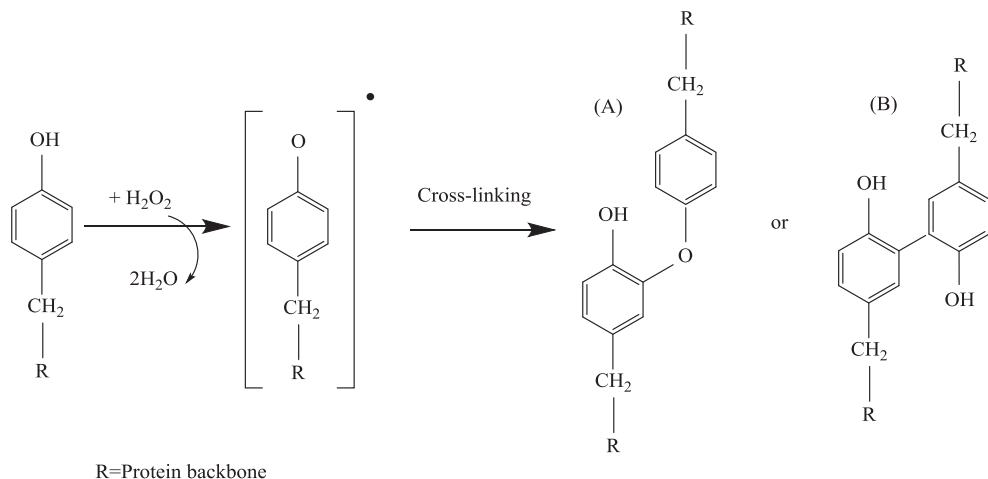


Figure.3. Peroxidase-catalyzed cross-linking of tyrosine via radicals: (A) *ortho-ortho* dityrosine; (B) isodityrosine.

The free radicals that are formed can further interact with a variety of groups. In the case of excessive H₂O₂, the reaction of compound II with H₂O₂ leads to a modification of the heme group, resulting in the so-called "suicide inhibition" of the peroxidase (18). Since excessive H₂O₂ leads to enzyme inhibition, a step-wise addition of peroxide is preferred to induce extended enzymatic cross-linking of proteins (19). The catalytic cycle of peroxidase can be monitored using UV-Vis spectroscopy. In the resting state, the enzyme has an absorption peak at 403 nm, while in its active state, the enzymes has an absorption peak at 417 nm (20).

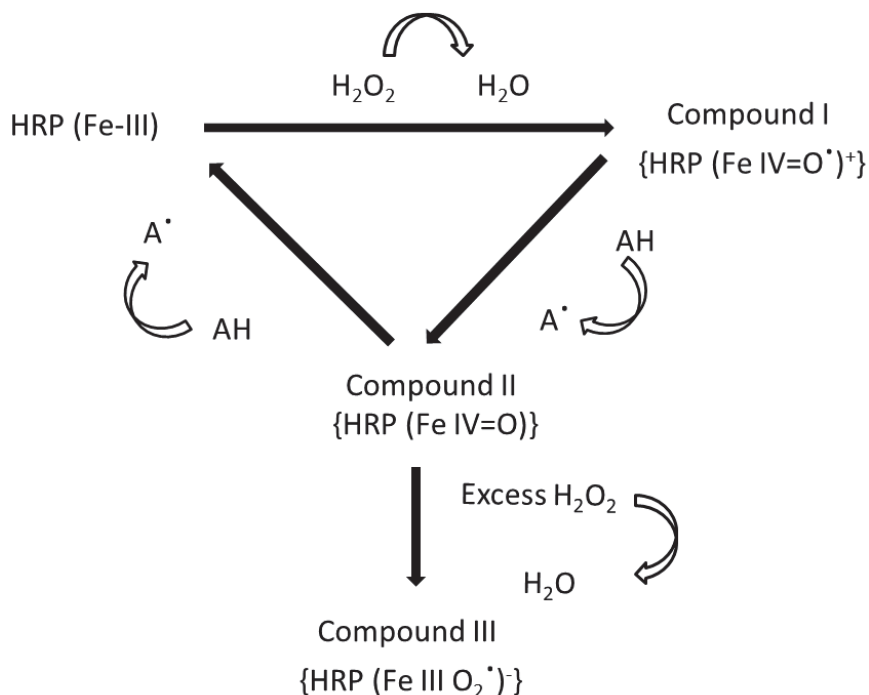


Figure.4. Catalytic cycle of peroxidase in the presence of H_2O_2 (17)

Laccase

Laccases are copper-containing oxidases that catalyze oxidation of the variety of phenolic compounds with the reduction of molecular oxygen to water (21). Oxidation of phenolic compounds by laccase results in the formation of free radicals that may further react with other compounds, leading to polymerization (22). Laccases can catalyze the oxidation of tyrosine in protein with a mechanism similar to that for peroxidases. Oxidation of tyrosines by the enzyme leads to the formation of either an *ortho-ortho* dityrosine (**A**, 3,3'-dityrosine) or an isodityrosine (**B**, 3,o'-dityrosine) bond (Fig.5) (21). Laccase-induced cross-linking of peptides and proteins has also been shown to lead to oxidation of tryptophans (Trp), and cysteines (Cys) (23). The main types of bonds formed under the influence of laccase appear to be disulphide bonds between cysteines and isodityrosine bonds between tyrosines (24-26).

PEROXIDASE-CATALYZED CROSS-LINKING

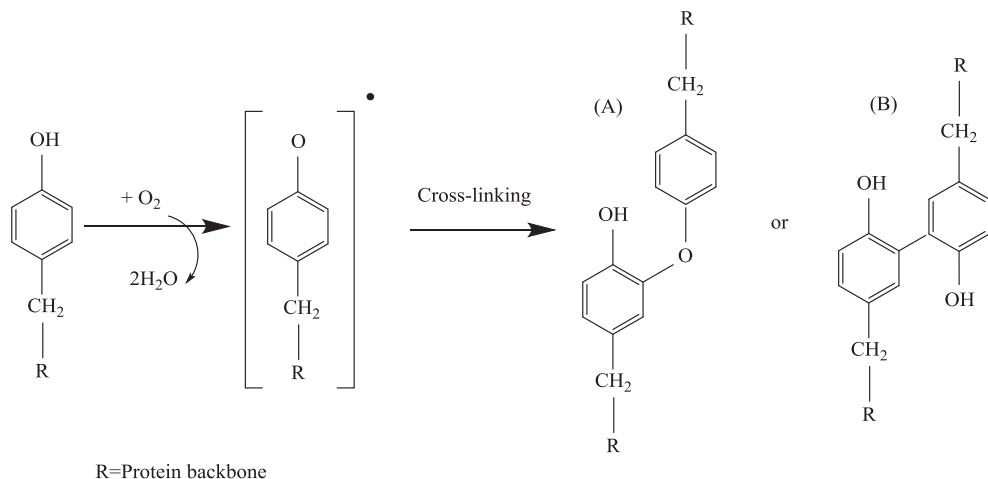


Figure.5. Laccase-catalyzed cross-linking of tyrosine radicals: (A) *ortho-ortho* dityrosine; (B) isodityrosine

Due to the broad substrate specificity of laccase (including phenolic compounds, diamines, aromatic amines, benzenethiols and even some inorganic compounds such as iodine (27)), laccases have seen a growing interest in recent years for biotechnological applications (28). One advantage of laccases as compared to peroxidases is that the use oxygen rather than peroxide.

Tyrosinase

Tyrosinases are copper-containing enzymes catalyzing the oxidation of mono- and di-phenolic compounds to quinones with the concomitant reduction of molecular oxygen to water (29). The quinone formed upon enzymatic oxidation can further react with other nucleophiles non-enzymatically, e.g. amino groups (30). Tyrosinase has been shown to oxidize tyrosine residues in proteins to quinones that further react with tyrosine, cysteine, or lysine residues (31). Enzymatic oxidation of tyrosine and the subsequent protein cross-linking upon tyrosinase-catalyzed cross-linking is depicted in Fig.6.

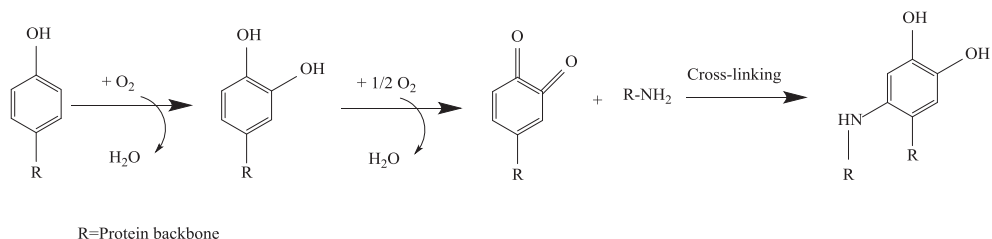


Figure.6. Tyrosinase-induced formation of a dopa *o*-quinone and the subsequent formation of a protein cross-link.

Accessibility of reactive groups

A major factor in determining the efficiency of enzymatic cross-linking reaction is the accessibility of the potentially reactive groups in the substrate protein to the cross-linking enzymes, which in turn, is determined by a range of physicochemical factors (23, 27, 30, 32-36). Flexible, unstructured proteins such as caseins have been found to be very good substrates for cross-linking enzymes, in contrast to globular food proteins with a compact folded structure such as whey proteins (8). Hence, globular food proteins are often pre-processed for improving cross-linking efficiency via the accessibility of the reactive groups.

A number of strategies are used:

1. **(Partial) protein unfolding.** By using heat, pressure, denaturants (e.g. *mercaptoethanol* (ME) or *dithiothreitol* (DTT)), or by changing extrinsic conditions (e.g. pH, ionic strength) (37-41).
2. **Addition of highly accessible cross-linking mediators.** For oxidative cross-linking, one can also resort to small cross-linking mediators such as caffeic acid (CA) and ferulic acid (FA). Enzymes indeed easily oxidize these highly accessible small molecules that can further react with target amino acids, and thus act as a bridge between proteins. A disadvantage of this approach is that the enzymatic

oxidation of these phenolic compounds typically leads to strong color formation (e.g. dark brown) (14, 30, 42, 43).

3. **Protein modification with cross-linking mediators** has also been recently used for improving the ability of oxidative enzymes to cross-link globular food proteins. For example, food proteins can be modified by the attachment of vanillic acid (VA) that can act as a highly accessible reactive site for enzymatic protein cross-linking (44).

Impact of cross-linking on physical and functional properties of food proteins

The enzyme microbial transglutaminase (mTG) is the most extensively studied enzyme for cross-linking of globular proteins (7). Commercially available preparation of this enzyme is approved for use in foods, and is indeed being used in many applications in the food industry (5, 7, 45). The main emphasis in the literature has been on the chemistry of cross-linking and on the improvements in food functionality that can be obtained by using it. Only a few authors have also studied the relation between the physical and functional properties of mTG-cross-linked whey proteins (46-49). In these studies, accessibility of the whey proteins to the enzymes was improved either by partial chemical and/or thermal denaturation. Differences between different transglutaminases have also been studied. For example, Matsumura et al. found that the initial cross-linking rate for the whey protein α -lactalbumin (α -lac), being cross-linked by gTG (from guinea pig liver) was substantially higher than for α -lac being cross-linked by mTG (from *Streptoverticillium mobaraense*) (46). However, prolonged incubation with mTG was found to eventually lead to the formation of cross-linked protein nanoparticles that are much larger than for gTG. Final structures of cross-linked protein nanoparticles were also different. Differences in the size-mass scaling exponent (obtained from size-exclusion coupled to multi-angle laser light scattering, SEC-MALLS) show that gTG-cross-linked α -lac nanoparticles were more compact than mTG-cross-linked α -lac nanoparticles. The exponent α in the size-mass scaling relation $R_g \propto M_w^\alpha$ was found to be $\alpha = 0.31$ for gTG but $\alpha = 0.44$ for mTG (46).

For whey protein isolate (WPI) it has been found that mTG cross-linking (without using chemical or thermal denaturation to improve accessibility) has no major influence on the secondary and tertiary structure of the globular whey proteins (47). Nevertheless it was observed that the cross-linking led to more protein precipitation in the pH range pH 4.0-4.5, when compared to native WPI. This was interpreted as being a consequence of the change of the hydrophobic-hydrophilic balance, due to the elimination of lysine charges (48). In contrast, mTG-treatment of chemically denatured WPI (8% (w/v) protein, 20 mM DTT) was reported to prevent hydrophobic interactions and thus to resulting in lower viscosities as compared to non-mTG-treated WPI solutions (49). This was attributed to the occlusion of hydrophobic patches of the partially unfolded, cross-linked proteins due to the supposedly compact structure of the mTG-cross-linked WPI.

Promising reports have now also been published on improvements in food protein functionality after oxidative protein cross-linking (14). Recently, the effect of tyrosinase (Tyr) from *Trichoderma reesei* on the rheology of milk gels has been compared with the corresponding effect of mTG (32). It was found that Tyr- and mTG-treated (heated) milk gels have different morphologies of the final casein protein particles. Protein particles formed in Tyr-treated heated milk (as judged from SEM images) are loosely connected aggregates of individual protein particles, suggesting no dramatic improvements in connectivity were induced by Tyr. In mTG-treated milk gel, however, protein particles appear to have improved connectivity. Even though the extent of mTG and Tyr-catalyzed cross-linking of casein was shown to be comparable, mTG treatment lead to a higher storage modulus and firmness as compared to Tyr-treated heated milk (32). This is consistent with the observation that mTG cross-linking of acid milk gels leads to the formation of a network of protein aggregates with a smaller pore size and hence a lower permeability (39).

In another study, after an mTG-treatment of WPI solutions (8% w/w protein in deionized water, pH 7.5, containing 10 mM dithiothreitol, 4-h enzymatic reaction at 40 °C) it was found that the temperature required for heat-induced gelation increased from 69 to 94 °C. The resulting gels exhibited a much lower storage modulus as compared to the corresponding untreated heat-induced WPI gels (50). Other authors have found that other

pre-treatment conditions (in particular, a lower extent of enzymatic cross-linking) may in fact lead to higher gel strengths and lower gelling temperatures instead (51, 52).

MTG-induced cross-linking has also been shown to enhance the thermal stability of food proteins. The denaturation temperature (T_d) of WPI solution increased from ~ 72 to ~ 78.5 °C when WPI solution was first incubated with mTG for 30 h. DSC thermograms for the cross-linked WPI show both an exothermic peak at 83 °C and an endothermic peak at 78.5 °C, indicating thermal aggregation at high temperature (≥ 83 °C). It was proposed that mTG-treatment of WPI solution leads to occlusion of hydrophobic patches in cross-linked proteins resulting in enhanced thermal stability (47).

MTG treatment of WPI has also been compared to a heating pretreatment in order to improve WPI stability against thermal aggregation (53). Partially denatured WPI solution (heated at 80 °C for 15 min) was cross-linked using mTG and compared to WPI solutions briefly heated at 138 °C. The mTG treated WPI exhibited higher resistance against thermal aggregation than the WPI that was only heat-pretreated. Both treatments increased the zeta potential (ζ) of the WPI from about -25mV (untreated WPI) to -36 mV for (pretreated WPI). The authors conclude that apparently, the enhanced zeta potential cannot be the main factor in improving stability against thermal aggregation. Indeed another concludes that an increase of the protein denaturation temperature T_d is more important in determining stability against thermal aggregation, than changes in zeta potential and surface hydrophobicity (54).

The above examples demonstrate that significant changes in the food functionality of proteins are induced by enzymatic cross-linking. They also indicate that the relation between these changes and changes in the structure and physical properties of the proteins across the relevant length scales (both the single protein level and the mesoscale level) are far from clear.

Apo- α -lactalbumin as a model substrate

Alpha-lactalbumin (α -lac) is a small (M_w of 14 kDa), Ca^{2+} -binding globular protein in whey (55). The native structure of α -lac is composed of two domains. A first domain is largely helical while the second domain has a significant content of β -sheets. The two domains

are divided by a deep cleft and connected to each other by a disulphide bridge between residues Cys73 and Cys91, forming the Ca^{2+} binding loop. Four disulfide bridges (Cys6–Cys120, Cys61–Cys77, Cys73–Cys91, and Cys28–Cys111) stabilize the overall structure of α -lac (56). Removal of the Ca^{2+} from α -lac leads to increased sensitivity to pH and ionic conditions (57). Ca^{2+} -binding to α -lac increases the thermal denaturation temperature (i.e. it shifts from 35 °C to 63 °C) (58). The conformation of α -lac changes dramatically with the removal of Ca^{2+} , inducing the formation of a partially unfolded structure, similar to the so-called molten globule state (Fig.7) (59).

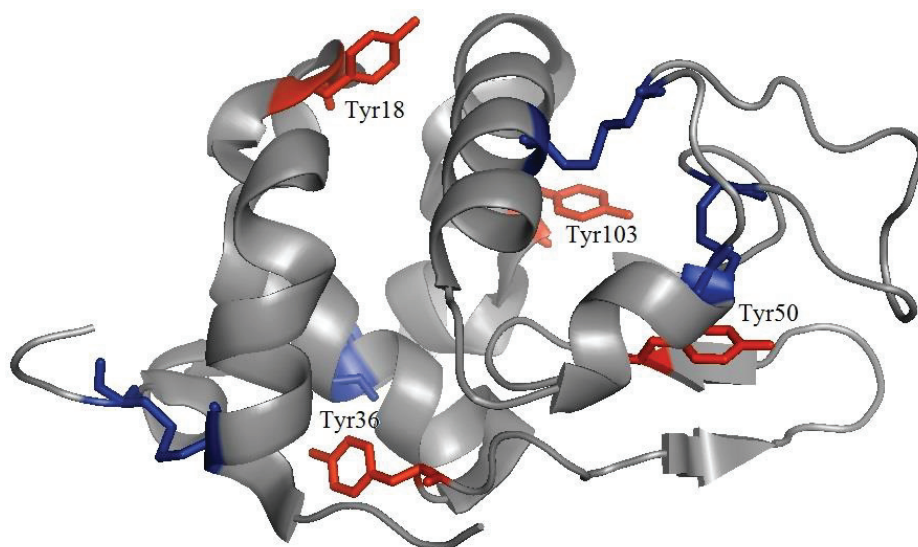


Figure.7. Crystal structure of bovine apo α -lactalbumin (PDB accession code 1f6r)(61). Tyr18, Tyr36, Tyr50 are indicated in red. Disulfide bridges are marked by blue.

In this molten globule state the tyrosine residues (Tyr⁵⁰ in the β -domain; Tyr¹⁸ and Tyr¹⁰³ in the α -domain; Tyr³⁶ at the surface (60)) will be much more accessible for oxidative cross-linking than in the Ca^{2+} containing holo form of the protein (10). This relatively controlled improvement of accessibility (as compared to partial denaturation using other means) makes apo- α -lactalbumin a very good model system to study the enzymatic cross-

linking of globular food proteins, the more so, since whey proteins (including α -lactalbumin) are food proteins with great economic significance.

Protein nanoparticles

There is a continued need in food technology for new strategies to tailor food protein functionality, and many approaches are under investigation. A general approach that is being explored more and more is to design protein nano- and micro-particles with controlled functional properties for particular food formulations (62). Within such a general approach, enzymatic protein cross-linking offers a means for either modifying protein properties (i.e. via intramolecular cross-linking) or for creating protein large protein clusters (i.e. via intermolecular cross-linking) (6). As compared to chemical modifications and heat-induced aggregation, a major advantage of enzymatic cross-linking is the high specificity of enzymes that is expected to lead to better control of the cross-links that can be formed, and hence to better tuning of physical and functional properties of protein particles (63). In this thesis, we focus on protein nanoparticles composed of apo- α -lactalbumin, created by enzymatic cross-linking using a range of oxidative enzymes. In this section, we briefly review protein particle properties that are important for their ultimate food functional properties.

Structure

The particle size, shape and internal architecture or in short, its structure (at all relevant lengthscales), is the most important parameter determining food functionality of protein nanoparticles. This is illustrated very nicely by the case of heat-induced protein aggregates. For instance, heating aqueous solution of globular proteins under different conditions results in the formation of spherical particles, flexible strands, semi-flexible fibril and fractal clusters (64). These structures may further assemble in fine stranded, mixed or particulate network in protein gels. All of this depends mainly on the pH and ionic strength at which the proteins are heated: fine stranded gels for $pI < pH < pI$ and at salt concentration < 0.1 M, particulate gels at $pH \approx pI$ or $pH > pI$ and at high salt concentration, and mixed gels at $pH > pI$ and at intermediate salt concentrations (65-67).

The different structures give rise to completely different physical properties and hence food functional properties. For instance, the fine-stranded gels have a translucent appearance whereas particulate and mixed gels are opaque (68). Textural properties of the different protein gels, that couple to their rheology, are also very different. For instance, fine-stranded gels made at $\text{pH} > \text{pI}$ exhibit strong elasticity whereas gels formed at $\text{pH} < \text{pI}$ are weak and brittle. Also, the water holding capacity of fine-stranded gels is better than that of particulate gels (68). The relation between the microstructure of protein networks, their rheology, and their ultimate food functional properties is a topic that has been addressed many different studies on heat-induced whey protein aggregation (69-71). Finally, the thermal stability against aggregation is another food functional property of proteins that can be tuned by a pretreatment in which the proteins are first heat-aggregated into protein nano- or microparticles with controlled physical properties (e.g. surface hydrophobicity, zeta potential) (72, 73).

In comparison to the enormous amount of literature available on heat-induced protein aggregates, very little work has been done on relating structures of enzymatically cross-linked protein (both at the single protein level and at the mesoscale) to their physical and food functional properties. To our knowledge, only Matsumura et al. have characterized particle structures resulting from enzymatic protein cross-linking in some detail, for the case of α -lactalbumin, being cross-linked by mTG (46). For the main system studied in this thesis, peroxidase catalyzed cross-linking of apo- α -lactalbumin, Heijnis et al. have shown that larger protein nanoparticles are formed when multiple low concentration additions of hydrogen peroxide (H_2O_2) were done, as compared to a single high concentration dose (74). The conversion of monomers into protein nanoparticles (the latter eluting in the void volume of their size-exclusion chromatography (SEC) column) was 73 % with a 6-times addition of H_2O_2 , as compared to the monomer conversion into particles of 27 % when a similar amount of peroxide was added at once. Size distributions for cross-linked protein, as determined from SEC showed significant variations when pH and ionic strength were changed. At low ionic strength, peroxidase-catalyzed cross-linking of α -lactalbumin led to more dimerization than high ionic strength. Similarly, more large oligomers occurred at pH 5.9 than at pH 6.8 (74). These observations indicate that

electrostatic interactions play an important role in determining nanoparticle growth when enzymatically cross-linking proteins.

To our knowledge, apart from the studies mentioned above, the structural properties of cross-linked protein and the mechanisms of nanoparticle formation have not been addressed yet in any detail in the literature for oxidative cross-linking enzymes. The different oxidative enzymes have somewhat different cross-linking chemistries that are not always completely understood yet, and these may give rise to different types of structures, and hence different types of physical properties and food functional properties. This is another topic on which as far as we know, no information is available in the literature.

Charge

For protein nanoparticles prepared by the enzymatic cross-linking of proteins, the electrostatic properties of the particles will depend on the pH and ionic strength (62). This means that the protein nanoparticles may be expected to swell and shrink under conditions of high or low electrostatic repulsion between their protein subunits. Also, conditions that lead to conformational changes such as extreme pH values, may lead to corresponding changes of protein subunits in the nanoparticles.

Depending on the type of enzyme used, the cross-linking reaction may or may not lead to changes in the net charge of the individual proteins (at given pH). For HRP the charge of the proteins is not changed upon cross-linking, since tyrosine is not a charged residues. For mTG, the loss of the free amino groups of lysine will result in an increase in the net negative charge of the protein (47, 54). Such changes may affect particle-particle interactions and hence may also affect both the physical properties of the particles, as well as their formation process.

Hydrophobicity & Protein Conformations

In native globular proteins, most of the hydrophobic amino acids are buried in the interior, while the polar amino acids are present on the exposed surface of the protein, stabilizing proteins from aggregation. Enzymatic cross-linking may alter the protein folding, and hence change which amino acids are buried and which ones are exposed (49). This will

result in changes of the physical properties of the individual protein subunits in enzymatically cross-linked protein. While most of the characterization of protein particles discussed so far deals with lengthscales beyond the size of the single protein subunit, the level of the individual protein subunits is equally important. Crucial issues that relate to cross-linking induced changes at this level are:

- (1) The possibility that cross-linking induced partial protein unfolding.
- (2) The possibility that the partial unfolding changes the surface properties of the individual protein subunits in cross-linked protein, in particular their surface hydrophobicity.

Such protein unfolding and the consequent surface hydrophobicity would favor the aggregation of enzymatically cross-linked protein nanoparticles, which is typically undesirable. On the other hand, some degree of hydrophobicity is required for some functionalities such as interfacial stabilization.

Outline of the thesis

In the first part of the thesis, **Peroxidase catalyzed cross-linking of apo- α -lactalbumin (Chapter 2 – 5)**, we mainly focus on understanding how peroxidase-catalyzed cross-linking alters mesoscale physical and functional properties of apo- α -lactalbumin nanoparticles at multiple length scale (from a single molecular level up to macroscale) (Fig.8). In the second part, **Comparison of peroxidase-, laccase- and tyrosinase-catalyzed cross-linking (Chapter 6 – 7)**, we investigate to what extent stability, physical and functional properties of protein nanoparticles differ when apo- α -lactalbumin is cross-linked by different oxidative enzymes.

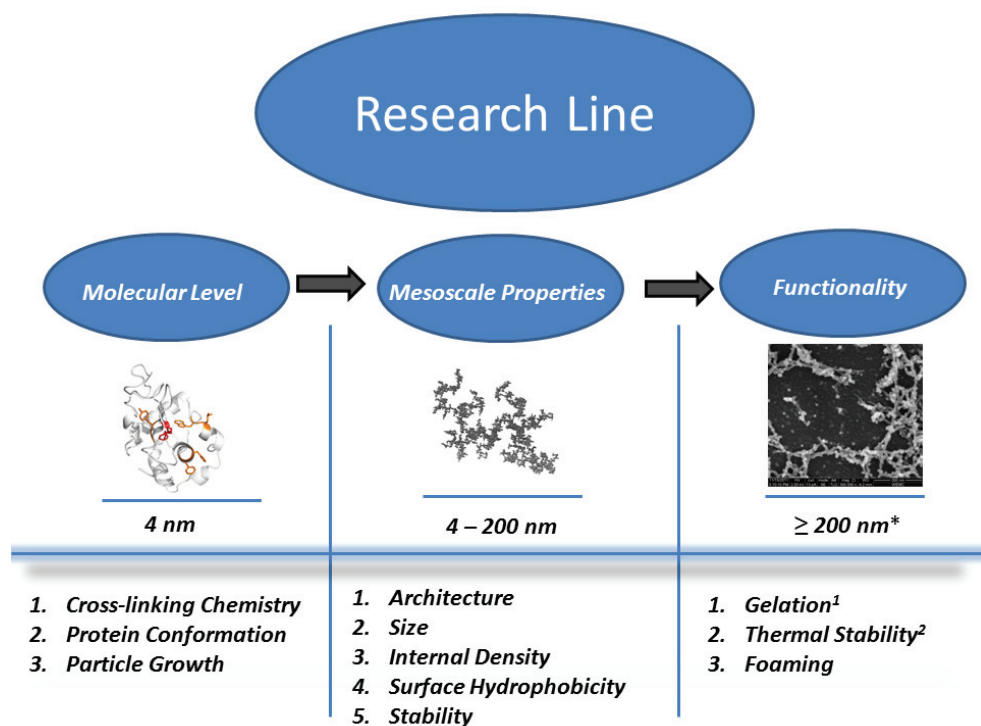


Figure.8. Graphical outline of the thesis.

¹ Gelation refers to physical protein hydrogel formed by jamming of dispersions of protein nanoparticles

² Thermal stability corresponds to stability against thermal aggregation

I. Peroxidase catalyzed cross-linking of apo- α -lactalbumin

Chapter 2 examines particle growth during horse-radish peroxidase-catalyzed cross-linking of apo- α -lac and the architecture of the final cross-linked protein nanoparticles.

In **Chapter 3**, we study changes in protein conformation and surface hydrophobicity of apo- α -lac upon cross-linking by horse-radish peroxidase.

Chapter 4 addresses the rheological properties of dispersions of the apo- α -lac nanoparticles characterized in detail in the previous chapters.

Chapter 5 investigates changes in the molecular conformation of the single protein subunits of enzymatically cross-linked apo- α -lac when the cross-linked nanoparticles are

heated, and considers the implications of these changes for heat stability of both dilute and concentrated solutions of the protein nanoparticles.

II. Comparison of peroxidase-, laccase- and tyrosinase-catalyzed cross-linking

Chapter 6 investigates differences in structure, and physical properties of protein nanoparticles prepared by either peroxidase or laccase-catalyzed cross-linking of apo- α -lac.

Chapter 7, the General Discussion, places the results of the earlier chapters in a broader perspective by providing a broad comparison between the structure, physical properties and functionalities of apo- α -lac nanoparticles produced by cross-linking with a range of oxidative enzymes (peroxidase, laccase, tyrosinase).

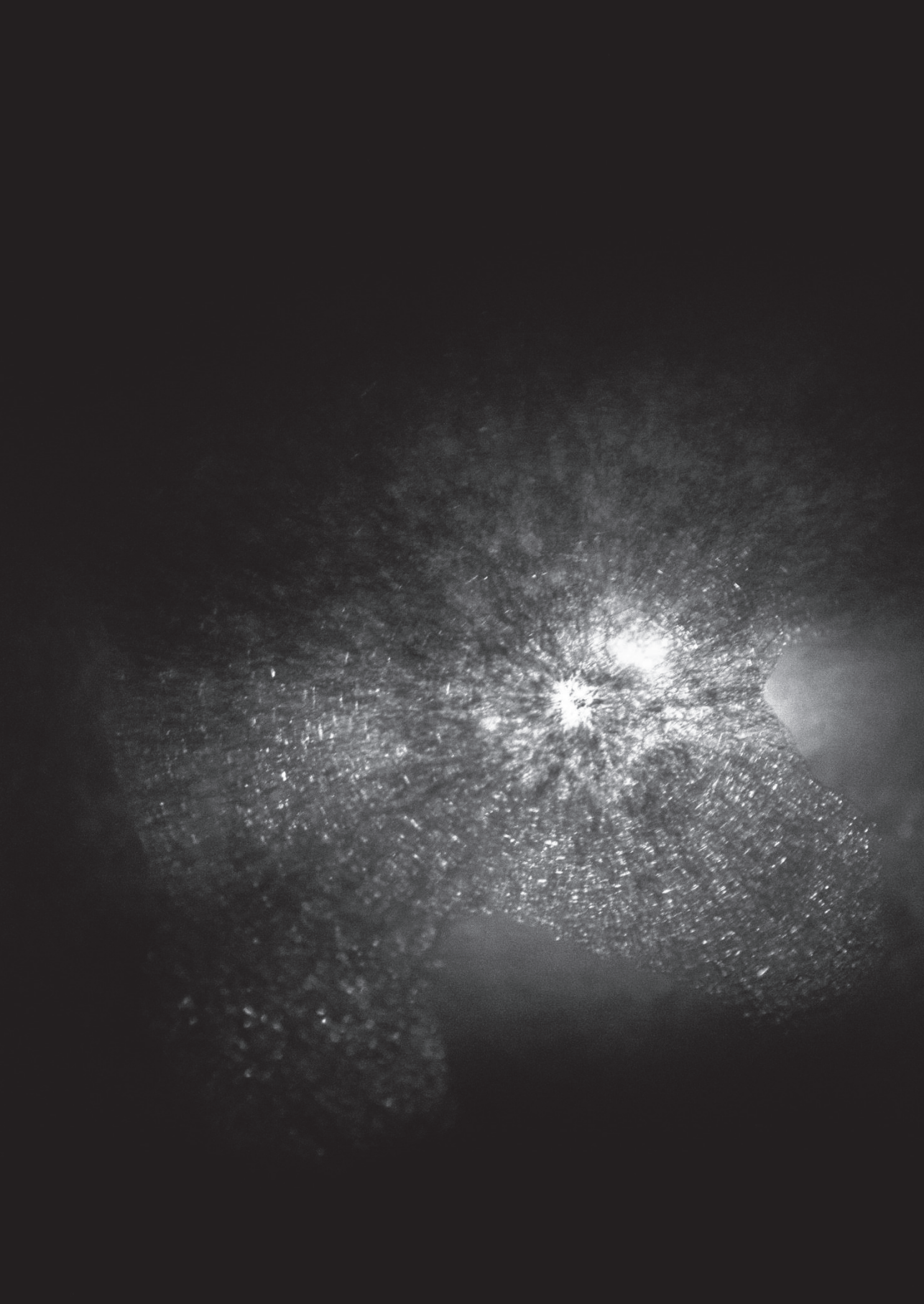
References

1. Foegeding, E. A.; Davis, J. P., Food protein functionality: A comprehensive approach. *Food Hydrocolloids* **2011**, *25*, 1853-1864.
2. Foegeding, E. A.; Davis, J. P.; Doucet, D.; McGuffey, M. K., Advances in modifying and understanding whey protein functionality. *Trends Food Sci. Technol.* **2002**, *13*, 151-159.
3. Kester, J. J.; Richardson, T., Modification of whey proteins to improve functionality. *J. Dairy Sci.* **1984**, *67*, 2757-2774.
4. Whitehurst, R. J.; Van Oort, M., *Enzymes in Food Technology*. Wiley: 2009.
5. Ozrenk, E., The use of transglutaminase in dairy products. *Int. J. Dairy Technol.* **2006**, *59*, 1-7.
6. Heck, T.; Faccio, G.; Richter, M.; Thony-Meyer, L., Enzyme-catalyzed protein crosslinking. *Appl. Microbiol. Biotechnol.* **2013**, *97*, 461-475.
7. Jaros, D.; Partschefeld, C.; Henle, T.; Rohm, H., Transglutaminase in dairy products: Chemistry, physics, applications. *J. Texture Stud.* **2006**, *37*, 113-155.
8. Kuraishi, C.; Yamazaki, K.; Susa, Y., Transglutaminase: Its utilization in the food industry. *Food Rev. Int.* **2001**, *17*, 221-246.
9. Yokoyama, K.; Nio, N.; Kikuchi, Y., Properties and applications of microbial transglutaminase. *Appl. Microbiol. Biotechnol.* **2004**, *64*, 447-454.
10. Oudgenoeg, G., Peroxidase catalyzed conjugation of peptides, proteins and polysaccharides via endogenous and exogenous phenols. *Wageningen University* **2004**.
11. Santhanam, N.; Vivanco, J. M.; Decker, S. R.; Reardon, K. F., Expression of industrially relevant laccases: prokaryotic style. *Trends Biotechnol.* **2011**, *29*, 480-489.
12. Fairhead, M.; Thony-Meyer, L., Bacterial tyrosinases: old enzymes with new relevance to biotechnology. *New Biotech.* **2012**, *29*, 183-191.
13. Motoki, M.; Seguro, K., Transglutaminase and its use for food processing. *Trends Food Sci. Technol.* **1998**, *9*, 204-210.
14. Buchert, J.; Cura, D. E.; Ma, H.; Gasparetti, C.; Monogioudi, E.; Faccio, G.; Mattinen, M.; Boer, H.; Partanen, R.; Selinheimo, E.; Lantto, R.; Kruus, K., Crosslinking Food Proteins for Improved Functionality. In *Annual Review of Food Science and Technology, Vol 1*, Doyle, M. P.; Klaenhammer, T. R., Eds. Annual Reviews: Palo Alto, 2010; Vol. 1, pp 113-138.
15. Veitch, N. C., Horseradish peroxidase: a modern view of a classic enzyme. *Phytochemistry* **2004**, *65*, 249-259.
16. Elliott, K. A., Oxidations catalysed by horseradish- and milk-peroxidases. *The Biochemical journal* **1932**, *26*, 1281-90.
17. Berglund, G. I.; Carlsson, G. H.; Smith, A. T.; Szoke, H.; Henriksen, A.; Hajdu, J., The catalytic pathway of horseradish peroxidase at high resolution. *Nature* **2002**, *417*, 463-468.
18. Arnao, M. B.; Acosta, M.; Delrio, J. A.; Varon, R.; Garcacanas, F., A kinetic-study on the suicide inactivation of peroxidase by hydrogen-peroxide. *Biochimica Et Biophysica Acta* **1990**, *1041*, 43-47.
19. Bhattacharyya, D. K.; Adak, S.; Bandyopadhyay, U.; Banerjee, R. K., Mechanism of inhibition of horseradish peroxidase-catalyzed iodide oxidation by edta. *Biochem. J.* **1994**, *298*, 281-288.
20. Andersen, M. B.; Hsuanyu, Y.; Welinder, K. G.; Schneider, P.; Dunford, H. B., Spectral and kinetic-properties of oxidized intermediates of coprinus-cinereus peroxidase. *Acta Chem. Scand.* **1991**, *45*, 1080-1086.
21. Thurston, C. F., The structure and function of fungal laccases. *Microbiology-(UK)* **1994**, *140*, 19-26.
22. Claus, H., Laccases: structure, reactions, distribution. *Micron* **2004**, *35*, 93-96.
23. Mattinen, M. L.; Hellman, M.; Permi, P.; Autio, K.; Kalkkinen, N.; Buchert, J., Effect of protein structure on laccase-catalyzed protein oligomerization. *J. Agric. Food Chem.* **2006**, *54*, 8883-8890.
24. Mattinen, M. L.; Kruus, K.; Buchert, J.; Nielsen, J. H.; Andersen, H. J.; Steffensen, C. L., Laccase-catalyzed polymerization of tyrosine-containing peptides. *Febs J.* **2005**, *272*, 3640-3650.

25. Labat, E.; Morel, M. H.; Rouau, X., Effects of laccase and ferulic acid on wheat flour doughs. *Cereal Chem.* **2000**, *77*, 823-828.
26. Figueroa-Espinoza, M. C.; Morel, M. H.; Rouau, X., Effect of lysine, tyrosine, cysteine, and glutathione on the oxidative cross-linking of feruloylated arabinoxylans by a fungal laccase. *J. Agric. Food Chem.* **1998**, *46*, 2583-2589.
27. Cura, D. E.; Lantto, R.; Lille, M.; Andberg, M.; Kruus, K.; Buchert, J., Laccase-aided protein modification: Effects on the structural properties of acidified sodium caseinate gels. *Int. Dairy J.* **2009**, *19*, 737-745.
28. Madhavi, V.; Lele, S. S., Laccase: properties and applications. *BioResources* **2009**, *4*, 1694-1717.
29. Faccio, G.; Kruus, K.; Saloheimo, M.; Thony-Meyer, L., Bacterial tyrosinases and their applications. *Process Biochem.* **2012**, *47*, 1749-1760.
30. Thalmann, C. R.; Lotzbeyer, T., Enzymatic cross-linking of proteins with tyrosinase. *Eur. Food Res. Technol.* **2002**, *214*, 276-281.
31. Selinheimo, E.; Lampila, P.; Mattinen, M. L.; Buchert, J., Formation of protein - Oligosaccharide conjugates by laccase and tyrosinase. *J. Agric. Food Chem.* **2008**, *56*, 3118-3128.
32. Cura, D. E.; Lille, M.; Partanen, R.; Kruus, K.; Buchert, J.; Lantto, R., Effect of *Trichoderma reesei* tyrosinase on rheology and microstructure of acidified milk gels. *Int. Dairy J.* **2010**, *20*, 830-837.
33. Zhang, L.; Zhang, L.; Yi, H.; Du, M.; Ma, C.; Han, X.; Feng, Z.; Jiao, Y.; Zhang, Y., Enzymatic characterization of transglutaminase from *Streptomyces mobaraensis* DSM 40587 in high salt and effect of enzymatic cross-linking of yak milk proteins on functional properties of stirred yogurt. *J. Dairy Sci.* **2012**, *95*, 3559-3568.
34. Hellman, M.; Mattinen, M. L.; Fu, B. A.; Buchert, J.; Permi, P., Effect of protein structural integrity on cross-linking by tyrosinase evidenced by multidimensional heteronuclear magnetic resonance spectroscopy. *J. Biotechnol.* **2011**, *151*, 143-150.
35. Mattinen, M. L.; Lantto, R.; Selinheimo, E.; Kruus, K.; Buchert, J., Oxidation of peptides and proteins by *Trichoderma reesei* and *Agaricus bisporus* tyrosinases. *J. Biotechnol.* **2008**, *133*, 395-402.
36. Partanen, R.; Torkkeli, M.; Hellman, M.; Permi, P.; Serimaa, R.; Buchert, J.; Mattinen, M. L., Loosening of globular structure under alkaline pH affects accessibility of beta-lactoglobulin to tyrosinase-induced oxidation and subsequent cross-linking. *Enzyme Microb. Technol.* **2011**, *49*, 131-138.
37. Eissa, A. S.; Bisram, S.; Khan, S. A., Polymerization and gelation of whey protein isolates at low pH using transglutaminase enzyme. *J. Agric. Food Chem.* **2004**, *52*, 4456-4464.
38. Lauber, S.; Noack, I.; Klostermeyer, H.; Henle, T., Oligomerization of beta-lactoglobulin by microbial transglutaminase during high pressure treatment. *Eur. Food Res. Technol.* **2001**, *213*, 246-247.
39. Faergemand, M.; Qvist, K. B., Transglutaminase: Effect on rheological properties, microstructure and permeability of set style acid skim milk gel. *Food Hydrocolloids* **1997**, *11*, 287-292.
40. Aeschbach, R.; Amado, R.; Neukom, H., Formation of dityrosine cross-links in proteins by oxidation of tyrosine residues. *Biochimica Et Biophysica Acta* **1976**, *439*, 292-301.
41. Stahmann, M. A.; Spencer, A. K.; Honold, G. R., CROSS LINKING OF PROTEINS INVITRO BY PEROXIDASE. *Biopolymers* **1977**, *16*, 1307-1318.
42. Lontie, R., *Copper proteins and copper enzymes*. CRC Press: 1984.
43. Steffensen, C. L.; Andersen, M. L.; Degn, P. E.; Nielsen, J. H., Cross-Linking Proteins by Laccase-Catalyzed Oxidation: Importance Relative to Other Modifications. *J. Agric. Food Chem.* **2008**, *56*, 12002-12010.
44. Ma, H.; Forssell, P.; Partanen, R.; Buchert, J.; Boer, H., Improving Laccase Catalyzed Cross-Linking of Whey Protein Isolate and Their Application as Emulsifiers. *J. Agric. Food Chem.* **2011**, *59*, 1406-1414.
45. Kieliszek, M.; Misiewicz, A., Microbial transglutaminase and its application in the food industry. A review. *Folia Microbiol.* **2014**, *59*, 241-250.
46. Matsumura, Y.; Lee, D. S.; Mori, T., Molecular weight distributions of alpha-lactalbumin polymers formed by mammalian and microbial transglutaminases. *Food Hydrocolloids* **2000**, *14*, 49-59.
47. Agyare, K. K.; Damodaran, S., pH-Stability and Thermal Properties of Microbial Transglutaminase-Treated Whey Protein Isolate. *J. Agric. Food Chem.* **2010**, *58*, 1946-1953.

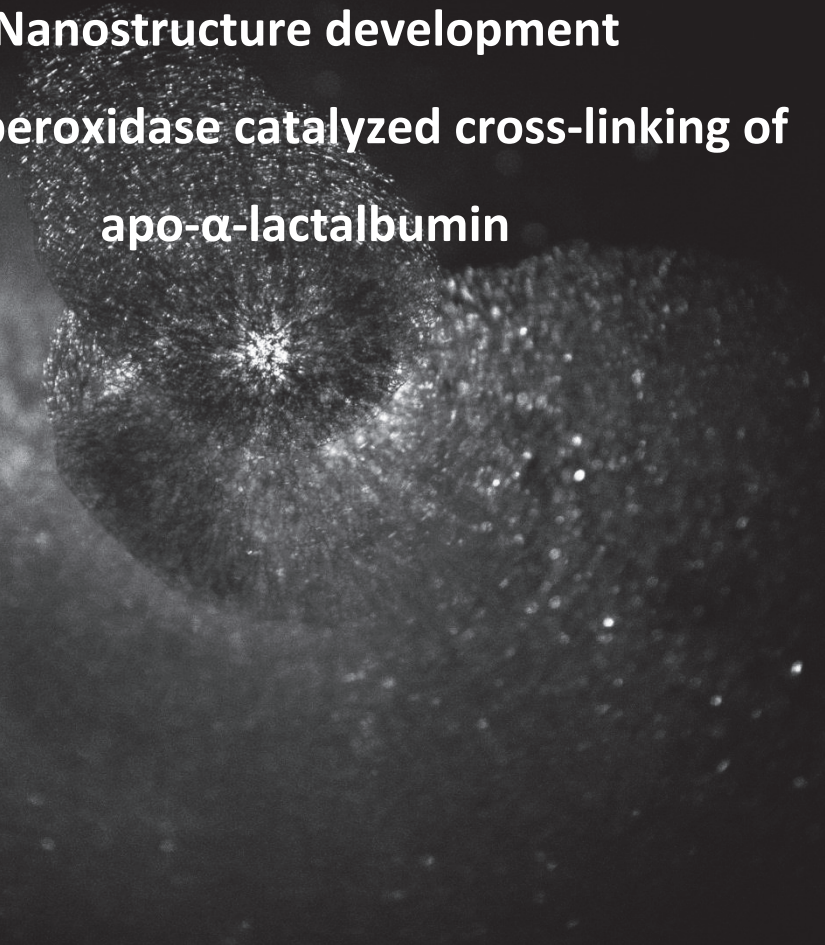
48. Damodaran, S.; Agyare, K. K., Effect of microbial transglutaminase treatment on thermal stability and pH-solubility of heat-shocked whey protein isolate. *Food Hydrocolloids* **2013**, *30*, 12-18.
49. Eissa, A. S.; Khan, S. A., Modulation of hydrophobic interactions in denatured whey proteins by transglutaminase enzyme. *Food Hydrocolloids* **2006**, *20*, 543-547.
50. Truong, V. D.; Clare, D. A.; Catignani, G. L.; Swaisgood, H. E., Cross-linking and rheological changes of whey proteins treated with microbial transglutaminase. *J. Agric. Food Chem.* **2004**, *52*, 1170-1176.
51. Wilcox, C. P.; Swaisgood, H. E., Modification of the rheological properties of whey protein isolate through the use of an immobilized microbial transglutaminase. *J. Agric. Food Chem.* **2002**, *50*, 5546-5551.
52. Wilcox, C. P.; Clare, D. A.; Valentine, V. W.; Swaisgood, H. E., Immobilization and utilization of the recombinant fusion proteins trypsin-streptavidin and streptavidin-transglutaminase for modification of whey protein isolate functionality. *J. Agric. Food Chem.* **2002**, *50*, 3723-3730.
53. Zhong, Q. X.; Wang, W.; Hu, Z. X.; Ikeda, S., Sequential preheating and transglutaminase pretreatments improve stability of whey protein isolate at pH 7.0 during thermal sterilization. *Food Hydrocolloids* **2013**, *31*, 306-316.
54. Wang, W.; Zhong, Q. X.; Hu, Z. X., Nanoscale Understanding of Thermal Aggregation of Whey Protein Pretreated by Transglutaminase. *J. Agric. Food Chem.* **2013**, *61*, 435-446.
55. Kataoka, M.; Kuwajima, K.; Tokunaga, F.; Goto, Y., Structural characterization of the molten globule of alpha-lactalbumin by solution X-ray scattering. *Protein Sci.* **1997**, *6*, 422-430.
56. Vanaman, T. C.; Brew, K.; Hill, R. L., Disulfide bonds of bovine alpha-lactalbumin. *J. Biol. Chem.* **1970**, *245*, 4583-&.
57. Griko, Y. V.; Remeta, D. P., Energetics of solvent and ligand-induced conformational changes in alpha-lactalbumin. *Protein Sci.* **1999**, *8*, 554-561.
58. Atri, M. S.; Saboury, A. A.; Yousefi, R.; Dalgalarrrondo, M.; Chobert, J. M.; Haertle, T.; Moosavi-Movahedi, A. A., Comparative study on heat stability of camel and bovine apo and holo alpha-lactalbumin. *J. Dairy Res.* **2010**, *77*, 43-49.
59. Kuwajima, K., The molten globule state as a clue for understanding the folding and cooperativity of globular-protein structure. *Proteins* **1989**, *6*, 87-103.
60. Lyon, C. E.; Suh, E. S.; Dobson, C. M.; Hore, P. J., Probing the exposure of tyrosine and tryptophan residues in partially folded proteins and folding intermediates by CIDNP pulse-labeling. *J. Am. Chem. Soc.* **2002**, *124*, 13018-13024.
61. Chrysina, E. D.; Brew, K.; Acharya, K. R., Crystal structures of apo- and holo-bovine alpha-lactalbumin at 2.2-A resolution reveal an effect of calcium on inter-lobe interactions. *J. Biol. Chem.* **2000**, *275*, 37021-37029.
62. Jones, O. G.; McClements, D. J., Functional Biopolymer Particles: Design, Fabrication, and Applications. *Compr. Rev. Food. Sci. Food Saf.* **2010**, *9*, 374-397.
63. Faergemand, M.; Otte, J.; Qvist, K. B., Cross-linking of whey proteins by enzymatic oxidation. *J. Agric. Food Chem.* **1998**, *46*, 1326-1333.
64. Nicolai, T.; Durand, D., Controlled food protein aggregation for new functionality. *Curr. Opin. Colloid Interface Sci.* **2013**, *18*, 249-256.
65. Clark, A. H.; Judge, F. J.; Richards, J. B.; Stubbs, J. M.; Suggett, A., Electron-microscopy of network structures in thermally-induced globular protein gels. *Int. J. Pept. Protein Res.* **1981**, *17*, 380-392.
66. Foegeding, E. A.; Gwartzney, E. A.; Errington, A. D., Functional Properties of Whey Proteins in Forming Networks. In *Functional Properties of Proteins and Lipids*, American Chemical Society: 1998; Vol. 708, pp 145-157.
67. Stading, M.; Langton, M.; Hermansson, A. M., Microstructure and rheological behavior of particulate beta-lactoglobulin gels. *Food Hydrocolloids* **1993**, *7*, 195-212.
68. Hudson, H. M.; Daubert, C. R.; Foegeding, E. A., Rheological and physical properties of derivitized whey protein isolate powders. *J. Agric. Food Chem.* **2000**, *48*, 3112-3119.
69. Verheul, M.; Roefs, S., Structure of particulate whey protein gels: Effect of NaCl concentration, pH, heating temperature, and protein composition. *J. Agric. Food Chem.* **1998**, *46*, 4909-4916.

- 70.** Verheul, M.; Roefs, S., Structure of whey protein gels, studied by permeability, scanning electron microscopy and rheology. *Food Hydrocolloids* **1998**, *12*, 17-24.
- 71.** Verheul, M.; Roefs, S.; Mellema, J.; de Kruif, K. G., Power law behavior of structural properties of protein gels. *Langmuir* **1998**, *14*, 2263-2268.
- 72.** Ryan, K. N.; Vardhanabhuti, B.; Jaramillo, D. P.; van Zanten, J. H.; Coupland, J. N.; Foegeding, E. A., Stability and mechanism of whey protein soluble aggregates thermally treated with salts. *Food Hydrocolloids* **2012**, *27*, 411-420.
- 73.** Ryan, K. N.; Zhong, Q. X.; Foegeding, E. A., Use of Whey Protein Soluble Aggregates for Thermal StabilityA Hypothesis Paper. *J. Food Sci.* **2013**, *78*, R1105-R1115.
- 74.** Heijnis, W. H.; Wierenga, P. A.; Berkel, W. J. H.; Gruppen, H., Directing the Oligomer Size Distribution of Peroxidase-Mediated Cross-Linked Bovine alpha-Lactalbumin. *J. Agric. Food Chem.* **2010**, *58*, 5692-5697.



Chapter 2

Nanostructure development during peroxidase catalyzed cross-linking of apo- α -lactalbumin

A grayscale electron micrograph showing a complex, fibrous nanostructure. The structure appears as a dense, interconnected network of fine filaments, with a brighter, more concentrated central region. The overall shape is somewhat irregular and elongated, with many small, bright spots scattered throughout the darker, more diffuse areas, suggesting a heterogeneous composition or varying degrees of cross-linking.

This chapter is published as: Y. Saricay, P. A. Wierenga, R. de Vries.

Food Hydrocolloids **2013**, 33, 280-288.

Abstract

Whereas extensive work has been done on the food functional and chemical aspects of enzymatic protein cross-linking, relatively little is known about the nanostructure and physical-chemical properties of enzymatically cross-linked protein. We investigate how nanostructure develops during enzymatic cross-linking of the 4 tyrosine residues of the globular protein apo- α -lactalbumin. Protein cross-linking is catalyzed by Horseradish Peroxidase, under the periodic addition of peroxide. We use on-line static and dynamic light scattering, combined with on-line UV-spectroscopy to simultaneously probe the development of nanostructure, the extent of dityrosine formation, and the catalytic state of the enzyme, as a function of the number of peroxide additions. It is found that initially, the rate of dityrosine formation is high, whereas the increase in the solution size of the cross-linked protein is limited. At later stages, the increase in solution size is significant whereas dityrosine formation slows down. Finally, the reaction stops due to enzyme inactivation. Off-line size exclusion chromatography shows that the initial phase corresponds to a fast cross-linking of monomers into small oligomers, followed by a slower joining of oligomers into large protein polymers. Consistent with this, Atomic Force Microscopy shows very heterogeneous polymers, apparently consisting of subunits that we identify with the oligomers formed in the first phase of the reaction. The dependence of the solution size on the molar mass of the cross-linked protein is determined using static and dynamic light scattering on fractionated reaction products. For sizes ranging from 30 nm to 80 nm, the protein polymers consist of 100-1000 α -lactalbumin subunits, and have molar masses of 10^6 - 10^7 g/mol. Apparent internal protein densities of the protein polymers calculated from these numbers are only a few weight percent, indicating a very dilute, open architecture of the cross-linked protein.

Introduction

Whereas enzymatic protein hydrolysis has a long history in food technology, the use of protein cross-linking enzymes is more recent, but very promising (1). For the commercially important whey proteins, functional effects that have been found upon cross-linking include enhanced foaming and foam stability, enhanced emulsion stability, enhanced thermal stability and improvements of gelation properties (2-5). In addition to food applications, various novel non-food applications of enzymatic protein cross-linking are also under investigation, for example in tissue engineering and for wool and leather (6). A lot of work has focused on the influence of microbial Transglutaminase (TGase) on the functionality and texture of dairy system (7-10). For milk proteins, TGase is very efficient at cross-linking the caseins, but less so for the commercially important whey proteins β -lactoglobulin and α -lactalbumin due to their rigid globular structure (11). Typically, reducing reagents such as DTT are used in order to increase substrate accessibility during TGase-mediated cross-linking for these proteins. For example, Eissa et al. report that the viscosity of denatured WPI solutions was decreased by several orders of magnitude after a TGase-treatment. This was attributed to a decrease of hydrophobic interactions after enzymatic cross-linking (12). It has also been reported that the thermal stability of β -lactoglobulin in heat-shocked WPI is enhanced by a TGase-treatment, with an increase in denaturation temperature of 6-7 °C (13). For food applications it would be better if reducing agents could be avoided, and some progress in this direction has been made for TGase-induced cross-linking of whey proteins (14).

An enzymatic cross-linking route that is complementary to cross-linking using TGase is oxidative cross-linking catalyzed by enzymes such as laccase, tyrosinase and various peroxidases (15). Whereas TGase introduces cross-links between γ -carboxyamide group and primary amines typically located on the outside and therefore typically reasonably accessible, the oxidative enzymes such as tyrosinase, laccase and peroxidase catalyze the formation of cross-links involving phenols. The phenols may be either located on tyrosine residues of proteins, or on side groups of polysaccharides such as arabinoxylan, containing reactive ferulic acid residue (16). Research in this area has largely

focused on determinants of chemical reactivity and accessibility of reactive groups (17-19). But, in the meantime, promising effects on food functionality have also been reported for oxidative enzymatic cross-linking (20-22). A major issue that so far has not been addressed in any detail is architecture of clusters of cross-linked globular food proteins, and the relation between this architecture and changes in food functionality induced by enzymatic cross-linking.

Indeed, an understanding of the functional effects of enzymatic protein cross-linking first of all requires a thorough characterization of structural evolution induced by enzymatic cross-linking of proteins. Very little work has been performed however, on the structural characterization of enzymatically cross-linked proteins, even for the commercially important case of microbial transglutaminase. An exception is the work of Matsumura et al. (23), who performed a detailed analysis of α -lactalbumin “protein-polymers” prepared by cross-linking α -lactalbumin using mammalian guinea pig liver (gTGase) and Microbial Streptovorticillium mobaraense MTGase in the presence of DTT. By using SEC with a multi-angle laser light scattering (SEC-MALLS) detector system, it was found that α -lactalbumin polymers were formed with solution molecular weights between 3.0×10^6 and 7.0×10^6 . The relation between solution size (radius of gyration R_g) and solution molecular weight was found to be $R_g \sim M^a$ with an exponent $a \approx 0.33$ and 0.44 respectively for protein-polymers produced by mTGase and gTGase, indicating a compact architecture. A few other studies have also reported on the effect of enzymatic cross-linking on protein structures (24-26).

Previously, we have been interested in the chemistry of enzymatic cross-linking reactions that involve phenol groups, such as oxidative protein cross-linking catalyzed by peroxidases, tyrosinase or laccase. Specifically, we have considered the case of the cross-linking of the globular whey protein α -lactalbumin via dityrosine bonds, catalyzed by Horseradish Peroxidase (HRP) (16, 27), in the presence of peroxide. For each catalytic cycle that ends with the formation of two phenol radicals (that may combine to form a phenol-phenol crosslink), HRP requires one molecule of H_2O_2 . Other oxidative cross-linking enzymes (tyrosinase, laccase) require dissolved oxygen rather than peroxide and an advantage of using peroxidase for studies of oxidative cross-linking is that the

concentration of peroxide is more easily controlled than the concentration of dissolved oxygen. However, HRP is rather sensitive to excess peroxide, which leads to various side reactions and eventually to inactivation of the enzyme (28). Therefore the supply of peroxide during the reaction must be tuned carefully (29). We also here use step-wise addition of peroxide, which enables us to control the reaction kinetics and particle size development during the reaction.

High conversion and high molecular weight products are found when performing the reactions at pH 7, in 0.1 M ammonium acetate (NH_4Ac) at 37 °C, using a simple scheme of multiple additions of small amounts of H_2O_2 (27). Also, the calcium depleted, and partly unfolded, apo-form of α -lactalbumin was found to be much more sensitive towards HRP-catalyzed cross-linking than the calcium containing holo form (16). Not all four tyrosines are equally reactive. Previous experimental data suggests that the first cross-link that is being formed is between Tyr18 and Tyr50 (30).

Whereas previous work (30) has mainly dealt with accessibility and reactivity in the early stages of the reaction, the aim of the present work is to perform a detailed nano-structural characterization of the formation of protein polymers if these reactions are ran to completion. Rather than varying reaction conditions (which has been done in previous work, (27), we here consider a single reaction condition that is known to lead to high conversion and high molecular weight products. For this condition, reactions run to completion in a number of hours, which allows for a detailed on-line probing of the reaction using dynamic and static light scattering, as well as UV-spectroscopy. Off-line analyses that are performed on both aliquots taken during the reaction and on the final reaction products include assays for enzyme activity, size-exclusion chromatography, and Atomic Force Microscope (AFM) imaging.

Materials and methods

Materials

Ca⁺²-depleted- α -lactalbumin (L6010) was supplied by Sigma-Aldrich and was used without any purification. The calcium content reported is less than 0.3 mol Ca²⁺ per mol of α -lactalbumin. Horseradish peroxidase (HRP) type VI-A (P6782), ABTS (2,2'-azino-bis(3-ethylbenzthiazoline-6-sulfonic acid) was also supplied by Sigma-Aldrich. All other chemicals used were of analytical grade.

Sample preparation

Stock solutions of α -lactalbumin were prepared by dissolving 12 g/L in 0.1 M NH₄Ac at 25 °C. After centrifugation (3h, 45000g, 25°C), the pH of the supernatant was adjusted to pH 6.8 using 0.1 mM HCl, and was filtered using a 0.1 μ m syringe filter. Finally, the protein concentration was determined spectrophotometrically assuming an absorbance $A_{280} = 20.1$ for a 1% (w/v) solution of α -lactalbumin (31). HRP stock solutions were prepared by dissolving 15 g/L in 0.1 M NH₄Ac. Concentration of HRP solutions were checked using UV spectrophotometry assuming a molar extinction coefficient of $\epsilon_{403} = 102.1 \text{ mM}^{-1}\text{cm}^{-1}$ (32). For preparing Hydrogen peroxide (H₂O₂) stock solutions, an aqueous solution of 30% (w/w) of peroxide was diluted with deionized water to a concentration of 0.05 M. Before use, concentrations of H₂O₂ stock solutions were checked spectrophotometrically assuming a molar extinction coefficient of $\epsilon_{240} = 43.6 \text{ M}^{-1}\text{cm}^{-1}$ (33).

Light scattering combined with titration and UV spectroscopy

For on-line probing of the enzymatic cross-linking reaction, a cell was developed that allows for simultaneous titration of H₂O₂, UV spectroscopy and light scattering at an angle of 90°. The measurement cell is illustrated in Fig 1. A fiber optic UV-probe, titration tube and stirrer are placed in a cylindrical quartz cell with a diameter of 2.5 cm. Periodic injections of hydrogen peroxide into the reaction solution are done using a computer controlled Schott Geräte TA01 titration system. Reactants are automatically mixed using a small glass stirrer.

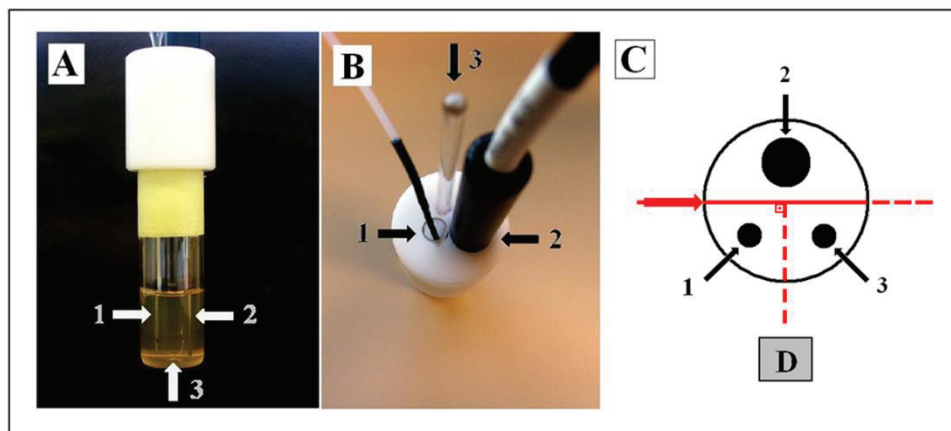


Figure.1. Cell used for Light scattering combined with titration and UV-spectrophotometry. A) Side view, the cell is filled with the reaction solution, which is slightly colored due to the heme group of the enzyme and oxidation of tyrosine B) Top view, 1= titration tube, 2= UV-Dip Probe, 3= Stirrer. C) Top view, schematically, red lines are the laser and the light scattered at 90°, detected by the detector D.

For light scattering experiments, this cell was used in an ALV goniometric light scattering instrument equipped with an ALV-5000/60X0 external digital correlator and a 300 mW solid state laser (Cobolt Samba-300 DPSS laser) operating at a wavelength of 532 nm. The angle of detection was 90°. A refractive index matching bath of filtered cis-decalin surrounded the cylindrical scattering cell, and the temperature was controlled at 37 ± 0.1 °C. Light scattering data was acquired in runs of 1min. No data was acquired during stirring or titration. UV absorbance was measured using a fiber-optic probe (Avantes FDP-UV-micro-1 1/16" Micro Dip Probe, UV/VIS) connected to a UV/Vis spectrometer (AvaSpec-128 Fiber optic Spectrometer). In order to accurately measure potentially large absorbance and to minimize potential effects of light scattering, UV probes were used with a short optical path length of 1 mm. UV spectra (between 250 nm and 500 nm) were acquired continuously with an integration time of 1 min. The average size reported is obtained by applying a second-order cumulant analysis to the correlation data. This is appropriate for samples with some size polydispersity around a single average size. Also, particle sizes that were found were always well below 100 nm, well within the range of

validity of the DLS technique. Dityrosine formation during the reaction was monitored via the increase in the absorbance at 318 nm. In order to examine the catalytic state of the enzyme, changes in the Soret absorption region between 350 nm and 450 nm were monitored on-line (16). Here the absorbance at 403 nm and 417 nm are related to the resting state of HRP and the state in which HRP has reacted with H_2O_2 , respectively. The catalytic state of HRP here was monitored through the change in the absorbance at 417 nm due to a peak that occurs at maximum after each titration step as a function of time.

Determination of peroxidase activity

In order to spectroscopically determine enzyme activity (34-37), ABTS stock solutions were prepared by dissolving 10 mg of ABTS in 2 mL 0.1 M NH_4Ac (pH 6.8). Peroxidase activity was determined for aliquots taken from the reaction mixture at various stages of the cross-linking reaction. Each aliquot was diluted 1000X with 0.1M NH_4Ac (pH 6.8). Next, 16 μL of the diluted aliquots was added to 1 mL of 5 mg/mL ABTS and incubated for 10 min. Finally, 33 μL of 0.3% (w/w) H_2O_2 was added, and the oxidation of ABTS was followed by measuring the absorbance at 405 nm as a function of time, for 10 min. The initial slope of ΔA_{405} versus time was used as a relative measure for the enzyme activity (27) during the cross-linking reaction (% of activity as compared to activity at the start of the reaction). For our experiments, we have found that the variation of enzyme activity from batch to batch was less than about 12 %, which is less than the range specified by the supplier (950 units/mg - 2000 units/mg).

Determination of monomers, oligomer and polymer fractions

For determining what fraction of the α -lactalbumin monomers was incorporated into protein oligomers and protein polymers, size exclusion chromatography was performed on 100 μL aliquots taken from the reaction mixture at various reaction times. The aliquots were injected on a Bio-Silect® SEC 400-5 300 mm x 7.8 mm column, connected to a Biologic DuoFlow Chromatography system. Elution was done using 0.1 M NH_4Ac (pH 6.8), detection at 280 nm. Prior to injection, the column was equilibrated with the elution buffer. For determining (weight) fractions of monomers, oligomer and protein polymers,

chromatograms were divided into three regions. The non-(intermolecularly) cross-linked α -lactalbumin monomers eluted from 11 mL to 12.2 mL. The exclusion limit of the Bio-Silect® SEC 400-5 column was reported to be around 106 g/mol for globular proteins, and for the purpose of the present determination, any cross-linked protein products eluting in the void (that is, at elution volumes smaller than 7.5 mL) were classified as “protein polymer” whereas cross-linked protein products at intermediate elution volumes (from 7.5 mL to 12.2 mL) were classified as “protein oligomers”. For all aliquots, the estimated error in the total area under chromatograms was about 5 %. The fraction of each species was taken to be the ratio of the area in the chromatogram for that particular species, divided by the total area for the three species combined. The whole experiment has been carried out in duplicate, with very similar results. The duplicate experiment was performed by using a Superose 6 10/300 GL column (GE Healthcare, Uppsala, Sweden) connected to an Akta Purifier system at room temperature. Samples were eluted with 0.1 M NH_4Ac buffer pH 6.8 at a flow rate of 0.5 mL/min, detection was done at 280 nm.

Determination of size-mass scaling exponent

For determining the relation between the size and molar mass of the species present in the final cross-linked reaction product, the latter was separated into chromatographic fractions on a Sephacryl S-500HR (GE Healthcare) column (exclusion limit is between 4×10^4 and 2×10^7 Da for Dextran standards), connected to an AKTA purifier system (GE Healthcare). A volume of 100 μL of final reaction product was injected onto the column, and eluted with 0.1M NH_4Ac (pH 6.8), at room temperature, at a flow rate of 0.8 mL/min. Prior to injection, the column was equilibrated with elution buffer. Detection was done using at 280 nm and 318 nm. Fractions of 0.5 mL were collected for elution volumes from 8 mL to 18 mL. For the light scattering analysis, the fractions were concentrated about 10 times using Amicon Ultra centrifugal filters (Cat No. UFC8000396). The protein concentration of the concentrated fractions was determined spectroscopically at 280 nm (see sample preparation). Static and dynamic light scattering experiments were done on each of the concentrated fractions using a Malvern Nanosizer ZS (Malvern) equipped with an Argon ion laser emitting vertically polarized light with a wavelength of 633 nm.

The scattering angle was 12.8°. Hydrodynamic radii RH reported are the major peak from the peak analysis as performed by the Malvern DTS software, version 6.20. Weight-averaged molar masses Mw were determined from the static light scattering intensities using the Rayleigh expression:

$$\frac{K_R C}{R_\theta} = \frac{1}{M_w} \quad (1)$$

where C is the weight concentration. The weight concentration C of cross-linked protein was determined using spectrophotometry, using the same molar extinction coefficient for protein polymers as that of the α -lactalbumin monomer. This is reasonable since cross-linking hardly affects the absorption at 280 nm (we have found changes of max. 5%). The constant K_R is the Rayleigh constant and R_θ is the Rayleigh ratio at the scattering angle of 12.8°. The constant K_R is given by:

$$K_R = \frac{4\pi^2 n_{solvent}^2 (dn/dC)^2}{\lambda^4 N_A} \quad (2)$$

We find $K_R = 2.46 \times 10^{-5} \text{ m}^2 \text{ mol/kg}^2$ using a refractive index increment $dn/dC = 0.188 \text{ mL/g}$ for α -lactalbumin (38). The Rayleigh ratio R_θ was calculated from

$$R_\theta = \frac{I_{sample} - I_{solvent}}{I_{toluene}} \frac{n_{solvent}^2}{n_{toluene}^2} R_{toluene} \quad (3)$$

using $R_{toluene} = 1.4 \times 10^{-5} \text{ cm}^{-1}$ (39) where I_{sample} , $I_{solvent}$, and $I_{toluene}$ are the scattered intensities of the sample, the solvent and the toluene standard, respectively.

Atomic force microscopy (AFM)

For Atomic Force Microscopy, the final reaction product was dialyzed against 0.1 M NH_4Ac at pH 6.8 at 4 °C with 300 kDa cellulose ester membrane (Spectra/Pro Biotech) to remove monomers from the reaction solution. The absence of monomers and small clusters by

was confirmed by SEC. The adsorption of the protein polymers to AFM substrates was tested at various pH values. Due to the high repulsive interaction, in general the polymers did not adhere to mica surfaces very strongly. pH values below pH 5 were avoided in view of possible protein aggregation. It was found that adsorption of the protein polymers without visible aggregation on unmodified mica required a pH of 5.5. To confirm that pH 5.5 instead of pH 6.8 does not affect the structure of the protein polymers as observed with AFM, we have also visualized protein polymers adsorbed on polylysine-modified mica surfaces at pH 6.8, with very similar results (see supporting information). For imaging, the dialyzed reaction product was diluted to 10 $\mu\text{g}/\text{mL}$ and the pH was adjusted to 5.5. Next, 20 μL of sample was incubated on a freshly cleaved mica surface for 1 minute, rinsed with deionized water and dried with nitrogen. AFM imaging was performed using a Digital Instruments NanoScope V Multimode Scanning Probe Microscopy with a noncontact ultrasharp silicon cantilever (NT-MDT CSCS11), in the Scan-assist imaging mode.

Reactions

For all reactions, the concentration of apo- α -lactalbumin was 10 mg/mL (or 0.7mM), that of horse-radish peroxidase 0.5 mg/mL. Reactions were carried out at 37 °C in 0.1M NH_4Ac pH 6.8. Small amounts of 50 mM peroxide were added periodically, every 11 minutes. Peroxide addition was done using computer controlled Schott Gerate TA01 titration systems, except when indicated otherwise. Every addition corresponded to a change in the peroxide concentration of $\Delta[\text{H}_2\text{O}_2] = 0.1 \text{ mM}$. Only reaction container, reaction volume, volume of 50 mM peroxide per addition, and mode of mixing were different for the different reactions R1-R4, as detailed below:

R1: Cylindrical quartz cell with a diameter of 2.5 cm, containing a UV probe, stirrer and titration tube, as illustrated in Fig.1 reaction volume 10 mL. After the 30 s injection of peroxide, the glass stirrer was operated for 30 s to ensure complete mixing.

R2: 1.5 mL Eppendorf tubes, reaction volume of 1 mL. Peroxide was added manually every 11 min. A thermomixer was used that provided continuous mixing as well as temperature control.

R3: Same as reaction R1, except using a 10 mL glass cell containing a titration tube and stirrer, but no UV probe, and using a smaller reaction volume of 5 mL.

R4: Water-jacketed reaction vessel, 50 mL reaction, continuous stirring using a magnetic stirrer bar.

Results and discussion

Growth of polymer size and number of dityrosine bonds during reaction

In this study, we will refer to the cross-linked protein structures as "protein polymers". On-line light scattering is often used to follow heat-induced protein aggregation (40-42), but has not yet been used to study enzymatic protein cross-linking. Here, we use simultaneous on-line light scattering and UV-spectroscopy to follow the growth of the protein polymers. The absorbance at 318 nm is a measure for the number of dityrosine bonds (43), the light scattering intensity is a measure for the weight average molar mass, and an analysis of autocorrelation functions from the dynamic light scattering, gives the average hydrodynamic radius of the reaction mixture. Results (reaction R1) for the absorbance at 318 nm, the average hydrodynamic radius and the light scattering intensity as a function of the number of additions of H_2O_2 are shown in Fig. 2.

The dityrosine signal starts increasing immediately after the first additions of peroxide, and increases to quite large values at the end of the reaction. Note that in order to reliably determine the quite large values of the UV absorbance in the presence of significant light scattering due to the large protein polymers, it was crucial to use UV-probes with short optical path lengths (1 mm). As compared to the dityrosine signal, the light scattering intensity and in particular the average hydrodynamic radius are lagging behind. The initial average hydrodynamic radius is somewhat larger than expected for an α -lactalbumin monomer, because of a small fraction of protein aggregates in the starting solution. This becomes evident from CONTIN fits of the dynamic light scattering data that gives scattering intensity weighted size distributions. The development of the size distribution of the protein polymers during the reaction is shown in Fig.3.

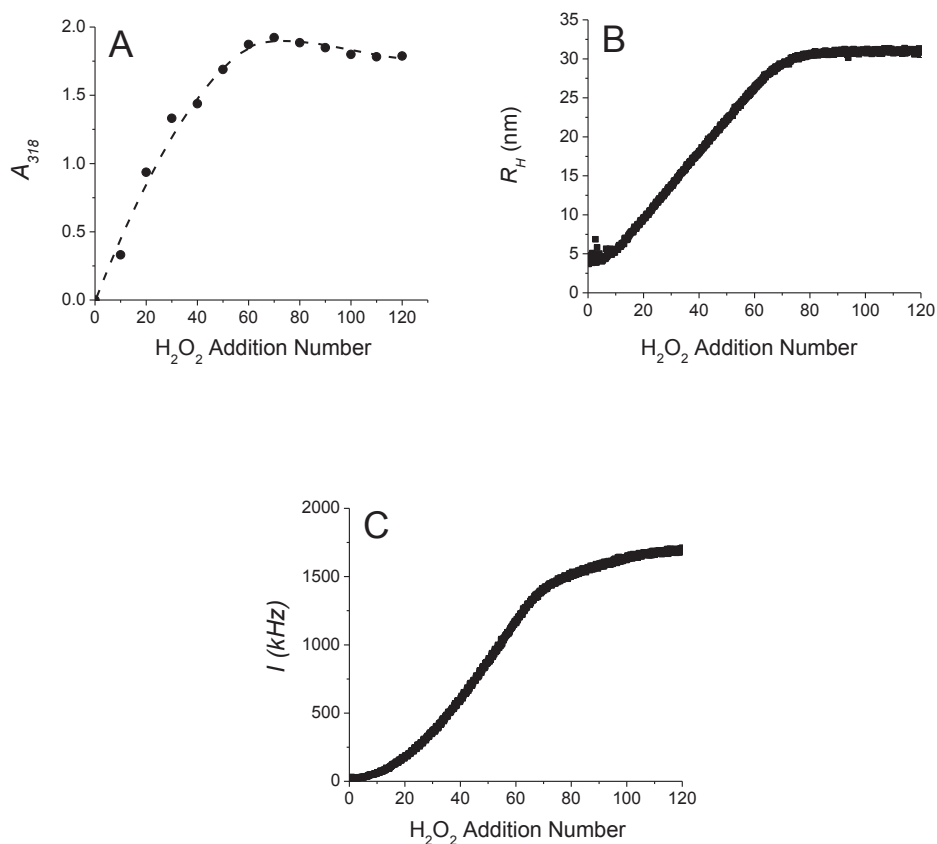


Figure.2. On-line characterization of the cross-linking of apo α -lactalbumin catalyzed by horseradish peroxidase under the periodic addition of peroxide, $\Delta[H_2O_2]=0.1$ mM, every 11 min (Reaction R1). Buffer is 0.1 M NH_4Ac , protein concentration is 10 g/L and the enzyme/protein ratio is 1:20 (w/w) **(A)** Absorbance at 318 nm, **(B)** Average hydrodynamic radius as determined using dynamic light scattering, **(C)** light scattering intensity. All quantities are plotted versus the peroxide addition number.

The curve at the beginning of the reaction clearly shows a monomer peak at a hydrodynamic radius of 2.65 nm, plus a smaller peak at about 50 nm, presumably corresponding to a small amount of aggregated/denatured protein material in the starting solution. After 9 additions, there is a single broad peak at a hydrodynamic radius of about 5 nm, corresponding to α -lactalbumin oligomers. At a later stage in the reaction, a dominant peak due to large protein polymers are observed (hydrodynamic radii of 18 nm and 32 nm after, respectively, 36 and 93 additions of H_2O_2) and a smaller peak due to

protein oligomers (hydrodynamic radii of about 5 nm and 10 nm after, respectively, 36 and 93 additions of H_2O_2). Since the peaks are scattering-intensity weighted, and small particles scatter much less than large ones, the size-distribution data implies that even in the later stages of the reaction there is still a significant fraction of protein oligomers. The fact that the DLS distribution is dominated by a single well-defined peak implies that the use of an average hydrodynamic radius as a simple on-line measure for the particle size is justified. But, given the extreme bias of DLS towards large particles, this should not be taken to mean that the reaction mixture is monodisperse during any stage of the reaction.

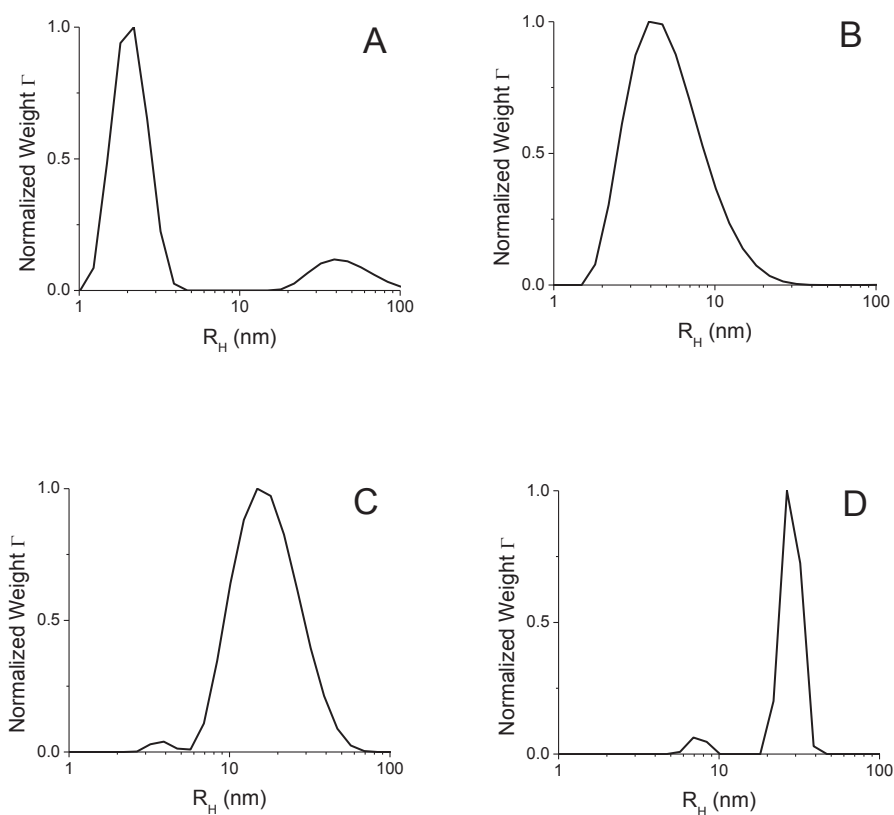


Figure.3. Development of the protein polymers size distribution (relative contribution to the light scattering as a function of hydrodynamic radius) as determined using CONTIN fits of the dynamic light scattering (DLS) autocorrelation functions. Curves are shifted and scaled in the Y-direction for clarity. The curves are obtained after 0 (A), 9 (B), 36 (C) and 93 (D) additions of H_2O_2 .

Activity of enzyme during the reaction

The catalytic state of the horseradish peroxidase enzyme can be monitored at 417 nm (44, 45). Immediately after a peroxide addition, absorbance at 417 nm increases, signifying that the enzyme has reacted with H_2O_2 . Meanwhile, absorbance at 403 nm decreases whereas the absorbance at 425 nm increases as is expected for the so-called Soret shift (16) (data not shown). As more and more of the peroxide is used up, the absorbance at 417 nm relaxes again. Fig.4 shows the time course of the absorbance at 417 nm immediately after the addition of peroxide, for a range of addition numbers (reaction R1). The peroxide added is used by the enzyme in 3, 4 and 6 minutes after addition number 9, 28 and 36, respectively.

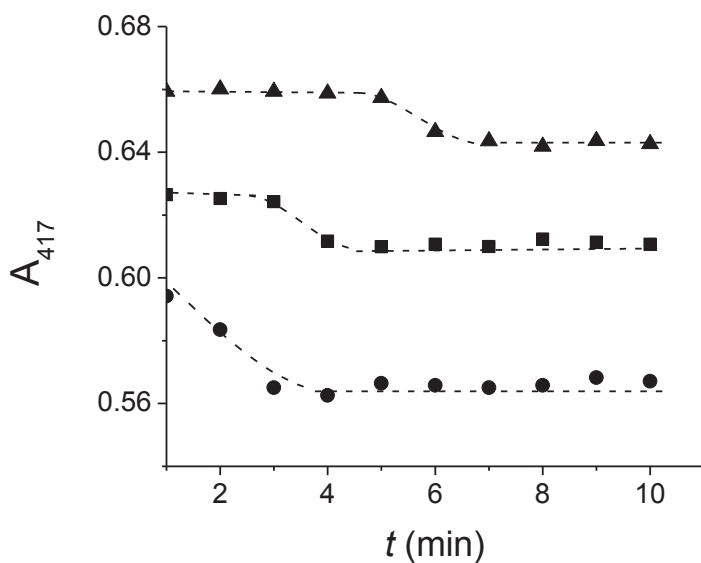


Figure.4. Catalytic state of the HRP during the reaction: absorbance A_{417} at 417 nm versus the time after addition of peroxide. Addition numbers: 9 (spheres), 28 (squares), 37 (triangles). From duplicate experiments, the reproducibility of the time at which the A_{417} has decreased to half its initial value is about 10 %.

Hence, as the reaction progresses, the enzyme stays in the peroxide-active state longer and longer, as was also found in previous work (16). The difference between the absorbance at the beginning and the end of the addition cycles decreases steadily and eventually completely disappears. At very high addition numbers, the enzyme no longer responds to H_2O_2 and apparently has become completely inactive. Gradual inactivation during the reaction has also been shown directly using an ABTS assay: after 18 additions (equivalent to 3 hours of reaction time) the activity of the enzyme has decreased by 20 %. Finally, adding fresh enzyme at the end of the reaction, after 120 additions, while continuing the additions of peroxide, leads to resumed polymer growth (data not shown). Clearly, the reaction eventually stops due to enzyme inactivation rather than due to a lack of accessible tyrosine groups.

Conversion of monomers into oligomers and protein polymers

The light scattering is dominated by the scattering of the largest polymers in the reaction mixture, and hence cannot be used to reliably quantify the conversion of α -lactalbumin monomer into oligomers and protein polymers. Fractions of monomeric α -lactalbumin, protein oligomers and protein polymers were determined by performing size exclusion chromatography on aliquots taken at various times from the reaction mixture (reactions R2, R3). Representative chromatograms (at the start of the reaction, after addition 10 and after addition 87) are shown in Fig.5, together with the boundaries used to separate the various fractions (monomers, oligomers, protein polymers). There is obviously no sharp distinction between protein oligomers and polymers. The choice we make here is to define anything that can be separated by the column we have used (exclusion limit is between 2×10^4 and 1×10^6 kDa for protein standards) as “oligomers”, and anything that elutes in the void as “protein polymers”. Conversions determined from chromatographic areas for the fractions as a function of addition number are shown in Fig. 6. The reaction very clearly has two distinct phases. In the first phase, up to about the 15th addition, monomers are very rapidly converted into oligomers.

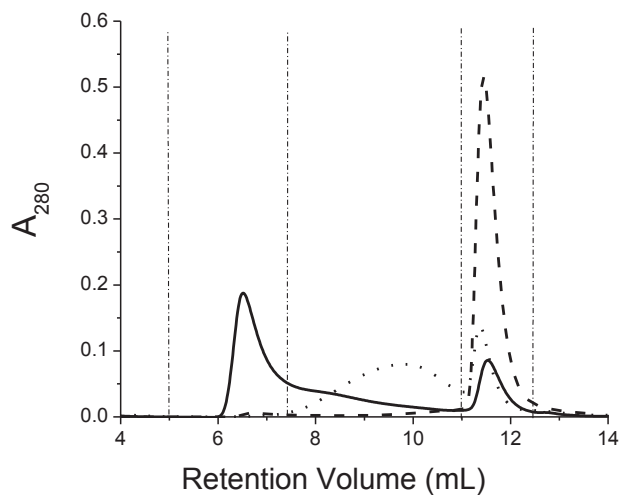


Figure.5. Polymer growth at various reaction time in SEC. Chromatograms in SEC are monomers (dash line), oligomers after a 10-addition of H_2O_2 (dot line) (reaction R2) and polymers after an 87-addition of H_2O_2 (solid line) (reaction R3)

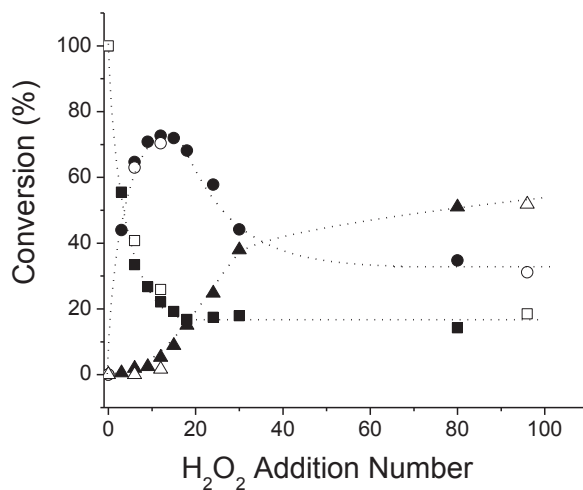


Figure.6. Conversion (%) of monomers to polymers during the cross-linking reaction. Data was obtained by calculating the peak areas under SEC chromatograms (for monomers (\blacksquare ; \square), oligomers (\bullet ; \circ) and polymers (\blacktriangle ; Δ)) in Fig.5. Open and closed symbols are from two different experiments.

The first phase of fast oligomer formation is followed by a second phase of slow cross linking of oligomers into high molecular weight protein polymers. In the second phase, very little additional monomeric α -lactalbumin is converted into either oligomers or protein polymers. Note that since an appreciable part of the cross-linked protein elutes in the void of the column, the shape of the chromatogram does not represent the true distribution. As has been argued previously (46), the about 30 % of α -lactalbumin monomers that are not converted, most likely correspond to the fraction of holo α -lactalbumin still present in the starting material (see materials and methods).

Size-mass scaling exponent of protein polymers

In order to estimate the internal density of the protein polymers, and the dependence of this density of particle size, we have fractionated the final reaction product (reaction R3) using size exclusion chromatography (see chromatogram in Fig.7). It is interesting to note that the monomer fraction does not have an enhanced absorption at 318 nm, indicating that cross-linking is predominantly inter-molecular rather than intra-molecular. For the fractions indicated in Fig.7, we have determined the weight-averaged molar mass M_w and the average hydrodynamic radius R_H of fractions containing the protein polymers using static and dynamic light scattering.

Results are shown in Table 1. The protein polymers consist of 100-1000 α -lactalbumin monomers, and have hydrodynamic sizes ranging from 30-80 nm. As illustrated in Fig.8, the size-mass scaling is $R_H \propto M_w^\alpha$, with $\alpha \approx 0.4$. The internal protein concentration C_{int} of the protein polymers, based on the hydrodynamic size and weight averaged molar mass of the fractions is:

$$C_{int} = \frac{1}{N_{Av}} \frac{M_w}{\frac{4}{3} \pi R_H^3} \propto M_w^{(1-3\alpha)} = M_w^{-0.2} \quad (4)$$

For the fractions listed in Table 1, values for the internal protein concentration are rather low and range from $C_{int} = 11$ g/L for the largest, to $C_{int} = 16$ g/L for the smallest polymers. Since the swelling exponent α is rather close to $1/3$, values for C_{int} vary only slowly with the molar mass of the protein polymers. It should be remarked however, that sufficient separation was only achieved over a rather narrow range of solution sizes (less than a decade), such that the actual value of the swelling exponent that we find here should be considered as a rough estimate only. Instead, the main point of the analysis is that the protein polymers are very dilute, and must have a very open internal structure.

Table 1. Results of light scattering analysis (DLS/SLS) of chromatographic fractions (Fig.7). N is number of α -lactalbumin monomers per protein polymer.

Fraction	$M_w (10^6 \text{ Da})$	$R_H \text{ (nm)}$	N
A	15.4	81	1065
B	5.50	51.8	376
C	3.40	41.6	236
D	2.20	34.5	155
E	1.70	35.8	118
F	1.18	30.6	82

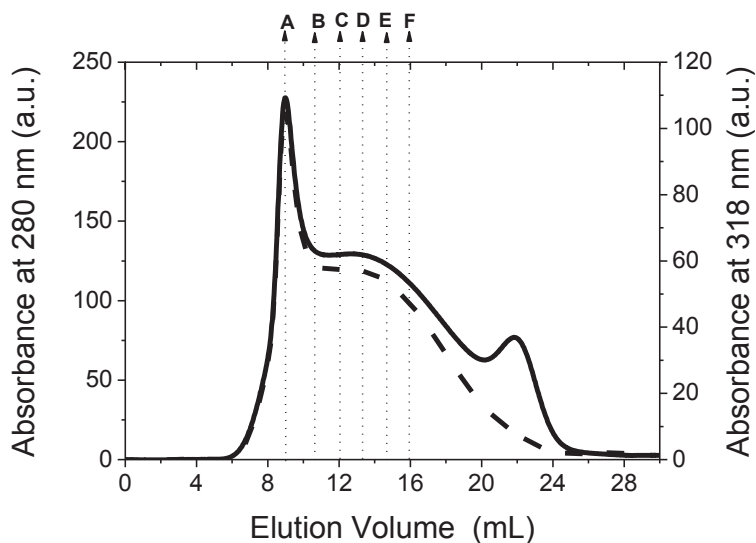


Figure.7. Chromatogram used for size-mass scaling, indicating fractions A-F. The solid line is the UV absorbance at 280 nm, which is proportional to the total protein concentration. The dotted line is the UV absorbance at 318 nm, which is proportional to the amount of dityrosines.

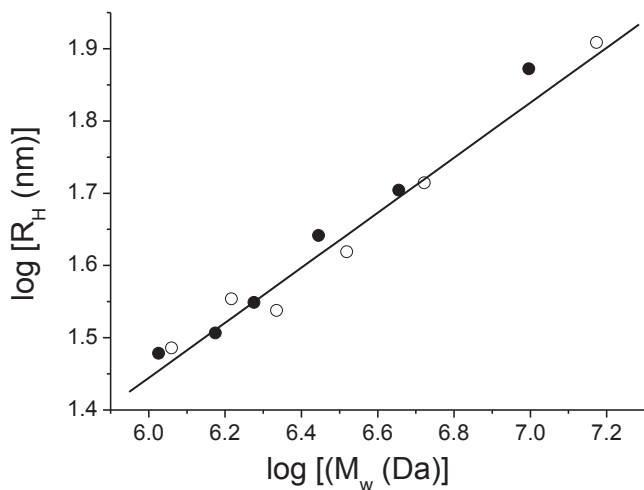


Figure.8. R_H (DLS) versus M_w (SLS) for fraction of table 1. Open and closed symbols are for two different experiments.

AFM imaging of protein polymers

Further insight into the architecture of the protein polymers is obtained by AFM imaging (in air) of protein polymers (reaction R4) adsorbed on mica from 0.1 M NH_4Ac at pH 5.5. In order to avoid any influence of the unreacted monomers and small oligomers on imaging the large protein polymers using AFM, the reaction product was first dialyzed using a 300 kDa cut-off membrane. AFM images show a very broad size distribution of the polymers (Fig.9).

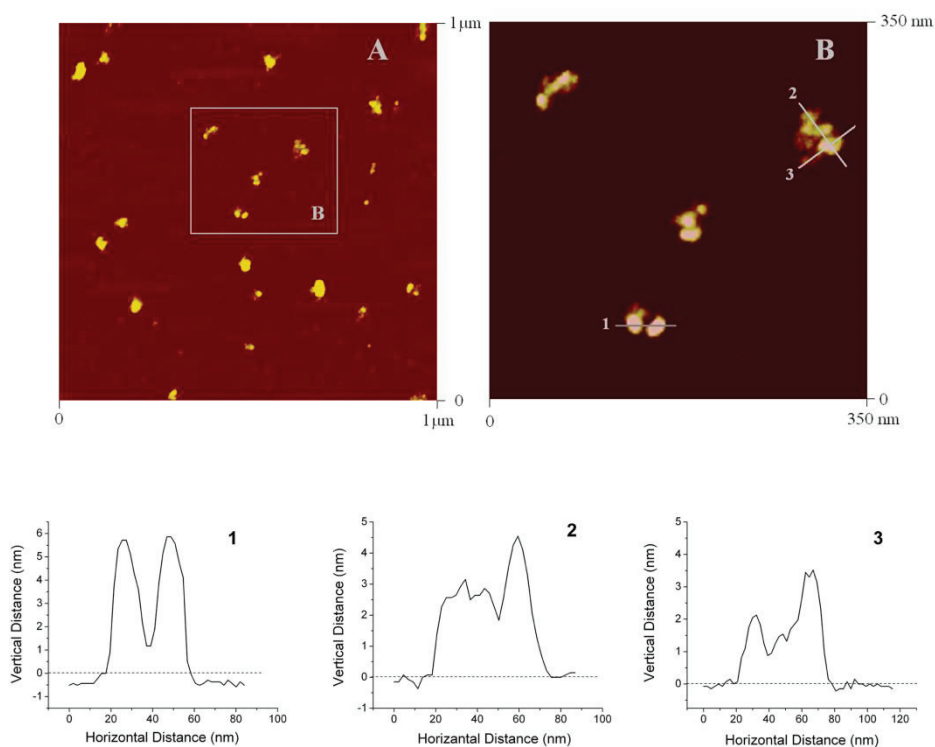


Figure.9. AFM images of the dried protein polymers on mica. (A) 2D height images of the polymers at 1 μm x 1 μm (B) 2D height high resolution images of the polymers at 350 nm x 350 nm. (From 1 to 3) Different cross-sections of the polymers on AFM image at 350 nm x 350 nm.

During drying the protein polymers apparently spread on the surface, forming layers a few proteins thick, with heights varying between 3 and 20 nm. This is to be expected, given the very low average protein content of the protein polymers (a few weight percent), which implies that these structures may not be expected to be able to withstand air-drying. Consistent with the notion of spreading induced by drying, the lateral sizes of dried polymers are larger than those inferred from the DLS measurements. Most importantly, the AFM images and height profiles very clearly show that the polymers are extremely heterogeneous, consisting of clusters of distinct “subunits” that are covalently coupled together rather loosely. We have checked that the proteins themselves do not aggregate when imaged on mica surfaces at pH 5.5 (supporting information). It has been shown previously that neither SDS nor DTT destroys the structural integrity of the polymers (27). Hence, the possibility that hydrophobic bonds or sulfur bridges are involved in joining the “subunits” is excluded. Finally, we have also imaged protein polymers adsorbed on polylysine-modified mica from 0.1 M NH_4Ac at pH 6.8 (these are the reaction condition). These AFM images (supporting information) are very similar to AFM images of protein polymers at pH 5.5 on non-modified mica.

Concluding remarks

Taken together, our data provide a rather clear picture of the process of the protein polymer formation during enzymatic cross-linking. In a fast first stage of the reaction, monomeric protein is converted into protein oligomers. In the second, much slower stage (during which the activity of the enzyme starts dropping as a consequence of peroxide-induced damage to the enzyme) oligomers are coupled together into protein polymers.

The data on the size-mass scaling indicates that the protein polymers that are formed in the present system are rather dilute, with internal protein concentrations of only a few percent. The low internal density of the protein polymers suggests that the average number of intermolecular cross-links per protein, which can be called the cross-link functionality f , never reaches its theoretical maximum of $f = 4$ (if all tyrosines form intermolecular dityrosine cross-links). In the latter case, a much denser network structure would have been expected, with much higher internal protein concentrations. A rather

low average cross-link functionality may be caused by large reactivity differences for the many possible tyrosine-tyrosine cross-links, with only a few types of cross-links being actually formed in appreciable numbers. This is consistent with our previous finding that, at least in the initial stages of the reaction, there is a very strong preference for Tyr 18 – Tyr 50 cross-links to be formed (30). Similar results have also been found for the cross-linking of apo- α -lactalbumin by microbial transglutaminase (47), where it was found that only 3 out of 12 lysines and 1 out of 7 glutamine residues were accessible for cross-linking. In such a scenario, the main determinant of the large-scale architecture of cross-linked protein is the distribution of cross-link functionalities f . For example, dilute gel-like structures formed from oligomers as we have observed, may be formed if the dominant cross-link functionalities are $f = 1$ and 2 (corresponding to a chain-like architecture) with occasional functionalities of $f = 3$ and 4.

In comparison with TGase-cross-linked α -lactalbumin with added DTT, HRP-cross-linked α -lactalbumin has very different properties. Matsumura reported that TGase induces the formation of dense compact particle rather than open polymer-like structures (23). Actually, this is to be expected in view of the use of DTT which leads to a large number of highly reactive and accessible groups on the protein surface. As a consequence, TGase-induced cross-linking of α -lactalbumin is also much faster than the HRP-induced reaction. In the former reaction, the formation of polymers occurs in 15 min. This already indicates the difference in the polymerization mechanism. A more relevant comparison to elucidate possible generalities in the development of nanostructure during enzymatic cross-linking of globular proteins, would be with the TGase-induced cross-linking of apo- α -lactalbumin without DTT.

While it is a challenge to control the architecture of polymers prepared via enzymatic cross-linking, our approach does give insight into architectural development during the reaction, and could be applied to different enzymes such as other oxidative enzymes and TGase, to reveal possible generalities.

Possible food- and other applications of enzymatically cross-linked protein will depend strongly on the internal density of the cross-linked proteins, and hence on the average cross-linking functionality f . For example, whereas dilute protein polymers may

have applications as protein-based thickeners much denser cross-linked protein polymers may have applications as protein-based Pickering stabilizers of foams and emulsions or as ingredient in protein-fortified drinks. Hence, the issue of the actual cross-linking functionality achieved during enzymatic cross-linking of globular proteins, and the resulting network structure of the cross-linked protein (open and dilute, or dense and compact) appears to be an interesting topic for future research.

Acknowledgement

This work is part of the Industrial Partnership Programme (IPP) Bio(-Related)Materials of the Stichting voor Fundamenteel Onderzoek der Materie (FOM), which is financially supported by the Nederlandse Organisatie voor Wetenschappelijk Onderzoek (NWO). The IPP BRM is co-financed by the Top Institute Food and Nutrition and the Dutch Polymer Institute.

References

1. Dickinson, E., Enzymic crosslinking as a tool for food colloid rheology control and interfacial stabilization. *Trends Food Sci Tech* **1997**, *8*, 334-339.
2. Eissa, A. S.; Bisram, S.; Khan, S. A., Polymerization and gelation of whey protein isolates at low pH using transglutaminase enzyme. *J Agr Food Chem* **2004**, *52*, 4456-4464.
3. Dickinson, E.; Ritzoulis, C.; Yamamoto, Y.; Logan, H., Ostwald ripening of protein-stabilized emulsions: effect of transglutaminase crosslinking. *Colloid Surface B* **1999**, *12*, 139-146.
4. Faergemand, M.; Otte, J.; Qvist, K. B., Enzymatic cross-linking of whey proteins by a Ca^{2+} -independent microbial transglutaminase from *Streptomyces lydicus*. *Food Hydrocolloids* **1997**, *11*, 19-25.
5. Truong, V. D.; Clare, D. A.; Catignani, G. L.; Swaisgood, H. E., Cross-linking and rheological changes of whey proteins treated with microbial transglutaminase. *J. Agric. Food Chem.* **2004**, *52*, 1170-1176.
6. Zhu, Y.; Tramper, J., Novel applications for microbial transglutaminase beyond food processing. *Trends in Biotechnology* **2008**, *26*, 559-565.
7. Jaros, D.; Heidig, C.; Rohm, H., Enzymatic modification through microbial transglutaminase enhances the viscosity of stirred yogurt. *J Texture Stud* **2007**, *38*, 179-198.
8. Ercili-Cura, D.; Lille, M.; Legland, D.; Gaucel, S.; Poutanen, K.; Partanen, R.; Lantto, R., Structural mechanisms leading to improved water retention in acid milk gels by use of transglutaminase. *Food Hydrocolloids* **2013**, *30*, 419-427.

9. Norziah, M. H.; Al-Hassan, A.; Khairulnizam, A. B.; Mordi, M. N.; Norita, M., Characterization of fish gelatin from surimi processing wastes: Thermal analysis and effect of transglutaminase on gel properties. *Food Hydrocolloids* **2009**, *23*, 1610-1616.
10. Wilcox, C. P.; Swaisgood, H. E., Modification of the rheological properties of whey protein isolate through the use of an immobilized microbial transglutaminase. *J Agr Food Chem* **2002**, *50*, 5546-5551.
11. Traore, F.; Meunier, J. C., Cross-Linking activity of placental F-XIIIa on whey proteins and caseins. *J Agr Food Chem* **1992**, *40*, 399-402.
12. Eissa, A. S.; Khan, S. A., Modulation of hydrophobic interactions in denatured whey proteins by transglutaminase enzyme. *Food Hydrocolloids* **2006**, *20*, 543-547.
13. Damodaran, S.; Agyare, K. K., Effect of microbial transglutaminase treatment on thermal stability and pH-solubility of heat-shocked whey protein isolate. *Food Hydrocolloids* **2013**, *30*, 12-18.
14. Chuan-He Tang, C.-Y. M., Modulation of the thermal stability of β -lactoglobulin by transglutaminase treatment. *European Food Research and Technology* **2007**, *225*, 649-652.
15. Buchert, J.; Cura, D. E.; Ma, H.; Gasparetti, C.; Monogioudi, E.; Faccio, G.; Mattinen, M.; Boer, H.; Partanen, R.; Selinheimo, E.; Lantto, R.; Kruus, K., Crosslinking Food Proteins for Improved Functionality. *Annu Rev Food Sci T* **2010**, *1*, 113-138.
16. Oudgenoeg, G. Peroxidase catalyzed conjugation of peptides, proteins and polysaccharides via endogenous and exogenous phenols. Wageningen University, Wageningen, 2004.
17. Mattinen, M. L.; Lantto, R.; Selinheimo, E.; Kruus, K.; Buchert, J., Oxidation of peptides and proteins by *Trichoderma reesei* and *Agaricus bisporus* tyrosinases. *J Biotechnol* **2008**, *133*, 395-402.
18. Hakulinen, N.; Kiiskinen, L. L.; Kruus, K.; Saloheimo, M.; Paananen, A.; Koivula, A.; Rouvinen, J., Crystal structure of a laccase from *Melanocarpus albomyces* with an intact trinuclear copper site. *Nat Struct Biol* **2002**, *9*, 601-605.
19. Thalmann, C. R.; Lotzbeyer, T., Enzymatic cross-linking of proteins with tyrosinase. *Eur Food Res Technol* **2002**, *214*, 276-281.
20. Selinheimo, E.; Kruus, K.; Buchert, J.; Hopia, A.; Autio, K., Effects of laccase, xylanase and their combination on the rheological properties of wheat doughs. *J Cereal Sci* **2006**, *43*, 152-159.
21. Faergemand, M.; Otte, J.; Qvist, K. B., Cross-linking of whey proteins by enzymatic oxidation. *J Agr Food Chem* **1998**, *46*, 1326-1333.
22. Selinheimo, E.; Lampila, P.; Mattinen, M. L.; Buchert, J., Formation of protein-oligosaccharide conjugates by laccase and tyrosinase. *J Agric Food Chem* **2008**, *56*, 3118-28.
23. Matsumura, Y.; Lee, D. S.; Mori, T., Molecular weight distributions of alpha-lactalbumin polymers formed by mammalian and microbial transglutaminases. *Food Hydrocolloids* **2000**, *14*, 49-59.
24. Mattinen, M. L.; Hellman, M.; Permi, P.; Autio, K.; Kalkkinen, N.; Buchert, J., Effect of protein structure on laccase-catalyzed protein oligomerization. *J Agr Food Chem* **2006**, *54*, 8883-8890.
25. Eissa, A. S.; Puhl, C.; Kadla, J. F.; Khan, S. A., Enzymatic cross-linking of beta-lactoglobulin: Conformational properties using FTIR spectroscopy. *Biomacromolecules* **2006**, *7*, 1707-1713.

26. Hu, X.; Zhao, M. M.; Sun, W. Z.; Zhao, G. L.; Ren, J. Y., Effects of Microfluidization Treatment and Transglutaminase Cross-Linking on Physicochemical, Functional, and Conformational Properties of Peanut Protein Isolate. *J Agr Food Chem* **2011**, *59*, 8886-8894.
27. Heijnis, W. H.; Wierenga, P. A.; Berkel, W. J. H.; Gruppen, H., Directing the Oligomer Size Distribution of Peroxidase-Mediated Cross-Linked Bovine alpha-Lactalbumin. *J Agr Food Chem* **2010**, *58*, 5692-5697.
28. Hernandez-Ruiz, J.; Arnao, M. B.; Hiner, A. N. P.; Garcia-Canovas, F.; Acosta, M., Catalase-like activity of horseradish peroxidase: relationship to enzyme inactivation by H₂O₂. *Biochem J* **2001**, *354*, 107-114.
29. van de Velde, F.; van Rantwijk, F.; Sheldon, R. A., Improving the catalytic performance of peroxidases in organic synthesis. *Trends in Biotechnology* **2001**, *19*, 73-80.
30. Heijnis, W. H.; Dekker, H. L.; de Koning, L. J.; Wierenga, P. A.; Westphal, A. H.; de Koster, C. G.; Gruppen, H.; van Berkel, W. J. H., Identification of the Peroxidase-Generated Intermolecular Dityrosine Cross-Link in Bovine alpha-Lactalbumin. *J Agr Food Chem* **2011**, *59*, 444-449.
31. Kronman, M. J.; Andreotti, R. E., Inter- and Intramolecular Interactions of Alpha-Lactalbumin .I. Apparent Heterogeneity at Acid pH. *Biochemistry-Us* **1964**, *3*, 1145-&.
32. Ohlsson, P. I.; Paul, K. G., Molar absorptivity of horseradish-peroxidase. *Acta Chemica Scandinavica Series B-Organic Chemistry and Biochemistry* **1976**, *30*, 373-375.
33. Noble, R. W.; Gibson, Q. H., Reaction of ferrous horseradish peroxidase with hydrogen peroxide. *J. Biol. Chem.* **1970**, *245*, 2409-&.
34. Pütter, J., and Becker, R. , *Methods of Enzymatic Analysis* 3rd ed.; Verlag Chemie: Deerfield Beach, FL 1983; Vol. III.
35. Dept, B. M. G. B., *Biochemica information*. Boehringer Mannheim GmbH: 1973.
36. Keesey, J., *Biochemica Information* 1st ed.; Boehringer Mannheim Biochemicals: Indianapolis, IN, 1987.
37. Dept, B. M. G. B., *Biochemica information*. Boehringer Mannheim GmbH.
38. McGuffey, M. K. Thermal Stability of α-Lactalbumin. North Carolina State University, Raleigh, 2004.
39. Gimel, J. C.; Durand, D.; Nicolai, T., Structure and Distribution of Aggregates Formed after Heat-Induced Denaturation of Globular-Proteins. *Macromolecules* **1994**, *27*, 583-589.
40. Jung, J. M.; Savin, G.; Pouzot, M.; Schmitt, C.; Mezzenga, R., Structure of heat-induced beta-lactoglobulin aggregates and their complexes with sodium-dodecyl sulfate. *Biomacromolecules* **2008**, *9*, 2477-2486.
41. Arnaudov, L. N.; de Vries, R., Strong impact of ionic strength on the kinetics of fibrillar aggregation of bovine beta-lactoglobulin. *Biomacromolecules* **2006**, *7*, 3490-3498.
42. Arnaudov, L. N.; de Vries, R., Thermally induced fibrillar aggregation of hen egg white lysozyme. *Biophys J* **2005**, *88*, 515-526.
43. Michon, T.; Wang, W.; Ferrasson, E.; Gueguen, J., Wheat prolamine crosslinking through dityrosine formation catalyzed by peroxidases: improvement in the modification of a poorly accessible substrate by "indirect" catalysis. *Biotechnology and bioengineering* **1999**, *63*, 449-58.
44. Bhattacharyya, D. K.; Adak, S.; Bandyopadhyay, U.; Banerjee, R. K., Mechanism of Inhibition of Horseradish Peroxidase-Catalyzed Iodide Oxidation by Edta. *Biochem J* **1994**, *298*, 281-288.

- 45.** Andersen, M. B.; Hsuanyu, Y.; Welinder, K. G.; Schneider, P.; Dunford, H. B., Spectral and Kinetic-Properties of Oxidized Intermediates of Coprinus-Cinereus Peroxidase. *Acta Chem Scand* **1991**, *45*, 1080-1086.
- 46.** Heijnis, W. H. Peroxidase-mediated cross-linking of bovine α -lactalbumin. Wageningen University, Wageningen, 2010.
- 47.** Matsumura, Y.; Chanyongvorakul, Y.; Kumazawa, Y.; Ohtsuka, T.; Mori, T., Enhanced susceptibility to transglutaminase reaction of alpha-lactalbumin in the molten globule state. *Bba-Protein Struct M* **1996**, *1292*, 69-76.

Supplementary Data

Atomic Force Microscopy

Materials & Methods

For Atomic Force Microscopy, the final reaction product was dialyzed against 0.1 M NH_4Ac at pH 6.8 at 4 °C with 300 kDa cellulose ester membranes (Spectra/Pro Biotech) to remove monomers and small oligomers from the reaction solution. The absence of monomers and small oligomers was confirmed using SEC. The dialyzed reaction product was diluted to 10 $\mu\text{g}/\text{mL}$ in NH_4Ac at pH 6.8. Polylysine solution (40 μL) was dropped onto freshly cleaved mica surfaces, and incubated for 1 min. Next, it was rinsed with deionized water and immediately dried with nitrogen. For imaging, 20 μL of sample was incubated on a polylysine-modified mica surface for 1 minute, rinsed with deionized water and dried with nitrogen. AFM imaging was performed using a Digital Instruments NanoScope V Multimode Scanning Probe Microscopy with a noncontact ultrasharp silicon cantilever (NT-MDT CSCS11), in the Scan-assist imaging mode. Note that proteins were incubated on mica surface at pH 5.5 according to the procedure in Materials & Methods (in paper).

Results

Bare Mica Surface

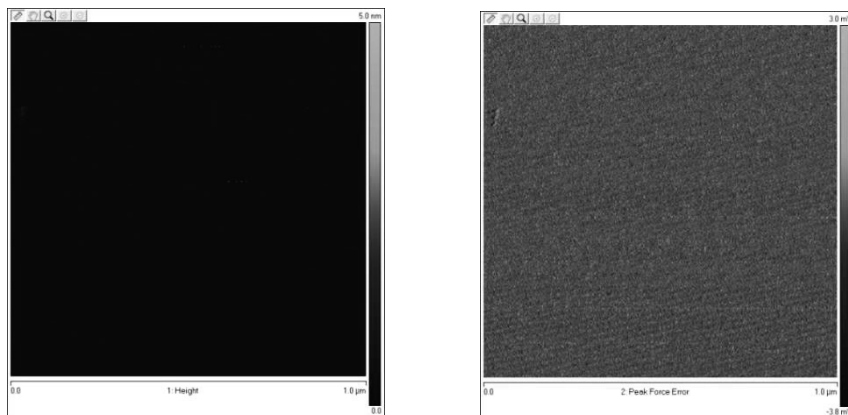


Figure.10. AFM images of the mica surface. (A) 2D height images of the surface at 1 μm x 1 μm (A) Peak error images of the surface at 1 μm x 1 μm

AFM images of pure α -lactalbumin at pH 5.5

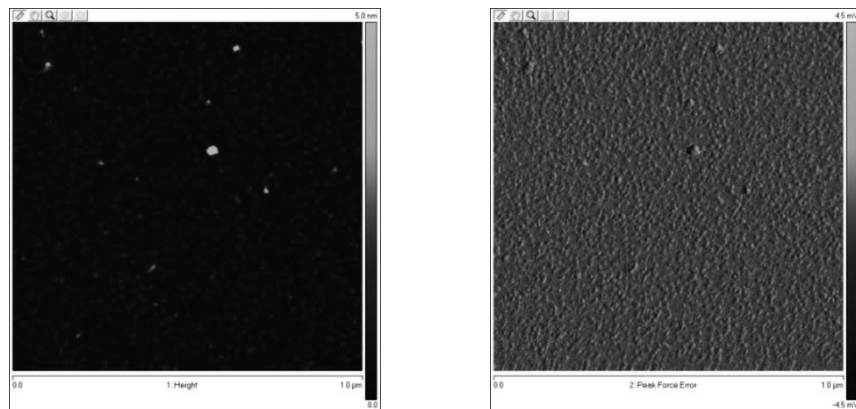


Figure.11. AFM images of pure α -lactalbumin, adsorbed on mica at pH 5.5 and dried before imaging. (A) 2D height images of the proteins at $1\ \mu\text{m} \times 1\ \mu\text{m}$ (A) Peak error images of the proteins at $1\ \mu\text{m} \times 1\ \mu\text{m}$

Multiple AFM images of protein polymers at pH 6.8 on polylysine-modified mica

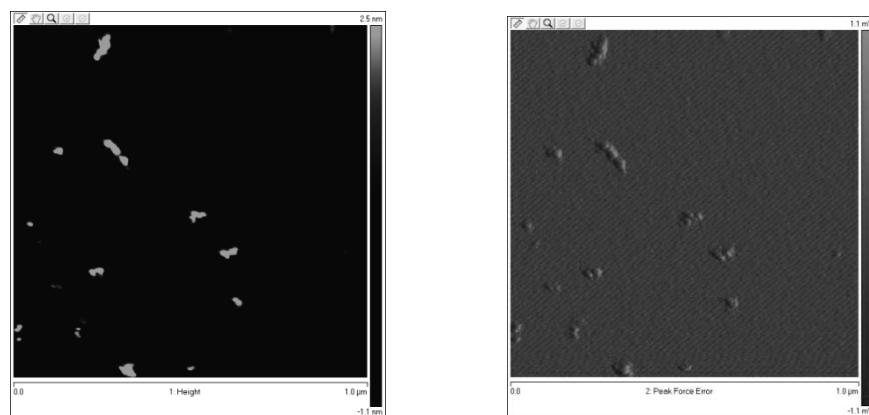


Figure.12. AFM images of protein polymers adsorbed on polylysine-modified mica at pH 6.8 and dried before imaging. (A, left) 2D height images of the polymers at $1\ \mu\text{m} \times 1\ \mu\text{m}$ (B, right) Peak error images of the polymers at $1\ \mu\text{m} \times 1\ \mu\text{m}$

On-line UV Analysis

Enzymatic cycle and dityrosine formation were obtained from spectra between 250 nm and 500 nm during enzymatic cross-linking by using a fiber-optic probe (Avantes FDP-UV-micro-1 1/16" Micro Dip Probe, UV/VIS). We here preferred to use the UV probe of which optical pathlength was 0.1 cm in order to avoid saturated absorption. Only 5% increase in absorbance at 280 nm was determined during HRP-induced cross-linking of α -lactalbumin. In view of this small change of A_{280} , we have used the same molar extinction coefficient for both protein monomers and protein polymers in our measurements.

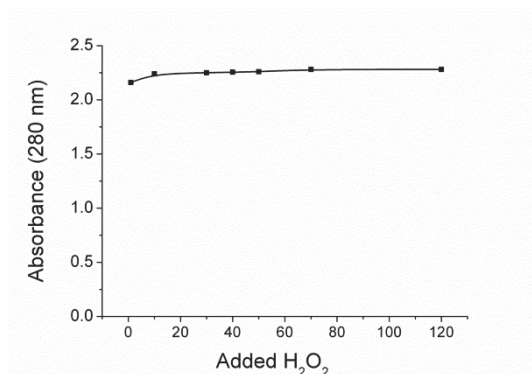


Figure.13. The absorbance at 280 nm during enzymatic cross-linking.

Chapter 3

Changes in protein conformation and surface hydrophobicity upon peroxidase-catalyzed cross-linking of apo- α -lactalbumin

This chapter is published online as: Y. Saricay, P. A. Wierenga, R. de Vries.

J. Agric. Food Chem. **2014** (<http://pubs.acs.org/doi/pdf/10.1021/jf502664q>).

Abstract

Enzymatic protein modifications for modulating- or obtaining new protein functionalities often lead to conformational changes and hence are often associated with changes in protein surface hydrophobicity. Here we explore the effect of peroxidase-catalyzed cross-linking on the molecular conformation of apo- α -lactalbumin (apo- α -lac) and the resulting changes in protein surface hydrophobicity. In studying conformational changes, we distinguish between early stages of the reaction (“partial cross-linking”) in which only small protein oligomers are formed, and a later stage, (“full cross-linking”) in which larger (25 nm) protein particles are formed. Partial cross-linking induces a moderate loss of α -helical content. Surprisingly, further cross-linking leads to a partial return of α -helices that are lost upon early cross-linking. At the same time, for fully cross-linked apo- α -lac, almost all tertiary structure is lost. Protein surface hydrophobicity follows the trend of the changes around local environment of cross-linked dityrosines in going from partially to fully cross-linked apo- α -lac: it first increases upon partial cross-linking, but then decreases again at full cross-linking. Our results highlight the subtle changes in protein conformation and the resulting changes in protein functionality that may take place upon enzymatic cross-linking.

Introduction

A key factor that determines protein functionality in food and biotechnology is the protein molecular conformation. Changes in protein conformation induced by external conditions allow for modulation of the protein functionality but may also result in detrimental effects on protein functionality. Techno-functional properties of proteins can be modulated by various treatments such as chemical modifications, enzymatic modifications, and processing steps such as heating (1, 2). For all these treatments it is crucial to understand the changes in protein molecular conformation that they induce, and how these changes alter protein functionality. Such an understanding eventually allows for a better ability to tune protein functionality, for example to design modifications for specific applications in food and biotechnology (3).

Whereas chemical cross-linking can be used to modulate physical properties of proteins, it is not typically used in food technology (4). Instead, in order to modulate protein functionality for food applications, one typically uses heat- or pressure treatments (5). In particular, disulfide cross-linking is the result of the oxidative coupling of two cysteine residues, and is commonly achieved by heat treatment, which leads to thiol exchanges in thermally denatured food proteins (6, 7). Such reactions play a key role in the production of protein particles with tunable techno-functional properties (8-14).

Another common type of modification is the Maillard reaction, in which proteins are covalently conjugated to polysaccharides, via the condensation between an available amino group and a carbonyl-containing moiety (15). Often the functionality of food proteins can be changed significantly using Maillard reactions, while retaining much of the native structure of the protein (16).

For more specific chemical reactions, many enzymes are used in the food industry. Advantages of enzymatic modifications are the typically mild reaction conditions and the fact that these modifications often induce quite specific chemical modifications that only induce modest changes in protein molecular conformation. An important example is the commercially available cross-linking enzyme microbial Transglutaminase (mTG) (17). Different kinds of improvements of food protein functionality have been reported for

mTG-induced cross-linking, such as enhanced foaming and foam stability, enhanced emulsion stability, enhanced thermal stability and solubility, and improvements in rheological and gelation properties (18-21).

For globular proteins such as the whey proteins α -lactalbumin (α -lac) and β -lactoglobulin (β -lac), at present it is unclear which changes in functionality upon cross-linking are related to changes in the protein molecular conformation and which changes are a consequence of the fact that the proteins have been linked into larger protein structures. Most work on conformational changes of globular proteins induced by mTG has been done for the whey protein β -lac which is a very poor substrate for mTG-catalyzed cross-linking (22-24). In order to improve accessibility for enzymatic cross-linking, β -lac needs to be partially unfolded which is typically achieved by either the addition of denaturants, or by heat treatment (25, 26). Hence, structural changes are already induced before enzymatic cross-linking, such that it becomes difficult to assess the role of conformational changes induced by enzymatic cross-linking.

An alternative to mTG-catalyzed protein cross-linking is oxidative cross-linking of endogenous or exogenous phenolic compounds such as tyrosine residues, caffeic acid or ferrulic acid that can be used to cross-link to either protein or polysaccharides (e.g. arabinoxylan) using various oxidative enzymes (27-29). While tyrosine is the most reactive residue for enzymatic oxidation, oxidative enzymes are capable of reacting with tryptophan, phenylalanine, tryptophan and cysteine and thus results in a range of different types of chemical bonds (tyrosine-tyrosine; lysine-tyrosine; cysteine-tyrosine) (30-32). The functional and technological impacts of oxidative enzymes as an alternative mTG are still under investigation. Whereas promising results of enhanced functionality have already been reported for various oxidative enzymes (33-36), no studies have been reported yet on conformational changes of globular proteins induced by oxidative cross-linking.

Previously, we have investigated the development of protein nanostructures during Peroxidase-mediated cross-linking of apo- α -lactalbumin, and have also investigated the impact of cross-linking on rheology (37-39). The apo- or calcium-free form of the protein has a “molten globule” structure that is quite accessible to enzymatic cross-linking

making, such that it is convenient model system for studying the enzymatic cross-linking of globular proteins (40). Heijnis et al. have shown that peroxidase induces the initial step of cross-linking between Tyr 18 and Tyr 50 in apo-form (41). We have found that nanostructures evolve in a two-stage process: (1) In an initial phase, with rapid conversion of tyrosines, monomers are cross-linked to form oligomers. (2) Upon prolonged cross-linking, protein nanoparticles are formed via cross-linking of the oligomers. In this last phase, the conversion rate of the remaining tyrosines is much slower than in the first phase. The final protein nanoparticles have a very open structure, are very heterogeneous in size and architecture, and exhibit a size-mass scaling of $R_H = M^a$, with an exponent $a \approx 0.4$, where R_H is hydrodynamic radius and M_w is molar mass. The internal protein density of the protein nanoparticles is approximately 9 % (w/v) for particles with a molar mass M_w of 10^6 Da and a hydrodynamic radius R_H of 30 nm (38, 39). In order to link the impact of cross-linking on food-functionality across all length scales, we here investigate conformational changes in apo- α -lac upon peroxidase-catalyzed cross-linking. We consider both conformational changes in the initial phase of cross-linking, and the changes that occur upon prolonged cross-linking, and find significant differences between these two cases. As we will show, these differences correlate with changes in the surface hydrophobicity that we also quantify, thus linking structure to techno-functionality of cross-linked apo- α -lac also at molecular length scales.

Materials and methods

Materials

A commercial preparation of calcium free α -lactalbumin (here simply referred to as apo- α -lac) was supplied by Davisco Foods International Inc. (Le Sueur, MN, USA). The preparation is reported to consist of 85% apo-form (Ca^{+2} -depleted) and 15% holo-form (Ca^{+2} -saturated). Horseradish peroxidase (HRP) type VI-A (P6782) and 2,2'-azino-bis 2,2'-azino-bis(3-ethylbenzothiazoline-6-sulphonic acid) (ABTS) were also supplied by Sigma-Aldrich. All other chemicals used were of analytical grade.

Enzyme activity

In order to determine peroxidase activity, a 2,2'-azino-bis 2,2'-azino-bis(3-ethylbenzothiazoline-6-sulphonic acid) (ABTS) assay was performed according to the published procedure (38). The activity of the enzyme preparation as given by the manufacturer is ~900 - 2000 units/mg). This is in agreement with our own determinations, for which we find variation of enzyme activity from batch to batch of less than about 15%.

Sample preparation

Stock solutions of apo- α -lac and peroxidase were separately prepared by dissolving 12 g/L and 15 mg/mL in 0.1 M NH_4Ac at 25 °C, respectively. After centrifugation (3h, 45000g, 25 °C) of the protein solution, the pH was adjusted to pH 6.8 using 0.1 mM HCl. Finally, the protein concentration was determined using UV spectroscopy assuming an absorbance $A_{280} = 20.1$ for a 1% (w/v) solution of α -lactalbumin (42). The concentration of HRP solutions was also determined using UV spectroscopy, assuming a molar extinction coefficient of $\epsilon_{403} = 102 \text{ mM}^{-1}\text{cm}^{-1}$ (43). To prepare hydrogen peroxide (H_2O_2) stock solutions, an aqueous solution of 30% (w/w) of peroxide was diluted into deionized water to a concentration of 0.05 M. Before use, the precise concentration of the H_2O_2 stock solution was determined using UV spectroscopy, assuming a molar extinction coefficient of $\epsilon_{240} = 43.6 \text{ M}^{-1}\cdot\text{cm}^{-1}$ (44).

Reactions

Reaction 1: Conditions for the reaction leading to “partially” cross-linked apo- α -lac, were similar to those published before (37, 38). The concentration of apo- α -lac in the reaction mixture was 10 mg/mL (or 0.7 mM). The reaction mixture was incubated in a 50 mL water-jacket glass vessel with under continuously stirring at 37 °C in 0.1M NH_4Ac at pH 6.8 for 1h. Next, peroxidase stock solution was added to a final concentration of the enzyme of 0.5 mg/mL. Finally, small amounts (2 μL per mL of reaction mixture) of 50 mM peroxide were added periodically, every 10 minutes. Peroxide addition was done using computer controlled Schott Geräte TA01 titration systems. Every addition corresponded to a change in the peroxide concentration of $\Delta[\text{H}_2\text{O}_2] = 0.1 \text{ mM}$. The total reaction consisted of 15

additions of peroxide into the reaction mixture. The final reaction product was cooled down at room temperature and stored at 4 °C. Analysis on the mixture was performed the following day, without any further purification and filtration.

Reaction 2: Conditions for the reaction leading to “fully” cross-linked apo- α -lac, were identical to the conditions for reaction R1, except that 80 additions of peroxide were used, in a 250 mL water-jacketed glass vessel.

Freeze-drying and dialysis

For long-term preservation of reaction mixture 2, it was cooled down to 25 °C. The reaction mixture was mixed with 1M sucrose in a volume ratio of 1:1. Next, the reaction mixture was freeze-dried at -80 °C. The resulting powder was stored at -80 °C. We have shown before that this procedure does not affect the particle properties, when the freeze-dried powder is redissolved (37). For sample preparation, the powder was redissolved in 10 mM sodium phosphate buffer and dialyzed against 10 mM sodium phosphate buffer using a 300 kDa cellulose ester membrane (Spectra/Por CE dialysis) to remove the sucrose and low molecular weight reaction products. The concentration of protein nanoparticles was determined using UV spectroscopy, assuming an absorbance $A_{280} = 20.1$ for a 1 % (w/v) solution of fully cross-linked apo- α -lac nanoparticles. Dialyzed samples (fully cross-linked apo- α -lac nanoparticles, $M_w > 300$ kDa) from the same batch were used for all experiments.

Size exclusion chromatography (SEC) fractionation

Reaction products were analysed and fractionated by size exclusion chromatography using a Superose 6 column (separation range reported for globular proteins between $5 \times 10^3 - 5 \times 10^6$ Da; exclusion limit 4×10^7 Da) connected to an AKTA purifier system (GE Healthcare). A volume of 100 μ l of reaction product was injected into the column and eluted with 10 mM sodium phosphate buffer at a flow rate of 0.5 mL/min. The UV absorbance of the eluate was monitored at wavelengths of 280 and 318 nm. For fractionation of reaction mixture R1, SEC fractions were collected into 10-mL tubes at 1-mL intervals, with a collection volume of 0.5 mL for each fractionation step. Protein particles (F), oligomers

(from P1 to P7) and un-cross-linked, native apo- α -lac were collected based on retention volume: F: 7.5 mL ($M_w > 2000$ kDa) ; P7: 9 mL and P6: 10 mL (2000 kDa $> M_w > 660$ kDa); P5: 11 mL (660 kDa $> M_w > 440$ kDa); P4: 12 mL, P3: 13 mL, and P2: 14 mL (440 kDa $> M_w > 66.5$ kDa); P1: 15 mL (66.5 kDa $> M_w > 18.4$ kDa) and α -Lac: 16.6 mL ($M_w \approx 14$ kDa). For further analysis, SEC fractions were concentrated by a factor of 10 in volume using centrifugal filter devices (50 kDa cut-off). Concentrations of concentrated fractions were determined using UV spectroscopy, assuming an absorbance $A_{280} = 20.1$ for a 1% (w/v) solution of α -lac. Finally, concentrations were adjusted to the required values by dilution with buffer.

Secondary structure analysis

Far-UV CD spectra (190-260 nm) were acquired using a Jasco J-715 spectropolarimeter (Tokyo, Japan) equipped with a PTC-348WI Peltier temperature control system. Quartz cuvettes (Starna, Hainault, UK) with 1-mm cell length were used as a sample container. The concentration of all samples was 0.12 mg/mL. CD spectra of samples and blanks were recorded by averaging 20 scans. CD spectra of samples were corrected by subtracting spectra of blanks (10 mM sodium phosphate buffer). From the far-UV spectra, contents of secondary structure (α -helix, β -strands, β -turns and random coil) were estimated using the ridge regression algorithm CONTINLL as implemented by the Dichroweb server (45-47).

Tertiary structure analysis

Near-UV CD spectra (250-350 nm) of nanoparticle solutions (1 mg/mL) were recorded in 3 mL quartz cuvettes (path length 1 cm) (Starna, Hainault, UK) at 20 °C for reaction 2. CD spectra of samples and blanks were determined by averaging 20 scans. CD spectra of samples were corrected by subtracting spectra of the blanks (10 mM sodium phosphate buffer).

Secondary structure of extensively heat-denatured α -lactalbumin

Extensively heat-denatured apo- α -lac was used for structural comparison with enzymatically cross-linked protein. In order to prepare the denatured protein according to

published procedure (48), apo- α -lac (1 mg/mL or 0.07 mM) was dissolved into 10 mM sodium phosphate buffer at pH 7.0 at 25 °C containing 2-mercaptoethanol (2-ME) (1 mM) (sigma, M6250). In order to allow for complete protein denaturation, the protein solution was heated for 24 h at 90 °C. Next, the sample was quickly cooled down using running tap water and diluted to final concentrations of 0.12 mg/mL and 1 mg/mL for far UV CD spectroscopy (performed as described above).

Determination of hydrodynamic radius (R_H) and zeta (ζ) potential

Dynamic light scattering (DLS) and electrophoretic light scattering (ELS) experiments were done on dialyzed reaction products using a Malvern Nanosizer ZS (Malvern) equipped with an Argon ion laser emitting vertically polarized light with a wavelength of 633 nm. For DLS measurements, the scattering angle was 173°. For ELS measurements, the scattering angle was 12.8°. Average hydrodynamic radii R_H and ζ -Potential reported are the major peak from the peak analysis as performed by the Malvern DTS software, version 6.20. For DLS, protein samples were measured in a low-volume quartz batch cuvette (ZEN2112). For ζ -Potential measurements, a disposable capillary cell (DTS1070) was used. For both measurements, concentration of sample is 1 mg/mL.

Fluorescence spectroscopy

Fluorescence spectra of apo- α -lac, partially and fully cross-linked apo- α -lac nanoparticles were obtained using a Perkin Elmer Luminescence Spectrometer LS 50 B spectrofluorimeter at 25 °C. In all experiments, a quartz cuvette with a 1-cm excitation path length was used. For partially and fully cross-linked apo- α -lac, samples were diluted to final concentrations of 0.12 mg/mL in 10 mM sodium phosphate buffer at pH 7.0 at 25 °C. In order to monitor fluorescence from cross-linked tyrosines, in particular dityrosines, an excitation wavelength was used of 315 nm. Emission was monitored for wavelengths between 330 nm and 550 nm. Excitation and emission slits were set at 5 nm.

In order to compare with the spectrum of free dityrosine, we synthesized dityrosine using peroxidase-catalyzed cross-linking of L-Tyrosine. First, 0.72 mg of L-tyrosine was dissolved in 20 mL of 10 mM sodium phosphate buffer at pH 8.0 and

transferred into 2 mL of Eppendorf tubes. In order to ensure complete dissolution, L-tyrosine solutions were heated at 95 °C for 15 min in a thermal incubator (Thermomixer comfort, Eppendorf, Harmburg, Germany). A peroxidase stock solution was prepared by dissolving 1.77 mg of peroxidase in 0.2 mL of 10 mM sodium phosphate buffer at pH 8.0. Next, protein and enzyme solutions were mixed at a molar ratio of protein to enzyme of 1000. The enzymatic reaction was performed by the periodic addition of peroxide (2 µl of 0.03% into 2 mL) every 210 s at 37 °C for 2 h. For fluorescence measurements, the reaction mixture (containing L-tyrosine and dityrosine) was diluted to a final concentration of 0.12 mg/mL (based on the initial concentration of L-tyrosine) with 10 mM sodium phosphate buffer, pH 7.0.

Surface hydrophobicity

The anionic fluorescent probe ANSA was used to measure exposed surface hydrophobicity of proteins and protein particles (49). First, an ANSA stock solution (2.4 mM) was prepared in 10 mM sodium phosphate buffer at pH 7.0 at 25 °C. The ANSA solution was stored at 4 °C overnight to ensure complete dissolution. Protein samples were diluted to a final concentration of 0.12 mg/mL using 10 mM sodium phosphate buffer at pH 7.0. Aliquots of ANSA stock solution (10 µl) were titrated into protein solutions (0.12 mg/mL, 1 mL). Between each addition, fluorescence emission spectra were recorded at wavelengths between 400 nm and 650 nm. The excitation wavelength was 385 nm, the scan rate of 120 nm/min. Excitation and emission slits were set at 5 nm. The system was thermostated at 20 °C. The relative exposed hydrophobicity of each sample was expressed as the difference between minimum and maximum area of integrated titration curve between 400 nm and 600 nm after blank subtraction.

Results and discussion

Partially and fully cross-linked α -lactalbumin

We refer to the apo- α -lac oligomers that are formed in the initial phase of the cross-linking process as “partially cross-linked” proteins (reaction 1: 150 min of reaction time, or 15 additions of peroxide in 10 min intervals).

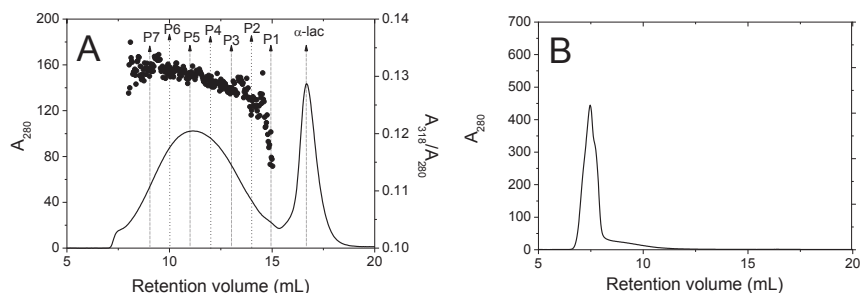


Figure.1. SEC chromatograms of peroxidase-cross-linked apo- α -lac (A) Solid line: UV absorption at 280 nm (A_{280}) versus retention volume for partially cross-linked apo- α -lac. Retention volumes of SEC fractions P1 to P7 used in further studies and monomeric protein (apo- α -lac) are indicated. Symbols: ratio A_{318}/A_{280} (a measure for tyrosine conversion) versus retention volume (B) UV absorption at 280 nm (A_{280}) versus retention volume for dialyzed fully cross-linked apo- α -lac nanoparticles (F). The fully cross-linked nanoparticles elute in the void of the column.

The larger hierarchical apo- α -lac particles that formed at later stages of the cross-linking reaction are referred to as “fully cross-linked” protein (reaction 2: 800 min of reaction time, or 80 additions of peroxide in 10 min intervals). Conformational changes as compared to apo- α -lac are studied separately for the two cases, such that we can also elucidate possible structural transitions in going from small oligomers to larger protein particles. In addition, in the early stages, the reaction mixture contains a mix of monomers and a range of oligomers (38) that possibly differ strongly in the extent of conformational change. Therefore, for partially cross-linked proteins (P), we focus on a fixed, short reaction time of 2.5h, separate the reaction mixture using size-exclusion chromatography (fractions P1-P7 from reaction 1), and study conformational changes as compared to apo- α -lac for all of the fractions. Fig.1A shows the size-exclusion chromatogram (SEC), and indicates the retention volumes corresponding to the different SEC fractions (apo- α -lac + P1-P7).

Cross-linked tyrosines (i.e. dityrosines) exhibit a strong absorption at 318 nm; hence Fig.1A also shows the ratio A_{318}/A_{280} which is a qualitative measure for the conversion of tyrosines into cross-linked reaction products, mainly dityrosines. As can be seen in Fig.1A, the conversion of tyrosines increases with oligomer size for the different fractions, whereas apo- α -lac fraction shows no signal at 318 nm, as expected. For fully

cross-linked protein (F; from reaction 2), we dialyze the reaction product (using a 300 kDa cut-off membrane) to remove small oligomers and any remaining monomers from the final reaction mixture. The fully cross-linked protein elutes in the void of the column (see Fig.1B).

Changes in secondary and tertiary structure upon enzymatic cross-linking

Changes in secondary structure upon enzymatic cross-linking for partially (P1-P7) and fully cross-linked protein (F) were quantified using CD spectroscopy. Far-UV CD spectra are shown in Fig.2 and compared with that of apo- α -lac. The latter exhibits a typical spectrum of α -helix-rich proteins, with two dips at 208 nm, and 222 nm. For partially cross-linked α -lac fraction P1, the ellipticity changes significantly as compared to the native apo- α -lac.

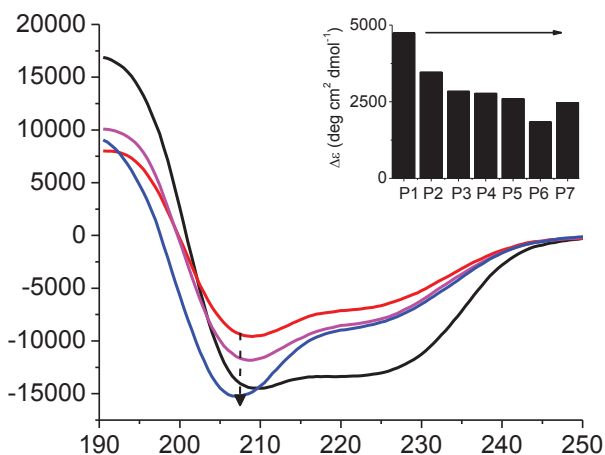


Figure.2. Far-UV CD spectra of apo- α -lac and cross-linked apo- α -lac. Black: native apo- α -lac. Navy: fully cross-linked protein nanoparticles (F). The inset shows the evolution of ellipticity at 208 nm [$\Delta\epsilon = \epsilon_1$ (ellipticity of SEC fractions) $- \epsilon_2$ (ellipticity of native α -lac)] for SEC fractions of partially cross-linked protein oligomers: from P1 (red) to P7 (magenta), as also indicated by the dotted arrow. The solvent is 10 mM sodium phosphate buffer, pH 7.0 at 25 °C. The protein concentration of all samples is 0.12 mg/mL.

For the fractions P2-P7 with a higher molar mass and a larger extent of cross-linking (as determined by their A_{318}/A_{280} ratio), there are no further major changes in the ellipticity with fraction number (Fig.2, the inset). The spectrum of fully cross-linked α -lac (F) is again distinctly different from that of the fractions P1-P7, with a pronounced dip at 205 nm. Hence it appears that it is the earliest cross-linking event that leads to the formation of the smallest oligomers P1 that induces the biggest changes in protein conformation. Also it appears that there are significant changes in conformation when going from partially to fully cross-linked protein (Fig.2, inset).

From the spectra, we have deduced approximate contents of secondary structure elements (α -helix, β -strands, β -turns and random coil) using the ridge regression algorithm CONTINLL as implemented by the Dichroweb server (45-47). The estimated percentages of secondary structure elements obtained from this analysis are reported in Table.1. A plot of the percentage of α -helix versus the fraction number is shown in Fig.3.

Table.1. Percentages of secondary structure elements for native apo- α -lac (N, native-form), partially cross-linked (fractions P1-P7), and fully cross-linked apo- α -lac (F) as deduced from the CD spectra of Fig.2.

Sample	α -helix	β -sheet	β -turns	Random coil
N	38.5	18.1	19.3	24.1
P1	23.8	24.8	21.3	30.1
P2	23.9	23.9	21.3	30.8
P3	26.4	23	20.8	29.6
P4	26.8	22.8	20.8	29.5
P5	26.9	21.4	21.1	30.6
P6	29.3	19.1	21.7	29.9
P7	27.5	21.8	20.7	29.9
F	31.2	17.2	21.8	29.8

Somewhat surprisingly, the analysis of the spectra (Fig.3) shows that the highest loss of α -helical content as compared to native apo- α -lac is observed for the partially cross-linked fraction P1 that has the lowest extent of tyrosine conversion, whereas the fully cross-linked α -lac (F) exhibited the lowest loss of α -helical content as compared to native apo- α -lac. This confirms that the first few tyrosines that are converted lead to the largest loss of α -helicity, with further conversion leading to a partial recovery of α -helicity

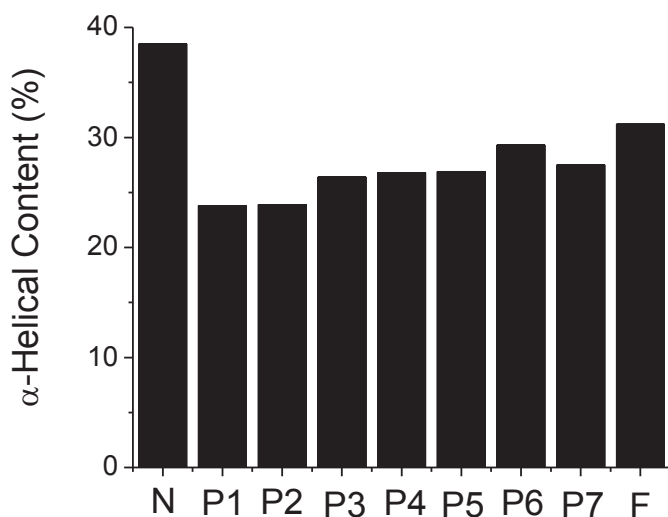


Figure.3. Total percentage of α -helix as deduced from CD spectroscopy for N: native apo- α -lac; P1 - P7: SEC fractions of partially cross-linked apo- α -lac; F: fully cross-linked apo- α -lac nanoparticles.

We have also compared the impact of peroxidase-induced cross-linking on protein conformation (as deduced from CD spectroscopy) with that of extensively heat-denaturation apo- α -lac (24h at 90 °C in 10mM sodium phosphate buffer at pH 7 in the presence of 1mM 2-ME). The far-UV CD spectrum of extensively heat-denatured apo- α -lac is shown in **Fig.4**, and compared with those of native apo- α -lac and fully cross-linked apo- α -lac (F).

As expected, conformational changes as compared to native apo- α -lac are largest for heat-denatured α -lac. From the far UV CD spectra in Fig.4, it appears that the

secondary structure of fully cross-linked apo- α -lac is intermediate between that of native- and extensively heat-denatured apo- α -lac. This analysis is confirmed by a more quantitative interpretation of the CD spectra in terms of approximate contents of secondary structure elements. Results for native, heat-denatured, and fully cross-linked α -lac are given in Table.2. Our findings indicate that fully cross-linked apo- α -lac has significantly higher secondary structure than fully denatured apo- α -lac.

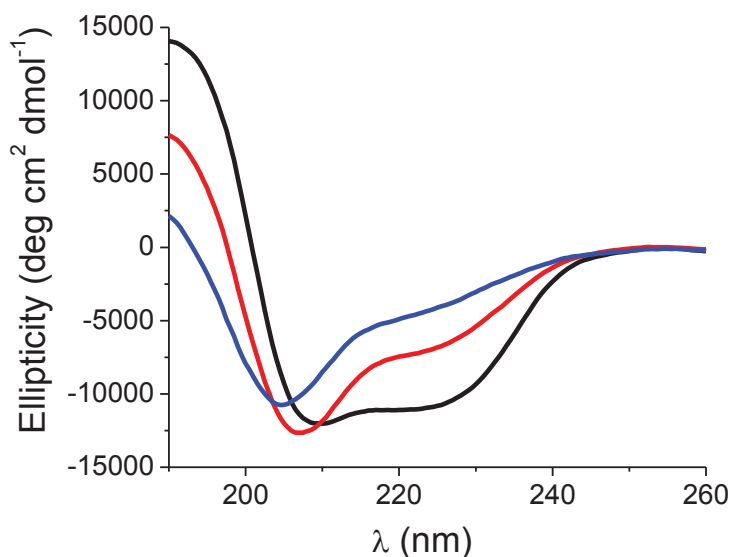


Figure.4. Far-UV CD spectra of native apo- α -lac (black line), fully cross-linked apo- α -lac (red line) and extensively heat-denatured apo- α -lac (blue line, 90 °C for 24h in the presence of 1mM 2-ME). Solution conditions for CD were 10 mM sodium phosphate buffer at pH 7.0 at 25 °C.

Table.2. Percentages of α -helix, β -strands, β -turns and random coil for native apo- α -lac (N), fully cross-linked apo- α -lac (F) and extensively heat-denatured apo- α -lac (D), estimated from the CD spectra of Fig.5.

Sample	α -helix	β -strands	β -turns	Random coil
N	38.5	18.1	19.3	24.1
F	31.2	17.2	21.8	29.8
D	20.5	23.3	24.2	32

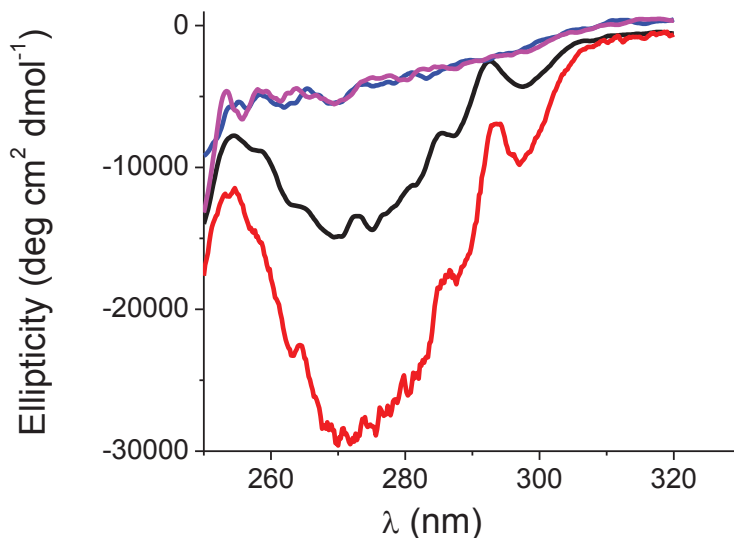


Figure.5. Near-UV spectra of apo- α -lac (0.07 mM) (black), apo- α -lac (0.07 mM) in the presence of Ca^{2+} (1 mM) (red), fully cross-linked apo- α -lac (0.05 mM) (blue) and fully cross-linked apo- α -lac (0.05 mM) in the presence of Ca^{2+} (1 mM) (magenta).

With regards to the tertiary structure, earlier investigations have shown that in the “molten globule” structure of calcium free apo- α -lac, much of the tertiary structure is already lost, as compared to holo- α -lac (50). In contrast, we find that the near-UV CD spectrum of fully cross-linked α -lac has lost all characteristic features and is nearly flat. Finally, whereas for native α -lac the change from apo- to holo- (by the addition or removal of Ca^{2+}) is reversible, we find that the near-UV CD spectra of fully cross-linked apo- α -lac are not affected by the addition of Ca^{2+} (Fig.5), indicating irreversible loss of tertiary structure.

Dityrosine fluorescence upon enzymatic cross-linking

In order to study the changes around the local environment of dityrosine, we recorded fluorescence emission spectra, using an excitation wavelength of 315 nm. At this wavelength it may be expected that mainly dityrosines are excited and that excitation of

tryptophans is negligible (51). First, in order to obtain a reference spectrum, we synthesized dityrosine by peroxidase-catalyzed cross-linking of tyrosine (see Materials and Methods). A comparison of fluorescence spectra (dityrosine reference, native apo- α -lac, partially cross-linked fractions P1-P7 and fully cross-linked α -lac (F)) is shown in Fig.6. As expected, native apo- α -lac does not exhibit any dityrosine fluorescence (Fig.6). Fluorescence first increases and then saturates with increasing fraction number of the partially cross-linked α -lac (P1-P7).

The fluorescence intensity of fully cross-linked protein (F) is much lower. Also, in going from partially cross-linked (P1-P7) to fully cross-linked protein (F), the peak position shifts to the red by about 11 nm, ending up very close to the peak position of free dityrosine (Fig.6). Most likely the increase and saturation of the fluorescence with increasing fraction number (from P1-P7) reflects the increase and then saturation of the number of dityrosines per molecule (and possibly trityrosines etc.).

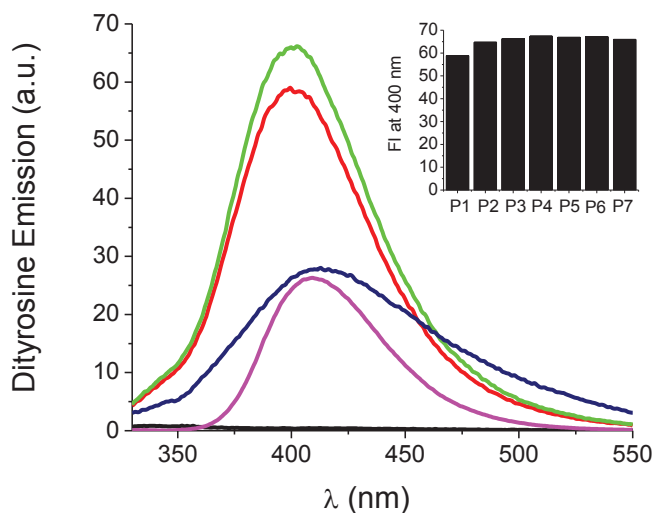


Figure.6. Fluorescence emission spectra of native apo- α -lac, partially and fully cross-linked apo- α -lac and dityrosine reference, excitation wavelength 315 nm. Black: native apo- α -lac (N), navy: fully cross-linked apo- α -lac, magenta: dityrosine reference. The inset shows the evolution of dityrosine fluorescence intensity at 400 nm for SEC fractions of partially cross-linked from P1 (red) to P7 (green).

This is consistent with a modest increase in dityrosine density (corresponding to $A_{318/280}$) from P2 to P7 (Fig.1A). On the other hand, the strong decrease of the fluorescence intensity for the fully cross-linked α -lac (F) most likely is due to quenching, that must be caused by a local structural rearrangement around the dityrosines. This process might arise from the change in inter- and intra-molecular interaction of dityrosine with solvent and neighbouring amino acid residues. Finally, the shift of the peak position towards the direction of free dityrosines suggests that the dityrosines are becoming more exposed to the solvent when going from partially to fully cross-linked protein.

Correlation of changes in conformation with changes in surface hydrophobicity

Changes in protein structure often correlate with changes in food functionality. Here we consider surface hydrophobicity as an underlying parameter that impacts properties such as emulsifying and foaming capacity, and protein aggregation. In order to get a qualitative measure of the exposed surface hydrophobicity of apo- α -lac and cross-linked protein, we use the ANSA fluorescent probe that shows a strong enhancement of fluorescence when binding to hydrophobic surfaces (49). The evolution of surface hydrophobicity of α -lac upon enzymatic cross-linking is shown in Fig.7.

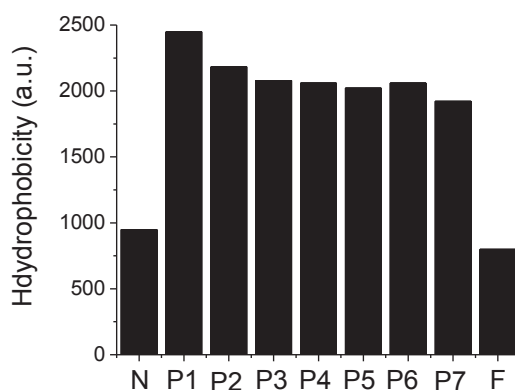


Figure.7. Surface hydrophobicity (arbitrary units) of native- (N), partially cross-linked (P1-P7), and fully cross-linked apo- α -lac (F) as determined using the fluorescent probe ANSA. Solution conditions: 10 mM sodium phosphate buffer at pH 7.0 at 25 °C.

Partial cross-linking rapidly induces a significant increase in hydrophobicity, which then saturates with increasing fraction number (P1-P7). Remarkably, full cross-linking leads to a decrease in surface hydrophobicity as compared with partially cross-linked protein (P1-P7), with final values that are (within the margin of error) similar to that of native apo- α -lac.

The remarkable changes in local structure upon going from native apo- α -lac to the smallest cross-linked oligomers (P1) with the lowest number of dityrosines (lowest ratio A_{318}/A_{280}), most probably relate to the initial steps of the cross-linking reaction. Heijnis et al. have shown that the initial step of cross-linking most likely involves a reaction between Tyr 18 and Tyr 50 (41). Our results show that apparently this first reaction already leads to a relatively large conformational change. The difference in dityrosine fluorescence and surface hydrophobicity for partially and fully cross-linked α -lac might be a consequence of conformational changes induced by the additional cross-linking reactions involving the other tyrosine residues (Tyr 36 and Tyr 103) that occur at later stage.

Concluding remarks

The objective of this study was to determine conformational transition in apo- α -lac in going from native apo- α -lac, to small oligomers, and then to larger protein particles upon peroxidase-catalyzed cross-linking. Our results show that, surprisingly, the surface hydrophobicity of apo- α -lac first increases upon partially cross-linking and then decreases upon fully cross-linking. Differences between partially- and fully cross-linked protein that are consistent with this result are also found for the local environment of the dityrosines (as probed using fluorescence), and for the secondary structure (as probed using CD).

With respect to the mTG-induced cross-linking of the globular whey proteins α -lac and β -lactoglobulin (β -lac), it has been found that α -lac, and in particular apo- α -lac, is a much better substrate for mTG than β -lac (23, 24), such that in WPI, in fact it may be expected that most of the cross-linking occurs for the α -lac fraction in WPI. For whey protein isolate (WPI) only minor changes in tertiary structure have been reported upon cross-linking with mTG, and then only for very long reaction times. Neither does mTG leads to no dramatic changes in secondary structure for WPI (23, 24). However, changes in

the apparent hydrophobicity have been reported for mTG-catalysed cross-linking of whey proteins. Surface hydrophobicity of WPI gradually decreased upon increasing cross-linking degree. A decrease of the apparent hydrophobicity of WPI after TG-catalyzed cross-linking (as detected using the fluorescent dye ANSA) was attributed to occlusion of hydrophobic cavities in protein (24). At the same time, however, it was reported that the reduction of net positive charge due to cross-linking of lysyl residues led to aggregation of TG-cross-linked WPI particles at acidic pH. In contrast, we find surface hydrophobicity of α -lac particles first increase with the first cross-linking. But, after full cross-linking, the surface hydrophobicity has decreased again to a value that is nearly the same of that of native α -lac. In contrast to TG-catalysed cross-linking, where the cross-linking led to changes in the surface charge that impacted colloidal stability, we have found that the zeta potential (ζ) of α -lac increases from -12.4 mV to -29.6 mV upon full cross-linking at neutral pH in 10 mM sodium phosphate buffer.

Taken together, we find that peroxidase-catalyzed cross-linking leads to physical properties of cross-linked protein that can be beneficial in beverages and for food structuring, in particular the highly hydrophilic nature and high zeta potential of the particles, as well as the fact that a significant fraction of secondary structure is retained. As we have observed in our previous work on the rheology of dispersions of these hydrophilic particles, the cross-linked apo- α -lac particles are interesting novel protein-based thickeners, with a completely reversible yield-stress and shear thinning behavior that is highly unusual for globular protein systems. Moreover, the tunability of the hydrophilicity/hydrophobicity may also have an impact on the interaction of the cross-linked α -lac with other molecules, and thus on their functionality as carrier molecules in delivery applications. For example, it is known that α -lac specifically interacts with oleic acid which has been exploited for applications in medicine (52).

In combination with our earlier work on the structure of cross-linked α -lac at larger lengthscales (37-39), by zooming in on the structural impact of enzymatic cross-linking at nanometer length scales, we now have a complete overview of the impact of peroxidase-catalyzed cross-linking of apo- α -lac across a range of lengthscales. Indeed, only by linking changes at nanometer length scales to the architecture and physical properties of cross-

linked protein at larger length scales, we will be able to rationally use enzymatic cross-linking to modulate food structure.

Acknowledgement

This work is part of the Industrial Partnership Programme (IPP) Bio(-Related)Materials of the Stichting voor Fundamenteel Onderzoek der Materie (FOM), which is financially supported by the Nederlandse Organisatie voor Wetenschappelijk Onderzoek (NWO). The IPP BRM is co-financed by the Top Institute Food and Nutrition and the Dutch Polymer Institute.

References

1. Jones, O. G.; McClements, D. J., Functional Biopolymer Particles: Design, Fabrication, and Applications. *Comprehensive Reviews in Food Science and Food Safety* 2010, 9, 374-397.
2. Panyam, D.; Kilara, A., Enhancing the functionality of food proteins by enzymatic modification. *Trends Food Sci. Technol.* 1996, 7, 120-125.
3. Foegeding, E. A.; Davis, J. P., Food protein functionality: A comprehensive approach. *Food Hydrocolloids* 2011, 25, 1853-1864.
4. Kluger, R.; Alagic, A., Chemical cross-linking and protein-protein interactions - a review with illustrative protocols. *Bioorganic Chem.* 2004, 32, 451-472.
5. Considine, T.; Patel, H. A.; Anema, S. G.; Singh, H.; Creamer, L. K., Interactions of milk proteins during heat and high hydrostatic pressure treatments - A review. *Innov. Food Sci. Emerg. Technol.* 2007, 8, 1-23.
6. Fass, D., Disulfide Bonding in Protein Biophysics. *Annu. Rev. Biophys.* 2012, 41, 63-79.
7. Shimada, K.; Cheftel, J. C., Sulfhydryl-group disulfide bond interchange reactions during heat-induced gelation of whey-protein isolate. *J. Agric. Food Chem.* 1989, 37, 161-168.
8. Nicolai, T.; Britten, M.; Schmitt, C., beta-Lactoglobulin and WPI aggregates: Formation, structure and applications. *Food Hydrocolloids* 2011, 25, 1945-1962.
9. Alting, A. C.; Hamer, R. J.; de Kruif, C. G.; Paques, M.; Visschers, R. W., Number of thiol groups rather than the size of the aggregates determines the hardness of cold set whey protein gels. *Food Hydrocolloids* 2003, 17, 469-479.
10. Foegeding, E. A.; Davis, J. P.; Doucet, D.; McGuffey, M. K., Advances in modifying and understanding whey protein functionality. *Trends Food Sci. Technol.* 2002, 13, 151-159.
11. Liu, X. M.; Powers, J. R.; Swanson, B. G.; Hill, H. H.; Clark, S., Modification of whey protein concentrate hydrophobicity by high hydrostatic pressure. *Innov. Food Sci. Emerg. Technol.* 2005, 6, 310-317.
12. Huebner, F. R.; Bietz, J. A.; Wall, J. S., Disulfide bonds: key to wheat protein functionality. *Advances in experimental medicine and biology* 1977, 86A, 67-88.

13. Okumura, K.; Miyake, Y.; Taguchi, H.; Shimabayashi, Y., Formation of stable protein foam by intermolecular disulfide cross-linkages in thiolated alpha-s1-casein as a model. *J. Agric. Food Chem.* 1990, 38, 1303-1306.
14. Schmitt, C.; Moitzi, C.; Bovay, C.; Rouvet, M.; Bovetto, L.; Donato, L.; Leser, M. E.; Schurtenberger, P.; Stradner, A., Internal structure and colloidal behaviour of covalent whey protein microgels obtained by heat treatment. *Soft Matter* 2010, 6, 4876-4884.
15. Miller, A. G.; Meade, S. J.; Gerrard, J. A., New insights into protein crosslinking via the Maillard reaction: Structural requirements, the effect on enzyme function, and predicted efficacy of crosslinking inhibitors as anti-ageing therapeutics. *Bioorg. Med. Chem.* 2003, 11, 843-852.
16. Oliver, C. M.; Melton, L. D.; Stanley, R. A., Creating proteins with novel functionality via the Maillard reaction: A review. *Crit. Rev. Food Sci. Nutr.* 2006, 46, 337-350.
17. de Goes-Favoni, S. P.; Bueno, F. R., Microbial Transglutaminase: General Characteristics and Performance in Food Processing Technology. *Food Biotechnol.* 2014, 28, 1-24.
18. Partanen, R.; Forssell, P.; Mackie, A.; Blomberg, E., Interfacial cross-linking of beta-casein changes the structure of the adsorbed layer. *Food Hydrocolloids* 2013, 32, 271-277.
19. Truong, V. D.; Clare, D. A.; Catignani, G. L.; Swaisgood, H. E., Cross-linking and rheological changes of whey proteins treated with microbial transglutaminase. *J. Agric. Food Chem.* 2004, 52, 1170-1176.
20. Ozrenk, E., The use of transglutaminase in dairy products. *Int. J. Dairy Technol.* 2006, 59, 1-7.
21. Jaros, D.; Partscheveld, C.; Henle, T.; Rohm, H., Transglutaminase in dairy products: Chemistry, physics, applications. *J. Texture Stud.* 2006, 37, 113-155.
22. Hu, X.; Zhao, M. M.; Sun, W. Z.; Zhao, G. L.; Ren, J. Y., Effects of Microfluidization Treatment and Transglutaminase Cross-Linking on Physicochemical, Functional, and Conformational Properties of Peanut Protein Isolate. *J. Agric. Food Chem.* 2011, 59, 8886-8894.
23. Eissa, A. S.; Puhl, C.; Kadla, J. F.; Khan, S. A., Enzymatic cross-linking of beta-lactoglobulin: Conformational properties using FTIR spectroscopy. *Biomacromolecules* 2006, 7, 1707-1713.
24. Agyare, K. K.; Damodaran, S., pH-Stability and Thermal Properties of Microbial Transglutaminase-Treated Whey Protein Isolate. *J. Agric. Food Chem.* 2010, 58, 1946-1953.
25. Faergemand, M.; Otte, J.; Qvist, K. B., Enzymatic cross-linking of whey proteins by a Ca^{2+} -independent microbial transglutaminase from *Streptomyces lydicus*. *Food Hydrocolloids* 1997, 11, 19-25.
26. Eissa, A. S.; Bisram, S.; Khan, S. A., Polymerization and gelation of whey protein isolates at low pH using transglutaminase enzyme. *J. Agric. Food Chem.* 2004, 52, 4456-4464.
27. Buchert, J.; Cura, D. E.; Ma, H.; Gasparetti, C.; Monogioudi, E.; Faccio, G.; Mattinen, M.; Boer, H.; Partanen, R.; Selinheimo, E.; Lantto, R.; Kruus, K., Crosslinking Food Proteins for Improved Functionality. In *Annual Review of Food Science and Technology*, Vol 1, Doyle, M. P.; Klaenhammer, T. R., Eds. Annual Reviews: Palo Alto, 2010; Vol. 1, pp 113-138.
28. Thalmann, C. R.; Lotzbeyer, T., Enzymatic cross-linking of proteins with tyrosinase. *Eur. Food Res. Technol.* 2002, 214, 276-281.

29. Faergemand, M.; Otte, J.; Qvist, K. B., Cross-linking of whey proteins by enzymatic oxidation. *J. Agric. Food Chem.* 1998, 46, 1326-1333.
30. Heck, T.; Faccio, G.; Richter, M.; Thony-Meyer, L., Enzyme-catalyzed protein crosslinking. *Appl. Microbiol. Biotechnol.* 2013, 97, 461-475.
31. Mattinen, M. L.; Hellman, M.; Permi, P.; Autio, K.; Kalkkinen, N.; Buchert, J., Effect of protein structure on laccase-catalyzed protein oligomerization. *J. Agric. Food Chem.* 2006, 54, 8883-8890.
32. Elliott, K. A., Oxidations catalysed by horseradish- and milk-peroxidases. *The Biochemical journal* 1932, 26, 1281-90.
33. Lantto, R.; Puolanne, E.; Katina, K.; Niemisto, M.; Buchert, J.; Autio, K., Effect of laccase and transglutaminase on the textural and water-binding properties of cooked chicken breast meat gels. *Eur. Food Res. Technol.* 2007, 225, 75-83.
34. Lantto, R.; Puolanne, E.; Kalkkinen, N.; Buchert, J.; Autio, K., Enzyme-aided modification of chicken-breast myofibril proteins: Effect of laccase and transglutaminase on gelation and thermal stability. *J. Agric. Food Chem.* 2005, 53, 9231-9237.
35. Ma, H.; Forssell, P.; Partanen, R.; Buchert, J.; Boer, H., Improving Laccase Catalyzed Cross-Linking of Whey Protein Isolate and Their Application as Emulsifiers. *J. Agric. Food Chem.* 2011, 59, 1406-1414.
36. Cura, D. E.; Lantto, R.; Lille, M.; Andberg, M.; Kruus, K.; Buchert, J., Laccase-aided protein modification: Effects on the structural properties of acidified sodium caseinate gels. *Int. Dairy J.* 2009, 19, 737-745.
37. Dhayal, S. K.; Gruppen, H.; de Vries, R.; Wierenga, P. A., Controlled formation of protein nanoparticles by enzymatic cross-linking of alpha-lactalbumin with horseradish peroxidase. *Food Hydrocolloids* 2014, 36, 53-59.
38. Saricay, Y.; Wierenga, P.; de Vries, R., Nanostructure development during peroxidase catalysed cross-linking of alpha-lactalbumin. *Food Hydrocolloids* 2013, 33, 280-288.
39. Yunus Saricay, A. P. W., Renko De Vries, Rheological properties of dispersions of enzymatically cross-linked α -lactalbumin nanoparticles *Food & Function* 2014.
40. Heijnis, W. H.; Wierenga, P. A.; Berkel, W. J. H.; Gruppen, H., Directing the Oligomer Size Distribution of Peroxidase-Mediated Cross-Linked Bovine alpha-Lactalbumin. *J. Agric. Food Chem.* 2010, 58, 5692-5697.
41. Heijnis, W. H.; Dekker, H. L.; de Koning, L. J.; Wierenga, P. A.; Westphal, A. H.; de Koster, C. G.; Gruppen, H.; van Berkel, W. J. H., Identification of the Peroxidase-Generated Intermolecular Dityrosine Cross-Link in Bovine alpha-Lactalbumin. *J. Agric. Food Chem.* 2011, 59, 444-449.
42. Kronman, M. J.; Andreotti, R. E., Inter- + intramolecular interactions of alpha-lactalbumin .i. apparent heterogeneity at acid pH. *Biochemistry* 1964, 3, 1145-&.
43. Ohlsson, P. I.; Paul, K. G., Molar absorptivity of horseradish-peroxidase. *Acta Chemica Scandinavica Series B-Organic Chemistry and Biochemistry* 1976, 30, 373-375.
44. Noble, R. W.; Gibson, Q. H., Reaction of ferrous horseradish peroxidase with hydrogen peroxide. *J. Biol. Chem.* 1970, 245, 2409-&.
45. Provencher, S. W.; Glockner, J., Estimation of globular protein secondary structure from circular-dichroism. *Biochemistry* 1981, 20, 33-37.

- 46.** Whitmore, L.; Wallace, B. A., DICHROWEB, an online server for protein secondary structure analyses from circular dichroism spectroscopic data. *Nucleic Acids Res.* 2004, 32, W668-W673.
- 47.** Whitmore, L.; Wallace, B. A., Protein secondary structure analyses from circular dichroism spectroscopy: Methods and reference databases. *Biopolymers* 2008, 89, 392-400.
- 48.** Chang, J. Y.; Li, L., The structure of denatured alpha-lactalbumin elucidated by the technique of disulfide scrambling - Fractionation of conformational isomers of alpha-lactalbumin. *J. Biol. Chem.* 2001, 276, 9705-9712.
- 49.** Wierenga, P. A.; Meinders, M. B. J.; Egmond, M. R.; Voragen, F.; de Jongh, H. H. J., Protein exposed hydrophobicity reduces the kinetic barrier for adsorption of ovalbumin to the air-water interface. *Langmuir* 2003, 19, 8964-8970.
- 50.** Yutani, K.; Ogasahara, K.; Kuwajima, K., Absence of the thermal transition in apo- α -lactalbumin in the molten globule state: A study by differential scanning microcalorimetry. *Journal of Molecular Biology* 1992, 228, 347-350.
- 51.** Harms, G.; Pauls, S.; Hedstrom, J.; Johnson, C., Fluorescence and Rotational Dynamics of Dityrosine. 1997, 7, 283-292.
- 52.** Svensson, M.; Fast, J.; Mossberg, A.-K.; Düringer, C.; Gustafsson, L.; Hallgren, O.; Brooks, C. L.; Berliner, L.; Linse, S.; Svanborg, C., α -Lactalbumin unfolding is not sufficient to cause apoptosis, but is required for the conversion to HAMLET (human α -lactalbumin made lethal to tumor cells). *Protein Science* 2003, 12, 2794-2804.

Chapter 4

Rheological properties of dispersions of enzymatically cross-linked apo- α -lactalbumin nanoparticles

Y. Saricay, P. A. Wierenga, R. de Vries.

This chapter has been submitted to *Food Hydrocolloids*.

Abstract

Whereas the chemical aspects and functional implications of enzymatic cross-linking of food proteins have been extensively studied, very little work has been done on relating the mesoscale structure of cross-linked proteins to their physical properties. Here we characterize the mesoscale structure of peroxidase-cross-linked α -lactalbumin (α -lac) nanoparticles. Atomic force microscopy (AFM) and scanning electron microscopy (SEM) images show that the nanoparticles have an open architecture that consists of protein oligomers that are linked together into branched, fractal-like networks. Approximate overlap concentrations for the nanoparticles are derived from their intrinsic viscosities, and were found to be 4-9% (w/v), for nanoparticles with hydrodynamic radii R_H decreasing from 100 to 25 nm. Next, we explore the rheological properties of dispersions of these nanoparticles as a function of concentration and particle size. Above the overlap concentration (C^*), the storage modulus (G') and apparent viscosity (η) increase exponentially with the concentration of nanoparticles. Both storage and loss modulus are nearly frequency independent. The nanoparticles dispersions are highly shear thinning, and no true zero-shear viscosity can be established. All these features are very similar to the rheology of glassy suspensions of model microgels that have been studied before. The enzymatically cross-linked nanoparticles offer the possibility to create protein hydrogels without using salt, multivalent ions or heating, with features normally not associated with heat-induced protein gels: transparent, reversibly yielding gels at rather low protein concentrations.

Introduction

Whey proteins have very favorable properties as food ingredients, both in terms of food structuring and in terms of nutritional properties (1). The formation of larger structures from proteins such as whey proteins can be induced by both physical (heat, pressure, solvent) and chemical means (2). In particular, heat treatment is most often used to structure food by creating larger protein structures. The most detailed account is probably available for the commercially important whey protein β -lactoglobulin from milk (3). Another important globular protein in whey is the globular protein α -lactalbumin. In contrast to β -lactoglobulin, this protein is rather heat stable, and does not rapidly form heat-induced aggregates (4).

Generally speaking, far away from the isoelectric point and at low ionic strength, heat-induced gels of β -lactoglobulin or whey protein isolate are transparent, having fibrous microstructures, whereas closer to the isoelectric point and at higher ionic strength, opaque gels are formed having fractal-like microstructures (5). Different types of gels can be prepared by tuning environmental conditions, but almost all of these protein gels break irreversibly, which limits their application for food structuring (6, 7).

In order to better control textural properties, some progress can be obtained by using multi-step processes such as cold gelation (8) or cold-set thickening (9). For cold gelation, soluble protein aggregates are induced in a first set of environmental conditions, typically by heating at low ionic strength. The soluble aggregates can be further aggregated into gels by a solvent change at room temperature, e.g. by the addition of salt (10). For cold-set thickening, heat-induced protein gels are freeze-dried and milled down to a derivatized whey protein powder with micron sized particles (11). Dispersions of both soluble protein aggregates and derivatized whey protein powder typically exhibit a high apparent viscosity, and notable shear thinning, usually with some degree of hysteresis at neutral pH (9, 11, 12). These dispersions have been suggested to be useful in a wide range of potential applications such as malted-milk beverages, protein drinks, and nutritious liquid formulations for athletes, infants, or the elderly (9).

In contrast, caseins do not need preprocessing in order to achieve high viscosities at somewhat higher concentrations: when the casein micelles and aggregates in dispersed caseinates start to overlap, the viscosity increases dramatically. Indeed, “jammed” casein micelles and aggregates in caseinate dispersions behave very similar as other soft-glassy materials such as multiarm star polymers (13).

One of the approaches, which is currently being explored to obtain even better control over protein structuring, is enzymatic protein cross-linking. This holds especially for cross-linking catalyzed by microbial transglutaminase, which is already used in various food products that are on the market (14). Microbial transglutaminase is used to increase the viscosity of protein solutions and to induce gelation or modify properties of heat-set protein gels (15-17). Other types of enzymes are also explored, in particular oxidative cross-linking enzymes such as horse-radish peroxidase, tyrosinase and laccase (18).

As opposed to the case of structure formation of proteins due to heating, virtually nothing is known about the structures created by enzymatic protein cross-linking at 1-100 nm length scales, nor is anything known about how these structures determine the final physical properties of the cross-linked protein materials, in particular the rheology. Indeed, food structuring is a complex multiscale issue such that a better understanding of structure-function relations for enzymatically cross-linked protein nanoparticles must be sought at multiple lengthscales. Previously, we have used on-line light scattering, on-line UV spectrophotometry, and Atomic Force Microscopy imaging to study the formation of protein particles during the cross-linking of the whey protein α -lactalbumin mediated by peroxide and the enzyme horse-radish peroxidase (19). The calcium free apo- α -lactalbumin has a molten-globule conformation that is very sensitive to the oxidative cross-linking of its 4 tyrosine residues (20).

The nanostructure during enzymatic cross-linking develops in two stages. In the first stage, protein monomers are cross-linked to form oligomers. Nearly all monomers are converted into oligomers in this stage in which the number of dityrosine bonds increases rapidly, but the solution size of the cross-linked proteins remains small. In the second stage, oligomers formed in the first stage of the reaction are connected to form nanoparticles. In this stage, the particle size increases rapidly, but the number of

dityrosine bonds increases more slowly than in the first stage of the reaction. Eventually the reaction stops due to inactivation of the peroxidase by excess peroxide. The final protein particles have a very open structure with internal protein concentrations of only a few weight percent. AFM images of collapsed and dried nanoparticles show very heterogeneous objects consisting of small subunits.

In addition, we have found that the protein nanoparticles are rather hydrophilic, and have a zeta (ζ) potential that is significantly higher than that of the native protein, making them very stable in solutions. Here we study the rheology of dispersions of these hydrophilic, negatively charged protein nanoparticles. By studying the rheology of dispersions of these well characterized enzymatically cross-linked protein nanoparticles, we can establish a clear relation between the structure of enzymatically cross-linked proteins at 1-100 nm length scales, and the physical properties of the materials that they form.

Materials and methods

Materials

Ca⁺²-depleted α -lactalbumin (apo-form, α -lac) was supplied by Davisco Foods International Inc. (Le Sueur, MN, USA, ~ 85% of α -lac). Horseradish peroxidase (HRP) type VI-A (P6782) and 2,2'-azino-bis 3-ethylbenzthiazoline-6-sulfonic acid (ABTS) were supplied by Sigma-Aldrich. All other chemicals used were of analytical grade.

Enzyme activity

In order to determine the Peroxidase activity before enzymatic reaction, 2,2'-azino-bis 3-ethylbenzthiazoline-6-sulfonic acid (ABTS) assay was performed according to the published procedure (19). We have found that the variation of enzyme activity (specified by the supplier as ~ 900-2000 units/mg) from batch to batch was less than about 12%.

Preparation of nanoparticle dispersion

In order to prepare the stock protein solutions, Peroxidase and α -lac were separately dissolved in ammonium acetate (NH₄Ac) buffer of 0.1 M at pH 6.8 at 25 °C. Before the

enzymatic reaction, α -lac solutions were filtered using 0.1 μm syringe filters to remove protein aggregates. For preparing hydrogen peroxide (H_2O_2) stock solutions, an aqueous solution of 30% (w/v) of peroxide was diluted with deionized water to a concentration of 0.05 M. Concentrations of α -lac, peroxidase and H_2O_2 solutions were determined spectroscopically, using $A_{280} = 20.1$ for a 1% (w/v) solution, $\epsilon_{402.5} = 102.1 \text{ mM}^{-1}\text{cm}^{-1}$ and $\epsilon_{240} = 43.6 \text{ M}^{-1}\cdot\text{cm}^{-1}$, respectively (21-23).

Previously we have found that cross-linking α -lac into nanoparticles changes the molar extinction coefficient by less than 5%, provided their hydrodynamic radius R_H is less than 50 nm (24). Therefore, the concentration of small nanoparticles (with $R_H \leq 50 \text{ nm}$) was determined using UV spectroscopy, using $A_{280} = 20.1$ for a 1% (w/v) solution. For α -lac nanoparticles with R_H of 100 nm, an approximate extinction coefficient is used of $A_{280} = 36$ for a 1% (w/v) solution, that is obtained by extrapolating the experimental values previously obtained for the smaller nanoparticles (24). For the enzymatic cross-linking reactions, α -lac solutions were first mixed with peroxidase solutions and incubated in a 250 mL water-jacketed glass vessel with continuous stirring at 37 $^{\circ}\text{C}$. The weight ratio of protein to enzyme ($R_{\alpha\text{-lac/HRP}} = 20$) was always kept constant for all reactions.

In order to induce the enzymatic cross-linking reaction, peroxide was added using a computer controlled Schott Geräte TA01 titration system. The number of peroxide additions $N(\text{H}_2\text{O}_2)$ and the time interval $\Delta t(\text{H}_2\text{O}_2)$ between H_2O_2 additions, were varied to obtain different particle sizes, as indicated in Table 1. For all enzymatic reactions, the change in the peroxide concentration per addition was $\Delta[\text{H}_2\text{O}_2] = 0.1 \text{ mM}$. After the reaction, nanoparticle dispersions were filtered using 0.45 μm syringe filters and hydrodynamic radii were measured using a Malvern Nanosizer. The specific conditions used in this study are the same as used in a previous study (24), and they are listed in Table 1.

Table.1. Reaction conditions used to produce nanoparticles with various R_H .

R_H (nm)	$C_{\alpha\text{-lac}}$ (mg/mL)	C_{HRP} (mg/mL)	Δt (H_2O_2) (min)	N (H_2O_2)
25	10	0.5	10	80
50	20	1	5	160
100	30	1.5	3.3	240

$C_{\alpha\text{-lac}}$: Concentration of $\alpha\text{-lac}$; C_{HRP} : Concentration of Horseradish peroxidase; Δt (H_2O_2): time intervals between H_2O_2 additions; $N(H_2O_2)$: Number of H_2O_2 additions.

In order to allow prolonged storage of the nanoparticles, reaction products were mixed with 1M sucrose at volume ratio of 1:1 and stored at -80°C for a day. Next, these mixtures were freeze-dried and stored at -20°C . After redissolution, they were excessively dialyzed against 10 mM phosphate buffer at 4°C via a 300 kDa cellulose ester membrane. Hydrodynamic radii of nanoparticles thus obtained by redissolving freeze-dried powders were found to be the same as those before freeze drying, as determined by DLS measurements (24). For experiments, the concentrations of redissolved and dialyzed protein nanoparticles were determined via UV spectroscopy at 280 nm, using the absorption coefficients A_{280} given above. Redissolved and dialyzed protein nanoparticles were concentrated to the final concentrations using Amicon ultra-15 (100 kDa) centrifugal filter units. First, the centrifugal filters were weighed with dialyzed nanoparticles. Next, samples were centrifuged at 8000 g at 10°C until obtaining the concentration required for experiments. Final concentrations were calculated using the weight of the buffer passed through the filter. The concentrated nanoparticle dispersions were then transferred into 1.5 mL Eppendorf tubes using a spatula. In order to remove air bubbles from samples, they were centrifuged at 4000 g for 2 min and stored at 4°C overnight. For each protein nanoparticle size, all experiments were performed using a single batch of freeze-dried nanoparticle powder.

Rheology

All rheological measurements were done using Anton Paar MRC 301 and 501 stress-controlled rheometers. Temperature was controlled by a Peltier system and kept at 20 °C for all experiments. In order to minimize water evaporation, a solvent trap was used for all measurements. After being taken from the 4 °C storage, samples were equilibrated at 20 °C in the rheometer for 15 min, before the start of each experiment. A couette geometry with an inner diameter of 10.835 mm and a gap width of 0.832 mm was used for protein concentration of 0.6; 1.1; 1.7; 2.2 (% w/v). A cone and plate geometry with a cone diameter of 24,969 mm and a cone angle of 0.993° was used for protein concentration of 3.4; 4.5, 5.6 and 10 (% w/v). A fixed sequence was used for the rheological measurements:

1. **Frequency sweep:** Measurements of storage modulus (G') and loss modulus (G'') were performed over an angular frequency range of 0.1 - 10 rad/sec. Strain was fixed at 0.5%, which was found to be within the linear regime. For each frequency sweep, 70 logarithmically spaced frequency points were used. The acquisition time for each frequency was set by the software and varied from 100 sec for the lowest frequency, to 0.1 sec for the highest frequency.
2. **Pause:** 10 min at 20 °C.
3. **Creep compliance:** Creep test were performed at constant stress of 1 Pa for diluted samples (0.2% - 3.4%) and 2 Pa for concentrated samples (4.5% - 5.6%). Both values were within linear regime, as conformed by prior trial experiments. For dilute nanoparticle dispersion (0.6% - 3.4% (w/v)), per test, 10000 measurements points were acquired, each with a measurement time of 0.1 sec. The most concentrated samples (4.5% - 5.6% (w/v)) exhibited very long relaxation times, such that the creep measurements took a very long time (many hours). In order to reduce total measurement time and associated problems such as evaporation, for the concentrated samples, the creep measurements were performed separately, on a new sample. For concentrated nanoparticle dispersions, per test, 10000 measurements points were acquired, each with a measurement time of 1 sec.
4. **Pause:** 10 min.

- 5. Flow curve:** Flow curves were recorded with a shear rate ($\dot{\gamma}$) ramp from 0.01 to 100 s⁻¹ and back to 0.01 s⁻¹. For each curve (either up or down), measurements were performed at 50 logarithmically spaced shear rates, each with a measurement time of 100 sec.

Atomic force microscopy (AFM)

The freeze-dried reaction product with sucrose was dialyzed against 10 mM phosphate buffer at pH 7.0 at 4 °C using 300 kDa cellulose ester membranes (Spectra/Pro Biotech) to remove small oligomers, unreacted monomers and sucrose from the sample solution. The concentration of stock nanoparticle dispersion was determined via UV spectroscopy, as described above. For imaging, dialyzed samples were diluted to 10 µg/mL with demineralized water. First, 20 µL of polylysine solution was incubated for 2 min on a freshly cleaved mica surface, in order to obtain a positively charged surface. Polylysine-coated mica was rinsed with demineralized water and immediately dried with nitrogen. Subsequently, 20 µL of dialyzed sample was incubated for 2 min on the polylysine-modified mica surface, and rinsed by demineralized water, and dried with nitrogen. AFM imaging was performed using a Digital Instruments NanoScope V Multimode Scanning Probe Microscopy with a noncontact ultrasharp silicon cantilever (NT-MDT CSCS11), in the Scan-assist imaging mode.

Scanning electron microscopy (SEM)

Freshly cleaved mica was modified with 0.2% Poly-L-lysine hydrobromide in water (Sigma-Aldrich, Inc., USA) and dried in air for 1h. 40 µL of nanoparticle dispersion (2% (w/v)) was incubated for 30 min on the poly-lysine modified mica. Samples were dehydrated by incubation in a series of acetone/water mixtures of increasing acetone concentration (30, 50, 70, 100% w/v, respectively) for 10 min at each step. Next, samples were dried in a critical point drying device (CPD 030, Baltec, Liechtenstein) and sputter-coated with 2 nm Tungsten.

Volume fraction measurement

The concentration of dialyzed nanoparticle dispersions with various R_H was determined via UV spectroscopy as described above. Next, a concentration series was prepared by diluting nanoparticle dispersions to concentrations ranging from 7.9 mg/mL to 1.1 mg/mL in 10 mM phosphate buffer at pH 7.0. The specific viscosity was measured using an Ostwald capillary viscometer with a 2 mL sample volume attached to a viscosity measurement unit (Schott AVS 350). During the measurements, the viscometer was placed into a water-bath at 25 (± 1) °C. Before the measurements, samples were first equilibrated at 25 °C for 10 min. Next, average flow time for each sample was automatically determined by viscosity measurement unit (Schott AVS 350). Each sample was run 10 times. Specific viscosities η_{sp} were determined from:

$$\eta_{sp} = 1 - \frac{t}{t_0} \quad (1)$$

where t_0 is flow time of buffer; t is flow time of nanoparticles dispersion. Intrinsic viscosities $[\eta]$ were determined from the intercepts of plots of η_{sp}/C versus C , where η_{sp} is the specific viscosity and C is the protein nanoparticle weight concentration (Huggins plot). The intrinsic viscosity is related to an approximate overlap concentration C^* via the Einstein equation for the viscosity of spherical particles:

$$[\eta] = 2.5 / C^* \quad (2)$$

Results and discussion

Meso-structure of peroxidase-cross-linked α -lactalbumin

Development of particle size during cross-linking

Previously, we have reported a procedure for precisely controlling particle size during peroxidase-mediated cross-linking of α -lactalbumin (α -lac) (24). The enzymatic cross-linking requires peroxide, and in order prevent enzyme inactivation, this is added in small

aliquots at regular time intervals. A first approach for controlling particle size is to tune the number of subsequent H_2O_2 additions during a reaction, for example at a fixed protein concentration of 3% (w/v)). A second approach, that we use here, is to vary the initial concentrations of protein and enzyme (this is done at a fixed weight ratio of protein to enzyme $R_{\alpha\text{-lac}/\text{HRP}} = 20$). Results for the development of particle size (hydrodynamic radius R_H determined using dynamic light scattering) during cross-linking at different initial concentrations are shown in Fig.1. Final hydrodynamic radii of the protein particles increase from 25 nm to 100 nm when increasing the initial concentration of α -lac from 1-3% (w/v).

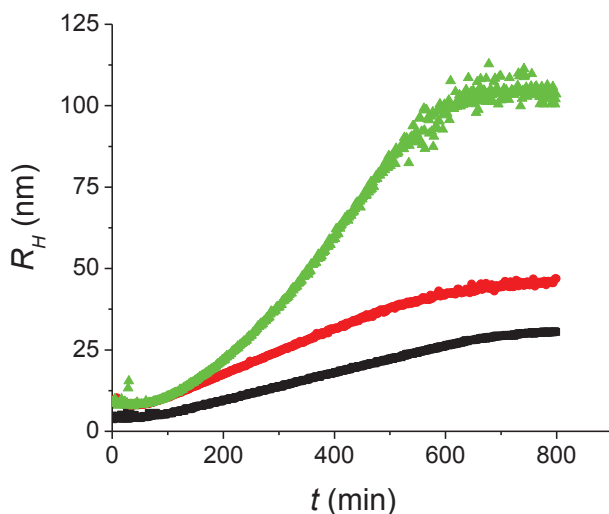


Figure.1. Hydrodynamic radius (R_H) as a function of reaction time during peroxidase-induced cross-linking of α -lac at 37 °C in 0.1 M NH_4Ac at pH 6.8 for different initial protein concentration at a constant weight ratio of protein to enzyme. Black: 1 %; red 2 %; and green: 3 % (w/v).

As can be seen in Fig.1, there is limited growth of particle size during the first 100 min, irrespective of protein concentration. However, the growth speed at later times, and the final particle sizes are strongly concentration dependent. Previously, we have already shown that particles cross-linked to different sizes have a similar branched architecture,

with a size-mass scaling of $R_g \sim M^a$ scaling exponent $a \approx 0.5$, such that the particles become more and more dilute with increasing particle size (19, 24). While most of the rheology results are for dispersions of particles of the largest size ($R_H \approx 100$ nm), the whole series of particles is used in a final section to address the effect of particle size on rheology.

Critical overlap concentration

In order to estimate the critical overlap concentrations (C^*) of cross-linked α -lac particles, we have measured their intrinsic viscosities $[\eta]$ using capillary viscosimetry.

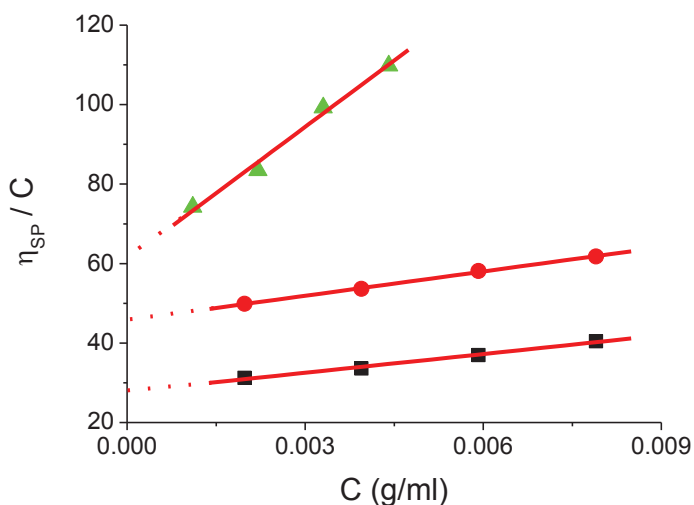


Figure.2. Huggins plots (η_{sp}/C versus C , where η_{sp} is the specific viscosity and C is the concentration) of protein particle dispersions with various hydrodynamic radii R_H : (■) 25 nm; (●) 50 nm; (▲) 100 nm. Solution conditions: 10 mM phosphate buffer at pH 7.0 at 25 °C.

Fig.2 shows Huggins plots for particles with hydrodynamic radii $R_H = 25, 50$ and 100 nm. Values for intrinsic viscosities $[\eta]$ and approximate overlap concentrations C^* (as determined from Eq. (1)) are given in Table 3, which also includes absolute molar masses determined for α -lac particles of similar sizes determined using static light scattering in a previous study (24).

Values for the internal concentration or overlap concentration C^* of the particles are consistent with estimates derived previously (19, 24). The overlap concentrations decrease from 9% (w/v) for the smallest particles with $R_H = 25$ nm, to about 4% (w/v) for the largest particles with $R_H = 100$ nm. As concluded before, the cross-linking mechanism is apparently such that the internal structure becomes more open as particle size increases.

Table.3. Structural properties of enzymatically cross-linked α -lac particles*

Particle Dispersion	R_H (nm)	M_w (10^6 Da)	$[\eta]$ (mL/g)	C^* % (w/v)
1	25	2.1	28	9
2	50	13.8	46	5.5
3	100	154	61	4

* Hydrodynamic radii R_H were obtained by DLS, absolute molar masses are from a previous study (24), and overlap concentrations C^* are estimated from intrinsic viscosities $[\eta]$ via Eq. (2).

AFM and SEM imaging of cross-linked protein

We have explored structural details of the largest particles (R_H of 100 nm) using both AFM and SEM. Fig.3 shows AFM images of dried particles, absorbed on poly-lysine-modified mica. The AFM images show a branched architecture that is very open, and very heterogeneous, as we have previously also observed (but less clearly) for smaller particles (19). The dilute, open structure is not preserved when the particles are adsorbed and dried, and the heights observed in AFM correspond to only a few protein layers. For SEM imaging, relatively high concentrations of the largest protein particles (R_H of 100 nm) were used. In an attempt to better preserve the open architecture and to prevent collapse and flattening, we have used critical point drying to prepare samples.

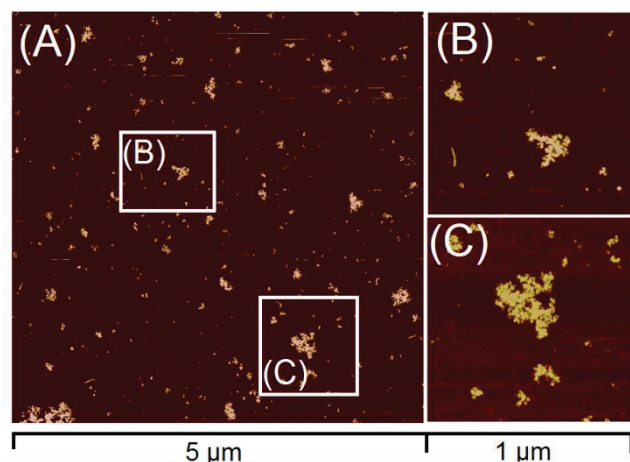


Figure.3. AFM images of dried enzymatically cross-linked α -lac nanoparticles (R_H of 100 nm in bulk) on poly-lysine-modified mica (A) at $5\ \mu\text{m} \times 5\ \mu\text{m}$. (B-C) high resolution AFM images at $1\ \mu\text{m} \times 1\ \mu\text{m}$

Unfortunately, we found that even this rather gentle procedure, cannot prevent collapse of the protein particles during drying. Individual particles cannot be distinguished in the SEM images shown in Fig.4, but a heterogeneous branched structure consisting of small globular objects can be clearly observed.

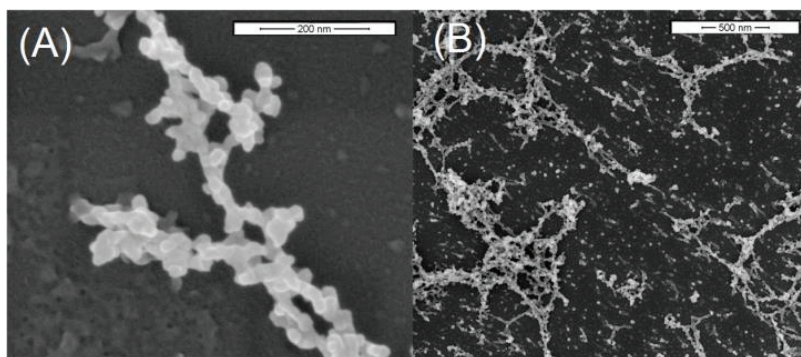


Figure.4. SEM images of enzymatically cross-linked α -lac nanoparticles (R_H of 100 nm) (A) at 400000X magnification (scale bar = 200 nm) (B) at 100000X magnification (scale bar = 500 nm). Samples were prepared using critical point drying.

Rheology

Concentration dependence of moduli

The rheology of dispersions of protein nanoparticles above their overlap concentration is first studied in some detail for the largest nanoparticles, with $R_H = 100$ nm. Frequency dependent storage (G') elastic and loss moduli (G'') are shown in Fig.5, for a range of protein nanoparticle concentrations. We find that storage moduli are higher than loss moduli for nanoparticle concentrations larger than 2.2 % (w/v), which is close to the overlap concentration $C^* = 4$ % (w/v) as estimated for these nanoparticles from viscosimetry. The nanoparticle dispersions have storage and loss moduli that are nearly frequency-independent in the frequency range of 0.1 rad/s – 10 rad/s above the overlap concentration $C^* = 4$ % (w/v). The frequency independent moduli are also found for soft glasses formed from microgels above their overlap concentration (25). At low concentration, such microgels exhibit Brownian motion, but they are kinetically arrested and jammed at higher concentrations (26).

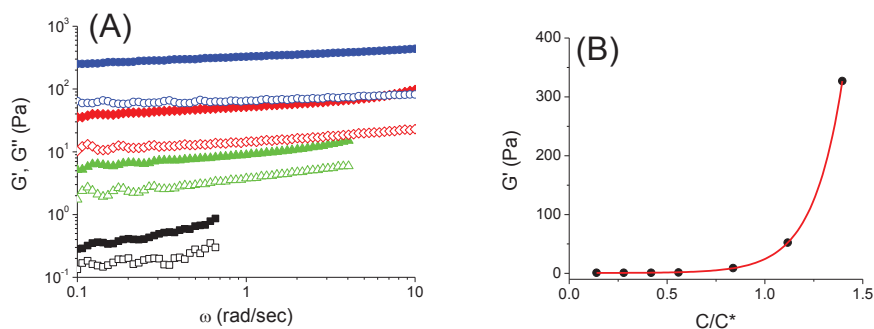


Figure.5. Rheology of dispersions of enzymatically cross-linked α -lac nanoparticles (R_H of 100 nm) in 10 mM phosphate buffer at pH 7.0 at 20°C. (A) Frequency dependence of elastic moduli at various concentrations: (black) (■): 2.2 % (w/v), green (▲): 3.4 % (w/v), red (◆): 4.5 % (w/v); blue (●): 5.6 % (w/v). Closed and open symbols refer G' and G'' , respectively. (B) Concentration dependence of the elastic modulus G' (Pa). The red curve is an exponential fit to the experimental data.

Storage moduli, as determined using oscillatory rheology, increase very rapidly with increasing the concentration of protein nanoparticles, as can be seen in Fig.5B, where the concentration axis has been scaled with the estimated overlap concentration derived from viscosimetry. Shear moduli are very low before the jamming point, and increase very rapidly above C^* . The increase of the shear modulus with concentration is described very well by an exponential function (see fit in Fig.5B), a feature that is highly characteristic of the rheology of dispersions of microgels, provided the micro-particles have internal moduli above a certain threshold (27).

Shear thinning

Another highly characteristic feature of the rheology of microgel dispersions is that their flow curves show extreme shear thinning. Apparent viscosities have no plateau values, and keep increasing with decreasing shear rates (28). We have also determined flow curves for our protein nanoparticle dispersions. Apparent viscosities are shown in Fig.6, for shear rates from 0.1 s^{-1} to 100 s^{-1} , for dispersions of a range of protein nanoparticle concentrations. We find that the highly viscous nanoparticle dispersions at higher concentrations (2.2 % - 5.6 % (w/v)) are extremely shear thinning, again confirming the similarity with the rheology of model microgel dispersions. In addition, flow-curves were very nearly reversible, when performed multiple times (see Fig.6), indicating the reversible nature of the interactions between the protein nanoparticles.

The apparent viscosity increases without bounds as the shear rate is decreased. To demonstrate that this behavior persists down to shear rates much lower than the lowest value of 0.1 s^{-1} used for the flow curves, we have performed creep compliance tests at a low fixed shear stress of 2 Pa, and derived effective viscosities from them. These are shown in Fig.7. For example, the viscosity found at a nanoparticle concentration of 5.6 % w/v from the creep experiment was $5 \cdot 10^6 \text{ Pa.s}$. At a stress of 2 Pa, this corresponds to a shear rate of $4 \cdot 10^{-5} \text{ s}^{-1}$. This should then be compared to an effective viscosity of only 540 Pa.s at shear rate of 0.1 s^{-1} . Hence, the apparent viscosity increases without bounds at lower and lower shear rates, similar to what has been found for model microgel (28) and caseinate dispersions (13).

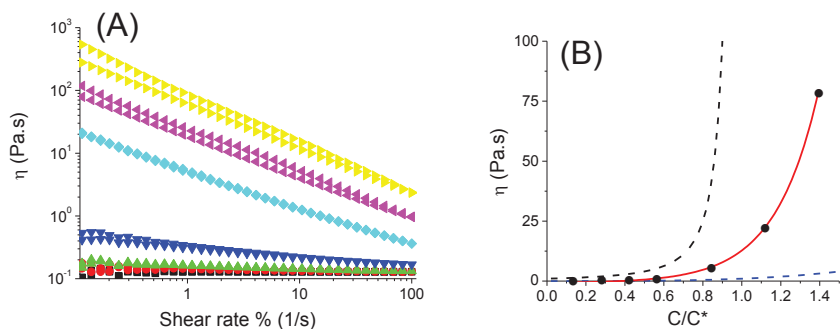


Figure.6. Viscosity of dispersions of enzymatically cross-linked α -lac nanoparticles (R_H of 100 nm, 10 mM phosphate buffer at pH 7.0 at 20 °C). (A) Dependence of apparent viscosity of α -lac nanoparticle dispersions on shear rate for various concentrations: (black (■): 0.6 % (w/v), red (●): 1.1 % (w/v) green (▲): 1.7 % (w/v), blue (▼): 2.2 % (w/v), cyan (◆): 3.4 % (w/v); magenta (◀): 4.5 % (w/v), yellow (▶): 5.6 % (w/v) (B) Apparent viscosity (η) at $d\gamma/dt$ of 1 s^{-1} . The blue dashed line is the characteristic dependence of viscosity on concentration observed for concentrated solutions of flexible polymers: $\eta = (C/C^*)^{3.4}$. The black line dashed is the simplified Krieger–Dougherty's model for hard spheres (black dash line): $\eta = (1 - C/C^*)^{-2}$, The red line is an exponential fit through the experimental data.

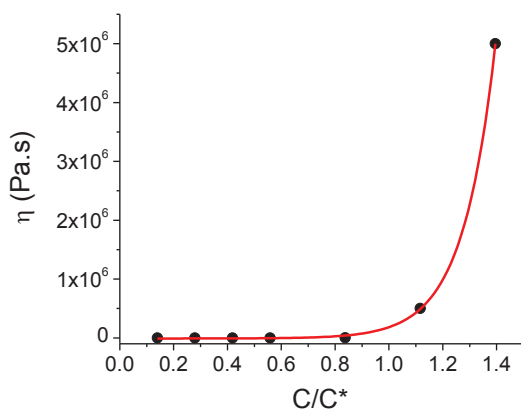


Figure.7. Dependence of apparent viscosity of dispersions of α -lac nanoparticles on concentration at very low shear rates. Apparent viscosities were determined from creep experiments at a low fixed stress of 2 Pa. (R_H of 100 nm, 10 mM phosphate buffer at pH 7.0 at 20 °C).

Finally, the concentration dependence of the apparent viscosity is also very steep, much steeper than the typical power law observed for concentrated flexible polymers (29), $\eta \propto (C/C^*)^{3.4}$, but less steep than for hard spheres (30) that show a true divergence at a critical concentration, $\eta \propto (1 - C/C^*)^{-2}$ (see Fig.6B). Also in this respect, the rheology of the protein nanoparticle dispersions is similar to that of model microgel dispersions studied before (31).

Yielding

The boundless increase of apparent viscosities at low shear rates is often associated with so-called “yield-stress” behavior (32), where a physical network first needs to be destroyed by a finite stress, before the materials will start to flow. Microgel dispersions are a key example of such behavior. Characteristic yielding behavior for microgel dispersions includes a more or less sudden decrease of the storage modulus above a critical value of the shear strain (when measuring in oscillatory deformation at a fixed frequency), accompanied by a peak in the loss modulus at that same critical value of the strain (33, 34). This peak in the loss modulus is sometimes attributed to enhanced dissipation due to elastic rearrangements related to the shear-induced decrease of the structural relaxation time (26). As is shown in Fig.8, this type of yielding behavior is also found for our protein nanoparticle dispersions.

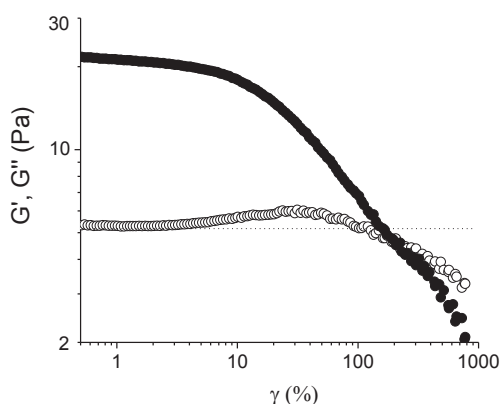


Figure.8. Yielding of dispersions of enzymatically cross-linked α -lac nanoparticles (R_H of 100 nm; 3.9% (w/v) at pH 7.0 in 10 mM phosphate buffer at 20 °C). Strain sweep at a constant frequency of 1 rad s⁻¹. Closed and open symbols refer to G' and G'' , respectively.

Dependence of rheology on nanoparticle size

Finally we investigate how the rheology of nanoparticle dispersions can be tuned by varying the size of the nanoparticle dispersions. The different overlap concentrations of differently sized nanoparticles leads to a different rheology in at least two ways: first, for nanoparticles with higher overlap concentrations, higher concentrations will be needed to achieve jamming. Secondly, higher overlap concentrations also indicate higher internal concentrations inside the nanoparticles and this may give rise to higher internal elastic moduli of the nanoparticles, and this may also affect the macro-scale rheology (35). The frequency-dependent storage and loss moduli of 10 % (w/v) dispersions of differently sized nanoparticles are shown in Fig.9A. Very roughly, we find $G' \sim R_H^3$ and this dependence must have contributions from both effects mentioned above. Finally, we have also performed flow curves for 10 % (w/v) dispersions of differently sized nanoparticles, and the results in Fig.9B shows that the reversible shear thinning of these gels, associated with their yielding behavior, is found for protein nanoparticles of all sizes, and that the nanoparticle size is an ideal parameter to tune the rheology of these protein hydrogels at a given concentration.

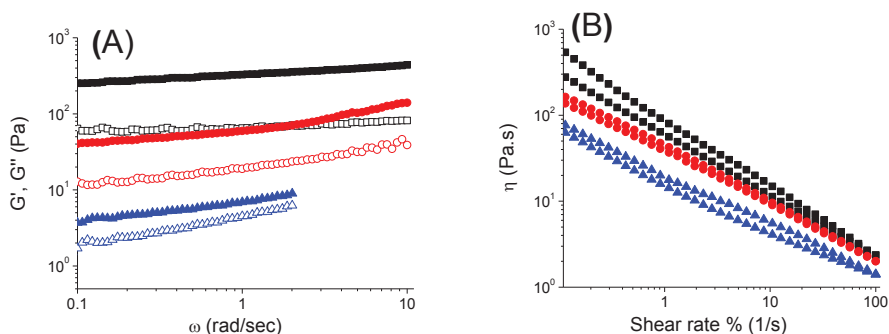


Figure.9. Dependence of rheology of dispersions of enzymatically cross-linked α -lac nanoparticles on particle size (solution conditions 10 mM phosphate buffer at pH 7.0 at 20 °C). (A) Frequency dependences of elastic moduli for a range of particle sizes: blue (\blacktriangle) R_H of 25 nm (C: 10% (w/v)); red (\bullet) R_H of 50 nm (C: 10% (w/v)); black (\blacksquare) R_H of 100 nm (C: 5.6% (w/v)). Closed and open symbols refer G' and G'' , respectively. (B) Dependence of apparent viscosity on shear rate. Labels are the same as in (A).

Concluding remarks

The aim of this study was to explore rheological features of dispersions of our well characterized enzymatically cross-linked protein nanoparticles. Our results highlight that dispersions of the enzymatically cross-linked protein nanoparticles behave very similar soft jammed materials. In view of possible food applications, we specifically compare our system with the rheological behavior of more traditional heat-induced protein microgels and casein micelles.

Many studies have focused on heat-induced whey protein aggregates as viscosifying or thickening agents (9, 12, 36). For modified powder prepared using a multistep process including heat-induced gelation at pH 3.3, freeze-drying and grinding, high viscosities with little hysteresis in apparent viscosity over a range of shear rates, 1.0 – 100 s⁻¹ have been reported for the microgels prepared at the critical concentration of around 7% (w/w) (11).

These systems were suggested to be good protein-based thickeners, useful over a wide range of temperatures and pH values in various in food formulation. These and other dispersions of derivatized whey protein typically exhibit some shear thinning behavior, and a Newtonian plateau at low shear rates (37).

A notable feature of the enzymatically cross-linked α -lac nanoparticles that we study here is their much larger apparent viscosity at similar concentrations and shear rates. For instance, the shear viscosity at 1 s⁻¹ of dispersions of our largest protein nanoparticles (R_H of 100 nm) is approximately 50 times higher than that of WPI microgels (9). Another distinguishing feature is that the dispersions of the enzymatically cross-linked α -lac nanoparticles show no Newtonian plateau, but instead have viscosities that increase without bound when lowering the shear rate. This behavior is fully in line with what is known for the rheology of jammed dispersions of model microgels (38), and is in fact reminiscent of the rheology of sodium caseinate (13), that forms small star-like aggregates in aqueous solution. Caseinate dispersions typically exhibit a strong increase in viscosity at concentrations larger than their overlap concentration C^* , which is about of 10% (w/v) at neutral pH at 20 °C. But, as opposed to dispersions of enzymatically cross-linked α -lac

nanoparticles, caseinate dispersions only exhibit shear-thinning at high shear rates and high concentrations ($C > 14\%$ (w/v)) (39).

Therefore, dispersions of enzymatically cross-linked α -lac truly behave very similar to model systems of repulsive glasses composed of soft, jammed particles (25, 27). The soft yielding, reversible rheology characteristic of these materials is highly desirable in many food applications, but is more typically found for physical networks of polysaccharides than for (heat-induced) protein gels, that are often brittle, and exhibit irreversible failure. While it may be possible to find similar behavior in concentrated dispersions of heat-induced protein aggregates, we believe that the enzymatic cross-linking route may offer additional advantages, and may be complementary to heat-induced aggregation for certain applications.

One possible advantage of enzymatic cross-linking over heat-induced aggregation is that the enzymatic approach may work in cases where heat-induced aggregation does not. For example, α -lac is known to be the most heat-stable whey protein, and typically does not give rise to heat-set gels. Enzymatic cross-linking then offers a route to use this protein (e.g. as a food protein thickener) for food structuring applications. Other possible advantages are that via the enzymatic cross-linking route it is possible to avoid or minimize the extent of heating during processing, and to form irreversible covalent rather than reversible physical bonds.

In order to profit from these and other possible advantages of enzymatic protein cross-linking, a detailed structural and physical characterization of enzymatically cross-linked protein is crucial, and the present work contributes to this by providing detailed insight into the structure-function relations for peroxidase-cross-linked α -lac nanoparticles.

Acknowledgement

This work is part of the Industrial Partnership Programme (IPP) Bio(-Related)Materials of the Stichting voor Fundamenteel Onderzoek der Materie (FOM), which is financially supported by the Nederlandse Organisatie voor Wetenschappelijk Onderzoek (NWO). The

IPP BRM is co-financed by the Top Institute Food and Nutrition and the Dutch Polymer Institute.

References

1. Purwanti, N.; van der Goot, A. J.; Boom, R.; Vereijken, J., New directions towards structure formation and stability of protein-rich foods from globular proteins. *Trends Food Sci. Technol.* **2010**, *21*, 85-94.
2. Totosaus, A.; Montejano, J. G.; Salazar, J. A.; Guerrero, I., A review of physical and chemical protein-gel induction. *Int. J. Food Sci. Technol.* **2002**, *37*, 589-601.
3. Nicolai, T.; Britten, M.; Schmitt, C., beta-Lactoglobulin and WPI aggregates: Formation, structure and applications. *Food Hydrocolloids* **2011**, *25*, 1945-1962.
4. McGuffey, M. K.; Epting, K. L.; Kelly, R. M.; Foegeding, E. A., Denaturation and aggregation of three alpha-lactalbumin preparations at neutral pH. *J. Agric. Food Chem.* **2005**, *53*, 3182-3190.
5. Foegeding, E. A.; Davis, J. P.; Doucet, D.; McGuffey, M. K., Advances in modifying and understanding whey protein functionality. *Trends Food Sci. Technol.* **2002**, *13*, 151-159.
6. Banerjee, S.; Bhattacharya, S., Food Gels: Gelling Process and New Applications. *Crit. Rev. Food Sci. Nutr.* **2012**, *52*, 334-346.
7. Li, H.; Errington, A. D.; Foegeding, E. A., Isostrength comparison of large-strain (fracture) rheological properties of egg white and whey protein gels. *J. Food Sci.* **1999**, *64*, 893-898.
8. Itling, A. C.; Hamer, R. J.; De Kruif, C. G.; Visschers, R. W., Cold-set globular protein gels: Interactions, structure and rheology as a function of protein concentration. *J. Agric. Food Chem.* **2003**, *51*, 3150-3156.
9. Hudson, H. M.; Daubert, C. R.; Foegeding, E. A., Rheological and physical properties of derivitized whey protein isolate powders. *J. Agric. Food Chem.* **2000**, *48*, 3112-3119.
10. Bryant, C. M.; McClements, D. J., Molecular basis of protein functionality with special consideration of cold-set gels derived from heat-denatured whey. *Trends Food Sci. Technol.* **1998**, *9*, 143-151.
11. Mudgal, P.; Daubert, C. R.; Foegeding, E. A., Cold-set thickening mechanism of beta-lactoglobulin at low pH: Concentration effects. *Food Hydrocolloids* **2009**, *23*, 1762-1770.
12. Daubert, C. R.; Hudson, H. M.; Foegeding, E. A.; Prabhasankar, P., Rheological characterization and electrokinetic phenomena of charged whey protein dispersions of defined sizes. *LWT-Food Sci. Technol.* **2006**, *39*, 206-215.
13. Panouille, M.; Durand, D.; Nicolai, T., Jamming and gelation of dense beta-casein micelle suspensions. *Biomacromolecules* **2005**, *6*, 3107-3111.
14. Jaros, D.; Partscheveld, C.; Henle, T.; Rohm, H., Transglutaminase in dairy products: Chemistry, physics, applications. *J. Texture Stud.* **2006**, *37*, 113-155.
15. Eissa, A. S.; Bislam, S.; Khan, S. A., Polymerization and gelation of whey protein isolates at low pH using transglutaminase enzyme. *J. Agric. Food Chem.* **2004**, *52*, 4456-4464.
16. Menendez, O.; Schwarzenbolz, U.; Rohm, H.; Henle, T., Casein gelation under simultaneous action of transglutaminase and glucono-delta-lactone. *Nahr.-Food* **2004**, *48*, 165-168.

17. Truong, V. D.; Clare, D. A.; Catignani, G. L.; Swaisgood, H. E., Cross-linking and rheological changes of whey proteins treated with microbial transglutaminase. *J. Agric. Food Chem.* **2004**, *52*, 1170-1176.
18. Buchert, J.; Cura, D. E.; Ma, H.; Gasparetti, C.; Monogioudi, E.; Faccio, G.; Mattinen, M.; Boer, H.; Partanen, R.; Selinheimo, E.; Lantto, R.; Kruus, K., Crosslinking Food Proteins for Improved Functionality. In *Annual Review of Food Science and Technology, Vol 1*, Doyle, M. P.; Klaenhammer, T. R., Eds. Annual Reviews: Palo Alto, 2010; Vol. 1, pp 113-138.
19. Saricay, Y.; Wierenga, P.; de Vries, R., Nanostructure development during peroxidase catalysed cross-linking of alpha-lactalbumin. *Food Hydrocolloids* **2013**, *33*, 280-288.
20. Heijnis, W. H.; Wierenga, P. A.; Berkel, W. J. H.; Gruppen, H., Directing the Oligomer Size Distribution of Peroxidase-Mediated Cross-Linked Bovine alpha-Lactalbumin. *J. Agric. Food Chem.* **2010**, *58*, 5692-5697.
21. Kronman, M. J.; Andreotti, R. E., Inter- + intramolecular interactions of alpha-lactalbumin .i. apparent heterogeneity at acid pH. *Biochemistry* **1964**, *3*, 1145-&.
22. Ohlsson, P. I.; Paul, K. G., Molar absorptivity of horseradish-peroxidase. *Acta Chemica Scandinavica Series B-Organic Chemistry and Biochemistry* **1976**, *30*, 373-375.
23. Noble, R. W.; Gibson, Q. H., Reaction of ferrous horseradish peroxidase with hydrogen peroxide. *J. Biol. Chem.* **1970**, *245*, 2409-&.
24. Dhayal, S. K.; Gruppen, H.; de Vries, R.; Wierenga, P. A., Controlled formation of protein nanoparticles by enzymatic cross-linking of alpha-lactalbumin with horseradish peroxidase. *Food Hydrocolloids* **2014**, *36*, 53-59.
25. Menut, P.; Seiffert, S.; Sprakel, J.; Weitz, D. A., Does size matter? Elasticity of compressed suspensions of colloidal- and granular-scale microgels. *Soft Matter* **2012**, *8*, 156-164.
26. Shao, Z.; Negi, A. S.; Osuji, C. O., Role of interparticle attraction in the yielding response of microgel suspensions. *Soft Matter* **2013**, *9*, 5492-5500.
27. Mattsson, J.; Wyss, H. M.; Fernandez-Nieves, A.; Miyazaki, K.; Hu, Z. B.; Reichman, D. R.; Weitz, D. A., Soft colloids make strong glasses. *Nature* **2009**, *462*, 83-86.
28. Ketz, R. J.; Prudhomme, R. K.; Graessley, W. W., Rheology of concentrated microgel solutions. *Rheol. Acta* **1988**, *27*, 531-539.
29. Heo, Y.; Larson, R. G., The scaling of zero-shear viscosities of semidilute polymer solutions with concentration. *Journal of Rheology* **2005**, *49*, 1117-1128.
30. Vlassopoulos, D., Colloidal star polymers: Models for studying dynamically arrested states in soft matter. *J. Polym. Sci. Pt. B-Polym. Phys.* **2004**, *42*, 2931-2941.
31. Omari, A.; Tabary, R.; Rousseau, D.; Calderon, F. L.; Monteil, J.; Chauveteau, G., Soft water-soluble microgel dispersions: Structure and rheology. *Journal of colloid and interface science* **2006**, *302*, 537-546.
32. Walls, H. J.; Caines, S. B.; Sanchez, A. M.; Khan, S. A., Yield stress and wall slip phenomena in colloidal silica gels. *Journal of Rheology* **2003**, *47*, 847-868.
33. Kobelev, V.; Schweizer, K. S., Yielding, strain softening and shear thinning in glassy colloidal suspensions. *Abstr. Pap. Am. Chem. Soc.* **2005**, *229*, U652-U652.

- 34.** Zhou, Z.; Hollingsworth, J. V.; Hong, S.; Cheng, H.; Han, C. C., Yielding Behavior in Colloidal Glasses: Comparison between “Hard Cage” and “Soft Cage”. *Langmuir : the ACS journal of surfaces and colloids* **2014**.
- 35.** Thaiboonrod, S.; Milani, A. H.; Saunders, B. R., Doubly crosslinked poly(vinyl amine) microgels: hydrogels of covalently inter-linked cationic microgel particles. *Journal of Materials Chemistry B* **2014**, *2*, 110-119.
- 36.** Eissa, A. S.; Mohamed, D. M.; Uoness, K. S.; Azab, M. M.; Abed, N. S.; Abu El-Aish, D., characterization of rheological and molecular properties of whey protein thickeners. *International Journal of Food Properties* **2014**, *17*, 570-586.
- 37.** Resch, J. J.; Daubert, C. R., Rheological and physicochemical properties of derivatized whey protein concentrate powders. *International Journal of Food Properties* **2002**, *5*, 419-434.
- 38.** Berli, C. L. A.; Quemada, D., Rheological modeling of microgel suspensions involving solid-liquid transition. *Langmuir : the ACS journal of surfaces and colloids* **2000**, *16*, 7968-7974.
- 39.** Pitkowski, A.; Durand, D.; Nicolai, T., Structure and dynamical mechanical properties of suspensions of sodium caseinate. *Journal of colloid and interface science* **2008**, *326*, 96-102.

Chapter 5

High stability of enzymatically cross-linked apo- α -lactalbumin nanoparticles against thermal aggregation

Y. Saricay, P. A. Wierenga, R. de Vries.

Manuscript in preparation.

Abstract

Avoiding the detrimental effects of heat-induced protein aggregation is a key requirement for food processing steps that involve heating. Here we explore oxidative cross-linking as a means to create heat-stable protein nanoparticles. Cross-linking of the tyrosine residues of calcium free α -lactalbumin (apo- α -lac) is induced by horseradish peroxidase under the periodic addition of peroxide. The enzymatic reaction leads to the formation of negatively charged, hydrophilic protein nanoparticles with hydrodynamic sizes $R_H = 25$ -100 nm and a low internal protein content, less than 9 % (w/v.) From circular dichroism (CD), we find that, when the cross-linked proteins are heated for 1h at 90 °C and at pH 5.7, there are only minor changes in the percentage of α -helical secondary structure. As also observed for native apo- α -lac under the same conditions, the changes in secondary structure that do occur upon heating are mostly reversible. Nevertheless the heat treatment leads to a strong increase of the surface hydrophobicity of native apo- α -lac, and even to thermal aggregation as deduced from turbidity measurements. In contrast, we find that under the same conditions, for the cross-linked apo- α -lac nanoparticles, the heat treatment even leads to a decrease of the surface hydrophobicity. The cross-linking leads to a more negative zeta-potential that is not influenced by heating, and we observe that the protein nanoparticles are highly resistant to thermal aggregation. Even dense dispersions of the protein nanoparticles (that form reversible, shear-thinning hydrogels) can be heated with only a minor influence on their rheology. For native apo- α -lac, differential scanning calorimetry (DSC) shows an endothermic transition at 35 °C, but for cross-linked apo- α -lac nanoparticles, we find a broad exothermic transition from 75-110 °C. The latter presumably points to the formation of some additional physical or chemical bonds in the particles during heating. These novel results on the structural changes and colloidal stability of cross-linked apo- α -lac under heating, provide insight in the enhanced heat stability of proteins upon enzymatic cross-linking, and may provide a new strategy to design heat stable protein nanoparticles for food applications.

Introduction

One of the challenges in food technology is to design heat stable protein particles that can be used as an ingredient in various (heat stable) food formulations (1). Whey proteins can serve a number of structural functions and enhance nutritional value in food products. Whereas whey proteins are widely used in food technology, they easily undergo unfolding above their melting temperature, which leads to exposed hydrophobicity and protein aggregation (2). Some of the detrimental effects of heat-induced protein aggregation in various food formulations may include e.g. sedimentation, flocculation, phase separation, and other undesirable changes in texture and sensory properties, which limit their application (3, 4).

One approach to limit the detrimental effects of thermal protein aggregation is to use soluble protein aggregates prepared using a heat preprocessing step. Soluble protein aggregates are obtained when whey protein solutions are heated below their critical gelation concentration (i.e. 12% w/w) (5, 6). Some physical properties of soluble protein aggregates have been hypothesized to enhance thermal stability (7): a high charge, small size, compact structure, and/or low surface hydrophobicity. Another form of protein preprocessing is micro and/or nanoparticulation of heat-denatured proteins, and this has also been utilized to improve the thermal stability of proteins (8, 9). Indeed, whey protein micro- and nano-particles have been reported to have higher thermal stability, resulting in reduced turbidities after heating as compared to native WPI (10). While a heat preprocessing step may lead to improved thermal stability, it may also have detrimental effects on the protein functionality and nutritional value (11).

An alternative approach to enhancing the thermal stability of proteins is through the use of enzymatic protein cross-linking (12). Enzymatic cross-linking is a versatile approach that can lead to various protein modifications at mild reaction conditions. Since it is highly specific and since stable covalent cross-links are generated due to the enzymatic reactions, it is expected to be a route that may ultimately lead to a very good control over protein modifications (13). Specifically, the cross-linking activity of the microbial enzyme transglutaminase (mTG) has been found to lead to an increase of the

denaturation temperature of β -lactoglobulin (β -Lg) at neutral pH (14-16). Cross-linking by mTG has also been shown to lead to a reduced increase in the turbidity of sodium caseinate after heating (17). Furthermore, mTG-treated milk has an improved thermal stability at pH > 6.5 (18). While these results are promising, mTG also leads to changes in the hydrophobic-hydrophilic balance of the substrate proteins upon enzymatic cross-linking (16), which, in turn, may lead to undesirable precipitation of cross-linked protein at pH 4.0 – 5.0.

Hence it would be very interesting to explore whether other cross-linking enzymes maybe lead to similar changes in heat-stability without these unfavorable shifts in the hydrophobic-hydrophilic balance of the substrate proteins. In particular, oxidative protein cross-linking (e.g. protein cross-linking catalyzed by laccase, peroxidase and tyrosinase) has seen a growing interest in food technology in recent years, since oxidative enzymes differ in cross-linking chemistry and may induce different techno-functional properties as compared to mTG (13). For instance, the thermal stability of myosin can be improved by Laccase treatment whereas mTG-catalyzed cross-linking reduces heat stability of this protein (19). Tyrosinase-catalyzed cross-linking of chicken breast myofibrils proteins leads to a decrease in denaturation temperature for myosin whereas it leads to an increase in the denaturation temperature of actin (20). These observations clearly imply that enzymatic cross-linking of proteins using different enzymes, leads to the different effects on thermal stability.

Previously, we have extensively characterized the formation, structure and physical properties of peroxidase-cross-linked nanoparticles of calcium free α -lactalbumin (apo- α -lac), but so far, the effect of the cross-linking on the heat-stability, has not been addressed (21-24). Therefore, we here investigate the thermal properties of protein particles created using peroxidase-catalyzed cross-linking.

For this system, particle formation occurs mainly through the formation of tyrosine-tyrosine bonds (25). Cross-linking leads to a moderate loss of the percentage of α -helical secondary structure, but the remaining degree of secondary structure is much larger than for the heat-denatured protein (24). The nanoparticles have typical hydrodynamic radii R_H = 25 – 100 nm, and a rather open structure, with internal protein concentrations ranging

from 4-9 % (w/v), depending on their size (23). The protein nanoparticles are very hydrophilic and have excellent colloidal stability from acidic to neutral pH, except in the narrow region of pH=4.5 – 5.5. Dense, jammed dispersions of the protein particles form soft, reversibly yielding physical hydrogels (23).

For potential applications, it will be crucial to know how these unique enzymatically cross-linked protein nanoparticles respond to heating. In particular, one would like to know whether the increased heat-stability reported to result from enzymatically cross-linking of proteins into small oligomers (14, 15) also occurs for our much larger enzymatically cross-linked nanoparticles. Therefore, we here systematically explore the effect of heating on protein nanoparticles produced by the oxidative cross-linking of apo- α -lac. As we will discuss at length, we indeed do find that the enzymatically cross-linked apo- α -lac nanoparticles exhibit remarkable heat stability, even at very high concentrations.

Materials and methods

Materials

Ca⁺²-depleted- α -lactalbumin (apo- α -lac) was supplied by Davisco and was used without any purification. This commercial preparation of apo- α -lac consists of about 85 % of apo-form and 15 % of holo-form (Ca⁺²-saturated- α -lactalbumin). The calcium content is reported to be less than 0.3 mol Ca⁺² per mol of α -lactalbumin. Horseradish peroxidase (HRP) type VI-A (P6782), ABTS (2,2'-azino-bis(3-ethylbenzthiazoline-6-sulfonic acid) was supplied by Sigma-Aldrich. All other chemicals used were of analytical grade.

Sample preparation

In order to prepare the stock protein solutions, Peroxidase and apo- α -lac were separately dissolved in an ammonium acetate (NH₄Ac) buffer of 0.1 M at pH 6.8, 25 °C. Before the enzymatic reaction, apo- α -lac solutions were filtered using 0.1 μ m syringe filters to remove protein aggregates. For preparing hydrogen peroxide (H₂O₂) stock solutions, an aqueous solution of 30 % (w/w) of peroxide was diluted with deionized water to a concentration of 0.05 M. Concentrations of α -lac, peroxidase and H₂O₂ solutions were

determined by UV spectroscopy, using $A_{280} = 20.1$ for a 1 % (w/v) solution (26), $\epsilon_{403} = 102.1 \text{ mM}^{-1}\text{cm}^{-1}$ (27) and $\epsilon_{240} = 43.6 \text{ M}^{-1}\text{cm}^{-1}$ (28) for α -lac, peroxidase and H_2O_2 , respectively.

Enzymatic reaction

For the enzymatic cross-linking reactions, α -lac solutions were first mixed with peroxidase solutions and incubated in a 250-mL water-jacketed glass vessel with continuous stirring at 37°C for 1 h. The weight ratio of protein to enzyme was $R_{\alpha\text{-lac}/\text{HRP}} = 20$, the molar ratio of H_2O_2 to enzyme was $R_{\text{H}_2\text{O}_2/\text{HRP}} = 10$. These ratios were always kept constant for all reactions. The H_2O_2 concentration refers to the amount added per 10 min. In order to induce the enzymatic cross-linking reaction, peroxide was periodically added using a computer controlled Schott Geräte TA01 titration system. The number of peroxide additions $N(\text{H}_2\text{O}_2)$ and the time interval $\Delta t(\text{H}_2\text{O}_2)$ between H_2O_2 additions, were varied for controlling particle size. For all enzymatic reactions, the change in the peroxide concentration per addition was always $\Delta[\text{H}_2\text{O}_2] = 0.1 \text{ mM}$. After each reaction, nanoparticle dispersions were filtered using $0.45 \mu\text{m}$ syringe filters and hydrodynamic radii were measured using a Malvern Nanosizer. The specific conditions to form nanoparticles that we tested in this study with various hydrodynamic radii R_H are the same as those used in a previous study (23). They are listed in Table 1.

Table.1. Reaction conditions used to produce nanoparticles with various hydrodynamic radii R_H .

R_H (nm)	$C_{\alpha\text{-lac}}$ (mg/mL)	C_{HRP} (mg/mL)	$\Delta t(\text{H}_2\text{O}_2)$ (min)	$N(\text{H}_2\text{O}_2)$
25	10	0.5	10	80
100	30	1.5	3.3	240

$C_{\alpha\text{-lac}}$: Concentration of apo- α -lactalbumin (mg/mL); C_{HRP} : Concentration of horseradish peroxidase (mg/mL); $\Delta t(\text{H}_2\text{O}_2)$: time intervals of added H_2O_2 (s); $N(\text{H}_2\text{O}_2)$: Number of H_2O_2 additions.

Freeze-drying and dialysis

In order to allow for prolonged storage of the nanoparticles, reaction products were first mixed by 1M sucrose at volume ratio of 1:1 and stored at -80°C for a day. This was

followed by freeze-drying and storage at -20°C . After redissolution, protein nanoparticles were extensively dialyzed against 10 mM sodium phosphate buffer at 4°C using 300 kDa cellulose ester membranes. Hydrodynamic radii of nanoparticles from redissolved freeze-dried powders (1 mg/mL) were found to be the same as those immediately after the reaction. Concentrations of protein nanoparticles with R_H of 25 nm and 100 nm were determined using UV spectroscopy, assuming $A_{280} = 20.1$ and $A_{280} = 36$ for a 1% (w/v) protein solution, respectively (23).

For measurements on dilute particle dispersions of the smallest particles ($R_H = 25$ nm), after the determination of the protein concentration, redissolved and dialyzed nanoparticles were diluted to the required concentrations and used immediately. For rheological measurements on concentrated dispersions of the larger nanoparticles (R_H of 100 nm), redissolved and dialyzed particles were concentrated using Amicon ultra-15 (100 kDa) centrifugal filter units. Samples were centrifuged at 8000 g and at 10°C until obtaining the desired final concentration. Final protein concentrations of the concentrated dispersions were determined by weighing the samples in the centrifugal filters before and after centrifugation, and by also weighing the amount of buffer that was extracted from the sample by centrifugation. Concentrated protein particle dispersions were transferred from the filter into 1.5 mL Eppendorf tubes using a spatula. In order to remove air bubbles from samples, they were first centrifuged at 4000 g for 2 min and subsequently stored at 4°C , overnight. All experiments were performed using a single batch of freeze-dried protein particle powder.

Structural analysis

Far-UV CD spectra were acquired using a Jasco J-715 spectropolarimeter (Tokyo, Japan) equipped with a PTC-348WI Peltier temperature control system. Quartz cuvettes (Starna, Hainault, UK) with a 1-mm cell length were used, measurements were performed at 20°C . Each spectrum is an average of at least 20 wavelength scans. Percentages of secondary structure elements (α -helix, β -strands, β -turns and random coil) were deduced from spectra (θ , milidegrees) using the ridge regression algorithm CONTINLL as implemented by the Dichroweb webserver provided by The University of London (29, 30).

Determination of hydrodynamic radius (R_H) and zeta (ζ) potential

Dynamic light scattering (DLS) and electrophoretic light scattering (ELS) experiments were done on dialyzed reaction products using a Malvern Nanosizer ZS (Malvern) equipped with an Argon ion laser emitting vertically polarized light with a wavelength of 633 nm. For DLS measurements, the scattering angle was 173° . For ELS measurements, the scattering angle was 12.8° . Average hydrodynamic radii R_H and ζ -Potential reported are the major peaks from a peak analysis as performed by the Malvern DTS software, version 6.20. For DLS, protein samples were measured in a low-volume quartz batch cuvette (ZEN2112). For ζ -potential measurements, a disposable capillary cell (DTS1070) was used. For both DLS and ζ -potential measurements, the protein concentration of the samples was 1 mg/mL. For only determining stability of protein particles at different pH upon heating, protein concentration of 4.4 mg/mL was used.

Fluorescence spectroscopy

Fluorescence spectra of native apo- α -lac and enzymatically cross-linked apo- α -lac particles were acquired using a Perkin Elmer Luminescence Spectrometer LS 50 B spectrofluorimeter. For all experiments, a quartz cuvette with a 1-cm excitation path length was used, and the temperature was 25°C . Protein samples were diluted to the required final concentrations (0.1 mg/mL) using 10 mM sodium phosphate buffer at pH 7.0 at 25°C . Emission spectra were acquired for wavelengths between 330 nm and 550 nm, using an excitation wavelength of 315 nm. Excitation and emission slits were set at 5 nm.

Surface hydrophobicity

A stock solution of 8-anilino-1-naphthalenesulfonic acid (ANSA) with a concentration of 2.4 mM was prepared in 10 mM sodium phosphate buffer, pH 7.0 at 25°C . The ANSA stock solution was stored at 4°C overnight to ensure complete dissolution. Protein samples were diluted to their final concentrations (0.1 mg/mL) into 10 mM sodium phosphate buffer at pH 7.0 at 25°C . 10 μL aliquots of ANSA were titrated into 1 mL protein solutions. Fluorescence spectra were recorded for emission wavelengths between 400 and 650 nm,

using an excitation wavelength of 365 nm, a scan speed of 120 nm/min and excitation and emission slits of 5 nm. All measurements were done at 20 °C. The relative exposed hydrophobicity of each sample was taken to be the difference between minimum and maximum area integrated under titration curve between 400 nm and 600 nm after blank subtraction.

Differential scanning calorimeter

Differential scanning calorimetry was performed using a MicroCal VP-DSC. Apo- α -lac or enzymatically cross-linked apo- α -lac (both 4 mg/mL) in 10 mM sodium phosphate buffer at pH 7.0 were placed in the sample cell while the reference cell was filled with 10 mM sodium phosphate buffer at pH 7.0. After 10 min of equilibration, the heat flow was recorded while increasing the temperature from 20 °C to 120 °C at a rate of 60 °C/h. Next, the system was immediately cooled down 20 °C, and another temperature scan was initiated. All measurements were done in triplicate. Final DSC curves were obtained by averaging the multiple measurements.

Turbidity measurements

Turbidity measurements were carried out using Hitachi spectrophotometer at a wavelength of 400 nm. Temperature of sample holder was controlled by a temperature controller SPR-10. The turbidity was determined for 1.5 mL samples in a 1 cm path length quartz cuvette, at a temperature of 90 °C. The turbidity τ was defined as:

$$\tau = -\ln(I / I_0) \quad (1)$$

where I/I_0 is the ratio of the intensities of the transmitted and incoming light.

Rheology

For detecting changes in rheology of concentrated samples of protein nanoparticles, samples were heated at 80 °C for 15 min or 60 min in an oven. Next the samples were rapidly cooled down using running cold tap water. After being kept at 25 °C for 15 min, samples were equilibrated at 20°C in the rheometer for another 15 min, before the experiments were started. All rheological measurements were done using an Anton Paar

MRC 301 stress-controlled rheometer. The temperature was controlled by a Peltier system and kept at 20 °C for all experiments. In order to minimize water evaporation, a solvent trap was used for all measurements. Rheological measurements were carried out in a cone-plate geometry with a cone diameter of 24,969 mm and a cone angle of 0.993°. A fixed sequence was used for rheological measurements on all samples:

- (1) **Frequency sweep:** Storage moduli (G') and loss moduli (G'') were determined for an angular frequency range of 0.1 - 10 rad/sec at a fixed strain of 0.5 %. This was found to be within the linear strain regime. For each frequency sweep, 100 points were acquired on a logarithmically spaced frequency axis. Acquisition time for each frequency was set by the instrument software and varied from 200 sec for the lowest frequency, to 0.1 sec for the highest frequency.
- (2) **Pause:** 10 min at 20 °C.
- (3) **Flow curve:** Apparent viscosities were determined for shear rates from $\dot{\gamma} = 0.01 \text{ s}^{-1}$ to 100 s^{-1} and then back to 0.01 s^{-1} . For each curve (either up or down), measurements were performed at 50 logarithmically spaced shear rates, each with a measurement time of 100 sec.

Results and discussion

The effect of pH on heat stability

As compared to the β -lactoglobulin, the whey protein α -lactalbumin is much more stable against heat-induced aggregation. Nevertheless, there are certainly conditions under which it undergoes aggregation upon heating (31). We use turbidity and light scattering for a first evaluation of the thermal stability of enzymatically cross-linked apo- α -lac nanoparticles, as compared to that of native apo- α -lac. Fig.1 shows that the turbidity of native apo- α -lac solutions remains close to zero at pH 3.0 and 7.0 during heating, but rapidly increases when heating at pH 5.7 (90 °C for 3 min.), indicating protein aggregation. For cross-linked apo- α -lac nanoparticle solutions, however, the turbidity does not change upon heating at pH 5.7 (even though the initial turbidity is much higher due to the much larger particle size and adsorption of cross-linked apo- α -lac nanoparticles).

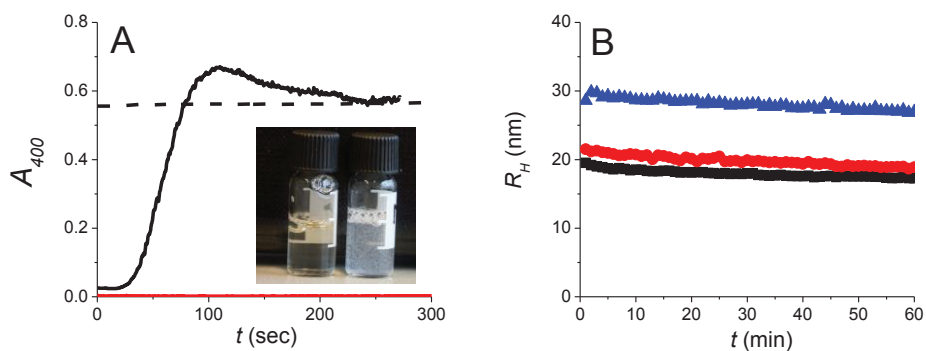


Figure.1. Stability of apo- α -lac and cross-linked apo- α -lac nanoparticles against thermal aggregation as a function of pH. (A) Turbidity as a function of time during heating at 90 °C: apo- α -lac at pH 3.0 (blue), pH 5.7 (black), pH 7.0 (red) and α -lac nanoparticles (dash black line) in 10 mM sodium phosphate buffer (B) Hydrodynamic radius (R_H) of α -lac nanoparticles as a function of time during heating at 90 °C: pH 3.0 (blue), pH 5.7 (red), pH 7.0 (black) in 10 mM sodium phosphate buffer. For turbidity and DLS measurements, protein concentration of 4.4 mg/mL was used.

We have also shown that turbidity of α -lac nanoparticle solution does not change when heating at higher salt concentrations at pH 5.7 (up to 0.5 M NaCl, see supplementary data). For a more sensitive probe of aggregation, we also used DLS to follow the hydrodynamic radius of the cross-linked apo- α -lac nanoparticles as a function of time during heating. As shown in Fig.1B, hydrodynamic radii of apo- α -lac nanoparticles at both acidic and neutral pH remain very nearly constant upon heating at 90 °C, showing only a slight decrease over the particle radii over time. Hence, there is no aggregation of apo- α -lac nanoparticles when they are heated, for a wide range of pH values and salt concentrations. However, during zeta-potential measurements (to be discussed below), we did note that there is a narrow range of pH values (pH 4.5 - 5.5) for which the samples become somewhat turbid (visual observation, data not shown).

Hence, we find that that solutions of apo- α -lac nanoparticles prepared by full oxidative cross-linking show no turbidity increase when heated at pH 5.7, whereas under the same conditions, the native apo- α -lac aggregates rapidly, leading to a fast increase of turbidity. Similar reductions of turbidity after heating have been reported for proteins

cross-linked using mTG (32). More specifically it was shown for whey protein isolate that an increased incubation time with mTG leads to a lower turbidity after heating (33).

The effect of heating on physical properties

Zeta potential

The colloidal stability of protein nanoparticles sensitively depends on the balance between repulsive and attractive interactions of protein particles. A key role for colloidal stabilization is played by electrostatic repulsion, that can be assessed qualitatively by measuring the zeta potential (ζ) of the particles. Previously, we have found that the ζ -potential of apo- α -lac nanoparticles at neutral pH is more negative than that of native apo- α -lac (24). Here we extend these results by determining the ζ -potential of the apo- α -lac nanoparticles over a full range of pH values, both before and after heating, and compare with results for native apo- α -lac. Fig.2 shows the change of ζ -potential as a function of pH and heating time for both native apo- α -lac and apo- α -lac nanoparticles. Consistent with our previous measurement of the ζ -potential at neutral pH, we here find that in fact the apo- α -lac nanoparticles have a more negative ζ -potential than native apo- α -lac for all pH values above the α -lac isoelectric point, $pI \approx 4.3$. At pH 5.7, the ζ -potential of α -lac nanoparticles is twice higher than that of native apo- α -lac, leading to significant repulsive electrostatic interactions between the particles. We also found that heating does not significantly affect the ζ -potential of the protein nanoparticles. Representative results for the ζ -potential as a function of the heating time (for pH = 7.0) are shown in Fig.1B. This implies that the strong repulsion between the nanoparticles does not diminish upon heating, which may be one of the factors contributing to the higher stability of the apo- α -lac nanoparticles against heat-induced aggregation at pH 5.7, as compared to native apo- α -lac.

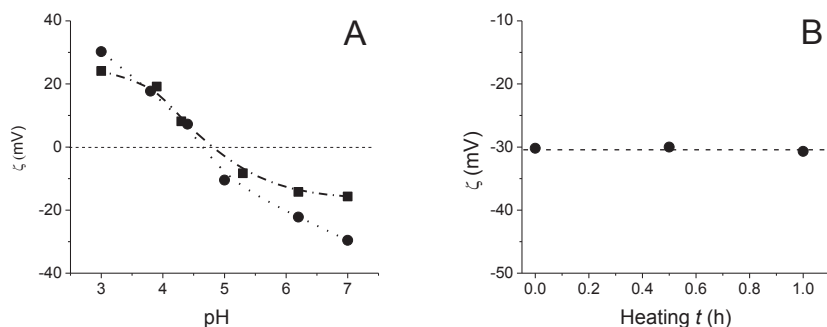


Figure.2. The change of ζ -potential of apo- α -lac nanoparticles and native apo- α -lac (A) ζ -potential as a function of pH (■: native α -lac; ●: α -lac nanoparticles) (B) ζ -potential of apo- α -lac nanoparticles as a function of heating time (h) at 90 °C at pH =7.0. Solution conditions: 10 mM sodium phosphate buffer, 25 °C. The protein nanoparticles have a hydrodynamic size of $R_H = 25$ nm.

Previously, mTG-catalyzed cross-linking has been found to induce slightly more negative ζ -potentials for whey protein isolate. mTG catalyzes the cross-linking of lysine to glutamine and thus leads to a reduction of the total positive charge (34). We expect that enzymatic oxidation induces no changes in the net charge of protein, but nevertheless we find much more negative values of the ζ -potential (above isoelectric point) for enzymatically cross-linked apo- α -lac nanoparticles, as compared to native apo- α -lac (Fig.2A).

For heat-induced protein aggregates prepared by heating WPI solutions above their pI, it has also been observed that these have a more negative ζ -potential (7). Since the relation between the titration charge and the electrophoretic mobility is a complicated one, a more negative ζ -potential, not necessarily means a larger net negative titration charge. Indeed, the structure of the protein nanoparticles (e.g. shape, size and hydrodynamic properties) influences their electrophoretic mobility and hence may lead to deviations since the model for calculating the ζ -potential from the electrophoretic mobility is that of a uniformly charged hard sphere. In fact, Schmitt et al. showed that ζ -potential of heat-induced WPI aggregates decreases with increasing salt concentration and decreasing pH. They indeed attribute the difference in ζ -potential observed to the differently structured aggregates that were formed (35).

Protein conformation

The molecular origin of heat-induced protein aggregation is that there are protein conformational changes upon heating. Therefore, when studying the heat-stability of the protein nanoparticles, it is crucial to also study conformational changes of the individual proteins constrained in the cross-linked nanoparticles upon heating. Here, we probe the changes in secondary structure upon heating for both native apo- α -lac and apo- α -lac nanoparticles by using far-UV CD spectroscopy. The percentage of α -helices was estimated from the far-UV CD spectra (θ in milidegree) using the ridge regression algorithm CONTINLL as implemented by the Dichroweb webserver, provided by University of London (29, 30).

Values for the percentage of α -helical secondary structure obtained from the far UV spectra are shown in Fig.3. For native apo- α -lac, we find a marked change in the percentage of α -helical structure upon heating to 90 °C. Cooling back to 25 °C after approximately 1h at 90 °C, leads to a nearly complete return to the spectrum observed at 25 °C before heating, suggesting reversible changes, at least at the level of secondary structure (see supplementary data). We have observed similar reversible changes in secondary structure for native apo- α -lac at pH 3.0 and pH 7.0.

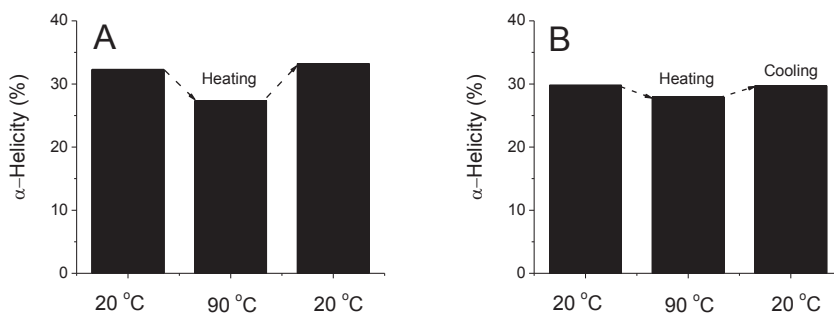


Figure.3. Reversible changes in percentage of α -helical secondary structure (as deduced from far UV CD spectroscopy) during heating and cooling of native apo- α -lac and enzymatically cross-linked apo- α -lac. (A) Native apo- α -lac (B) enzymatically cross-linked apo- α -lac. The content of α -helical secondary structure reported during heating is an average of values obtained at the start and end of heating. The protein concentration is 0.1 mg/mL, solution conditions are 10 mM sodium phosphate buffer at pH 5.7.

It is worth mentioning that we have found indications of at least some irreversible loss in tertiary structure under these same conditions, from near UV CD spectra (see supplementary data). Next consider the enzymatically cross-linked apo- α -lac nanoparticles. As we have shown before (24), at 25 °C, the proteins in the particles exhibit a far UV CD spectrum that is intermediate between that of native apo- α -lac and extensively heat-denatured apo- α -lac. The same holds for the percentage of α -helical secondary structure, deduced from these spectra. Upon heating the apo- α -lac nanoparticles for 1h at 90 °C, and then cooling back to 25 °C, we find hardly any irreversible changes to the far UV CD spectra, and consequently, a similar percentage of α -helical secondary structure, before and after heating (Fig.3B). Also, the decrease in the percentage of α -helical structure at 90 °C is only minimal. Whereas for the native apo- α -lac, near-UV CD spectra indicated some irreversible loss of tertiary structure, for the nanoparticles, essentially all tertiary structure had already been lost due to cross-linking, and no further changes to the near-UV CD spectrum take place upon heating (see supplementary data). The results shown in Fig.3 suggest that the α -helices that remain after enzymatic cross-linking are much less sensitive to thermal unfolding than those in the native apo- α -lac. This is a clear indication of the high structural stability of enzymatically cross-linked apo- α -lac, with respect to heating.

Surface hydrophobicity

Protein conformational changes caused by enzymatic cross-linking may lead to changes in the physical properties of the protein surface, in particular the protein surface hydrophobicity (36). Here we probe these changes using 8-anilino-1-naphthalenesulfonic acid (ANSA). The fluorescence intensity of ANSA significantly increases when it is bound to a hydrophobic site (37). Fig.4 shows the exposed surface hydrophobicity (S_o) determined using ANSA, both before and after heating, for both native apo- α -lac and enzymatically cross-linked apo- α -lac.

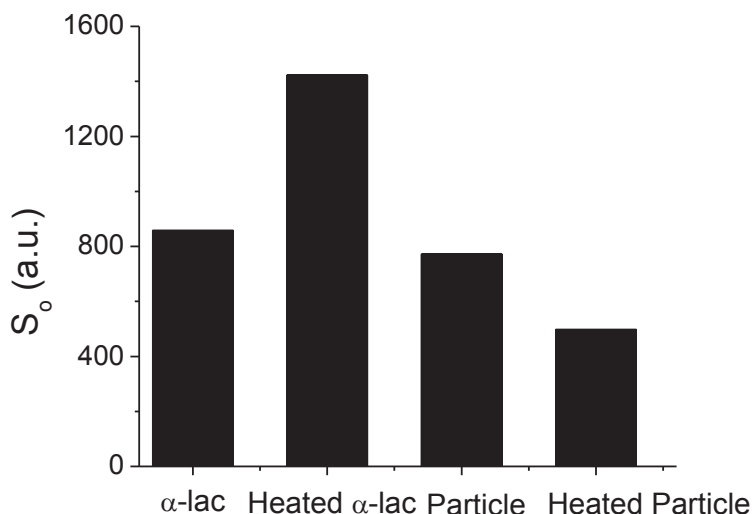


Figure.4. Relative exposed surface hydrophobicity of native apo- α -lac and enzymatically cross-linked apo- α -lac, before and after heating for 1h at 90 °C, pH 5.7, in 10 mM sodium phosphate buffer, as determined using ANSA. The ANSA assay was carried out at pH 7.0 in 10 mM sodium phosphate buffer at 25 °C.

The 1h-heated native apo- α -lac (after cooling back) has a significantly higher surface hydrophobicity, confirming that despite reversible changes in secondary structure, there are also irreversible conformational changes, as was also highlighted by the near-UV CD spectra (see supplementary data). However, for the enzymatically cross-linked apo- α -lac, the ANSA assay suggests that the exposed surface hydrophobicity even decreases after a heat treatment.

For heat-induced soluble protein aggregates, the surface hydrophobicity sensitively depends on environmental conditions. For some cases, a reduced surface hydrophobicity of aggregates as compared to native proteins has also been reported, in particular for soluble β -lactoglobulin aggregates formed by heating the protein at pH 6.0 and pH 7.0 (35, 38). Also, mTG-catalyzed cross-linking of WPI has been reported to results in a surface hydrophobicity after cross-linking that decreasing with increasing cross-linking time. At the same time, the solubility of WPI at pH 4.5 also decreases with increasing time of incubation with mTG, suggesting the enzymatic cross-linking enhances rather than

decreases the surface hydrophobicity of the protein, leading to protein aggregation nearby pI (15, 16). The authors argue that cross-linking does increase the protein surface hydrophobicity, but that this is not reported by the fluorescent probe due to the occlusion of hydrophobic cavities that limit the accessibility of the probe. In contrast, we find that peroxidase-catalysed cross-linking completely prevents thermal aggregation of apo- α -lactalbumin under conditions where the native protein rapidly aggregates (pH 5.7). We have also found that thermal aggregation of native apo- α -lac at pH 5.7 can be prevented by the addition of SDS, suggesting that hydrophobic interactions are the main driving force for thermal aggregation of the native protein. Taken together, this shows that the enzymatically cross-linked apo- α -lac is highly hydrophilic, and remains so after heating.

Thermal transition

Besides circular dichroism, another sensitive probe of heat-induced conformational changes of proteins is differential scanning calorimetry (DSC). We have performed DSC on both native apo- α -lac and enzymatically cross-linked apo- α -lac in 10 mM sodium phosphate buffer at pH 7.0. The results are shown in Fig.5. An endothermic peak occurs for native apo- α -lac at $T_d = 35 (\pm 0.5)^\circ\text{C}$, which is characteristic for the “molten globule” state of apo- α -lac (39). For the calcium containing holo- α -lac with a much better defined tertiary structure, the endothermic peak corresponding to denaturation occurs at a much higher temperature. Since our apo- α -lac preparation still contains about 15 % of holo- α -lac, we also find an endothermic transition at $T_d = 63.5 (\pm 0.5)^\circ\text{C}$, at a position is consistent with previous studies for holo- α -lac (31). We have confirmed the assignment of these peaks by also preparing an apo- α -lac sample for which all Ca^{2+} was rigorously removed using EDTA. For this sample, indeed the endothermic peak occurring at $T_d = 35(\pm 0.5)$ is much more pronounced and the peak at $T_d = 63.5(\pm 0.5)^\circ\text{C}$ is much less pronounced (see supplementary data). Next consider the enzymatically cross-linked apo- α -lac. Our data in Fig.5 shows that this does not exhibit an endothermic denaturation transition, but instead shows a broad exothermic transition centered at $99.1 (\pm 0.5)^\circ\text{C}$. This suggests that certain conformational changes take place when heating the enzymatically cross-linked apo- α -lac at 99.1°C . The exothermic nature of the transition indicates that it must involve

the establishment of some new (physical or chemical) bonds during heating (40-42). This is also consistent with a slight increase (about 10 %) in dityrosine bonds that we have found (as judged from the development of the UV absorbance at 318 nm during heating) (data not shown) and the permanent decrease in surface hydrophobicity after heating.

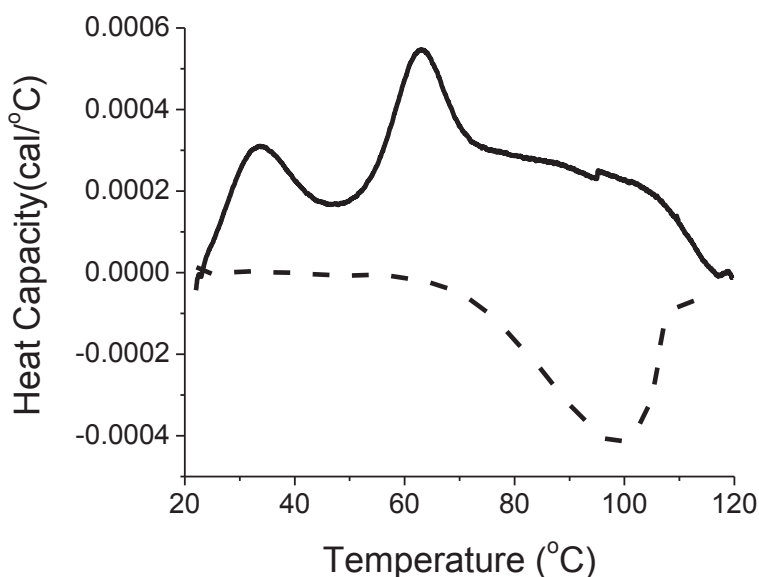


Figure.5. DSC thermograms of native apo- α -lac (solid line) and enzymatically cross-linked apo- α -lac (dash line) in 10 mM sodium phosphate buffer at pH 7.0.

Rheology

Having observed that enzymatically cross-linked apo- α -lac hardly exhibits any changes in secondary structure or particle size upon heating, and in contrast to native apo-a-lac, does not become more hydrophobic, we turn to the most stringent test of heat stability by considering how the rheology of dense dispersions of enzymatically cross-linked apo- α -lac changes upon heating. Previously, we have found that in dense dispersions of enzymatically cross-linked apo-a-lac particles (hydrodynamic radius $R_H = 100$ nm) jamming occurs above the overlap concentration of the particles (at around 4% (w/v) for the $R_H = 100$ nm particles) (23). This leads to the formation of a transparent, reversibly

yielding gel. We have heated their dense dispersions for 15 min and for 60 min at 80 °C, cooled back to 20 °C, and determined the effect of this heating step on their rheology. Fig.6 shows the frequency dependent storage (G') and loss moduli (G'') of the protein hydrogels before and after heating. Remarkably, the influence of the heating on the storage and loss moduli versus frequency is very limited. In particular the short-term heating (15 min at 80 °C) hardly affects the rheology of the protein gels. Consistent with the observation that prolonged heating leads to a gradual decrease of the size of the enzymatically cross-linked apo- α -lac particles (data not shown), we find that prolonged heating leads to a decrease in elastic moduli.

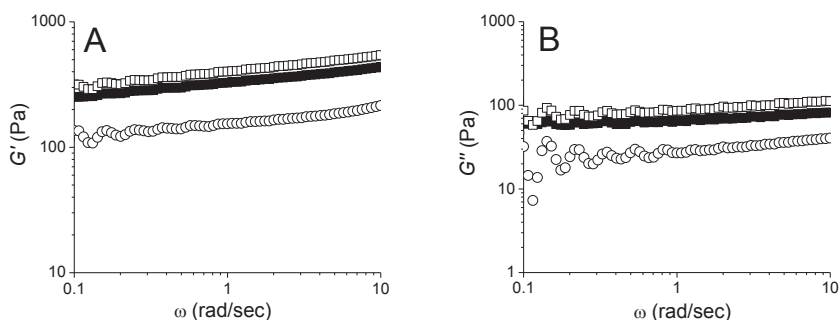


Figure.6. Frequency dependences of storage moduli (G') (**A**) and loss moduli (G'') (**B**) of apo- α -lac nanoparticles dispersion (R_H of 100 nm; 5.6 % (w/v)) in 10 mM sodium phosphate buffer at pH 7.0 at 20 °C before (■) and after heated for 15 min (□) and 60 min (○).

Another characteristic rheological feature of these hydrogels is their extreme, reversible shear thinning. In order to determine the effect of heating on this property, we determined flow curves before and after heating. Fig.7A shows apparent viscosities for shear rates from 0.1 s⁻¹ to 100 s⁻¹, for unheated and heated (for 15 min and 60 min) protein nanoparticle dispersions (R_H of 100 nm). All samples exhibit a strongly shear thinning behavior. The flow curves for heated and unheated dispersions nearly overlap. Only after prolonged heating we find that the slow decrease in particle size leads to a moderate decrease of the apparent viscosity of dispersions (Fig.7B). The rheology of dense dispersions is extremely sensitive to even small changes in size, hydrophobicity, and

interactions of the particles that make up the dispersion. Hence we conclude again that the enzymatically cross-linked apo- α -lac particles exhibit a high hydrophilicity that is also very heat stable.

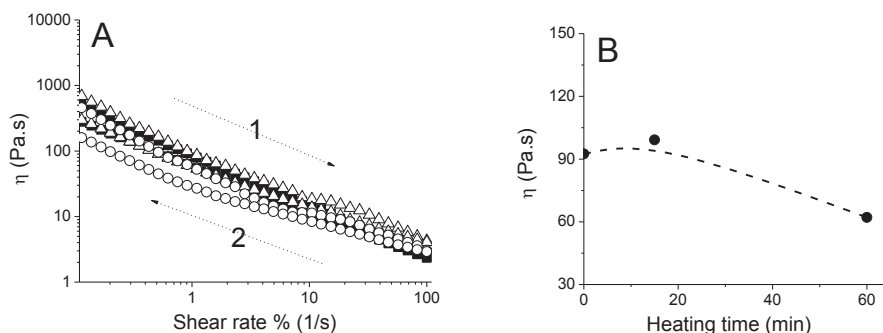


Figure.7. (A) Dependence of apparent viscosity of α -lactalbumin nanoparticle dispersions (R_H of 100 nm, 5.6 % (w/v)) on shear rate in 10 mM sodium phosphate buffer at pH 7.0 at 20 °C after heating at 90 °C for 1 min (■); for 15 min (□); for 60 min (○). **(B)** The change of apparent viscosity at shear rate % of 1 s^{-1} upon heating in 10 mM sodium phosphate buffer at pH 7.0.

Conclusion

The objective of this study was to examine the potential of oxidative cross-linking to create heat stable apo- α -lac nanoparticles. Our results have shown that α -lac nanoparticles (R_H of 25 – 100 nm) resulting from peroxidase-catalyzed cross-linking indeed exhibit a very high stability against thermal aggregation, over a wide range of pH values (pH 3.0 – 7.0) and salt concentrations (up to 0.5 M NaCl). Only in a narrow pH range around the pI (pH 4.5 – 5.5), we have observed indications of particle aggregation upon heating at 90 °C.

Due to their heat stable secondary structure, hydrophilic nature and high ζ -potential, the interaction between the particles is strongly repulsive, which stabilizes them against thermal aggregation. The most extreme illustration of this is the fact that the rheological properties of dense dispersions of the apo- α -lac nanoparticles are hardly affected by heating. Our study has demonstrated an enzymatic cross-linking route to create very heat stable, hydrophilic, negatively charged α -lac nanoparticles that form

reversibly yielding, heat stable and transparent hydrogels. The unique results may be a basis for also designing other heat stable protein colloids and heat-stable protein hydrogels with possible applications in novel food formulations, including high protein beverages.

Acknowledgement

This work is part of the Industrial Partnership Programme (IPP) Bio(-Related)Materials of the Stichting voor Fundamenteel Onderzoek der Materie (FOM), which is financially supported by the Nederlandse Organisatie voor Wetenschappelijk Onderzoek (NWO). The IPP BRM is co-financed by the Top Institute Food and Nutrition and the Dutch Polymer Institute.

References

1. Dissanayake, M.; Ramchandran, L.; Donkor, O. N.; Vasiljevic, T., Denaturation of whey proteins as a function of heat, pH and protein concentration. *Int. Dairy J.* **2013**, *31*, 93-99.
2. Mezzenga, R.; Fischer, P., The self-assembly, aggregation and phase transitions of food protein systems in one, two and three dimensions. *Rep. Prog. Phys.* **2013**, *76*, 43.
3. Fox, P. F.; McSweeney, P. L. H., *Advanced Dairy Chemistry: Volume 1: Proteins, Parts A&B: Protein*. Kluwer Academic/Plenum: 2003.
4. Raikos, V., Effect of heat treatment on milk protein functionality at emulsion interfaces. A review. *Food Hydrocolloids* **2010**, *24*, 259-265.
5. Purwanti, N.; Smiddy, M.; van der Goot, A. J.; de Vries, R.; Alting, A.; Boom, R., Modulation of rheological properties by heat-induced aggregation of whey protein solution. *Food Hydrocolloids* **2011**, *25*, 1482-1489.
6. Ryan, K. N.; Vardhanabhuti, B.; Jaramillo, D. P.; van Zanten, J. H.; Coupland, J. N.; Foegeding, E. A., Stability and mechanism of whey protein soluble aggregates thermally treated with salts. *Food Hydrocolloids* **2012**, *27*, 411-420.
7. Ryan, K. N.; Zhong, Q. X.; Foegeding, E. A., Use of Whey Protein Soluble Aggregates for Thermal StabilityA Hypothesis Paper. *J. Food Sci.* **2013**, *78*, R1105-R1115.
8. Saglam, D.; Venema, P.; de Vries, R.; Sagis, L. M. C.; van der Linden, E., Preparation of high protein micro-particles using two-step emulsification. *Food Hydrocolloids* **2011**, *25*, 1139-1148.
9. Zhang, W. N.; Zhong, Q. X., Microemulsions as nanoreactors to produce whey protein nanoparticles with enhanced heat stability by thermal pretreatment. *Food Chem.* **2010**, *119*, 1318-1325.
10. Saglam, D.; Venema, P.; de Vries, R.; Shi, J.; van der Linden, E., Concentrated whey protein particle dispersions: Heat stability and rheological properties. *Food Hydrocolloids* **2013**, *30*, 100-109.

11. Vachon, C.; Gauthier, S. F.; Jones, J. D.; Savoie, L., Enzymatic digestion method with dialysis to assess protein damage - application to alkali-treated proteins containing lysinoalanine. *Nutr. Res.* **1982**, *2*, 675-688.
12. Tang, C. H.; Yang, X. Q.; Chen, Z.; Wu, H.; Peng, Z. Y., Physicochemical and structural characteristics of sodium caseinate biopolymers induced by microbial transglutaminase. *J. Food Biochem.* **2005**, *29*, 402-421.
13. Buchert, J.; Cura, D. E.; Ma, H.; Gasparetti, C.; Monogioudi, E.; Faccio, G.; Mattinen, M.; Boer, H.; Partanen, R.; Selinheimo, E.; Lantto, R.; Kruus, K., Crosslinking Food Proteins for Improved Functionality. In *Annual Review of Food Science and Technology, Vol 1*, Doyle, M. P.; Klaenhammer, T. R., Eds. Annual Reviews: Palo Alto, 2010; Vol. 1, pp 113-138.
14. Truong, V. D.; Clare, D. A.; Catignani, G. L.; Swaisgood, H. E., Cross-linking and rheological changes of whey proteins treated with microbial transglutaminase. *J. Agric. Food Chem.* **2004**, *52*, 1170-1176.
15. Agyare, K. K.; Damodaran, S., pH-Stability and Thermal Properties of Microbial Transglutaminase-Treated Whey Protein Isolate. *J. Agric. Food Chem.* **2010**, *58*, 1946-1953.
16. Damodaran, S.; Agyare, K. K., Effect of microbial transglutaminase treatment on thermal stability and pH-solubility of heat-shocked whey protein isolate. *Food Hydrocolloids* **2013**, *30*, 12-18.
17. Flanagan, J.; Gunning, Y.; FitzGerald, R. J., Effect of cross-linking with transglutaminase on the heat stability and some functional characteristics of sodium caseinate. *Food Res. Int.* **2003**, *36*, 267-274.
18. O'Sullivan, M. M.; Kelly, A. L.; Fox, P. F., Effect of transglutaminase on the heat stability of milk: A possible mechanism. *J. Dairy Sci.* **2002**, *85*, 1-7.
19. Lantto, R.; Puolanne, E.; Kalkinen, N.; Buchert, J.; Autio, K., Enzyme-aided modification of chicken-breast myofibril proteins: Effect of laccase and transglutaminase on gelation and thermal stability. *J. Agric. Food Chem.* **2005**, *53*, 9231-9237.
20. Lantto, R.; Puolanne, E.; Kruus, K.; Buchert, J.; Autio, K., Tyrosinase-aided protein cross-linking: Effects on gel formation of chicken breast myofibrils and texture and water-holding of chicken breast meat homogenate gels. *J. Agric. Food Chem.* **2007**, *55*, 1248-1255.
21. Saricay, Y.; Wierenga, P.; de Vries, R., Nanostructure development during peroxidase catalysed cross-linking of alpha-lactalbumin. *Food Hydrocolloids* **2013**, *33*, 280-288.
22. Dhayal, S. K.; Gruppen, H.; de Vries, R.; Wierenga, P. A., Controlled formation of protein nanoparticles by enzymatic cross-linking of alpha-lactalbumin with horseradish peroxidase. *Food Hydrocolloids* **2014**, *36*, 53-59.
23. Yunus Saricay, P. A. W. a. R. d. V., Rheological properties of dispersions of enzymatically cross-linked α -lactalbumin nanoparticles *submitted manuscript* **2014**.
24. Yunus Saricay, P. A. W. a. R. d. V., Changes in protein conformation and surface hydrophobicity upon peroxidase-catalyzed cross-linking of apo- α -lactalbumin *submitted manuscript* **2014**.
25. Surender. K. Dhayal, H. G., Renko de Vries and Peter A. Wierenga Determination of Cross-linking bonds upon peroxidase-catalyzed cross-linking of α -lactalbumin *manuscript in preparation* **2014**.
26. Kronman, M. J.; Andreotti, R. E., Inter- + intramolecular interactions of alpha-lactalbumin .i. apparent heterogeneity at acid pH. *Biochemistry* **1964**, *3*, 1145-&.

27. Ohlsson, P. I.; Paul, K. G., Molar absorptivity of horseradish-peroxidase. *Acta Chemica Scandinavica Series B-Organic Chemistry and Biochemistry* **1976**, *30*, 373-375.
28. Noble, R. W.; Gibson, Q. H., Reaction of ferrous horseradish peroxidase with hydrogen peroxide. *J. Biol. Chem.* **1970**, *245*, 2409-8.
29. Provencher, S. W.; Glockner, J., Estimation of globular protein secondary structure from circular-dichroism. *Biochemistry* **1981**, *20*, 33-37.
30. Whitmore, L.; Wallace, B. A., DICHROWEB, an online server for protein secondary structure analyses from circular dichroism spectroscopic data. *Nucleic Acids Res.* **2004**, *32*, W668-W673.
31. McGuffey, M. K.; Epting, K. L.; Kelly, R. M.; Foegeding, E. A., Denaturation and aggregation of three alpha-lactalbumin preparations at neutral pH. *J. Agric. Food Chem.* **2005**, *53*, 3182-3190.
32. Anuradha, S. N.; Prakash, V., Altering functional attributes of proteins through cross linking by transglutaminase - A case study with whey and seed proteins. *Food Res. Int.* **2009**, *42*, 1259-1265.
33. Wang, W.; Zhong, Q. X.; Hu, Z. X., Nanoscale Understanding of Thermal Aggregation of Whey Protein Pretreated by Transglutaminase. *J. Agric. Food Chem.* **2013**, *61*, 435-446.
34. Zhong, Q. X.; Wang, W.; Hu, Z. X.; Ikeda, S., Sequential preheating and transglutaminase pretreatments improve stability of whey protein isolate at pH 7.0 during thermal sterilization. *Food Hydrocolloids* **2013**, *31*, 306-316.
35. Schmitt, C.; Bovay, C.; Rouvet, M.; Shojaei-Rami, S.; Kolodziejczyk, E., Whey protein soluble aggregates from heating with NaCl: Physicochemical, interfacial, and foaming properties. *Langmuir* **2007**, *23*, 4155-4166.
36. Eissa, A. S.; Puhl, C.; Kadla, J. F.; Khan, S. A., Enzymatic cross-linking of beta-lactoglobulin: Conformational properties using FTIR spectroscopy. *Biomacromolecules* **2006**, *7*, 1707-1713.
37. Wierenga, P. A.; Meinders, M. B. J.; Egmond, M. R.; Voragen, F.; de Jongh, H. H. J., Protein exposed hydrophobicity reduces the kinetic barrier for adsorption of ovalbumin to the air-water interface. *Langmuir* **2003**, *19*, 8964-8970.
38. Zhu, H. M.; Damodaran, S., Heat-induced conformational-changes in whey-protein isolate and its relation to foaming properties. *J. Agric. Food Chem.* **1994**, *42*, 846-855.
39. Relkin, P.; Launay, B.; Eynard, L., Effect of sodium and calcium addition on thermal-denaturation of apo-alpha-lactalbumin - a differential scanning calorimetric study. *J. Dairy Sci.* **1993**, *76*, 36-47.
40. Rodriguez-Cabello, J. C.; Reguera, J.; Alonso, M.; Parker, T. M.; McPherson, D. T.; Urry, D. W., Endothermic and exothermic components of an inverse temperature transition for hydrophobic association by TMDSC. *Chem. Phys. Lett.* **2004**, *388*, 127-131.
41. Arntfield, S. D.; Murray, E. D., The influence of processing parameters on food protein functionality .1. differential scanning calorimetry as an indicator of protein denaturation. *Canadian Institute of Food Science and Technology Journal-Journal De L Institut Canadien De Science Et Technologie Alimentaires* **1981**, *14*, 289-294.
42. Basturkmen, M.; Hacaloglu, J.; Kisakurek, D., Effect of N-methylimidazole and 3,5-dimethylpyrazole ligands on the polymerization of di(2,6-dichlorophenolato) Cu(II) Co(II) complexes in the solid state. *J. Appl. Polym. Sci.* **2004**, *91*, 3797-3805.

Supplementary data

Turbidity of nanoparticles as a function of NaCl concentration.

First, freeze-dried powder of apo- α -lac nanoparticles (R_H of 25 nm) (please see procedure for preparation of powder in materials & methods) was dissolved in demi H₂O and extensively dialyzed against demi H₂O. Then, the concentration of apo- α -lac nanoparticles dispersion was spectroscopically determined using $A_{280} = 20.1$ for a 1% (w/v) protein solution, which was determined as 4.4 mg/mL. To balance pH value, 0.1 mL of 1 M sodium phosphate buffer was mixed with aqueous solution of protein nanoparticles. Hydrodynamic radii of apo- α -lac nanoparticles (1mg/mL) were obtained as R_H of 25 nm using Malvern Nanosizer ZS.Next, stock NaCl solution (5M) was diluted into protein nanoparticles to obtain the desired salt concentrations (0.1 M, 0.25 M and 0.5 M) in 10 mM sodium phosphate buffer at pH 7.0. Finally, pH of solutions was adjusted to pH 5.7 using 0.1 mM HCl at 25 °C. The stability of protein nanoparticles against thermal aggregation as a function of salt concentration at pH 5.7 was monitored using UV-vis spectrophotometer at 400 nm. Fig.8 shows the change in turbidity (absorbance at 400 nm, A_{400}) as a function of NaCl concentration at pH 5.7 after heating for 15 min. The turbidity of apo-apo- α -lac nanoparticles solution remains constant with increasing NaCl concentration at pH 5.7 upon heating at 90 °C for 15 min. This suggests that apo-apo- α -lac nanoparticles exhibit very high stability against thermal aggregation at pH 5.7 where native apo- α -lac rapidly undergoes thermal aggregation even in 10 mM sodium phosphate buffer under the same conditions.

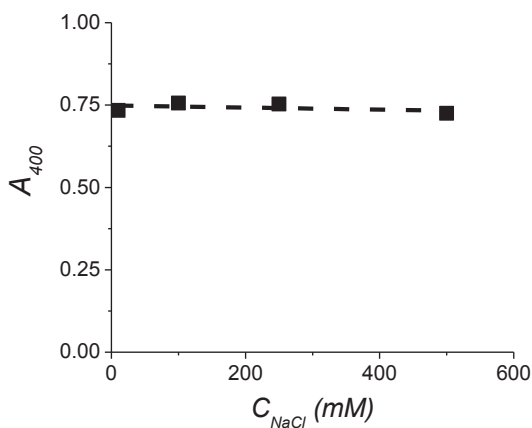


Figure.8. The change in turbidity (A_{400}) of apo-apo- α -lac nanoparticles (Concentration: 4.4 mg/mL; R_H of 25 nm) as a function of NaCl concentration after heating particle solution at pH 5.7 for 15 min at 90 °C.

Thermal transition of apo-lactalbumin.

First, ethylenediaminetetraacetic acid disodium salt dihydrate (EDTA) solution was prepared by dissolving EDTA (10% (w/v) or 0.29 M) in demi H₂O. Next, α -lac (10 % w/v/ or 7 mM), which according to the manufacturer mainly consists of the Ca²⁺-depleted apo-form (85 %), and for the remainder of the Ca²⁺-containing holo-form (15 %) was dissolved into the EDTA solution. The protein solution was incubated with EDTA at 4 °C overnight. Next, it was dialyzed against demi H₂O. Finally, differential scanning calorimeter (DSC) was used to monitor thermal transition of α -lac, from which remaining Ca²⁺ was removed using EDTA. Fig.9 shows DSC thermogram of apo- α -lac after removal of Ca²⁺. The endothermic transition at 35 °C (corresponding to apo- α -lac) becomes more pronounced after removal of Ca²⁺ from α -lac. This suggests the endothermic transition at 63.5 °C corresponds to holo-apo- α -lac and peak ratio of apo-form to holo-form in DSC shifts to apo-form after removal of Ca²⁺ from holo-form with EDTA.

Structural Transition upon Heating

Protein nanoparticle solution was prepared from freeze-dried powder as mentioned in materials & methods. For near and far-UV CD measurements, apo- α -lac nanoparticles (R_H

of 25 nm) dispersion was extensively dialyzed against 10 mM sodium phosphate buffer at 4 °C.

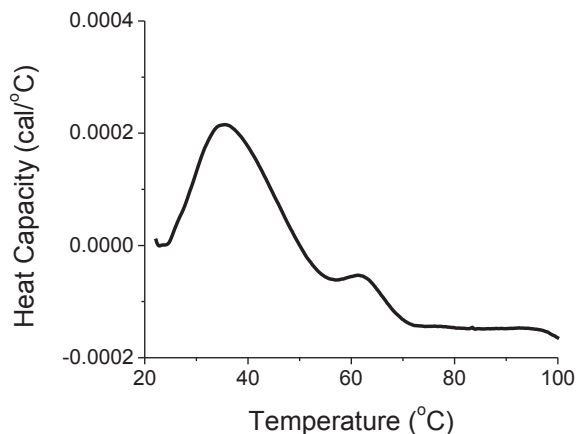


Figure.9. DSC thermogram of apo- α -lac in 10 mM sodium phosphate buffer at pH 7.0 after removal of Ca^{2+} by EDTA

For far- and near-UV CD measurements, proteins concentrations were 1 mg/mL and 0.1 mg/mL, respectively. The far- and near-UV CD spectra was used to explore the structural transitions in secondary and tertiary structure for native and cross-linked apo- α -lac upon heating. Fig.10 shows the change at 222 nm (corresponding to α -helices) in far-UV CD spectrum at different pH upon heating at 90 °C. The far-UV CD spectra of apo- α -lac show that CD signal at 222 nm first decreases upon heating and then returns back initial value at all pH (Fig.10, left). This suggests the refolding of α -helices upon heating and then cooling down, indicating reversible changes. Like, far-UV CD spectra of apo- α -lac nanoparticles at all pHs exhibit the reversible changes in CD signal at 222 nm upon a heating-cooling cycle. However, the changes in CD signal at 222 nm ($\Delta_{CD_{222}}$) for apo- α -lac nanoparticles are less than those of native apo- α -lac whereas initial CD signal for apo- α -lac nanoparticles is also low as compared to native apo- α -lac (Fig.10, right).

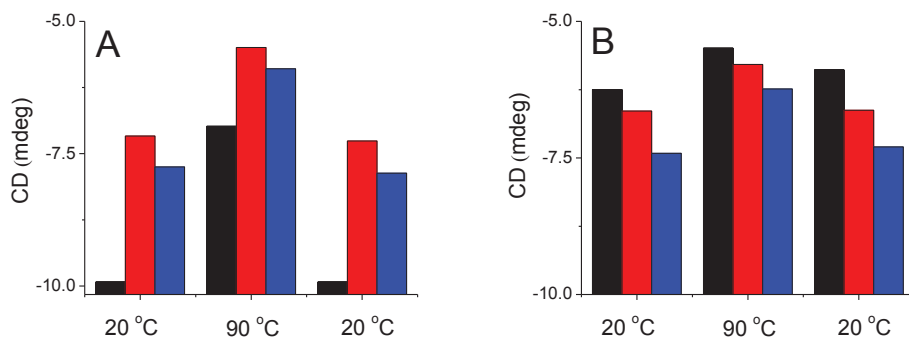


Figure.10. The changes in CD signal at 222 nm (corresponding to α -helicity) during a heating-cooling cycle in 10 mM sodium phosphate buffer for native apo- α -lac (A) and apo- α -lac nanoparticles (B) at pH 7.0 (black), pH 5.7 (red) and pH 3.0 (blue). Note that signals that we here presented are average of signals recorded for 30 min.

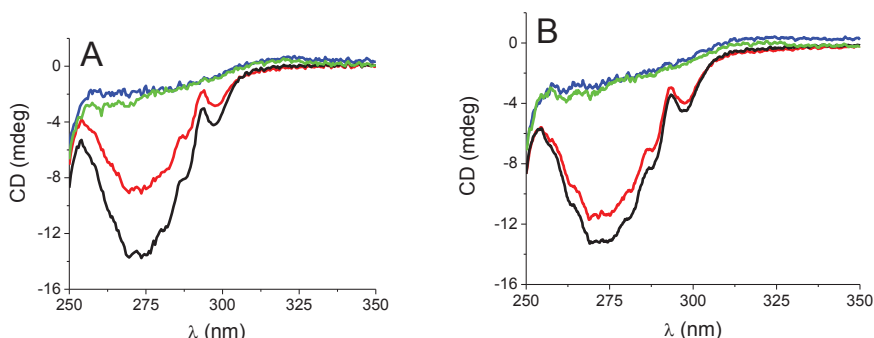
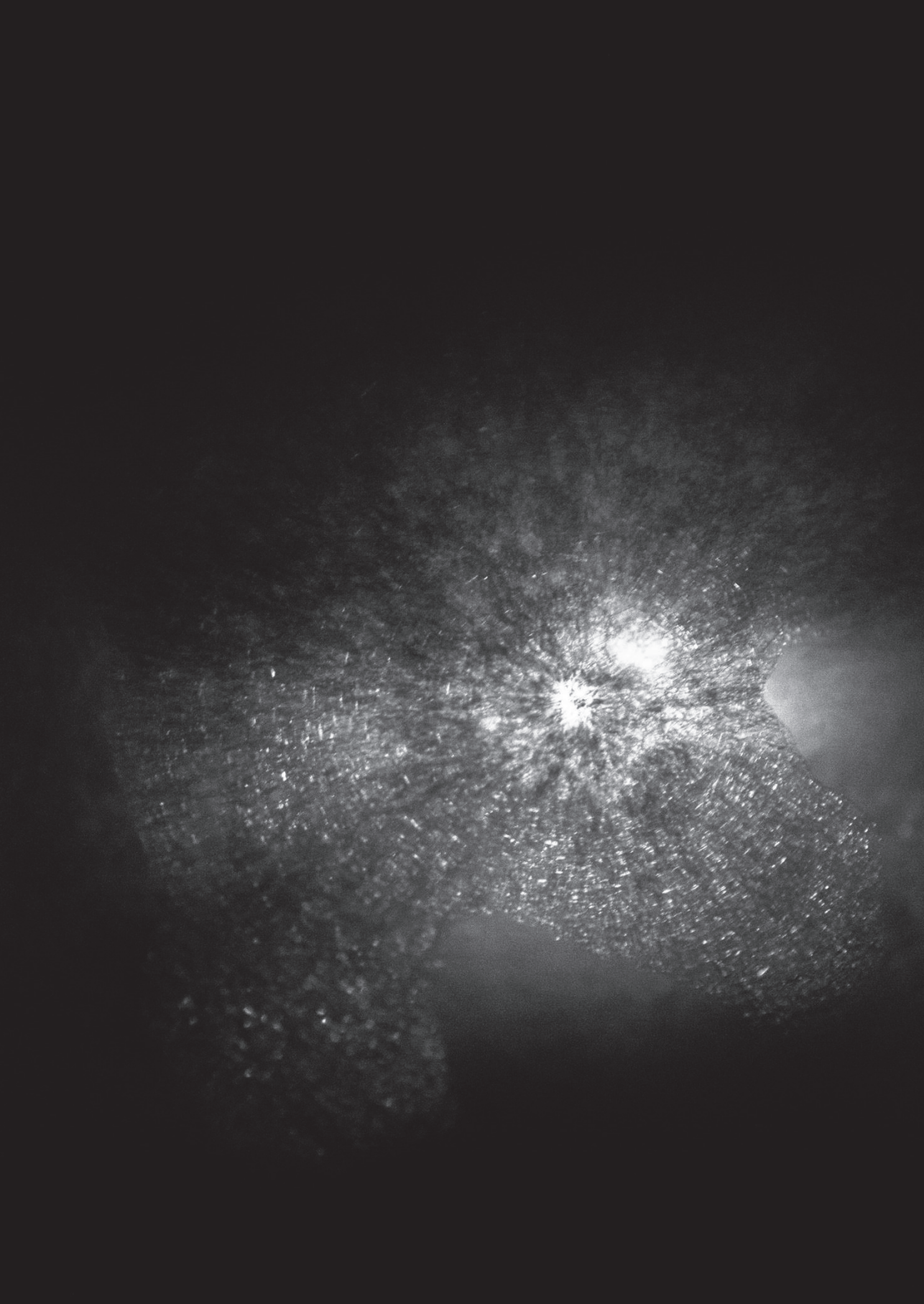


Figure.11. Near-UV CD spectra of native apo- α -lac and apo- α -lac nanoparticles at pH 7.0 (A) and at pH 5.7 (B) in 10 mM sodium phosphate buffer. For native α -lac, red and black cruves refer before heating and after heating at 90 °C and then cooling down 25 °C for 1h, respectively. For apo- α -lac nanoparticles, blue and green cruves refer before heating and after heating at 90 °C and then cooling down 25 °C for 1h, respectively.

The near-UV CD spectra of native apo- α -lac and apo- α -lac nanoparticles are depicted in fig.11. Heating of native apo- α -lac solution at 90 °C results in the reduction of CD signal, indicating some extent of irreversible loss in tertiary structure. Previously, we have shown full cross-linking of apo-apo- α -lac leads to nearly entire loss in tertiary structure. However, no further loss changes in near-UV CD spectra upon heating at 90 °C occurs for apo- α -lac nanoparticles.



Chapter 6

Structural and physical properties of enzymatically cross-linked apo- α -lactalbumin nanoparticles: Laccase versus peroxidase

Y. Saricay, S.K. Dhayal, P. A. Wierenga, R. de Vries.

Manuscript in preparation.

Abstract

Different oxidative enzymes are currently under investigation for cross-linking food proteins in order to tailor their functionality. This study elucidates to what extent peroxidase and laccase-catalyzed protein cross-linking leads to cross-linked protein nanoparticles that differ in stability, structural and physical properties. We consider cross-linking of a single substrate, apo- α -lactalbumin (apo- α -lac). Protein nanoparticles produced by both enzymes exhibit a similar scaling of size with molar mass: $R_g \sim M_W^a$ with a scaling exponent $a \approx 0.5$. They both have a zeta potential (at pH = 7.0) that is about 2.5 times more negative than that of native apo- α -lac, and are both highly resistant against heat-induced aggregation. In both type of protein nanoparticles, the tertiary structure of the protein subunits is lost completely, while a significant fraction of the original α -helical secondary structure is retained. Besides similarities, there are also pronounced differences between the two types of nanoparticles. Peroxidase-catalyzed cross-linking of apo- α -lac hardly affects the surface hydrophobicity, whereas for laccase-catalyzed cross-linking the surface hydrophobicity increases significantly (about 3 times) as compared to that the native apo- α -lac. We also find that laccase cross-linked nanoparticles show a significant disassociation in the presence of DTT while HRP-nanoparticles remain intact under these conditions, thus implicating disulfide bridges as a contributor to the stability of the laccase cross-linked nanoparticles. Our results demonstrate that a judicious choice of a certain type of oxidative cross-linking enzyme can be used to create protein nanoparticles with different physical and functional properties.

Introduction

Enzyme-induced protein modification have seen a growing interest in food technology in recent years since it offers the prospect to enhance protein functionality using mild and food-grade chemistry (1). The commercially available protein cross-linking enzyme, microbial transglutaminase (mTG) has been found to enhance protein gel strength, water-holding capacity, stability, rennetability and mechanical properties of dairy products (2). Other possible cross-linking enzymes for modulating the food functionality of proteins are still under investigation. In particular, many oxidative enzymes such as peroxidase, laccase, tyrosinase have a great potential for modulating the food functionality of proteins in ways that are alternative to mTG (3). To indeed benefit from the possibilities of oxidative protein cross-linking in food technology, it is crucial to also understand the effect of different types of cross-links on the overall physical and functional properties of the proteins, as catalyzed by different types of oxidative enzymes.

Oxidative enzymes can catalyze reactions of a wide variety of phenolic compounds (e.g. diphenols, polyphenols, aromatic amines, benzenethiols) including tyrosine, cysteine, and tryptophan in proteins, with different cross-linking mechanism (4). Peroxidases catalyze oxidations in the presence of a co-substrate (H_2O_2), but laccases and tyrosinases are capable of catalyzing oxidation using molecular oxygen in solution (5-7). Laccases and peroxidases-catalyzed reactions result in the formation of free radicals (8, 9). However, tyrosinases catalyze the conversion of monophenols into *o*-diphenols and their oxidation to *o*-quinones, which can react with a range of chemical groups in proteins and other biomolecules (10).

Oxidative enzymes have also been shown to catalyze the formation of cross-links in- and between various food proteins including casein, WPI, lysozyme, BSA, ovalbumin, apo- α -lactalbumin and β -lactoglobulin (4). The cross-linking efficiency can be enhanced in the presence of mediators (11). Moreover, cross-linking between carbohydrates, peptides, phenolic compounds, and/or proteins can be also achieved using oxidative cross-linking (11, 12).

Laccase (LC, copper-containing oxygen oxidoreductase) is a versatile oxidative enzyme, which is being investigated for use in food and biotechnology, bioremediation applications, personal and medical care applications and biosensor and analytical applications (13). The pH optimum of many fungal LC is in the acidic pH range. In general, these enzymes are active and stable in temperature ranges of about 30-60 °C. LC typically exhibits a poor cross-linking activity with many (globular) proteins, due to either limited tyrosine accessibility or a high redox potential of the protein (14). Therefore, it typically requires small cross-linker agents or/and unfolding for efficient cross-linking (15). LC-catalyzed cross-linking is mostly found to result in the formation of an ether bond that is formed with connection of an oxygen atom with two alkyl or aryl group as well as small amount of dityrosine coupling (16). LC-catalyzed cross-linking has been shown to lead to improved structural properties and water-holding capacity of protein gels, as well as to enhanced thermal stability of proteins (17, 18).

The heme-binding peroxidases are another major type of oxidative enzymes that also oxidize amino acids including Tyr, Phe, Trp, His, and Cys (19). However, Tyr is found to be the most reactive residue during peroxidase catalyzed protein cross-linking (20). Tyr reacts to form either *ortho-ortho* dityrosine or an isodityrosine bonds. Whereas the optimal pH of HRP is 6.0-6.5, the enzyme still exhibits a high activity at higher pH values (84% of maximum activity at pH 7.5) (21). A few studies have also shown possible functional effects of peroxidase-induced cross-linking on the gelation of polysaccharide-based building blocks including chitosan or dextran derivatives for applications in tissue engineering and the production of protein hydrogels (22-24).

Previously, we extensively characterized the formation, structure and physical properties of peroxidase cross-linked nanoparticles of apo- α -lac (HRP-nanoparticles) (25-27). We have found that protein nanoparticles are formed in a two-stage process: (1) first, monomers are rapidly cross-linked together to form small oligomers (2) next, the oligomers are coupled to each other via additional cross-links produced in a second, much slower part of the reaction, to finally form hierarchical protein nanoparticles (25). The development of nanostructure upon peroxidase-catalyzed cross-linking results in a self-similar architecture for the nanoparticles, over lengthscales from 20 nm – 150 nm, with a

fractal dimension of ~ 2 (26). The internal protein density of the nanoparticles decreases from 9 % to 4 % (w/v) when the particle hydrodynamic radius (R_H) increases from 25 nm to 100 nm (in chapter 4). In the nanoparticles, the proteins retain a significant degree of secondary structure (30 % α -helicity). Interestingly, the surface hydrophobicity of the protein nanoparticles (R_H of 25 nm) is nearly the same as that of the native apo- α -lac protein (in chapter 2). Also, we have found that their zeta potential is about twice higher than that of the native apo- α -lac monomers. Furthermore, the protein nanoparticles are very heat stable (chapter 5).

While we have thoroughly investigated the formation of hierarchical apo- α -lac particles at pH 7.0 by HRP, very little is known about the structure, formation and physical properties of protein nanoparticles produced using other oxidative enzymes. Therefore, we here explore the effect of the type of oxidative cross-linking on the structural and physical properties of apo- α -lac nanoparticles.

Oxidative enzymes differ in substrate specificity and different oxidative enzymes can induce different types of cross-links even when acting on the same protein substrate. Previously, the potential of at least some oxidative enzymes for tuning the food-functional properties of globular food proteins has been compared in the literature with that of transglutaminase. A question however, that has not yet been addressed is how different oxidative enzymes, acting on a single globular protein substrate, lead to the formation of cross-linked structures with different physical and functional properties. In this study we examine to what extent two different oxidative cross-linking enzymes, peroxidase and laccase, differ in altering the physical and functional properties of the whey protein (apo) α -lactalbumin.

Materials and methods

Materials

Ca⁺²-depleted- α -lactalbumin (apo-form) was supplied by Davisco Foods International Inc. (Le Sueur, MN, USA, contains ~ 85 % of calcium-free apo- α -lac and 15 % of calcium-containing holo- α -lac. Laccase from *Trametes versicolor* ≥ 10 U/mg (51639), peroxidase

from horseradish type VI-A (P6782) and 2,2'-azino-bis 3-ethylbenzthiazoline-6-sulfonic acid (ABTS) were supplied by Sigma-Aldrich. Peroxidase was used without any purification; laccase is purified as explained below. All other chemicals used were of analytical grade.

Preparation of enzyme solution & laccase activity

In order to prepare the laccase stock enzyme solution of protein powder (50 mg/mL) was dissolved in 10 mM sodium phosphate buffer at pH 7.0 at 25 °C. We observed a very poor solubility of laccase from *Trametes versicolor*. Therefore, stock solutions were first centrifuged at 20,000 rpm for 1 h to remove insoluble components from the crude enzyme preparation. Next, for desalting and removal of other low molar mass components, the stock enzyme solution was washed with 10 mM sodium phosphate buffer 6 times by using centrifugal filter units (Amicon ultra-4, 3 kDa cut-off). Finally, the solution was again centrifuged at 20,000 rpm for 1h. For the enzyme activity assay, stock LC solution (stock1) was diluted 100 times into 10 mM sodium phosphate buffer (Stock2).

The enzyme activity of purified laccase was determined via an assay based on the oxidation of 2,2'-azino-bis(3-ethylbenzothiazoline-6-sulphonic acid or ABTS (28). First the ABTS (0.5 mM) as dissolved in 10 mM sodium phosphate buffer at pH 6.0. It was incubated in 2 mL quartz cuvettes for 10 min at 25 °C in a UV-1601 spectrophotometer equipped with a CPS-240A cell positioner (Shimadzu SI, Columbia, MD, USA). In order to induce oxidation, LC solution (20 µl, stock2) was added into the ABTS solution (2 mL). Oxidation of ABTS was monitored by determining the increase in absorption at 420 nm for 5 min (29). The slope of $\Delta A_{420nm}/minute$ was used to calculate the enzymatic activity at 25 °C, according to given equation below:

$$\text{Enzyme Activity (Units/mL)} = \frac{(\Delta A_{420nm}/minute)(V_T)(d_f)}{(\epsilon_{420})(V_E)} \quad (1)$$

where $\Delta A_{420nm}/minute$ is the slope determined from oxidation of ABTS, V_T is a total volume of assay mixture (2.02 mL), d_f is a dilution factor (100), is ϵ_{420} a molar extinction coefficient of 36 mM⁻¹cm⁻¹ (28), V_E is a volume of enzyme added in assay solution (0.02 mL). The enzyme activity of stock laccase solution was found to be 4 U/mL.

Enzymatic reactions with laccase

Optimization of reaction conditions

First, an apo- α -lac stock solution was prepared by dissolving the protein (3% w/v) in 0.1 M sodium phosphate buffer at pH 7.0 at 25 °C. It was filtered using 0.25 μ m syringe filters to remove protein aggregates. The concentration of stock protein solution was determined using UV spectroscopy, assuming $A_{280} = 20.1$ for a 1% (w/v) solution (30). To prepare samples of different apo- α -lac concentrations, stock solutions (~ 3% w/v) were diluted with 0.1 M sodium phosphate buffer at pH 7.0. For samples at lower pH values, pH was adjusted using 1M HCl. For the enzymatic reactions, apo- α -lac stock solutions and LC solutions of the appropriate concentrations were mixed and incubated in the 10-mL glass tubes with continuous stirring at 40 °C overnight in a climate chamber. In order to maintain oxygen saturation of the buffer, the lids of glass tubes were kept open. For most experiments, enzyme concentrations used correspond to an activity of 0.2 U/mL; some experiments were done at different enzyme concentrations, as indicated.

Production of protein nanoparticles

Protein solutions were prepared by dissolving apo- α -lac (4 % w/v) in 0.1 M sodium phosphate buffer at pH 7.0 at 25 °C. The pH of the protein solution was adjusted to 6.0 using 1 M HCl. It was filtered using 0.25 μ m syringe filters to remove protein aggregates. Finally, the concentration of stock protein solution was spectroscopically determined, using $A_{280} = 20.1$ for a 1% (w/v) solution (30). Protein solution (3.5 % (w/v), 80 mL) was mixed with enzyme solution (4 U/mL, 5 mL) into a 100 mL Schott glass bottle. Enzyme concentration used corresponds to an activity of 0.25 U/mL. Enzymatic reaction was catalyzed at 40 °C overnight in a climate chamber with a continuous stirring by using a 2.5-cm magnetic stirrer. In order to supply enough oxygen saturation, a lid of a 100 mL Schott glass was kept open during enzymatic reaction.

Freeze drying and redissolution of cross-linked protein nanoparticles

In order to allow prolonged storage of the nanoparticles, reaction products were mixed with 1M sucrose at volume ratio of 1:1 and stored at -80 °C for a day. Next, these mixtures

were freeze-dried and stored at $-20\text{ }^{\circ}\text{C}$ (26). After redissolution, they were excessively dialyzed against 10 mM sodium phosphate buffer at $4\text{ }^{\circ}\text{C}$ via a 300 kDa cellulose ester membrane. Hydrodynamic radii of nanoparticles thus obtained were found to be the same as those before freeze drying, as determined by DLS measurements. For experiments, the concentrations of redissolved and dialyzed protein nanoparticles were determined via UV spectroscopy at 280 nm, using the absorption coefficients $A_{280}=2.01$ for 1 % (w/v) α -lac solution. Like the HRP-nanoparticles, the LC particles used for the structural and physical characterization experiments were freeze-dried in the presence of a cryoprotectant, redissolved and dialyzed. In this way, all experiments could be performed over a longer period of time, from a batch prepared using a single reaction

Peroxidase activity

In order to determine peroxidase activity, a 2,2'-azino-bis(3-ethylbenzothiazoline-6-sulphonic acid) (ABTS) assay was performed according to the published procedure (27). The activity of the enzyme preparation as given by the manufacturer is $\sim 900 - 2000$ units/mg). This is in agreement with our own determinations, for which we find variation of enzyme activity from batch to batch of less than about 15%,

Enzymatic reactions with peroxidase

Before performing peroxidase-catalyzed cross-linking, particle size of laccase-cross-linked apo- α -lac nanoparticles was determined. To create protein nanoparticles with a similar size (R_H of 50 nm), peroxidase-catalyzed cross-linking of apo- α -lac was performed at reaction conditions according to published procedure (28): $C_{\alpha\text{-lac}} = 20\text{ mg/mL}$; $C_{\text{HRP}} = 1\text{ mg/mL}$, $\Delta t\text{ (H}_2\text{O}_2\text{)} = 5\text{ min}$, $N\text{ (H}_2\text{O}_2\text{)} = 160$. Here, symbols refer protein concentration, enzyme concentration, time interval of added H_2O_2 , number of added H_2O_2 , respectively.

Freeze drying and redissolution of cross-linked protein nanoparticles

The reaction mixture prepared upon peroxidase-catalyzed cross-linking of apo- α -lac was first freeze-dried and then dialyzed against 10 mM sodium phosphate buffer according to the procedure aforementioned above.

Size exclusion chromatography (SEC)

The molecular mass distribution of final reaction products was analyzed using size exclusion chromatography. Aliquots of reaction products were first diluted to 1 % (w/v) into 10 mM sodium phosphate buffer at pH 7.0. Next, aliquots (100 μ l, 1% (w/v)) were injected onto a Superose 6 column (for globular proteins between $5 \times 10^3 - 5 \times 10^6$ Da; exclusion limit is 4×10^7 Da) connected to an AKTA purifier system (GE Healthcare). Elution was done at a flow rate of 0.5 mL/min in 10 mM sodium phosphate buffer at pH 7.0 at 25 °C. The eluate was monitored at 280 (for proteins) and 318 nm for dityrosine (5). For quantifying conversion, SEC chromatograms were divided into three regions: (1) Region I: monomeric apo- α -lac eluted between 15.3 mL and 20 mL, these are the “unreacted proteins” ($M_w = 14$ kDa) (2) Region II: for the purpose of quantifying conversion, the reaction products eluting between 15.3 mL and 8.0 mL are called “protein oligomers” ($2000 \text{ kDa} < M_w < 14 \text{ kDa}$) (3) Region III: for the purpose of quantifying conversion, reaction products eluting between 5.0 mL and 8.0 mL (in the void of the column) are called “protein nanoparticles” ($M_w > 2000 \text{ kDa}$). The conversion (%) of each fraction reported is the area under the respective curves of the SEC chromatogram. Experiments were performed in duplicate, to confirm reproducibility.

Determination of hydrodynamic radius (R_H) and zeta (ζ) potential

Dynamic light scattering and electrophoretic light scattering experiments were done using a Malvern Nanosizer ZS (Malvern) equipped with an Argon ion laser emitting vertically polarized light with a wavelength of 633 nm. The scattering angle was 173°. Average hydrodynamic radii R_H and ζ -Potential reported are the major peak from the peak analysis as performed by the Malvern DTS software, version 6.20. For DLS, a low-volume quartz batch cuvette was used (ZEN2112). For ζ -Potential measurements, a disposable capillary cell (DTS1070) was used. For both measurements, the protein concentrations were 1 mg/mL, and the buffer was 10 mM sodium phosphate, at the indicated pH. To monitor the change in particle size upon heating at 90 °C online, protein concentration was 4 mg/mL. For heating experiments, a 2-mL quartz cuvette was used.

Asymmetrical flow field flow fractionation (AF4) system

A Wyatt Eclipse 2 AF4 system (Wyatt Technology, Dernbach Germany) combined with a HPLC unit (Agilent Technologies, Palo Alto, USA) equipped with UV and IR detection and Wyatt Eos multi-angle laser light scattering (MALLS) detector was also used to analyze protein nanoparticles according to published procedure (26). The separation channel was equipped with a spacer having a gap of 350 μm (350 W), the membrane was a 10 kDa cut-off regenerated cellulose membrane. For AF4 separations, 50 μL of protein nanoparticles (10-30 μg) was injected at a flow rate of 0.2 mL/min and first focused for 8 min. Meanwhile, the detector flow rate was kept constant at 1 mL/min. For elution, the cross flow rate (V_x) was first kept constant at 2 mL/min for 5 min and then exponentially decreased to 0.1 mL/min with a decay time constant of 5 min. The exponential decay was achieved by eight linear decays of 1 min duration, followed by seven linear decays of 2 min duration. After this, V_x was kept constant at 0.1 mL/min for 5 min and finally decreased to 0 mL/min and kept at 0 mL/min for 10 min. All samples were measured in duplicate to confirm reproducibility. The weight averaged molar masses (M_w) and gyrations of radii (R_g) were determined from the extrapolated light scattering signals, using data from scattering angles from 29.6° to 140° , using a 1st order Berry fit. The apparent protein density inside the nanoparticles, (ρ) and the number of proteins per nanoparticle (N) were determined from:

$$\rho = \frac{M_w}{N_A \frac{4}{3} \pi R_g^3} \quad (2)$$

$$N = \frac{(M_w)_{\text{particle}}}{(M_w)_{\text{protein}}} \quad (3)$$

where, ρ is the internal density, M_w is the weight averaged molar mass, R_g is the z-averaged radius of gyration, and N_A is the Avogadro's number. The RI signal was used to determine the protein concentration while calculating M_w , using a value for the refractive index increment dn/dc of 0.185 mL/g, a typical value for proteins (26). Data were

corrected using a blank subtraction, normalization and peak alignment as described manufacturer (Wyatt Technology). All calculation was performed using the ASTRA 6.0.2 software package.

Secondary structure analysis

Far-UV CD spectra were acquired by using a Jasco J-715 spectropolarimeter (Tokyo, Japan) equipped with a PTC-348WI Peltier temperature control system. For far-UV CD spectra (190-250 nm) quartz cuvettes were used with a 1-mm cell length (Starna, Hainault, UK). The temperature was controlled at 20 °C. Signal-to-noise was improved by accumulating at least 20 scans for a single spectrum. The final CD spectra of samples is determined by subtracting the buffer spectrum from that acquired for the protein sample and by smoothing the features of the spectrum using software the spectra manager. From the measured CD (θ , mdeg) as a function of the wavelength, percentages of secondary structure elements ((α -helix; β -sheets; β -turns and unordered structure) were deduced using the ridge regression algorithm CONTINLL from Dichroweb provided by The University of London (31, 32).

Tertiary structure analysis

Near-UV CD spectra (250-350 nm) of both native α -lac, LC and HRP-nanoparticles were recorded in 3 mL quartz cuvettes (path length 1 cm) (Starna, Hainault, UK) at 20 °C. The signal-to-noise ratio was improved by accumulating at least 20 scans for a single spectrum. The final CD spectra of samples is determined by subtracting the buffer spectrum from that acquired for the protein sample and by smoothing the features of the spectrum using software the spectra manager.

Surface hydrophobicity

A 2.4 mM stock solution of 8-anilino-1-naphthalenesulfonic acid (ANSA) (2.4 mM) was prepared in a 10 mM sodium phosphate buffer at pH 7.0. The ANSA solution was kept at 4 °C overnight with continuous stirring to ensure complete dissolution (33). Protein samples were diluted to a concentration of 0.1 mg/mL using 10 mM sodium phosphate buffer at pH 7.0 at 25 °C. Next, Protein solutions (1 mL) were titrated by a 10 μ L aliquots of ANSA

solution. Fluorescence spectra were recorded using a steady-state spectrofluorometry (The Fluorolog 3.22, (Jobin Yvon-Spex)) between 400 nm and 650 nm upon excitation at 365 nm, using a scan speed of 120 nm/min. Excitation and emission slits were set at 5 nm. The system was thermostated at 20 °C.

Foaming

The foamability of the protein nanoparticles was measured using a foamsan (Teclis, Longessaigne, France) (34). The foam formation and breakdown were monitored by combination of optical (CCD camera) and conductimetric measurements. Conductivity electrodes were placed along the foam tube to monitor the liquid content of foam as well as the volume of liquid drained out of foam and collected at the bottom. Pressurized air was sparged at a flow rate of 200 mL/min. through a metallic plate containing square grid of tapered holes of 30 μm diameter. The foaming tube had an inner diameter of 3.5 cm and the temperature was maintained at 22 ± 1 °C by circulating the water from the water bath (Julabo F25) through outer jacket of the foam tube. A 40-mL of nanoparticle solution (0.25 mg/mL, 10 mM sodium phosphate buffer, pH 7) was used for testing. The electrodes were calibrated with the test solutions before starting the sparging. The foam generation was programmed to produce a fixed volume i.e. 200 mL of foam and if this was not possible then the sparging was stopped after five minutes and the decay of foam volume with time was monitored. The slope of the generated foam volume versus sparging time was used as an indication of foamability of the solution. The time required for the foam volume to reduce to half of its starting volume (t_{half}) was used as indication of foam stability. The data collection and analysis were done by “sampler” and “cell size” software supplied by Teclis along with the “Foamsan”.

Results and discussion

Characterization of laccase-catalyzed cross-linking

Optimization of reaction conditions

In order to be able to compare the $R_H = 25\text{-}100$ nm protein particles produced using HRP, with those produced by LC, we first explored conditions required for the formation of large protein nanoparticle ($R_H > 25$ nm) upon oxidative cross-linking using LC. Size exclusion chromatography (SEC) was used to determine particle formation upon oxidative cross-linking.

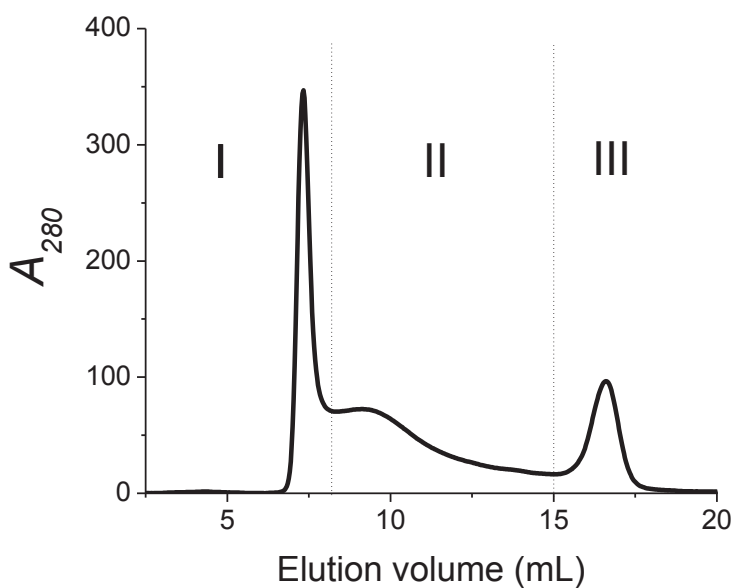


Fig.1. Typical SEC chromatogram of LC cross-linked apo- α -lac, with elution volumes indicated used for estimating conversion of apo- α -lac “protein monomers” (region III, 15-20 mL) into “protein oligomers” (region II, 8-15 mL) and “protein nanoparticles” (region I, 5–8 mL, in the void of the column). The chromatogram shown is for 3 % (w/v) apo- α -lac incubated with laccase (activity: 0.2 U/mL) in 0.1M sodium phosphate buffer, pH 6.0, $T=40$ °C, reaction time $t=15$ h. Elution solution is 10 mM sodium phosphate buffer, pH 7.0.

To analyze the conversion into different types of reaction products, the reaction products eluting in the void of the column are referred to as “protein nanoparticles” ($M_w > 2000$ kDa). Unreacted “protein monomers” ($M_w = 14$ kDa) eluted in a peak around 17 mL. Reactions products eluting at intermediate volumes are referred to as “protein oligomers” ($2000 \text{ kDa} > M_w > 14 \text{ kDa}$). Fig. 1 shows a typical chromatogram with elution volumes indicated corresponding to the regions I (“protein nanoparticles”), II (“protein oligomers”) and III (“protein monomer”). The conversion (%) of monomeric apo- α -lac into protein nanoparticles and protein oligomers at different reaction conditions was determined by determining the normalized areas under the SEC curves for regions I and II, respectively. These are shown in Fig.2.

At pH 6.0, the conversion of protein particle increases from 10 % to 30 % with increasing enzyme activity, mainly at the expense of conversion into oligomers (Fig.2A). At a fixed enzyme concentration of 0.064 U/mL, increasing the initial protein concentration also leads to a higher conversion into protein nanoparticles (Fig.2B). The pH has a strong influence on conversion into either oligomers or nanoparticles: while essentially no protein particles are formed at pH 7.0, we find that by lowering the pH to 6.0, about 30 % of protein monomers are converted into protein nanoparticles (Fig.2C). Finally, we find that the reactions consume enough oxygen such that a high stirring speed is required to maintain oxygen saturation in the reaction mixture (Fig.2D).

The pH dependency of nanoparticle development upon LC-catalyzed cross-linking that we observed agrees with the pH optimum of catalytic activity of laccase reported (13, 14). Based on these results, we continue with the following reaction conditions in order to further characterize the LC protein nanoparticles: a 0.1 M sodium phosphate buffer at pH 6.0, using a high stirring speed (400 rpm and a 3-cm magnetic stirrer), a 3.5 % (w/v) protein concentration, a 0.25 U/ml enzyme concentration. The reaction time is carried out for 15h in a climate chamber maintained at 40 °C, in a 100 mL Schott bottle without a lid (to maintain O_2 saturation).

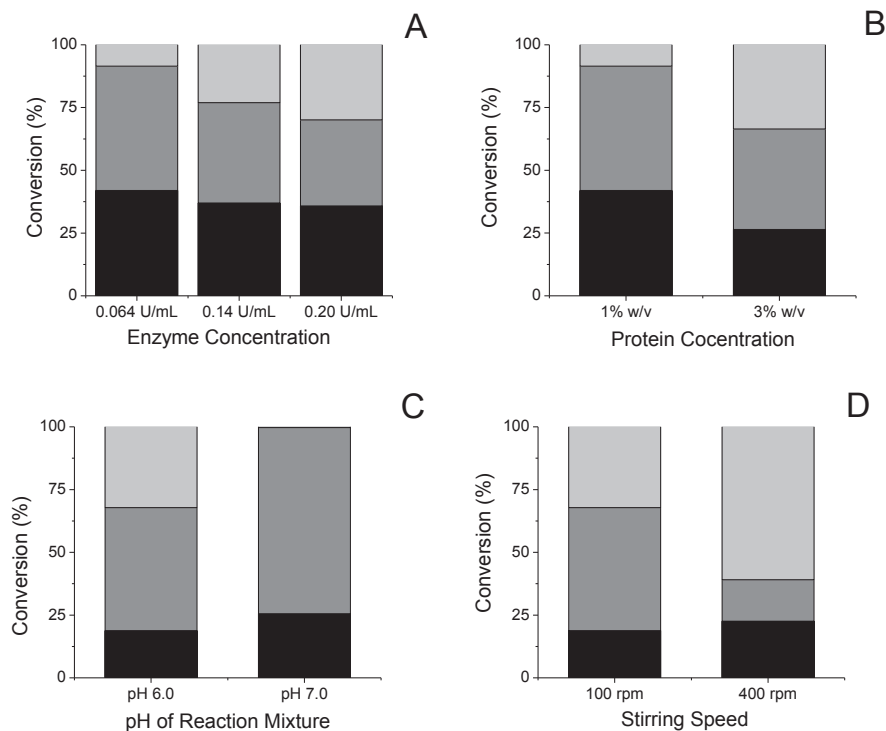


Figure 2. Effect of reaction conditions on conversion (%) upon LC-catalyzed cross-linking of apo- α -lac at 40 °C in 0.1 M sodium phosphate buffer (A) Enzyme concentration added into apo- α -lac solution (α -lac concentration: 1 % w/v) at pH 6.0 (B) Initial protein concentration at pH 6.0 (enzyme concentration: 0.064 U/mL) (C) pH of reaction mixture (α -lac concentration: 3 % w/v, enzyme concentration: 0.064 U/mL) (D) Speed of stirring for reaction at pH 6.0 (α -lac concentration: 3% w/v, enzyme concentration: 0.064 U/ml for 100 rpm, 0.2 U/ml for 400 rpm). Black: “protein monomer”, dark grey: “protein oligomer”, light grey: “protein nanoparticle”.

Analysis of covalent protein cross-linking

SDS-PAGE was used to test whether the protein nanoparticles observed in SEC are indeed held together by covalent cross-links, or that physical bonds also play a role. SDS-PAGE was performed on both peroxidase (HRP) and laccase (LC)-cross-linked nanoparticles were performed in the presence of the reducing agent DTT. We find that the HRP-nanoparticles do not enter the SDS-PAGE gels, while the LC-nanoparticles show a smear on SDS-PAGE, for molecular weights in the range of 14 – 200 kDa (data not shown). This suggests that HRP indeed induces the formation of large, covalently cross-linked protein particles,

whereas the LC-catalyzed cross-linking only gives rise to oligomers. Since the SEC chromatograms clearly show the formation of significant amounts of large protein nanoparticle that elute in the void volume of the column, this must mean that LC cross-linked nanoparticles disintegrate in the presence of DTT and SDS. DLS was used to monitor the possible disintegration of apo- α -lac nanoparticles in the presence of either SDS alone, or both SDS and DTT, in real time. Fig.3 shows the time evolution of the hydrodynamic radii of dialyzed LC- and HRP-nanoparticles.

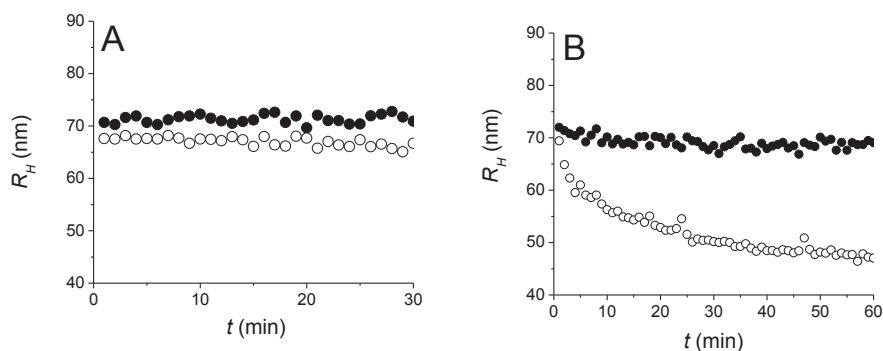


Fig.3. The changes in hydrodynamic radii of HRP nanoparticles (closed symbols) and LC-nanoparticles (open symbols) upon adding SDS or SDS+DTT. (A) with 1% (w/v) SDS (B) with 1% (w/v) SDS and 1% (w/v) DTT. The protein concentration is 0.5 mg/mL, solution conditions are pH 6.8, 10 mM sodium phosphate buffer, temperature 25 °C.

Both LC and HRP-nanoparticles are very stable in the presence of SDS such that R_H remains constant over time at 25 °C. However, the addition of DTT into nanoparticle dispersion (in the additional presence of SDS) leads to a gradually decrease in R_H of LC-nanoparticles over time. The HRP-nanoparticles on the other hand, show a stable hydrodynamic radius in the combined presence of SDS and DTT.

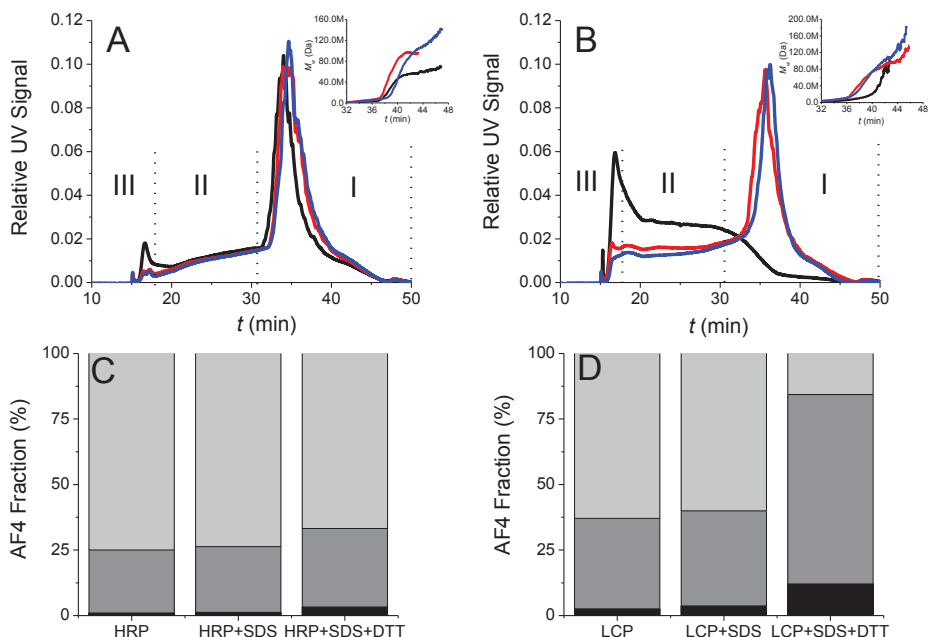


Figure.4. AF4 fractograms of protein nanoparticles that were dialyzed by 300 kDa cut-off membrane, in the absence of reducing agents (blue) and in the presence of 1% (w/v) SDS (red); 1% (w/v) SDS + 1% (w/v) DTT (black) (A) and (C) for HRP-nanoparticles (B) and (D) for LC-nanoparticles. AF4 fractions (%) in region I (Black: “protein monomers”), region II (Dark grey: “protein oligomers”) and region III (Light grey: “protein nanoparticles”).

The extent of disintegration and the M_w distribution of protein nanoparticles in the presence of DTT and SDS were further analyzed using a field flow fractionation (AF4) system. For AF4 analysis, nanoparticle solutions extensively dialyzed against 10 mM sodium phosphate buffer were first incubated with SDS (1% w/v), DTT (1% w/v), or both, for 24h at 25 °C. Next, they were injected and separated using the AF4. The fractograms in Fig.4-A and 4-B are used to estimate the disassociation of “protein nanoparticles” (region I in Fig.4-A, B) into “protein oligomers” (region II in Fig.4-A,B) and “protein monomers” (region III in Fig.4-A,B). The apo- α -lac monomers have a molar mass of $M_w \sim 14$ kDa, oligomers are assumed to have a molar mass in the range $14 \text{ kDa} < M_w < 1000 \text{ kDa}$, and reaction products with molar mass $M_w > 1 \text{ MDa}$ are termed “protein nanoparticles”.

The estimated conversions are shown in Fig.4-C, D. We find that the HRP-nanoparticles remain mostly intact in the presence of SDS and DTT, only a small amount of disintegration occurs for the largest protein nanoparticles (Fig.4-A, inset). In contrast, the combined presence of SDS and DTT (but not SDS alone) leads to significant disintegration of LC nanoparticles into protein oligomers and monomers (Fig.4-B). This observation is entirely consistent with the SDS-PAGE and DLS results.

Our results relating to particle disintegration clearly indicate that LC- and HRP-catalyzed cross-linking results in a different cross-linking chemistry. Previously, we have found that HRP induces mostly dityrosine cross-linking. Preliminary experiments have showed that HRP cross-links only tyrosine residues in a mixture of model amino acids solution including tyrosine, tryptophan and cysteine. Moreover, HRP-catalyzed cross-linking of tyrosine even induces the formation of polytyrosine (data not shown).

On the other hand, LC has been reported to have broad substrate specificity such as tyrosine, cysteine and tryptophan. It has been also found that LC-catalyzed cross-linking can result in an intra- or/and inter-molecular protein cross-linking (14). The particle disintegration that we observe in the presence of DTT clearly suggests disulfide cross-linking, but it is difficult to establish whether cysteine is directly involved in cross-links or not. In fact, the direct enzymatic oxidization of cysteines seems very difficult since α -lac has no free cysteines. On the other hand, we do find that the UV-absorption at 318 nm (corresponding to dityrosine) shows a strong increase during LC-catalyzed cross-linking of α -lac, suggesting that dityrosines are certainly one of the types of cross-links that are being formed. The final absorbance ratio A_{318}/A_{280} (which is a qualitative measure for conversion of tyrosines into dityrosines, trityrosines etc.) is about 25 % less than for HRP-nanoparticles. In summary, while it seems clear that LC induces the formation of dityrosine bonds, disulfide bridges might also be involved in some way. Since direct oxidation of the cysteines seems unlikely, it could be that disulfide-bridges in the protein are attacked by a reaction intermediate, freeing up other cysteine residues to be involved in the disulfide-bridge cross-linking.

Characterization of nanoparticles

Architecture

In order to compare the resulting physical and structural properties of α -lac nanoparticles upon LC and HRP-catalyzed cross-linking, we first characterized protein nanoparticles using AF4 connected to a triple detector system (MALS, UV and IR detectors). Zeta potential of the protein nanoparticles was measured using a Zetasizer Nano ZS. The major physical properties that we quantified for both LC- and HRP-nanoparticles are summarized in table.1.

Table.1. Molecular weight (M_w), gyration of radius (R_g), hydrodynamic radius (R_H), shape factor (R_g/R_H), number of cross-linked monomer (N), internal density (C^*) and zeta potential (ζ) of apo- α -lac nanoparticles.

Nanoparticles	Mw (MDa)	R_g (nm)	R_H (nm)	R_g/R_H	N	C^* (%)	ζ (mV)
HRP	63.3	120.3	65	1.85	4521	1.44	-27.1
LC	51.1	120	62	2.0	3651	1.17	-22.4

We found that the molar mass M_w (calculated from a Berry plot of the angle-dependent light scattering intensity) for HRP-nanoparticles is nearly 10 MDa higher than that for the LC- nanoparticles. Since the size of the HRP- and LC-nanoparticles is nearly the same, this implies that the LC-nanoparticles have a somewhat more open structure, and lower internal density than the HRP-nanoparticles. Both LC and HRP-nanoparticles have a zeta potential that is around twice more negative than that of monomeric apo- α -lac at neutral pH.

More detailed information can be extracted from the AF4-MALLS analysis by plotting the radius of gyration of the eluting species versus their molar mass. Typically an approximate relationship $R_g \sim M_w^a$ holds, and the exponent a is a function of the architecture of the nanoparticles. For example, for a compact (collapsed) structure, $a \approx 0.3$, for random coils, as well as for many types of particle aggregates, $a \approx 0.5$ - 0.6 , and

finally, for rod-like objects, $a = 1.0$ (35). The plots of R_g versus M_w for HRP and LC-nanoparticles are given in fig.5-A.

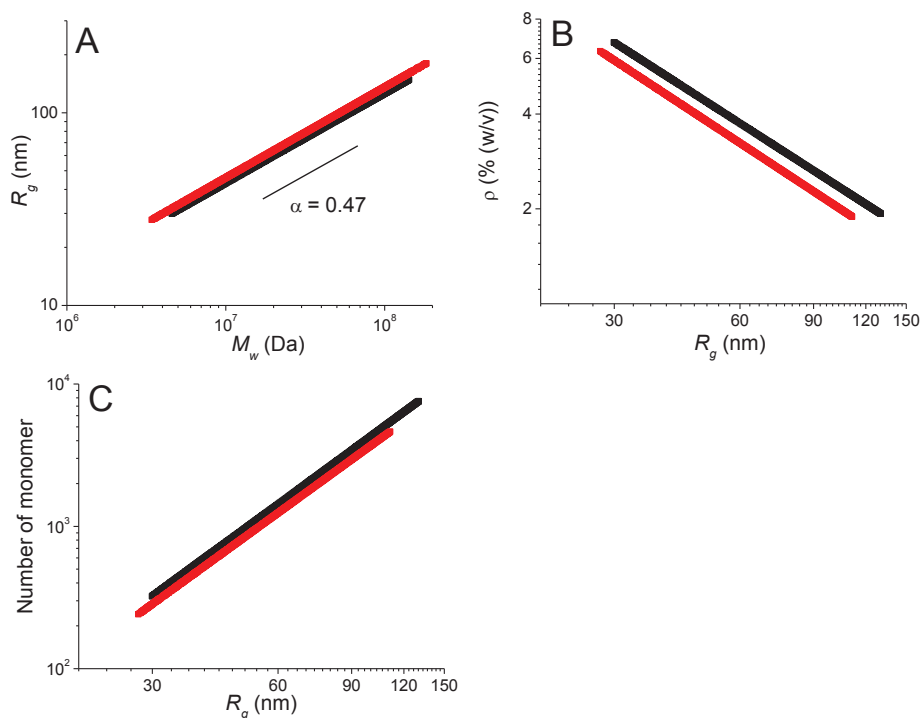


Figure.5. Structural Properties of LC- and HRP nanoparticles (A) Size-mass scaling, radius of gyration R_g versus molar mass M_w (obtained for the same separations as those shown in Fig.4-B) (B) Apparent molar mass averaged density ρ versus radius of gyration R_g (C) Number of monomers N per nanoparticle versus nanoparticle radius of gyration R_g . For all plots, black lines are for HRP-nanoparticles and red lines are for LC-nanoparticles, for elution volumes between 36 min and 45 min in the AF4 fractograms, where elution was done using a 10 mM sodium phosphate buffer at pH 7.0 at 25 °C.

The scaling exponents for both LC and HRP-nanoparticle are nearly identical, $a \approx 0.5$ indicating a self-similar structure with fractal dimension of $d_f = 1/a \approx 2$. As expected for such a self-similar structure, the internal densities decrease with increasing particle size (Fig.5-B). We have also plotted the number of protein monomers making up protein nanoparticles with a certain size (Fig.5-C). In summary, the AF4 analysis clearly indicates that the structural properties of protein nanoparticles made upon both HRP- and LC-catalyzed cross-linking apo- α -lac are very similar, and correspond to rather dilute

structures with an average internal protein concentration in the particles on the order of 1% (w/v) to a few % (w/v).

Secondary and tertiary structure

Circular Dichroism (CD) was used to study conformational changes of apo- α -lac upon the oxidative cross-linking using either HRP or LC. The secondary structure can be determined by CD spectroscopy in the "far-UV" spectral region (190-250 nm) corresponding to wavelengths of peptide bond absorption, whereas the "near-UV" spectral region (250-350 nm) is sensitive to tertiary structure via changes in the relative distances and orientation of aromatic amino acids and disulfide bonds that have near-UV absorption (36). Fig.6 shows the far-UV and near-UV CD spectra of apo- α -lac, LC- and HRP-cross-linked apo- α -lac nanoparticles. The native apo- α -lac exhibits the typical feature of α -helix rich protein in far-UV CD spectra: two minima, at respectively 208 nm and 222 nm wavelength. We find that both types of oxidative cross-linking of apo- α -lac lead to a decrease of the depth of the minimum at 222 nm (Fig.7-A). This indicates that some extent of secondary structure is lost upon oxidative cross-linking. In the near-UV CD spectra, both LC- and HRP- catalyzed cross-linking leads to a complete loss of the characteristic spectral features for native apo- α -lac.

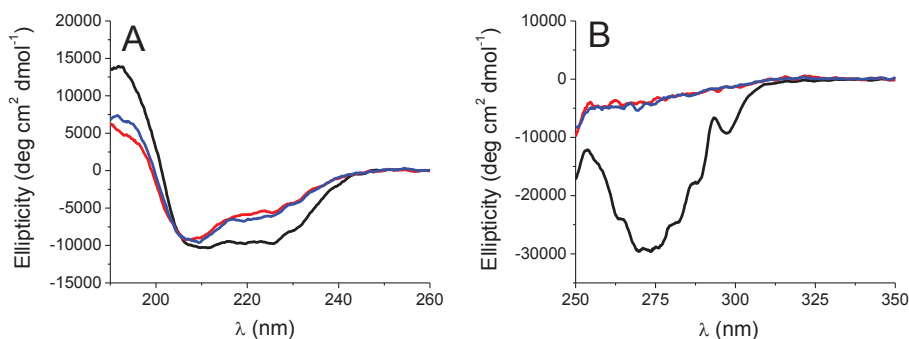


Figure.6. Far-UV and near-UV CD spectra of HRP and LC cross-linked apo- α -lac, compared to spectra for native apo- α -lac. (A) The far-UV spectra and (B) near-UV CD spectra of native α -lac (black), LC-nanoparticles (blue) and HRP- nanoparticles (red) in 10 mM sodium phosphate buffer at pH 7.0 at 25 °C.

Hence, cross-linked proteins in both types of apo- α -lac nanoparticles have lost practically all tertiary structure as compared to native apo- α -lac. In summary, we find very similar changes in both near-UV and far-UV CD-spectra upon for LC and HRP-catalyzed cross-linking, indicating a similar conformational changes: a partial loss of the predominantly α - helical secondary structure and a complete loss of tertiary structure. The quantitative analysis confirms that there is indeed a noticeable decrease of the percentage of α - helices, of about 30%, such that about 70% of the original α -helices remain after cross-linking (Table.2)

Table.2. Percentages of α -helix, β -sheet, β -turns and random coil of native apo- α -lac; HRP-nanoparticles and LC-nanoparticles.

Sample	α -helix	β -sheet	β -turns	Random Coil
Apo- α -lac	36	19.7	18.5	25.9
HRP-nanoparticles	24.8	23.8	20.7	30.7
LC-nanoparticles	26.9	22.2	20.9	30

Exposed surface hydrophobicity

Somewhat unexpectedly, we find that the surface hydrophobicity (S_o) slightly decreases upon HRP-catalyzed cross-linking as compared to that of native apo- α -lac (Fig.7) In contrast, LC cross-linked apo- α -lac has a significantly higher surface hydrophobicity S_o , corresponding to a threefold higher fluorescence as compared to native apo- α -lac and HRP cross-linked apo- α -lac nanoparticles.

In summary, we find that HRP nanoparticles are very hydrophilic, even more so than the native apo- α -lac, whereas LC cross-linked apo- α -lac nanoparticles are significantly more hydrophobic. This again highlights the fact that the different cross-linking chemistry of HRP and LC leads to different molecular conformations and hence to different physical properties.

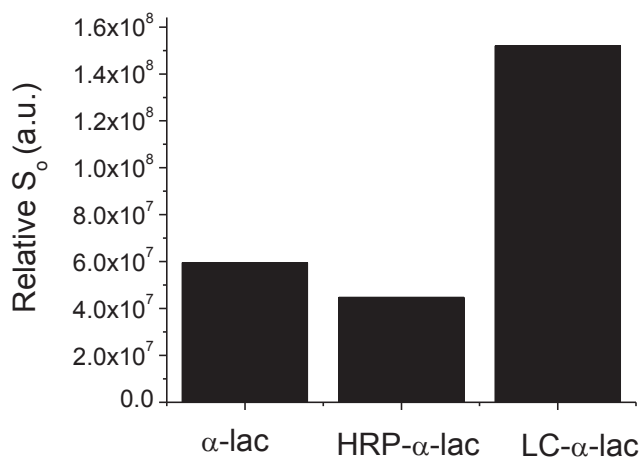


Figure.7. Exposed surface hydrophobicity (S_0 , arbitrary units) as determined using the fluorescent probe ANSA, for native apo- α -lac (α -lac), HRP cross-linked (HRP- α -lac) and LC-cross-linked apo-a-lac (LC- α -lac). Solution conditions were a 10 mM sodium phosphate buffer at pH 7.0 at 25 °C.

Functionality

Foamability

The surface activity of molecules and molecular assemblies at air-water interfaces, and hence their ability to increase foamability and foam stability, directly correlates with their surface hydrophobicity (S_0) (37). To elucidate the relation between the surface hydrophobicity and the influence of the protein nanoparticles on foamability and foam stability, we have performed foaming experiments with solutions of HRP- and LC-nanoparticles. We found that for the more hydrophobic LC-nanoparticles, the foam volume reached 189.5 cm³ after sparging at a flow rate of 200 mL/min for 80 sec. In contrast, for HRP-nanoparticles we were not able to make stable foam even after very longer sparging times (300 sec), a difference that is also reflected in the very different foaming rates (Table.3).

Table.3. The parameters for foam properties of both LC- and HRP-nanoparticles as determined a sparging test. Solution conditions are a pH 7.0 in 10 mM sodium phosphate buffer at 25 °C, with a protein concentration of 0.25 mg/mL.

Sample	Foam volume (cm ³)	Sparging time (sec)	<i>t</i> _{1/2} (sec)	Foaming rate (cm ³ /sec)
LC-NP	189.5	80	2931	2.6
HRP- NP*	54.5	300	ND**	0.23

* NP: Nanoparticles; ** ND: Not determined,

Hence it is clear that the hydrophobic nature of the LC-nanoparticles facilitates their adsorption at the water/air interface. When adsorbed at the interface, they can possibly rearrange to make inter-particle connections, and also the interface may induce further unfolding of the protein subunits, both leading to further stabilization of the foam. It is equally clear that the HRP-nanoparticles are simply too hydrophilic to efficiently adsorb at the interface, an effect presumably amplified by the large zeta-potential that leads to strong electrostatic repulsions.

Thermal stability

The thermal stability of the different protein nanoparticles was characterized using dynamic light scattering and turbidity measurements. To compare thermal stability of LC- and HRP-nanoparticles, the time evolution of the size of the nanoparticles during heating was monitored in real-time using DLS (Fig.10-A). Hydrodynamic radii (*R_H*) of HRP-nanoparticles very slowly decrease during heating for 1h. For LC-nanoparticles, however, the *R_H* decreases much more rapidly, such that after one hour of heating, the LC-nanoparticles only have about half their original size.

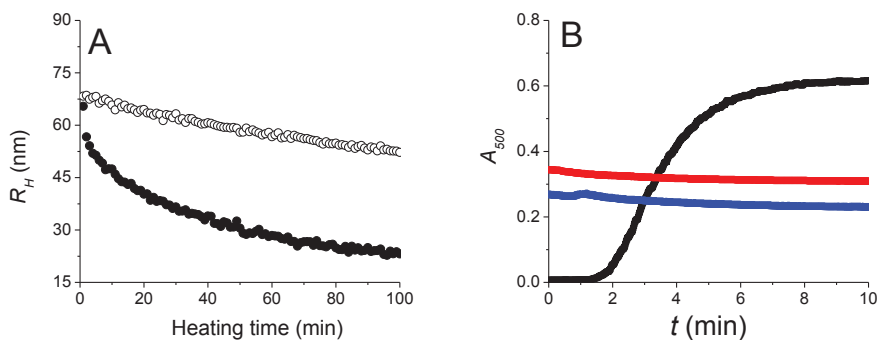


Figure.8. Thermal stability of apo- α -lac nanoparticles versus that of native apo- α -lac (A) Hydrodynamic radii (R_H) for LC-nanoparticles (solid spheres) and HRP-nanoparticles (open spheres) during heating at 90 °C at pH 6.8 (B) Turbidity at 400 nm for native α -lac (black), LC-nanoparticles (blue) and HRP-nanoparticles (red) at pH 5.7 during heating at 90 °C. Protein concentration is 5.3 mg/mL for all samples, 10 mM sodium phosphate buffer.

This suggests the LC-nanoparticles easily undergo thermal disintegration whereas the disintegration at neutral pH of the HRP-nanoparticles is limited. The particle disintegration observed upon heating LC-nanoparticles is consistent with our earlier observation that disulfide-bridges are somehow involved in stabilizing the LC-nanoparticles, since disulfide bridges are known to be able to re-arrange during heating.

Previously, we found that HRP-nanoparticles are completely stable against thermal aggregation at pH 5.7, a pH at which native apo- α -lac easily aggregates upon heating (in chapter 5). Fig.10-B shows a comparison of the time evolution of the turbidity of native apo- α -lac, HRP and LC-nanoparticles at pH 5.7 upon heating at 90 °C. In view of their much larger size, the initial turbidity is much larger for the nanoparticles, but within a few minutes of heating the turbidity of the native apo- α -lac increases to large values, indicating fast and extensive aggregation of the protein. Instead, the turbidity for the nanoparticles decreases slightly during the heating, presumably due to the slight decrease in particle size that takes place during the 10-minute of heating (see Fig. 10-A). Hence, the oxidative cross-linking of apo- α -lac appears to prevent protein aggregation at pH 5.7, both for the hydrophilic HRP- and for the hydrophobic LC-nanoparticles. Previously, we have shown that it is the hydrophilic nature, structural stability and strongly repulsive colloidal

interactions of the HRP nanoparticles that determine their stability against heat-induced aggregation. Although the LC-nanoparticles are much more hydrophobic, likewise high zeta potential (which we have shown is not affected by heating) and their high structural stability apparently are sufficient to also make the LC-nanoparticles highly stable against heat-induced aggregation.

Concluding remarks

The aim of this study was to examine to what extent two different oxidative cross-linking enzymes, peroxidase and laccase alter the physical and functional properties of when acting on the common substrate apo- α -lac. We found that the nanoparticles formed under the influence of both enzymes, have a self-similar architecture with a rather low content of protein inside the nanoparticles (a few % w/v). Also, for both enzymes, protein monomers within the nanoparticles retain a significant part of the original protein α -helical secondary structure, while all tertiary structure is lost due to cross-linking. Again, for both enzymes, the oxidative cross-linking leads to a higher resistance against thermal aggregation, although for LC this effect is less pronounced than for HRP. We also find differences: the LC nanoparticles partially disintegrate when heated in the presence of DTT, pointing to a role for disulfide bridges in stabilizing these particles. This is not the case for the HRP particles. Also, whereas the HRP particles are very hydrophilic and cannot efficiently stabilize foams, the LC particles are more hydrophobic and do adsorb to the air-water interface, leading to foam stabilization.

Overall, our findings indicate that different types of cross-linking bonds must be involved in stabilizing the two different kinds of protein nanoparticles. This presumably also leads to different kinds of rearrangements at the interfaces of the proteins, induced by the cross-linking. As a consequence, even though the structures are quite similar at the mesoscale, they have quite different physical and functional properties. This implies that differences between oxidative enzymes can be exploited to tailor the properties of protein nanoparticles. The use of oxidative enzymes also expands the repertoire of functionalities that can be obtained as compared to transglutaminase. Future studies will be necessary to learn more about the detailed differences in the chemistry of the oxidative cross-linking of

the different enzymes that determine the differences in physical and functional properties that we observe here.

Acknowledgement

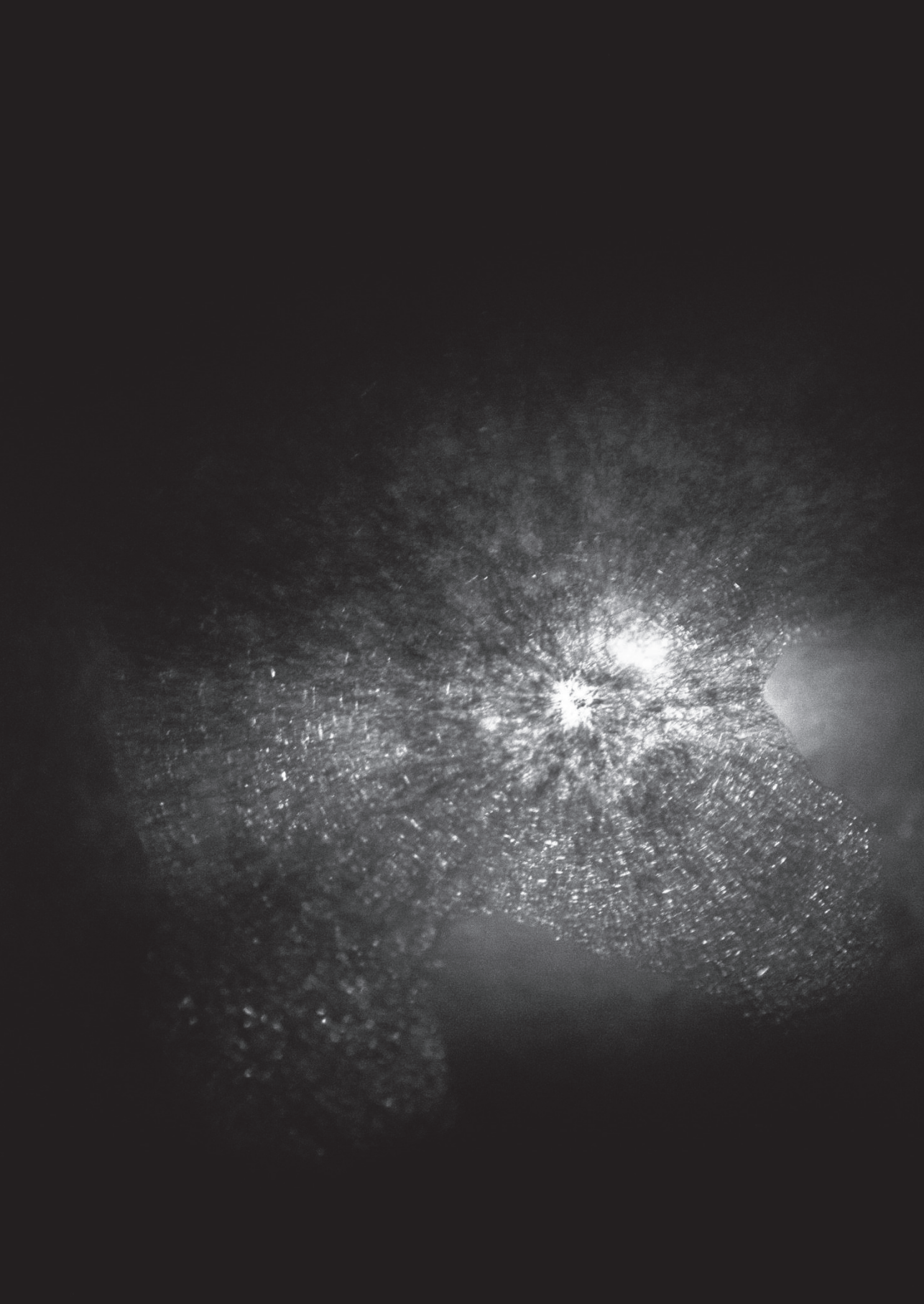
This work is part of the Industrial Partnership Programme (IPP) Bio(-Related)Materials of the Stichting voor Fundamenteel Onderzoek der Materie (FOM), which is financially supported by the Nederlandse Organisatie voor Wetenschappelijk Onderzoek (NWO). The IPP BRM is co-financed by the Top Institute Food and Nutrition and the Dutch Polymer Institute.

References

1. Heck, T.; Faccio, G.; Richter, M.; Thony-Meyer, L., Enzyme-catalyzed protein crosslinking. *Appl. Microbiol. Biotechnol.* **2013**, *97*, 461-475.
2. Ozrenk, E., The use of transglutaminase in dairy products. *Int. J. Dairy Technol.* **2006**, *59*, 1-7.
3. Faergemand, M.; Otte, J.; Qvist, K. B., Cross-linking of whey proteins by enzymatic oxidation. *J. Agric. Food Chem.* **1998**, *46*, 1326-1333.
4. Buchert, J.; Cura, D. E.; Ma, H.; Gasparetti, C.; Monogioudi, E.; Faccio, G.; Mattinen, M.; Boer, H.; Partanen, R.; Selinheimo, E.; Lantto, R.; Kruus, K., Crosslinking Food Proteins for Improved Functionality. In *Annual Review of Food Science and Technology, Vol 1*, Doyle, M. P.; Klaenhammer, T. R., Eds. Annual Reviews: Palo Alto, 2010; Vol. 1, pp 113-138.
5. Heijnis, W. H.; Wierenga, P. A.; Berkel, W. J. H.; Gruppen, H., Directing the Oligomer Size Distribution of Peroxidase-Mediated Cross-Linked Bovine alpha-Lactalbumin. *J. Agric. Food Chem.* **2010**, *58*, 5692-5697.
6. Thurston, C. F., The structure and function of fungal laccases. *Microbiology-(UK)* **1994**, *140*, 19-26.
7. Faccio, G.; Kruus, K.; Saloheimo, M.; Thony-Meyer, L., Bacterial tyrosinases and their applications. *Process Biochem.* **2012**, *47*, 1749-1760.
8. Selinheimo, E.; Autio, K.; Krijus, K.; Buchert, J., Elucidating the mechanism of laccase and tyrosinase in wheat bread making. *J. Agric. Food Chem.* **2007**, *55*, 6357-6365.
9. Veitch, N. C., Horseradish peroxidase: a modern view of a classic enzyme. *Phytochemistry* **2004**, *65*, 249-259.
10. Thalmann, C. R.; Lotzbeyer, T., Enzymatic cross-linking of proteins with tyrosinase. *Eur. Food Res. Technol.* **2002**, *214*, 276-281.
11. Selinheimo, E.; Lampila, P.; Mattinen, M. L.; Buchert, J., Formation of protein - Oligosaccharide conjugates by laccase and tyrosinase. *J. Agric. Food Chem.* **2008**, *56*, 3118-3128.
12. Oudgenoeg, G., Peroxidase catalyzed conjugation of peptides, proteins and polysaccharides via endogenous and exogenous phenols. *PhD Thesis, Wageningen University* **2004**.
13. Madhavi, V.; Lele, S. S., Laccase: properties and applications. *BioResources* **2009**, *4*, 1694-1717.

14. Kiiskinen, L. L.; Viikari, L.; Kruus, K., Purification and characterisation of a novel laccase from the ascomycete *Melanocarpus albomyces*. *Appl. Microbiol. Biotechnol.* **2002**, *59*, 198-204.
15. Lantto, R.; Schonberg, C.; Buchert, J.; Heine, E., Effects of laccase-mediator combinations on wool. *Text. Res. J.* **2004**, *74*, 713-717.
16. Mattinen, M. L.; Kruus, K.; Buchert, J.; Nielsen, J. H.; Andersen, H. J.; Steffensen, C. L., Laccase-catalyzed polymerization of tyrosine-containing peptides. *Febs J.* **2005**, *272*, 3640-3650.
17. Lantto, R.; Puolanne, E.; Kalkkinen, N.; Buchert, J.; Autio, K., Enzyme-aided modification of chicken-breast myofibril proteins: Effect of laccase and transglutaminase on gelation and thermal stability. *J. Agric. Food Chem.* **2005**, *53*, 9231-9237.
18. Lantto, R.; Puolanne, E.; Katina, K.; Niemisto, M.; Buchert, J.; Autio, K., Effect of laccase and transglutaminase on the textural and water-binding properties of cooked chicken breast meat gels. *Eur. Food Res. Technol.* **2007**, *225*, 75-83.
19. Elliott, K. A., Oxidations catalysed by horseradish- and milk-peroxidases. *The Biochemical journal* **1932**, *26*, 1281-90.
20. Heijnis, W. H.; Dekker, H. L.; de Koning, L. J.; Wierenga, P. A.; Westphal, A. H.; de Koster, C. G.; Gruppen, H.; van Berkel, W. J. H., Identification of the Peroxidase-Generated Intermolecular Dityrosine Cross-Link in Bovine alpha-Lactalbumin. *J. Agric. Food Chem.* **2011**, *59*, 444-449.
21. Schomberg, D., Salzmann, M., and Stephan, D., Enzyme Handbook, 7, EC 1.11.1.7:1-6 **1993**.
22. Jin, R.; Teixeira, L. S. M.; Dijkstra, P. J.; Karperien, M.; van Blitterswijk, C. A.; Zhong, Z. Y.; Feijen, J., Injectable chitosan-based hydrogels for cartilage tissue engineering. *Biomaterials* **2009**, *30*, 2544-2551.
23. Jin, R.; Teixeira, L. S. M.; Dijkstra, P. J.; van Blitterswijk, C. A.; Karperien, M.; Feijen, J., Enzymatically-crosslinked injectable hydrogels based on biomimetic dextran-hyaluronic acid conjugates for cartilage tissue engineering. *Biomaterials* **2010**, *31*, 3103-3113.
24. Sofia, S. J.; Singh, A.; Kaplan, D. L., Peroxidase-catalyzed crosslinking of functionalized polyaspartic acid polymers. *J. Macromol. Sci.-Pure Appl. Chem.* **2002**, *A39*, 1151-1181.
25. Saricay, Y.; Wierenga, P.; de Vries, R., Nanostructure development during peroxidase catalysed cross-linking of alpha-lactalbumin. *Food Hydrocolloids* **2013**, *33*, 280-288.
26. Dhayal, S. K.; Gruppen, H.; de Vries, R.; Wierenga, P. A., Controlled formation of protein nanoparticles by enzymatic cross-linking of alpha-lactalbumin with horseradish peroxidase. *Food Hydrocolloids* **2014**, *36*, 53-59.
27. Saricay, Y.; Dhayal, S. K.; Wierenga, P. A.; de Vries, R., Protein cluster formation during enzymatic cross-linking of globular proteins. *Faraday Discuss.* **2012**, *158*, 51-63.
28. Bourbonnais, R.; Leech, D.; Paice, M. G., Electrochemical analysis of the interactions of laccase mediators with lignin model compounds. *Biochim. Biophys. Acta-Gen. Subj.* **1998**, *1379*, 381-390.
29. Majcherczyk, A.; Johannes, C.; Huttermann, A., Oxidation of polycyclic aromatic hydrocarbons (PAH) by laccase of *Trametes versicolor*. *Enzyme Microb. Technol.* **1998**, *22*, 335-341.
30. Kronman, M. J.; Andreotti, R. E., Inter- + intramolecular interactions of alpha-lactalbumin .i. apparent heterogeneity at acid pH. *Biochemistry* **1964**, *3*, 1145-&.

31. Provencher, S. W.; Glockner, J., Estimation of globular protein secondary structure from circular-dichroism. *Biochemistry* **1981**, *20*, 33-37.
32. Whitmore, L.; Wallace, B. A., DICHROWEB, an online server for protein secondary structure analyses from circular dichroism spectroscopic data. *Nucleic Acids Res.* **2004**, *32*, W668-W673.
33. Wierenga, P. A.; Meinders, M. B. J.; Egmond, M. R.; Voragen, F.; de Jongh, H. H. J., Protein exposed hydrophobicity reduces the kinetic barrier for adsorption of ovalbumin to the air-water interface. *Langmuir* **2003**, *19*, 8964-8970.
34. Schwenzfeier, A.; Lech, F.; Wierenga, P. A.; Eppink, M. H. M.; Gruppen, H., Foam properties of algae soluble protein isolate: Effect of pH and ionic strength. *Food Hydrocolloids* **2013**, *33*, 111-117.
35. Nilsson, L., Separation and characterization of food macromolecules using field-flow fractionation: A review. *Food Hydrocolloids* **2013**, *30*, 1-11.
36. Kelly, S. M.; Price, N. C., The Use of Circular Dichroism in the Investigation of Protein Structure and Function. *Curr. Protein Pept. Sci.* **2000**, *1*, 349-384.
37. Damodaran, S., 1997. Protein-stabilized foams and emulsions. In: Damodaran, S., Paraf, A. (Eds.), *Food Proteins and their Applications*. Marcel Dekker, Inc., New York, United States, pp. 57–110).



Chapter 7

General Discussion

**Apo- α -lactalbumin cross-linking by peroxidase, laccase and tyrosinase –
A comparison of the formation, physical and functional properties of
the resulting nanoparticles**

Introduction

In this thesis, we have studied the effects of enzymatic cross-linking on the molecular and mesoscale properties of apo- α -lactalbumin (apo- α -lac), in order to explore and understand the possible food functional properties of enzymatically cross-linked protein nanoparticles in food formulations. In this chapter, we will summarize our key findings obtained for peroxidase and laccase. To this, we add some preliminary observation on tyrosinase-catalyzed cross-linking of apo- α -lac, and some additional observations on the influence of Ca^{2+} on peroxidase cross-linked particles. In this way, we arrive at a broad overview of the enzymatic cross-linking of apo- α -lac into nanoparticles by a range of oxidative enzymes.

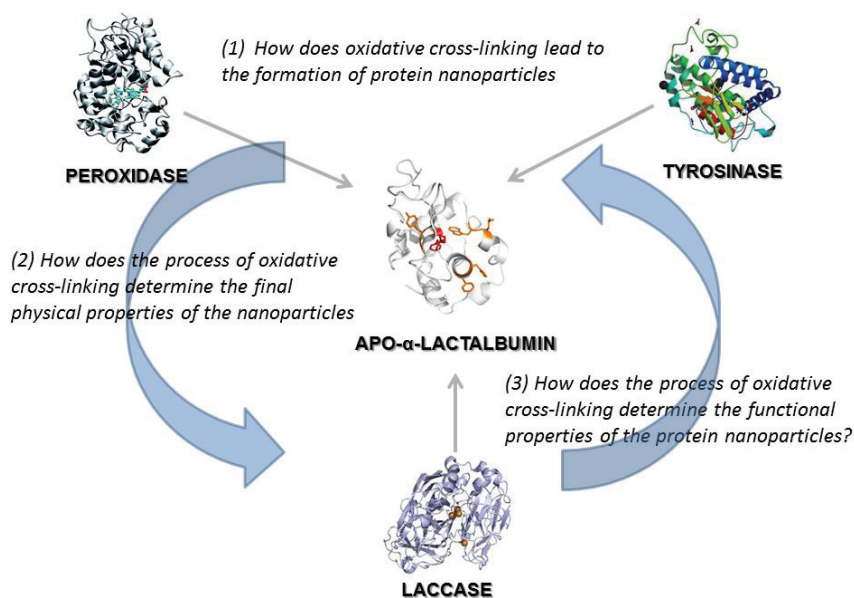


Figure.1. Graphical summary of the main topics of the General Discussion

Our overview focuses on similarities and differences between the different enzyme systems (illustrated in fig.1) with respect to the nanoparticle formation process and the key factors influencing it, and the physical and functional properties of the nanoparticles.

Nanoparticle formation

Peroxidase & laccase versus tyrosinase

As discussed in the introduction, for globular food proteins, the limited accessibility of reactive groups is the main factor preventing the formation of enzymatically cross-linked nanoparticles consisting of many protein subunits. **In chapter 2 and 4**, we have shown that the peroxidase-catalyzed cross-linking of apo- α -lac nevertheless can lead to the formation of large protein nanoparticles. **In chapter 6**, we have found that the same holds for laccase. Here we also include tyrosinase in the comparison. We first present data for the conversion of apo- α -lac “monomers” into protein nanoparticles, as quantified using size exclusion chromatography (SEC). We refer the reaction products that occur in the void volume of the column (V_e of 5 -8 mL, $M_w \geq 10^6$ Da) as “protein nanoparticles”. Reaction products with intermediate elution volumes (V_e of 8-15 mL, 10^6 Da $\geq M_w \geq 10^4$ Da) are called “protein oligomers”. The highest elution volumes correspond to “protein monomers” (V_e of 15 - 20 mL, $M_w \approx 10^4$ Da). Fig.2 shows SEC chromatograms of the final reaction products of enzymatically cross-linked apo- α -lac for a set of representative reaction conditions for the different enzymes.

When comparing the enzymes with respect to the ability to convert as much protein monomers as possible into large protein nanoparticles (which is what we want here), for pH 7.0, it is clear that peroxidase is by far the most effective enzyme for the conditions that we have explored. (Fig.2-A). For tyrosinase, we did not find conditions that led to the efficient conversion of protein monomers into large protein nanoparticles, for reaction pH values in the range pH 3.0-7.0 (Fig.2-B) (data obtained for pH 3.0, 7.0 is not shown). At pH 7, laccase-catalyzed cross-linking only induced the formation of protein oligomers with M_w in the range of 14 kDa – 660 kDa (Fig.2-C). By lowering the pH to pH 6.0, laccase was also capable of creating larger soluble protein nanoparticles than those formed at pH 7.0 (R_H of 50 nm; M_w of 10^7 Da). We find that all oxidative enzymes catalyze the conversion of about the same amount of protein monomers into oligomers and nanoparticles at pH 6.0 and 7.0, namely around 80% while typical particle sizes differed for the various oxidative enzymes (Fig.2).

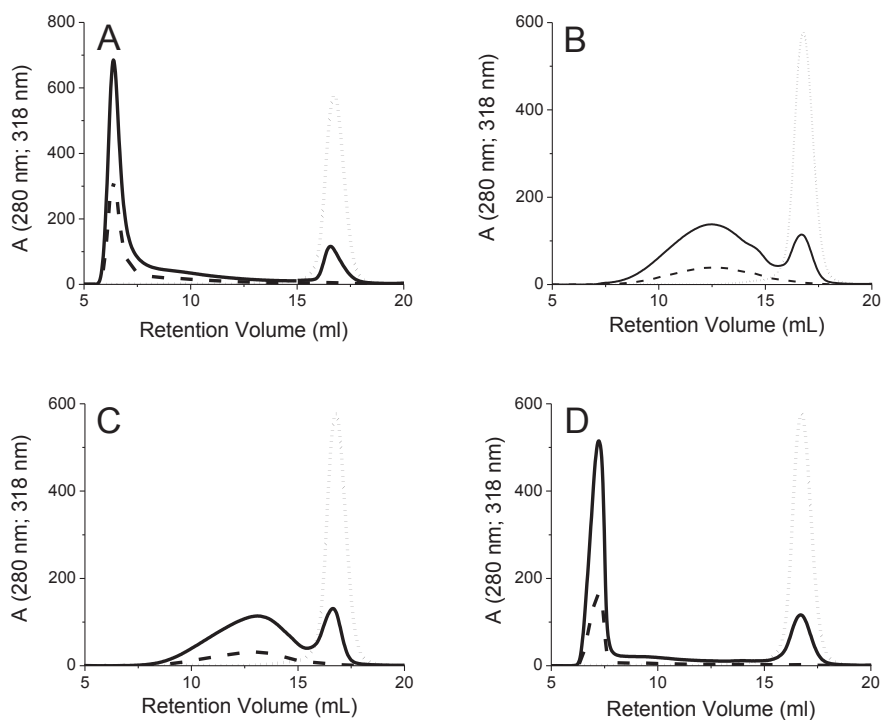


Figure.2. SEC chromatograms of apo- α -lac cross-linked using various oxidative enzymes (A) Peroxidase-cross-linked apo- α -lac (Reaction conditions: $C_{apo-\alpha-lac}$ = 1% (w/v), C_{HRP} = 0.5 mg/mL, buffer: 0.1 M ammonium acetate, pH 6.8, T = 37 °C, $t_{reaction}$ = 15 h) (B) Tyrosinase-cross-linked apo- α -lac (Reaction conditions: $C_{apo-\alpha-lac}$ = 3.5% (w/v), C_{TYR} = 1.5 mg/mL, buffer: 0.1 M sodium phosphate buffer, pH 6.0, T = 40 °C, $t_{reaction}$ = 15 h) (C) Laccase-cross-linked apo- α -lac at pH 7.0 (Reaction conditions: $C_{apo-\alpha-lac}$ = 3.0% (w/v), C_{LC} = 0.2 U/mL, buffer: 0.1 M sodium phosphate buffer, pH 7.0, T = 40 °C, $t_{reaction}$ = 15 h, slow stirring (100 rpm)) (D) Laccase-cross-linked apo- α -lac at pH 6.0 (Reaction conditions: $C_{apo-\alpha-lac}$ = 3.5% (w/v), C_{LC} = 0.25 U/mL, buffer: 0.1 M sodium phosphate buffer, pH 6.0, T = 40 °C, $t_{reaction}$ = 15 h, fast stirring (400 rpm)). Eluent is 10 mM sodium phosphate buffer, pH 7.0, and column = Superose 6, flow rate = 0.5 min/mL, SEC chromatography: GE AKTA Micro.

These results show that the different oxidative enzymes (peroxidase, laccase and tyrosinase) induce nearly same final monomer conversion, but only peroxidase and laccase are capable of forming large hierarchical apo- α -lac nanoparticles with hydrodynamic radii R_H in the range of R_H = 25-150 nm.

Under the conditions we have explored, tyrosinase only leads to the formation of small oligomers. One reason for this might be that for the large tyrosinase enzyme ($M_w = 119.5$ kDa), accessibility of the reactive tyrosines in globular proteins is more problematic than for the smaller enzymes laccase and peroxidase. Another reason might be that tyrosinase, as compared to peroxidase and laccase, has a stronger tendency to catalyze the formation of intra-molecular cross-links. In addition to dityrosine cross-links, tyrosinase is known to be able to catalyze the formation of cross-links with other groups as well, which may enhance the possibility for intramolecular cross-links with amino, sulfhydryl, and pyrrolidine side chains of proteins (1). The formation of such intra-molecular cross-links may prevent the further inter-molecular cross-linking of the proteins into nanoparticles.

The optimum pH for cross-linking by tyrosinase, was reported to be pH 4.0-5.0, which is supposedly a consequence of an optimal accessibility of the active site to globular protein substrates in this pH range (1). Unfortunately, under these conditions (i.e. 1% w/v at pH 4.0-5.0 in 10 mM ammonium phosphate, at 37 °C), we also found significant aggregation of the substrate protein. On the other hand, at pH 3.0, 6.0 and 7.0, the substrate protein does not aggregate, but we observed little cross-linking. Hence we directed our attention to the narrow pH range pH 5-6 where we expect both some enzymatic activity, and where we do not expect to see any aggregation. Indeed, at pH 5.7, tyrosinase-catalyzed cross-linking clearly leads to the formation of a significant amount of cross-linked protein, including some (but not much) reaction product that elutes in the void volume of the column, i.e. protein nanoparticles.

A higher conversion of apo- α -lac into nanoparticles by tyrosinase was observed under slightly different reaction conditions, namely a higher initial protein concentration, a somewhat higher protein-to-enzyme ratio and a lower concentration of buffer. For this case, Fig.3 shows the SEC chromatograms of the reaction products at various reaction times (as indicated in the figure). Remarkably, at pH 5.7, for tyrosinase induced cross-linking, we observed the formation of specific protein oligomers at relatively short reaction times. These occur at elution volumes (V_e) of 15.5 mL (1) ($M_w \approx 18.4$ kDa); both 13.9 mL (2) and 13.2 mL (3) ($450 \text{ kDa} < M_w < 18.4 \text{ kDa}$) (Fig.3).

This indicates that tyrosinase-catalyzed cross-linking of apo- α -lac could possibly be used for creating well-defined small oligomers rather than large protein particles. Such oligomers might have very different functional properties as compared to the large protein nanoparticles that we mainly focus on here.

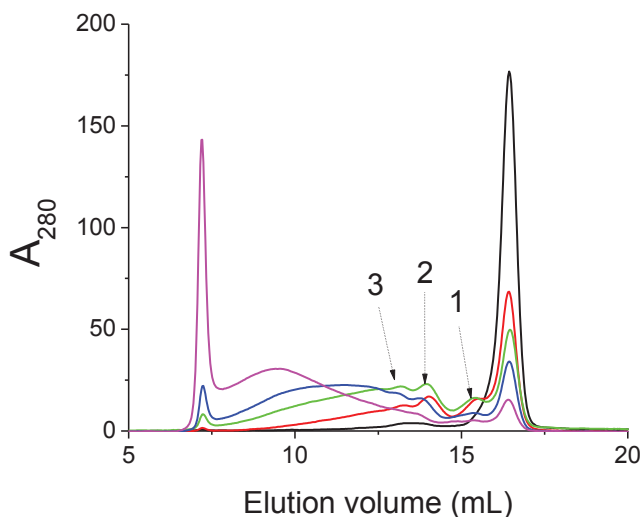


Figure.3. SEC chromatograms of native apo- α -lac (black) and tyrosinase-cross-linked apo- α -lac at various incubation times: red: 1h, green: 3h blue: 6h magenta: 18h (Reaction conditions: $C_{apo-\alpha-lac}$ = 5% (w/v), C_{TYR} = 2.5 mg/mL (Tyrosinase activity from *agaricus bisporus*, (Sigma T3824) is given by manufacturer as ≥ 1000 unit/mg solid for lyophilized powder), buffer: 0.01 M ammonium acetate, pH 5.7, $T = 37^\circ\text{C}$, $t_{reaction} = 18\text{h}$, no stirring. Eluent is 10 mM sodium phosphate buffer at pH 7.0.

An overview of the typical sizes and molar masses obtained by cross-linking with the different enzyme systems is given in Table 1. Clearly, for peroxidase and laccase, we find very large protein clusters, that given their hydrodynamic sizes are indeed appropriately called protein nanoparticles. Most other studies on enzymatic protein cross-linking report cluster sizes that are much smaller than this (1-4).

An exception is the work of Matsumura et al., who found that transglutaminase was capable of creating large α -lac particles (i.e. $M_w \geq 1$ and/or 10 MDa) in the presence of DTT (5). Our results show that peroxidase and laccase can also catalyze the formation of large apo- α -lac particles in the absence of DTT.

Table.1. Overview of molecular weight (M_w) and hydrodynamic radii (R_H) of protein particles created by peroxidase, laccase and tyrosinase.

Enzyme	M_w	R_H
<i>Peroxidase</i>	2 -150 MDa	4 -100 nm
<i>Laccase</i>	50 MDa	50 nm
<i>Tyrosinase</i>	≤ 2 MDa	≤ 20 nm

For laccase, significant cross-linking of WPI has so far only been reported for the case when the WPI is chemically modified with a small cross-linking mediator, vanillic acid (6). The molar mass M_w of these laccase-cross-linked WPI clusters ranged from 29 kDa to over 206 kDa (as judged from SDS-page). For unmodified WPI, however, the authors found only a very low cross-linking efficiency, both in the presence and absence of free vanillic acid (6). In the absence of a small molecule cross-linking mediator, the laccase only induced cross-linking of β -lactoglobulin into dimers. In the presence of ferulic acid as a cross-linking mediator, somewhat larger protein structures (trimers) were found (7). A previous report has also compared the cross-linking of whey proteins by a range of oxidative enzymes: microbial peroxidase, fungal laccase, and bovine plasma monoamine oxidase. These were found to differ in their mode of action (2). All enzymes catalyzed the formation of oligomers and to some extent the formation of true “protein polymers” or nanoparticles. It was found for that peroxidase mainly cross-linked α -lactalbumin rather than β -lactoglobulin. Similarly, for laccase it was found that in the presence of chlorogenic acid as a cross-linking mediator, only α -lac was cross-linked and not α -lactoglobulin. Only monoamine oxidase was able to cross-link both proteins. The molar mass of enzymatically cross-linked WPI polymers was found to be large: larger than about 600 kDa (as judged from the fact that they eluted in the void of the SEC chromatograms with superose 6 columns).

Other authors have reported that the conversion into large molar mass protein clusters can be improved for peroxidase, when using periodic addition of H_2O_2 (i.e. a 6-times addition, 1 mM H_2O_2 , a 10-min. intervals) rather than adding the same amount of peroxide at once (8). In summary, most reports on enzymatically cross-linked globular food proteins so far have been on cross-linked protein clusters that are significantly smaller than 1 MDa. Similar to Matsumura and Mori, who found α -lac particles with masses \gg 1MDa using TG in the presence of DTT (5), we have identified conditions to prepare extensively cross-linked apo- α -lac, with molar masses \gg 1 MDa, using both laccase and peroxidase, but without resorting to the use of DTT.

Key factors influencing nanoparticle formation

Peroxidase-catalyzed cross-linking

For peroxidase (HRP)-catalyzed cross-linking of apo- α -lactalbumin (apo- α -lac), control of the concentration of the co-substrate peroxide is a key factor for creating large protein nanoparticles (**chapter2, chapter 4**). Peroxidase efficiently catalyzes the cross-linking reaction at neutral pH such that cross-linking at higher concentrations and at a neutral pH leads to the formation of large protein nanoparticles (R_H of 25 - 150 nm; M_w of $10^6 - 10^9$ Da).

The peroxide is added step-wise ($\Delta C_{H_2O_2} = 0.1$ mM). Higher concentrations of H_2O_2 addition ($\Delta C_{H_2O_2} = 1$ mM) in each titration step lead to a faster inactivation of the enzyme (Fig.4-A). Consequently the enzyme is inactivated before the larger particle sizes are reached (data not shown). Even at very low concentrations of added H_2O_2 ($\Delta C_{H_2O_2} = 0.1$ mM), the particle growth stops after about 80 additions of H_2O_2 . After the addition of fresh enzyme into the reaction mixture, protein cross-linking resumes (Fig.4-B). This finding has three implications: (1) All peroxidase (0.1 mM) has apparently been completely inactivated after 80 additions of H_2O_2 (corresponding to 8mM). (2) Not all H_2O_2 that is added leads to the formation of a tyrosine-tyrosine cross-link: from stoichiometry, 30 additions of H_2O_2 (corresponding to 2.8 mM H_2O_2) should be sufficient to cross-linking all tyrosine residues (4 per protein). Nevertheless, there are still many unreacted tyrosine residues even after 80 additions of H_2O_2 (3).

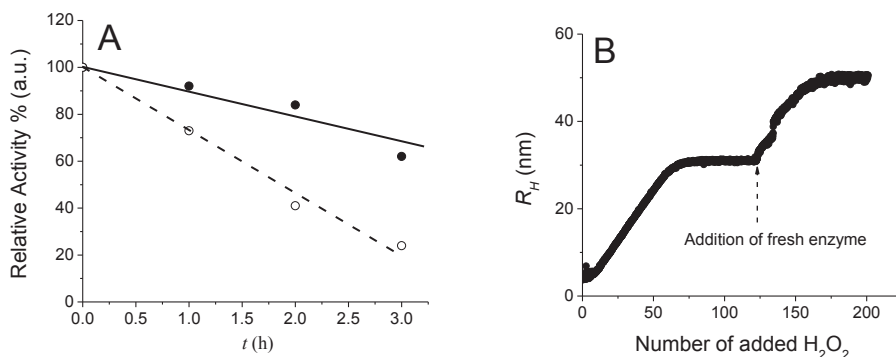


Figure 4. Inactivation of peroxidase. (A) Relative enzyme activity of peroxidase at 0.1 M NH_4Ac at pH 6.8 (determined by ABTS assay) as a function of reaction time. Solid line: $\Delta C_{H_2O_2}$: 0.1 mM per titration step, every 10 min (2 μ l of 0.05 M H_2O_2 in 1 mL); Dashed line: $\Delta C_{H_2O_2}$: 1 mM per titration step, every 10 min (2 μ l of 0.5 M H_2O_2 in 1 mL). A reaction time of 1h corresponds to 6 additions of H_2O_2 . (B) Hydrodynamic radius (R_H) as a function of number of H_2O_2 additions ($\Delta C_{H_2O_2}$: 0.1 mM in each titration step, every 10 min.) for peroxidase-catalyzed cross-linking of apo- α -lactalbumin Buffer: 0.1 NH_4Ac , $T=37^\circ C$, $C_{\alpha-lac} = 1\%$ (w/v), $C_{HRP}=0.5$ mg/mL (**Chapter 2**).

Peroxidase is known to have a “suicide” activity in which the enzyme inhibits itself, that depends on the concentration of peroxide (9, 10). Indeed, in **chapter 2**, we showed that peroxidase progressively loses its activity with an increasing number of H_2O_2 additions. This ultimately leads to an end of particle growth (after about 80-additions of H_2O_2 , for a ratio of substrate protein to enzyme of $R_{P/E} = 20$). When a higher ratio ($R_{P/E} = 60$) of protein to enzyme was used, particle growth continued for a longer time (fig.9). In chapter 6, we have also shown that particle size increases with increasing initial substrate protein concentration. These observations indicate that particle growth for peroxidase catalyzed cross-linking depends on the enzyme activity, initial substrate protein concentration and on the protein to enzyme ratio.

Laccase-catalyzed cross-linking

We have found that particle growth for laccase-catalyzed cross-linking is influenced by the speed of stirring of the reaction mixture, the pH, and to a lesser extent by the protein and enzyme concentrations (fig.5). Understanding the relation between oxygen consumption

and monomer conversion into oligomers and particles is obviously an important factor in controlling particle growth and in the efficiency of the cross-linking reaction (11). Our preliminary results also clearly indicate that maintaining saturation of the solution with O_2 is crucial for efficient cross-linking (see Fig.5). Therefore, for further improving the cross-linking efficiency of laccase to prepare protein nanoparticles, it is crucial to use a reactor in which O_2 levels can be controlled.

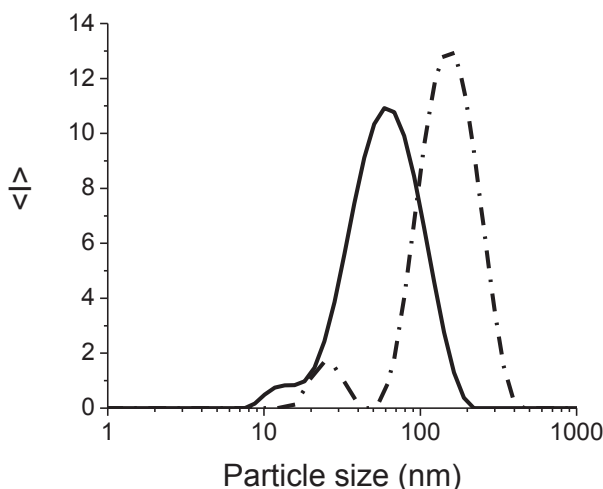


Figure.5. Size distribution of LC-cross-linked apo- α -lac under different conditions: Solid line: No stirring, 250 mg/mL of LC, 6% w/v of apo- α -lac, $T = 45^\circ\text{C}$, $\text{pH} = 5.8$, buffer: 10 mM sodium phosphate; Dash dot line: stirring at 400 rpm, 50 mg/mL of LC, 3.5 % w/v of apo- α -lac, $T = 40^\circ\text{C}$, $\text{pH} = 6.0$, buffer: 100 mM sodium phosphate

Alternatively O_2 levels could also be controlled by using the catalase enzyme that can convert H_2O_2 into O_2 , using periodic addition of H_2O_2 as we have done here for peroxidase. Such a strategy would certainly lead to a better control of the enzymatic reaction. Another factor is reaction pH. The formation of large protein particles at pH 6.0 rather than at pH 7.0 is consistent with the known pH optimum of laccase (12, 13). It is worth here mentioning that at the same concentration of substrate protein, nanoparticles produced by laccase catalyzed cross-linking are somewhat smaller than those produced by peroxidase-catalyzed cross-linking.

This may be caused by many factors: relative enzyme activities might be different, laccase may have a different inactivation profile than peroxidase during the reaction (an issue that we have not investigated).

Tyrosinase-catalyzed cross-linking

As we noted, tyrosinase is capable of catalyzing cross-linking reactions that lead to the formation of apo- α -lac protein nanoparticles, only in a narrow pH range (we focused on pH 5.7). Preliminary experiments showed that the size of these protein nanoparticles did not increase when the reaction mixture was stirred at higher speed. It was determined that at this higher speed, O₂ saturation was 70 % (data not shown). Hence, for tyrosinase, other factors than O₂ concentrations (such as pH) are rate limiting for particle growth.

Physical properties

Cross-linking bonds & stability

When comparing laccase- and peroxidase cross-linked apo- α -lac nanoparticles, a notable difference between the two is that for peroxidase the cross-links exclusively appear to involve tyrosines (**Chapter 2**) (i.e. even poly-tyrosine formation during peroxidase-catalyzed reactions was detected (14)), but for laccase, we find clear indications for the involvement of additional types of cross-linking bonds, in particular disulfide cross-linking (as deduced from our experiments on DTT-induced disassociation of laccase cross-linked nanoparticles, **Chapter 6**). Also, the conversion of monomeric tyrosine into cross-linked tyrosine appears to be less for the laccase cross-linked nanoparticles (based on the ratio of UV absorbances A_{318}/A_{280} which is a qualitative measure for the conversion of tyrosines into di- tri- and other cross-linked tyrosines; $A_{318}/A_{280} = 0.46$ for peroxidase and 0.35 for laccase). Also, in chapter 6, we have shown for laccase catalyzed cross-linking, that the large particles are stabilized by di-sulfide bridges, while dityrosines are most likely still responsible for stabilizing the smaller oligomeric structures that cannot be dissociated by DTT. The strikingly different colors for the different particles solutions also reflect the fact that the cross-linking chemistries are different for the different enzymes.

Colors of the reaction mixtures after oxidative cross-linking are brown for tyrosinase and yellowish for both peroxidase and laccase-catalyzed cross-linking (Fig.6).

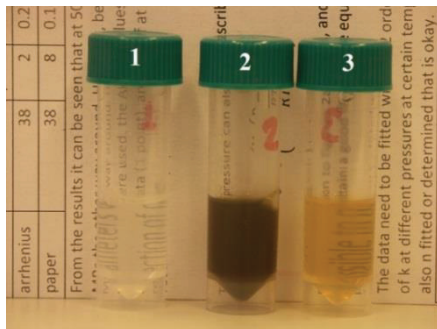


Figure.6. The appearance and turbidity of native apo- α -lac and enzymatically cross-linked apo- α -lac. (1) native apo- α -lac (6% w/v) heated at 45 °C for 15h at pH 6.0 (2) tyrosinase cross-linked apo- α -lac nanoparticles (6% w/v, $R_H=25$ nm) at pH 6.0 (3) laccase cross-linked apo- α -lac nanoparticles (6% w/v, $R_H=25$ nm) at pH 6.0. Reaction conditions: 6% (w/v), Tyr: 55 mg/mL; LC: 250 mg/mL, pH 6.0, 0.01 M sodium phosphate buffer, T=45 °C, t=15h.

Hence we conclude that these oxidative enzymes give rise to very different cross-linking chemistries even when acting on the same protein substrates (15-17). This may indeed be expected, due to the broad range of substrate specificities of oxidative enzymes, which may give rise to variety of types of cross-linking bonds (4, 18, 19). Enzyme properties that may determine different chemistry even when acting on the same protein substrate include their redox potential, structural properties, optimum pH, temperature (13). While it is known that laccase can induce oxidation of free cysteine (3), our finding that disulfide bridges are implicated in the stability of large, laccase catalyzed cross-linked nanoparticles is at the very least surprising since the substrate protein has no free cysteine, and this is certainly an issue that warrants further study.

Although we have found conditions for all three oxidative enzymes at which at least some amount of highly cross-linked protein nanoparticles can be formed (fig.2, 3), we have found that the peroxidase-cross-linked protein particles are by far the most stable protein particles (against heating, in the presence of DTT and SDS) when compared to both laccase and tyrosinase-cross-linked protein nanoparticles.

Results on the stability of the protein nanoparticles in the presence of SDS and DTT are summarized in table.2.

Table.2. Stability of protein nanoparticles in the presence of SDS and/or DTT.

Enzyme	Stability			
	No SDS & DTT	SDS & DTT	DTT	SDS
<i>Peroxidase</i>	+	+	+	+
<i>Laccase</i>	+	-	-	+
<i>Tyrosinase</i>	+	-	ND	ND

(+) No disassociation = stable, (-) Disassociation = instable, ND: Not determined.

Ca²⁺-stability of protein nanoparticles

In Chapter 3, we have shown that full cross-linking of apo- α -lac upon peroxidase-catalyzed cross-linking leads to a nearly complete loss of tertiary structure that cannot be recovered by the addition of Ca^{2+} . Here we further investigate the Ca^{2+} sensitivity of the peroxidase cross-linked apo- α -lac protein nanoparticles. We first explore the stability of protein nanoparticles in the presence of Ca^{2+} at 25 °C. Fig.7 shows the particle size for protein nanoparticles (R_H of 60 nm) as a function of the concentration of added Ca^{2+} . The hydrodynamic radii of the protein nanoparticles remains constant with increasing concentration of Ca^{2+} up to rather high molar ratio. However, at a molar ratio of Ca^{2+} to α -lac monomers (in particles) of ~ 4.3 , the hydrodynamic radius R_H of the protein nanoparticles starts to increase strongly, indicating Ca^{2+} -induced aggregation. In chapter 3, we showed that tertiary structure of the α -lac protein in cross-linked nanoparticles did not come back to the holo-form when adding Ca^{2+} , as happens for native apo- α -lac. Our results suggest that nevertheless some Ca^{2+} -binding capability is retained, since a reasonably large number of Ca^{2+} ions per protein is required to induce aggregation.

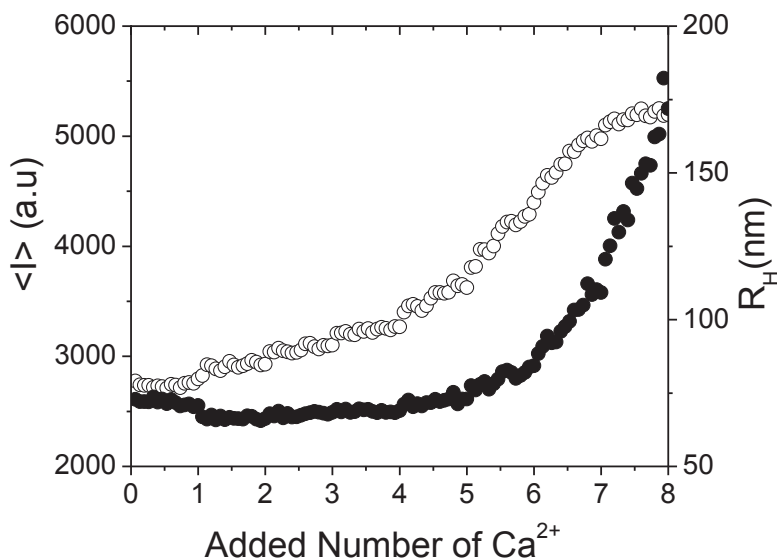


Figure.7. Hydrodynamic radii of HRP-nanoparticles ($R_H \approx 50$ nm) as a function of concentration of Ca^{2+} in demi H_2O at 25°C . Open and closed symbols refer to hydrodynamic radii and light scattering intensity, respectively.

Architecture

We have shown in chapter 2 that the size-mass scaling exponent a (obtained from $R_H \sim M_w^a$) of protein nanoparticles (the smallest in size, $R_H \leq 25$ nm) is 0.4 or D_f of 2.5. For larger protein particles ($R_H \approx 50$ nm), we have found in chapter 6 that protein nanoparticles formed upon laccase and peroxidase-catalyzed cross-linking have self-similar or fractal architectures with D_f of ≈ 2 or a of 0.5, irrespective of the type of cross-linking. In fact, peroxidase-catalyzed cross-linked protein nanoparticles (with a R_g range of 25 -200 nm) exhibit a self-similar structure with D_f of ≈ 2 at all lengthscales. Besides, their structure is not dramatically affected within the changes in environmental conditions (i.e. ionic strength and salt concentration) (20).

The mass-size scaling exponent of ≈ 2 that we obtained for protein nanoparticles suggests reaction limited aggregation during particle growth (21). It means that first primary protein aggregates form and then these primary aggregates assemble in a fractal-type structure (22). This indeed suggests a two-stage particle growth that we have shown in

chapter 2. The particle growth and fractal dimension of enzymatically cross-linked α -lactalbumin exhibit an analogy to heat-induced β -lactoglobulin at neutral pH (20). In contrast, for TG-catalyzed cross-linking of apo- α -lac it was found that this gives a more compact architecture with scaling exponent α of 0.3 from $R_g \sim M_w^\alpha$ (23). Whereas oxidative enzymes are capable of oxidizing tyrosines (4 residues), TG catalyzes the cross-linking reaction between lysine (12 residues) and glutamine (7 residues) (24). This suggests that the cross-linking functionality (the number of cross-linked residues per protein molecule), might be the key factor in determining the architecture upon enzymatic cross-linking. In order to prove this hypothesis, further research should certainly also focus on determining the average number of cross-linking bonds formed per protein for the different enzymatic cross-linking reactions.

Protein conformation

Oxidative cross-linking of apo- α -lac via various enzymes leads to subtle changes in secondary structure of the substrate proteins (Chapter 3, Chapter 6). The different enzymes give rise to different percentages of apo- α -lac α -helices that are lost upon cross-linking (Fig.8-A). Besides, almost all tertiary structure is lost upon all oxidative cross-linking (Fig.8-B). The content of helices in TYR-cross-linked apo- α -lac is intermediate (content of secondary structure was estimated as in Chapter 3 and Chapter 6). In fact, TYR-catalyzed cross-linking induces only 15% loss of α -helices while 30% of helices are lost upon LC-catalyzed cross-linking. In chapter 3, we have shown that full cross-linking of apo- α -lac upon peroxidase-catalyzed cross-linking induces a similar loss in α -helical content as LC-catalyzed cross-linking. We have also found that changes in α -helical content for peroxidase-catalyzed cross-linking differs between partially ($M_w < 2000$ kDa) and fully cross-linked ($M_w \approx 10^6$ kDa) apo- α -lac (Chapter 3).

Interestingly, we found that (peroxidase-catalyzed) partial cross-linking (only a small number of subsequent additions of peroxide) induces a much higher loss of α -helices in apo- α -lac as compared to TYR-cross-linked oligomers. These observations might imply that different cross-linking enzymes induce the oxidation of either different tyrosine residues or different phenolic compounds (e.g. tryptophan).

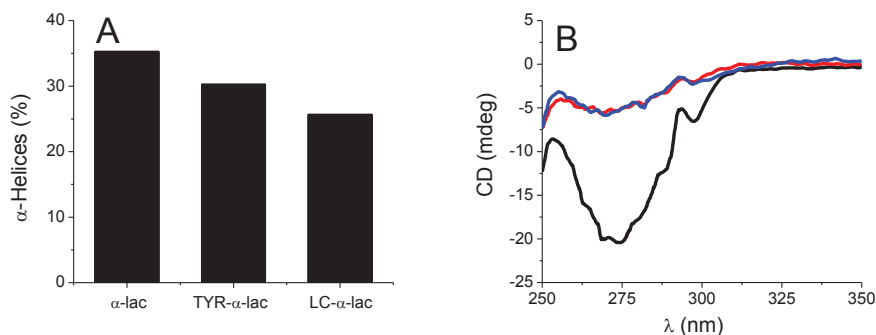


Figure.8. Percentages of α -helix in enzymatically cross-linked apo- α -lac; **α -lac:** native apo- α -lac, **TYR- α -lac:** tyrosinase-cross-linked apo- α -lac, **LC- α -lac:** laccase-cross-linked apo- α -lac (B) near-UV CD spectra of native α -lac (black), LC-nanoparticles (red) and TYR-oligomers (blue) in 10 mM sodium phosphate buffer at pH 7.0 at 25 °C. Note that reaction products still contain about 20 % of α -lac monomers.

This might then lead to different types of changes in protein conformation. It may be expected that cross-links involving amino acids on the protein surface induce less significant changes in protein conformation than cross-links involving (partially) buried amino acids. For instance, TG, which catalyzes the formation of cross-links between lysine and glutamine residues, that are typically located at the surface of globular proteins, induces almost no change in secondary and tertiary structure of WPI (25). Tyrosinase appears to catalyze the formation of cross-links involving tyrosines, without the major conformational changes that we observe for peroxidase.

A possible reason for this might be that it involves cross-linking of the rather accessible α -lac tyrosine Tyr¹⁰³, and not of the other, less accessible tyrosine residues. For peroxidase-catalyzed cross-linking, with prolonged cross-linking (continued additions of peroxide), we observe a small *increase* of the α -helical content with the extent of cross-linking, and it has also been shown that such prolonged cross-linking leads to the formation of poly-tyrosines. Hence, there is a possibility that the increased α -helical content is in fact related to the formation of the poly-tyrosines.

The different types of conformational changes due to cross-linking by the different enzymes also lead to different changes in the surface hydrophobicity of the cross-linked proteins. For peroxidase-catalyzed cross-linking, partially cross-linked apo- α -lac (only a

few additions of peroxide) has a surface hydrophobicity that is three times higher than that of fully cross-linked apo- α -lac (many additions of peroxide). We cannot yet fully explain why partial cross-linking induces higher surface hydrophobicity than full cross-linking. One reason might be that the anionic probe ANSA that is used to quantify surface hydrophobicity, cannot easily bind to large protein nanoparticles whereas it can interact with protein oligomers more easily. However, this explanation is at odds with our observations that the fully cross-linked apo- α -lac particles show a completely reversible rheology that is only consistent with very hydrophilic (and thermostable) particles (chapter 6).

We find that laccase-catalyzed cross-linking leads to a higher surface hydrophobicity than for peroxidase-catalyzed cross-linking (when comparing apo- α -lac nanoparticles of similar size). Possibly, for this case, the disulfide cross-linking that we suspect is (also) induced by laccase cross-linking can lead to different types of structural rearrangements, which could then lead a higher surface hydrophobicity. The differences that we observe between the hydrophobicities of the nanoparticles, as probed by ANSA (that are otherwise similar in size and zeta potential), is another argument against the idea that ANSA cannot reliably determine hydrophobicity of highly cross-linked proteins, but only for monomers or oligomers.

Control of particle size

We have shown that hydrodynamic radii of protein nanoparticles produced by peroxidase-catalyzed cross-linking can be precisely controlled by using three main routes. A first approach for controlling particle size is to simply vary the number of H_2O_2 additions of the reaction. In order to avoid gelation, the substrate protein concentration should not be higher than 3% (w/v), which we have shown is the critical gelation concentration at a fixed weight ratio of protein to enzyme of $R_{\alpha\text{-lac/HRP}} = 20$. The desired particle size can simply be selected by stopping the addition of H_2O_2 . A second approach is to vary the substrate protein concentration (at a fixed weight ratio of protein to enzyme $R_{\alpha\text{-lac/HRP}} = 20$), while staying below the critical concentration of 3% (w/v) (Fig.9, black, red, green) and letting the reaction go to completion (Chapter 4).

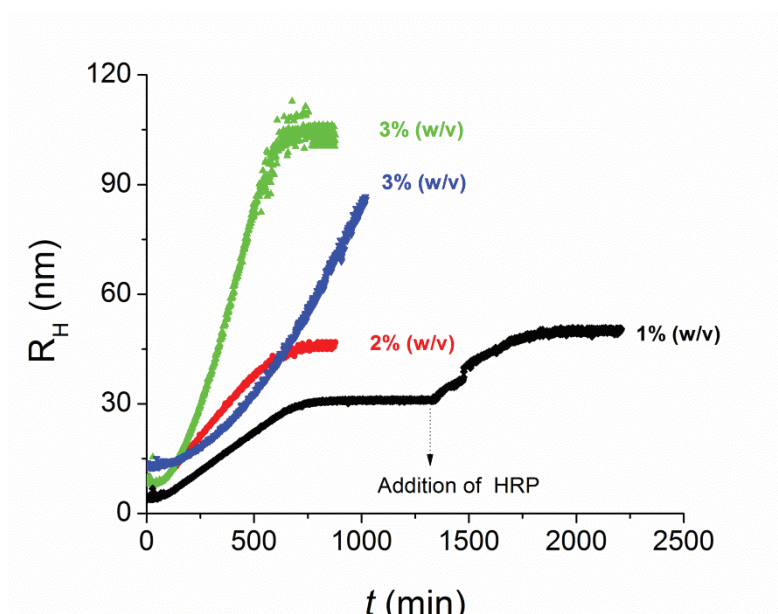


Figure.9. Particle size as a function of reaction time during peroxidase-catalyzed cross-linking of apo- α -lac. Black: $C_{apo-\alpha-lac} = 3.0\%$ (w/v), $R_{\alpha-lac/HRP} = 20$ (w/w); red: $C_{apo-\alpha-lac} = 2\%$ (w/v), $R_{\alpha-lac/HRP} = 20$ (w/w); green: $C_{apo-\alpha-lac} = 3\%$ (w/v), $R_{\alpha-lac/HRP} = 20$ (w/w); blue: 3% (w/v), $R_{\alpha-lac/HRP} = 60$ (w/w). All reactions were performed in 0.1 M NH_4Ac at pH 6.8 and at $37^\circ C$.

Finally, a third approach is to vary the weight ratio of protein to enzyme at fixed initial protein concentration (Fig.9, blue vs green curve), while letting the reaction go to completion. Of course, various combinations of these approaches are also possible. For laccase and tyrosine, controlling particles size precisely seems very difficult due to limitation of controlling O_2 concentration. For laccase, the only way to tune particle size might be to determine particle formation process, and, for desired particle size, to inhibit reaction using inhibitor or heat treatment.

Functionality

Stability against thermal aggregation

In chapter 5, 6, we have shown that HRP- and LC-nanoparticles have a very high stability against thermal aggregation at pH 5.7, a pH at which native apo- α -lac easily undergoes thermal aggregation. Interestingly, we found that oligomers produced by laccase and tyrosinase-catalyzed cross-linking also exhibit high resistance against thermal aggregation (data not shown). This suggests that in fact even partial oxidative cross-linking of apo- α -lac can improve the protein stability against thermal aggregation at pH 5.7 (a pH at which the protein itself is very sensitive to heat-induced aggregation).

Previously, enzymatic cross-linking has also been reported to improve thermal stability of enzymatically cross-linked proteins (25-27). In these reports, the most pronounced feature observed was a shift in the denaturation temperature of whey proteins to higher temperature upon enzymatic cross-linking (25). In contrast, for the proteins in the highly cross-linked nanoparticles, we have not been able to determine denaturation temperatures, but instead have shown that they are extremely stable against heat-induced aggregation.

Thermal aggregation of particles in the presence of Ca^{2+}

In a previous section we have shown that only high concentrations of Ca^{2+} destabilize HRP cross-linked apo- α -lac particles at 25 °C, and induce their aggregation. Here we also consider the question what the influence would be of lower concentrations of Ca^{2+} (that do not affect unheated particles) on the heat stability. To this end, we monitored particle sizes during heating at 90 °C for protein nanoparticles (R_H of 25 nm) at a mole ratio of Ca^{2+} to particles of ~ 2 . Recall that in the absence of Ca^{2+} the particles are perfectly stable against heating. With added Ca^{2+} , we observed that the hydrodynamic radius R_H of the protein nanoparticles gradually increases from 25 nm to 100 nm in a period of about 15h when heated (data not shown).

Fig.10 shows AFM images of the protein nanoparticles heated in the presence of Ca^{2+} . The AFM images show a heterogeneous mixture of elongated protein structures.

Hence, the addition of Ca^{2+} has led to a new type of structure being formed when the nanoparticles are heated. In chapter 3, we found that the tertiary structure of native holo- α -lac was not recovered for the protein subunits in nanoparticles when Ca^{2+} was added, while this is the case when Ca^{2+} is added to native apo- α -lac.

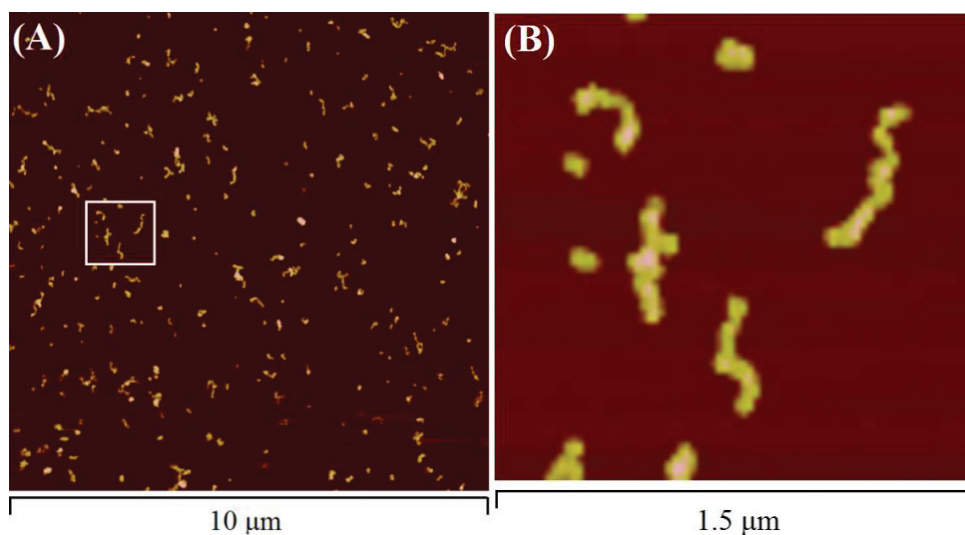


Figure 10. AFM images of α -lac nanoparticles heated at 90°C in the presence of Ca^{2+} (aggregates have been adsorbed on mica and dried before imaging). (A) 2D height images of Ca^{2+} -induced aggregates of protein nanoparticles (R_H of 30 nm in bulk) at $10\ \mu\text{m} \times 10\ \mu\text{m}$ (B) 2D height high resolution images of Ca^{2+} -induced aggregates of protein nanoparticles (R_H of 30 nm in bulk) at $1.5\ \mu\text{m} \times 1.5\ \mu\text{m}$.

As for the case of the stability against the addition of Ca^{2+} at room temperature, we again conclude, that some aspects of the Ca^{2+} binding must have been retained in the cross-linked protein since even rather small amounts of Ca^{2+} that do not affect their room temperature stability, have such a dramatic effect on the behavior of the particles when heated.

Gelation

For peroxidase-induced gelation, we have two important observations: (1) peroxidase induces the formation of an enzymatically (covalently) cross-linked protein gel when the

initial protein concentration was equal to, or above 4% (w/v) ($\Delta t=210$ sec, $C_{H_2O_2} = 0.1$ mM, $N=240$, $T=37$ °C (2) Consistent with observation (1), HRP-nanoparticles with a hydrodynamic radius $R_H = 100$ nm, start overlapping at about 4% (w/v) (i.e. a critical overlap concentration, C^*) and create a physical “jammed” protein nanoparticle hydrogel. In chapter 4, we showed that rheological properties of our protein nanoparticles have an analogy to soft jammed materials (28, 29). The property of the nanoparticles to exhibit a very high viscosity (comparable with polysaccharides) at low protein concentrations and to exhibit a “yield stress” behavior (again comparable to polysaccharides) implies that these protein nanoparticles might find applications in food as protein-based thickeners.

We did not observe any gelation for laccase and tyrosinase. Even at higher protein concentration (20 % (w/v)), these enzymes were not capable of inducing gelation. Possibly, gelation may be achieved with better control over the O_2 level during these reactions at high protein concentration. Our results are consistent with other reports that also found that various oxidative enzymes (i.e. microbial peroxidase, fungal laccase, and bovine plasma monoamine oxidase) induced the cross-linking of whey proteins, but not their gelation, not even at high concentrations of 10-20 % w/v (2).

Application

In addition to the HRP-nanoparticles, we also believe that the HRP-nanoparticles heat-aggregated in the presence of Ca^{2+} could have interesting applications as rheology modifiers for other heat-set protein gels. To demonstrate this possibility, we have studied the effect of the linearly aggregated protein nanoparticles on the rheological properties of heat-induced whey protein isolate gels. Fig.11 shows the evolution of storage moduli of a WPI solution (20% w/v/) during a heat-treatment, both in the absence and in the presence of a small amount (1% w/v) of HRP-nanoparticles previously heat-aggregated in the presence of Ca^{2+} . We find that this small addition leads to a 50% increase of the modulus of the WPI gels, an increase that does not occur when a similar amount of HRP cross-linked apo- α -lac particles are added that have not been previously heat-aggregated in the presence of Ca^{2+} .

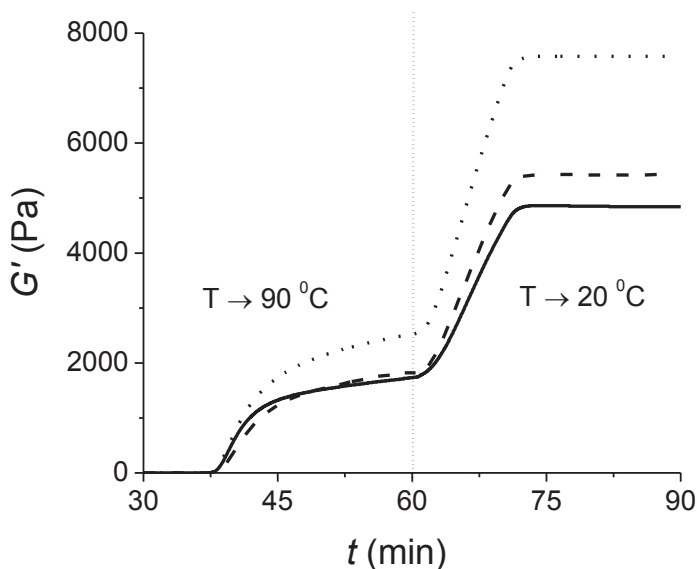


Figure.11. Storage modulus during heat treatment of WPI (20 % w/v) with a small amount of different types of added HRP-cross-linked apo- α -lac nanoparticles (1% w/v). Solid line: 20% (w/v) WPI and 1% (w/v) α -lac in demi H₂O, Dash line: 20% (w/v) WPI and 1% (w/v) α -lac nanoparticles (R_H of 60 nm) in demi H₂O; Dot line: 20% (w/v) WPI and 1% (w/v) nanoparticles (R_H of 60 nm) prepared in the presence of Ca²⁺ at a molar ratio of Ca²⁺ to protein of 2.

Outlook

Our results on comparing apo- α -lac cross-linked by different enzymes strongly suggests that the detailed differences in the cross-linking chemistry to a large extent determine the rather striking differences in the final nanoparticle physical properties (structure, stability, hydrophobicity) even within the class of oxidative enzymes. To better understand the effect of the cross-linking chemistry on the physical properties of cross-linked globular food proteins, the cross-linking chemistry would need to be understood in more detail than we do now.

We have found that for all oxidative enzymes, when protein nanoparticles are formed, they have an open structure, with a size-mass scaling $R \propto M^a$, with exponents $a = 0.4$ - 0.5 , with typical protein concentrations inside the protein particles of a few % (w/v).

Protein nanoparticles produced by mTG appear to be somewhat denser, but not by much (30). We have also found that the conditions for which cross-linking enzymes cross-link so efficiently that nanoparticles are produced, fall in a narrow range. Hence, there does not seem to be much room to tune particle structure by tuning reaction conditions. On the other hand, the formation of the worm-like aggregates in the presence of Ca^{2+} upon heating demonstrates that there may be ways to create different structures with enzymatically cross-linked protein by using post-processing.

Creating nanoparticles composed of the commercially important whey protein α -lactalbumin is difficult if traditional heat-induced aggregation processes are being used, since the α -lac proteins have very good heat stability. Enzymatic cross-linking is a facile, complementary route for making α -lac nanoparticles. In this case the high stability of apo- α -lac probably works in our advantage, since this is probably one of the key factors behind the high thermal stability of the enzymatically cross-linked protein nanoparticles. Indeed, the peroxidase-cross-linked apo- α -lac nanoparticles exhibit an extremely high stability against thermal aggregation for a wide range of pH values and salt concentrations. Although we suspect that the high zeta potential, hydrophilic nature and the structural stability of the cross-linked protein nanoparticles all contribute, we definitely need a more thorough understanding of what is behind the high stability of the nanoparticles against heat-induced aggregation.

The open architecture that we find typically develops due to enzymatic cross-linking, makes protein nanoparticles good candidates for structuring food (e.g. as protein based thickener). Solutions of only a few % (w/v) of protein nanoparticles exhibit a rheology that is comparable to that of polysaccharide thickeners. The fact that the protein nanoparticles form transparent physical (cold-set) protein hydrogels at neutral pH without using multivalent ions or heat treatment is also quite unique. Furthermore, the rheological properties of the nanoparticle hydrogels are not significantly affected upon heating, which can also be advantageous for many food applications.

Finally, we have found that the very hydrophilic peroxidase cross-linked apo- α -lac nanoparticles appear to behave as anti-foaming agents (31). Still, the more hydrophobic laccase-cross-linked apo- α -lac nanoparticles were found to exhibit a higher foamability

than the peroxidase-cross-linked apo- α -lac nanoparticles. With respect to the foamability, a next step should be to compare the foaming properties of oligomers, nanoparticles and different types of nanoparticles, produced by cross-linking with different enzymes, or post-processed in different ways.

Acknowledgement

This work is part of the Industrial Partnership Programme (IPP) Bio(-Related)Materials of the Stichting voor Fundamenteel Onderzoek der Materie (FOM), which is financially supported by the Nederlandse Organisatie voor Wetenschappelijk Onderzoek (NWO). The IPP BRM is co-financed by the Top Institute Food and Nutrition and the Dutch Polymer Institute.

References

1. Thalmann, C. R.; Lotzbeyer, T., Enzymatic cross-linking of proteins with tyrosinase. *Eur. Food Res. Technol.* **2002**, *214*, 276-281.
2. Faergemand, M.; Otte, J.; Qvist, K. B., Cross-linking of whey proteins by enzymatic oxidation. *J. Agric. Food Chem.* **1998**, *46*, 1326-1333.
3. Mattinen, M. L.; Hellman, M.; Permi, P.; Autio, K.; Kalkkinen, N.; Buchert, J., Effect of protein structure on laccase-catalyzed protein oligomerization. *J. Agric. Food Chem.* **2006**, *54*, 8883-8890.
4. Mattinen, M. L.; Lantto, R.; Selinheimo, E.; Kruus, K.; Buchert, J., Oxidation of peptides and proteins by *Trichoderma reesei* and *Agaricus bisporus* tyrosinases. *J. Biotechnol.* **2008**, *133*, 395-402.
5. Matsumura, Y.; Lee, D. S.; Mori, T., Molecular weight distributions of alpha-lactalbumin polymers formed by mammalian and microbial transglutaminases. *Food Hydrocolloids* **2000**, *14*, 49-59.
6. Ma, H.; Forssell, P.; Partanen, R.; Buchert, J.; Boer, H., Improving Laccase Catalyzed Cross-Linking of Whey Protein Isolate and Their Application as Emulsifiers. *J. Agric. Food Chem.* **2011**, *59*, 1406-1414.
7. Steffensen, C. L.; Andersen, M. L.; Degn, P. E.; Nielsen, J. H., Cross-Linking Proteins by Laccase-Catalyzed Oxidation: Importance Relative to Other Modifications. *J. Agric. Food Chem.* **2008**, *56*, 12002-12010.
8. Heijnis, W. H.; Wierenga, P. A.; Berkel, W. J. H.; Gruppen, H., Directing the Oligomer Size Distribution of Peroxidase-Mediated Cross-Linked Bovine alpha-Lactalbumin. *J. Agric. Food Chem.* **2010**, *58*, 5692-5697.
9. Arnao, M. B.; Acosta, M.; Delrio, J. A.; Varon, R.; Garcíacanas, F., A kinetic-study on the suicide inactivation of peroxidase by hydrogen-peroxide. *Biochimica Et Biophysica Acta* **1990**, *1041*, 43-47.
10. Nicell, J. A.; Wright, H., A model of peroxidase activity with inhibition by hydrogen peroxide. *Enzyme Microb. Technol.* **1997**, *21*, 302-310.
11. Mattinen, M. L.; Kruus, K.; Buchert, J.; Nielsen, J. H.; Andersen, H. J.; Steffensen, C. L., Laccase-catalyzed polymerization of tyrosine-containing peptides. *Febs J.* **2005**, *272*, 3640-3650.

12. Kiiskinen, L. L.; Viikari, L.; Kruus, K., Purification and characterisation of a novel laccase from the ascomycete *Melanocarpus albomyces*. *Appl. Microbiol. Biotechnol.* **2002**, *59*, 198-204.
13. Madhavi, V.; Lele, S. S., Laccase: properties and applications. *BioResources* **2009**, *4*, 1694-1717.
14. Surender K. Dhayal, H. G., Renko de Vries, Peter A. Wierenga, Determination of poly-tyrosine in peroxidase-cross-linked apo-alpha-lactalbumin. *In preparation* **2014**.
15. Bittner, S., When quinones meet amino acids: chemical, physical and biological consequences. *Amino Acids* **2006**, *30*, 205-224.
16. Monogioudi, E.; Creusot, N.; Kruus, K.; Gruppen, H.; Buchert, J.; Mattinen, M. L., Cross-linking of beta-casein by *Trichoderma reesei* tyrosinase and *Streptovorticillium mobaraense* transglutaminase followed by SEC-MALLS. *Food Hydrocolloids* **2009**, *23*, 2008-2015.
17. Buchert, J.; Cura, D. E.; Ma, H.; Gasparetti, C.; Monogioudi, E.; Faccio, G.; Mattinen, M.; Boer, H.; Partanen, R.; Selinheimo, E.; Lantto, R.; Kruus, K., Crosslinking Food Proteins for Improved Functionality. In *Annual Review of Food Science and Technology, Vol 1*, Doyle, M. P.; Klaenhammer, T. R., Eds. Annual Reviews: Palo Alto, 2010; Vol. 1, pp 113-138.
18. Thurston, C. F., The structure and function of fungal laccases. *Microbiology-(UK)* **1994**, *140*, 19-26.
19. Elliott, K. A., Oxidations catalysed by horseradish- and milk-peroxidases. *The Biochemical journal* **1932**, *26*, 1281-90.
20. Dhayal, S. K.; Gruppen, H.; de Vries, R.; Wierenga, P. A., Controlled formation of protein nanoparticles by enzymatic cross-linking of alpha-lactalbumin with horseradish peroxidase. *Food Hydrocolloids* **2014**, *36*, 53-59.
21. Foegeding, E. A.; Davis, J. P.; Doucet, D.; McGuffey, M. K., Advances in modifying and understanding whey protein functionality. *Trends Food Sci. Technol.* **2002**, *13*, 151-159.
22. Mezzenga, R.; Fischer, P., The self-assembly, aggregation and phase transitions of food protein systems in one, two and three dimensions. *Rep. Prog. Phys.* **2013**, *76*, 43.
23. Surender K. Dhayal, H. G., Renko de Vries, Peter A. Wierenga, Comparison of structural properties of peroxidase- and transglutaminase cross-linked apo-alpha-lactalbumin. *in preparation* **2014**.
24. Saricay, Y.; Dhayal, S. K.; Wierenga, P. A.; de Vries, R., Protein cluster formation during enzymatic cross-linking of globular proteins. *Faraday Discuss.* **2012**, *158*, 51-63.
25. Agyare, K. K.; Damodaran, S., pH-Stability and Thermal Properties of Microbial Transglutaminase-Treated Whey Protein Isolate. *J. Agric. Food Chem.* **2010**, *58*, 1946-1953.
26. Damodaran, S.; Agyare, K. K., Effect of microbial transglutaminase treatment on thermal stability and pH-solubility of heat-shocked whey protein isolate. *Food Hydrocolloids* **2013**, *30*, 12-18.
27. Flanagan, J.; Gunning, Y.; FitzGerald, R. J., Effect of cross-linking with transglutaminase on the heat stability and some functional characteristics of sodium caseinate. *Food Res. Int.* **2003**, *36*, 267-274.
28. Berli, C. L. A.; Quemada, D., Rheological modeling of microgel suspensions involving solid-liquid transition. *Langmuir* **2000**, *16*, 7968-7974.
29. Omari, A.; Tabary, R.; Rousseau, D.; Calderon, F. L.; Monteil, J.; Chauveteau, G., Soft water-soluble microgel dispersions: Structure and rheology. *J. Colloid Interface Sci.* **2006**, *302*, 537-546.

30. Surender K. Dhayal, H. G., Renko de Vries, Peter A. Wierenga, Comparison of structural properties of peroxidase and transglutaminase cross-linked apo- α -lactalbumin nanoparticles. *manuscript in preparation*

2014.

31. Heijnis, W. H., Peroxidase-mediated cross-linking of bovine α -lactalbumin. *PhD Thesis, Wageningen University* **2010.**

Summary

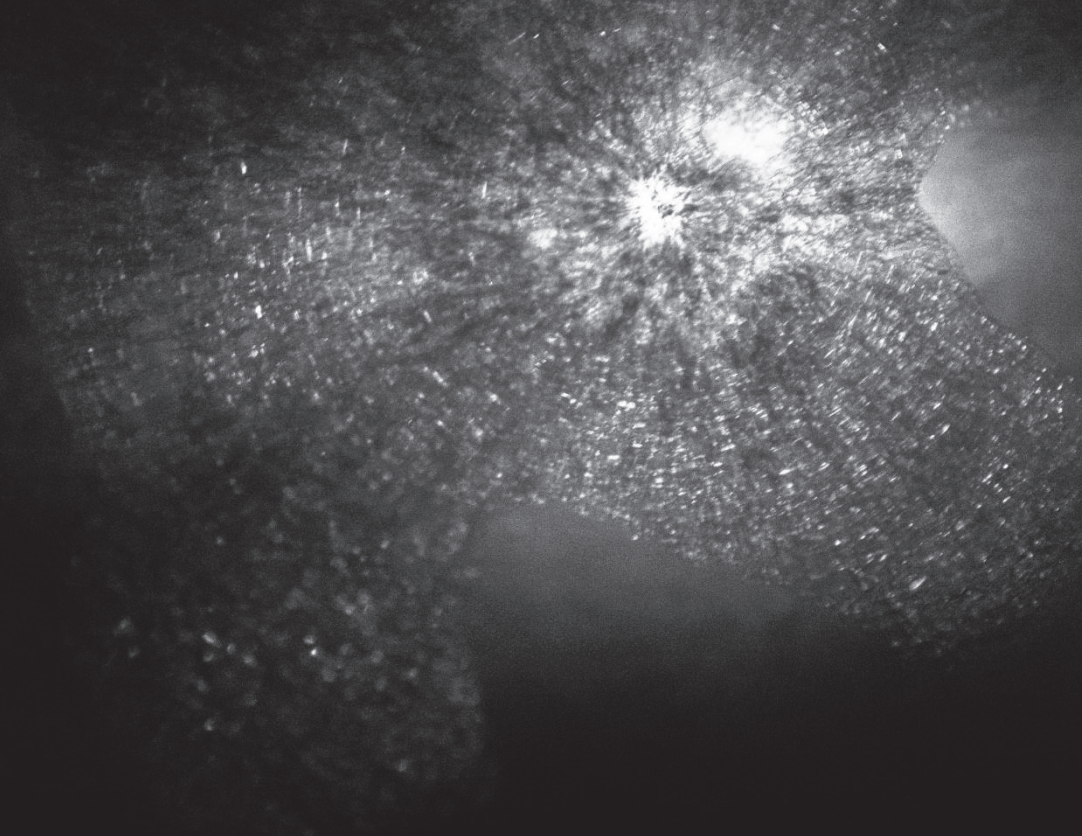
Samenvatting

List of publications

Acknowledgement

About the author

Overview of completed training activities



Summary

This thesis, we aim to elucidate the effects of oxidative enzymatic crosslinking on the molecular and mesoscale properties of apo- α -lactalbumin, and to apply these insights to understanding the functional properties of enzymatically cross-linked α -lactalbumin nanoparticles in food formulations. In the first part of the thesis, **Peroxidase catalyzed cross-linking of apo- α -lactalbumin**, we mainly focus on understanding how peroxidase-catalyzed cross-linking alters mesoscale physical and functional properties of apo- α -lactalbumin. In the second part, **Comparison of peroxidase-, laccase- and tyrosinase-catalyzed cross-linking** we investigate to what extent stability, physical and functional properties of protein nanoparticles differ when apo- α -lactalbumin is cross-linked by different oxidative enzymes.

First, in the **General Introduction, Chapter 1**, we first introduce the research question of this thesis and provide essential background information on the different oxidative cross-linking enzymes that feature in the thesis, as well as on the model globular protein substrate that we use, apo- α -lactalbumin. We use the cross-linking to prepare protein nanoparticles, and a further section deals with the role of protein nano- and microparticles in current food technology, and reviews properties and uses of such particles. Finally, we outline the remainder of the thesis.

Part I: Peroxidase catalyzed cross-linking of apo- α -lactalbumin

In **chapter 2**, we study the process of the peroxidase catalyzed *formation* of apo- α -lactalbumin nanoparticles. We find that there are two distinct stages. In the first stage of the reaction, which is short, monomeric proteins are converted into protein oligomers. In the second stage, which takes much longer, oligomers are coupled together into protein nanoparticles. We find that particle growth stops as a consequence of peroxidase-induced inactivation of the enzymes. The final particles have an open structure with a scaling of the hydrodynamic size R_H versus molar mass M_w of $R_H = M_w^\alpha$, for a value of the exponent of $\alpha = 0.4$.

In **chapter 3** we study conformational changes of α -lactalbumin proteins induced by peroxidase-catalysed cross-linking. We separately study conformational changes for the

two stages of the reaction that we found in chapter 2 (“partial cross-linking” and “full cross-linking”). We find that partial cross-linking leads to a significant loss of the mainly α -helical secondary structure of the proteins, and to a significant increase of their surface hydrophobicity. Remarkably, in fully cross-linked protein nanoparticles, part of the α -helical structure that was lost in the early stage of the reaction seems to come back, and the final particles turn out to be very hydrophilic, having a surface hydrophobicity that is close to that of the native protein monomer. Also, fully cross-linked nanoparticles have a zeta potential that is twice more negative than that of the native protein monomer, such that fully cross-linked alpha-lactalbumin nanoparticles are very stable in solution.

Chapter 4 deals with the rheology of concentrated solutions of the nanoparticles characterized in chapters 2 and 3. We find that overlap concentrations for the nanoparticles are 4-9 % (w/v), for nanoparticles with hydrodynamic radii R_H decreasing from 100 to 25 nm. Above the overlap concentration, the storage modulus (G') and apparent viscosity (η) rapidly increase with concentration. Nanoparticles solutions are highly shear thinning, and no true zero-shear viscosity can be established. We interpret these features in terms of what is known in the literature about soft, jammed materials. A major conclusion is this type of cross-linking can be used to create protein hydrogels with rheological features that are attractive for food structuring, and which are not normally associated with protein gels: transparent, reversibly yielding gels at rather low protein concentrations.

The impact of heat-treatments on protein-containing foods is a key topic in food technology, and in **chapter 5**, we study the effects of heating on the structure and physical properties of peroxidase cross-linked α -lactalbumin nanoparticles. We find that after cross-linking; heating does no longer lead to any significant changes in secondary structure, as it does for the native protein. The nanoparticles retain their hydrophilic character, and for a wide range of solution conditions, we find that heating does not lead to aggregation of the nanoparticles, in contrast to the native protein, which rapidly heat-aggregates for pH values close to pH 5.7. Hydrogels prepared from the nanoparticles can also be heated without major changes in their rheology. In summary, we have established that peroxidase cross-linked α -lactalbumin nanoparticles are extremely heat-stable.

Part II: Comparison of peroxidase-, laccase- and tyrosinase-catalyzed cross-linking

In **chapter 6** we compare cross-linking of apo- α -lactalbumin by two different oxidative enzymes, peroxidase (HRP) and laccase (LC). We find that nanoparticles produced by the two enzymes are similar in structure at the mesoscale: both have a size-mass scaling $R_g \sim M_W^a$ with an exponent of $a \approx 0.5$. Changes in secondary structure and zeta potential upon cross-linking are similar for the two enzymes. Also, for both enzymes, the nanoparticles do not aggregate upon heating. We also find significant differences: as opposed to HRP-induced cross-linking, LC-induced cross-linking leads to a strong increase of the surface hydrophobicity, as compared to the native protein. Also, the particles partially disintegrate in the presence of DTT, thus implicating disulfide bridges as a contributor to the stability of the LC-nanoparticles. In summary we find that LC catalyzed cross-linking leads to nanoparticles that in many ways are similar to those produced by HRP catalyzed cross-linking, except for being more hydrophobic, which can be important e.g. when designing protein nanoparticles that need to be surface active.

The General discussion, **Chapter 7** presents an overview of the formation, physical and food functional properties of oxidatively cross-linked α -lactalbumin nanoparticles. In addition to relying on the data in the other chapters of the thesis, the chapter also brings in some new data, in particular on α -lactalbumin nanoparticles produced using yet another oxidative enzyme, tyrosinase, and on how additives (in particular Ca^{2+} ions) can be used as a further handle on the properties of enzymatically cross-linked α -lactalbumin nanoparticles.

Samenvatting

In dit proefschrift willen we licht werpen op het effect van enzymatische verknoping op de moleculaire en mesoschaal eigenschappen van apo- α -lactalbumine, om vervolgens deze inzichten toe te passen op het begrijpen van de functionele eigenschappen van enzymatisch verknoopte α -lactalbumine nanodeeltjes in voedsel formuleringen. In het eerste deel van het proefschrift, **peroxidase gekatalyseerde verknoping van apo- α -lactalbumine**, leggen we de nadruk op het begrijpen van hoe peroxidase gekatalyseerde verknoping, fysieke en functionele eigenschappen van apo- α -lactalbumine nanodeeltjes op mesoschaal verandert. In het tweede deel, **Vergelijking van peroxidase-, laccase-en tyrosinase-gekatalyseerde verknoping**, onderzoeken we in hoeverre de stabiliteit, fysieke en functionele eigenschappen van eiwit nanodeeltjes afwijken wanneer apo- α -lactalbumine is verknoopt door verschillende oxidatieve enzymen.

Allereerst, in de **algemene inleiding, Hoofdstuk 1**, introduceren we de onderzoeksvraag van dit proefschrift, en geven we essentiële achtergrondinformatie over de verschillende oxidatieve enzymen die gebruikt worden in ons onderzoek, en over het model substraat wat we gebruiken: α -lactalbumine. De enzymatische verknoping wordt in dit proefschrift gebruikt om eiwit nanodeeltjes te maken. En volgende gedeelte van Hoofdstuk 1 behandelt de rol van eiwit nano- en microdeeltjes in de huidige voedseltechnologie. Tevens geven we in dit gedeelte een overzicht van de manieren waarop deze deeltjes gebruikt kunnen worden, en van hun eigenschappen. Tenslotte geven we in Hoofdstuk 1 een kort overzicht van de rest van het proefschrift.

Deel I: peroxidase gekatalyseerde verknoping van apo- α -lactalbumine

In **hoofdstuk 2** bestuderen we het proces van de peroxidase gekatalyseerde vorming van apo- α -lactalbumine nanodeeltjes. We hebben twee afzonderlijke fasen ontdekt. In de eerste fase van de reactie, die snel is, worden de eiwit monomeren omgezet in eiwit oligomeren. In de tweede fase, die veel langer duurt, worden de oligomeren met elkaar gekoppeld tot eiwit nanodeeltjes. We ontdekken dat deeltjesgroei stopt als gevolg van

peroxide geïnduceerde inactivatie van de enzymen. De uiteindelijke deeltjes hebben een open structuur met een schaling van de hydrodynamische grootte R_H versus molmassa M_w van $R_H = M_w^\alpha$, met als waarde van de exponent $\alpha = 0.4$.

In **hoofdstuk 3** bestuderen we conformatie veranderingen van de α -lactalbumine eiwitten geïnduceerd door de peroxidase-gekatalyseerde verknoping. We bestuderen conformatie veranderingen voor de twee fasen van de reactie afzonderlijk en staan beide beschreven in hoofdstuk 2 ("gedeeltelijke verknoping" en "volledige verknoping"). We ontdekken dat gedeeltelijke verknoping leidt tot een significant verlies van de voornamelijk α -helische secundaire structuur van de eiwitten en tot een aanzienlijke toename van de hydrofobiciteit van de eiwit oppervlakte. Opmerkelijk is dat in volledig verknoopte eiwit nanodeeltjes, een deel van de α -helixstructuur, die verloren ging in het beginstadium van de reactie, terug lijkt te komen. De uiteindelijke deeltjes zijn zeer hydrofiel en hebben een oppervlaktehydrofobiciteit die dicht bij die van het natieve eiwit monomeer ligt. Ook hebben volledig verknoopte nanodeeltjes een zeta potentieel dat tweemaal negatiever is dan die van het natieve eiwit monomeer. Zodoende zijn volledig verknoopte alfa-lactalbumine nanodeeltjes zeer stabiel in oplossing.

Hoofdstuk 4 behandelt de rheologie van geconcentreerde oplossingen van de nanodeeltjes die gekarakteriseerd zijn in hoofdstuk 2 en 3. We ontdekken dat de overlap concentraties voor de nanodeeltjes liggende tussen de 4 en 9% (w/v), voor nanodeeltjes met hydrodynamische radii R_H die afneemt van 100 tot 25 nm. Boven de overlap concentratie, neemt de opslagmodulus (G') en viscositeit (η) snel toe met toenemende concentratie. Nanodeeltjes oplossingen hebben een viscositeit die snel afneemt met toenemende afschuifspanning. Deze kenmerken worden geïnterpreteerd in termen van wat er in de literatuur bekend is over de rheologie van zachte, tegen elkaar aangedrukte bolletjes. Een belangrijke conclusie is dat de enzymatische verknoping kan worden gebruikt om eiwitten hydrogelen te maken met rheologische eigenschappen die aantrekkelijk zijn voor voedsel structureren, maar die niet normaal geassocieerd worden met eiwit gelen: transparante gelen bij vrij lage concentraties, die zacht worden onder afschuifspanning.

De invloed van warmte-behandelingen op eiwit-bevattende voedingsmiddelen is een belangrijk onderwerp in de levensmiddelentechnologie, en in **hoofdstuk 5**, bestuderen we de effecten van verhitting op de structuur en de fysische eigenschappen van peroxidase verknoopte α -lactalbumine nanodeeltjes. We ontdekken dat na verknoping; verhitting niet meer leidt tot significante veranderingen in de secundaire structuur, in tegenstelling voor het natuurlijke eiwit. De nanodeeltjes behouden hun hydrofiel karakter, en voor diverse oplossingsomstandigheden, vinden we dat verhitting niet leidt tot aggregatie van de nanodeeltjes, in tegenstelling tot de natieve eiwitten, die snel warmte-aggregeert voor pH-waarden dicht bij pH 5.7. Hydrogelen bereid uit de nanodeeltjes kunnen worden verhit zonder grote veranderingen in de rheologie. Samengevat: we hebben vastgesteld dat peroxidase verknoopt α -lactalbumine nanodeeltjes zeer hittestabiel zijn.

Deel II: Vergelijking van peroxidase-, laccase-en-tyrosinase gekatalyseerde cross-linking

In **hoofdstuk 6** vergelijken we verknoping van apo- α -lactalbumine door twee verschillende oxidatieve enzymen, peroxidase (HRP) en laccase (LC). We ontdekken dat nanodeeltjes geproduceerd door de twee enzymen vergelijkbaar zijn in structuur op mesoschaal: beide hebben een grootte-massa schaling $R_g \sim M_W^a$ met een exponent van een $a \approx 0.5$. Veranderingen in de secundaire structuur en zeta potentiaal na de verknoping zijn vergelijkbaar voor de twee enzymen. Tevens vind er voor beide enzymen er geen aggregatie van de nanodeeltjes plaats tijdens verhitting. We vinden ook significante verschillen: in tegenstelling tot HRP-geïnduceerde verknoping, LC-geïnduceerde verknoping leidt tot een sterke toename van de oppervlak hydrofobiciteit in vergelijking met het natieve eiwit. Ook desintegreren de deeltjes gedeeltelijk in de aanwezigheid van DTT, wat impliceert dat disulfidebruggen bijdragen aan de stabiliteit van de LC-nanodeeltjes. Samenvattend vinden we dat LC gekatalyseerde verknoping leidt tot nanodeeltjes die in veel opzichten vergelijkbaar zijn met de door HRP gekatalyseerde verknoping, alleen zijn deze wel meer hydrofoob, wat van belang kan zijn, bijvoorbeeld voor het ontwerpen van eiwit nanodeeltjes die oppervlakteactief moeten zijn.

De algemene discussie, **hoofdstuk 7**, geeft een overzicht van de formatie, de fysische en voedsel functionele eigenschappen van oxidatief verknoopte α -lactalbumine nanodeeltjes. In aanvulling op de gegevens in de andere hoofdstukken van het proefschrift, brengt dit hoofdstuk ook nieuwe gegevens, met name α -lactalbumine nanodeeltjes geproduceerd met nog een oxidatief enzym tyrosinase, en hoe additieven (in het bijzonder Ca^{2+} ionen) kunnen worden gebruikt om extra greep te krijgen op de eigenschappen van enzymatisch verknoopte α -lactalbumin nanodeeltjes.

List of publications

This thesis

Saricay, Y., Wierenga, P. A., de Vries, R., Changes in protein conformation and surface hydrophobicity upon peroxidase-catalyzed cross-linking of apo- α -lactalbumin. *J. Agric. Food Chem.* **2014**, published online (<http://pubs.acs.org/doi/pdf/10.1021/jf502664g>).

Saricay, Y., Wierenga, P. A., de Vries, R., Nanostructure development during peroxidase catalyzed cross-linking of apo- α -lactalbumin. *Food Hydrocolloids* **2013**, *33*, 280-288.

Saricay, Y., Dhayal, S.K., Wierenga, P.A., de Vries, R., Protein cluster formation during enzymatic cross-linking of globular proteins. *Faraday Discussions*, **2012**, *158*, 51 – 63.

Saricay, Y., Wierenga, P. A., de Vries, R., Rheological properties of dispersions of enzymatically cross-linked apo- α -lactalbumin nanoparticles. *Submitted to Food Hydrocolloids*.

Saricay, Y., Wierenga, P. A., de Vries, R., High Stability of Enzymatically Cross-linked apo- α -lactalbumin Nanoparticles against Thermal Aggregation. *Manuscript in preparation*.

Saricay, Y., Dhayal, S.K., Wierenga, P. A., de Vries, R., Structural and physical properties of enzymatically cross-linked apo- α -lactalbumin nanoparticles: Laccase versus peroxidase. *Manuscript in preparation*.

Saricay, Y., Wierenga, P. A., de Vries, R., The effect of Ca^{2+} on stability of enzymatically cross-linked apo- α -lactalbumin nanoparticles. *Manuscript in preparation*.

Dhayal, S., **Saricay, Y.**, Gruppan, H., de Vries, R., Wierenga, P. A., Rheological behaviour of enzymatically cross-linked α -lactalbumin particle dispersion: Transglutaminase versus peroxidase. *Manuscript in preparation*.

Other work

Cicek M., Mutlu O., Erdemir A., Ozkan E., **Saricay, Y.**, Turgut-Balik, D., Single Mutation in Shine-Dalgarno-Like Sequence Present in the Amino Terminal of Lactate Dehydrogenase of Plasmodium Effects the Production of an Eukaryotic Protein Expressed in a Prokaryotic System. *Molecular Biotechnology*, **2013**, *54*, 602-608.

Acknowledgement

This is going to be a very long acknowledgment! Because, you all made my life in The Netherlands and in this scientific adventure awesome! Without you, my PhD would be too scientific. With you, however, it has become so lively!

Firstly, I would like to express my deepest gratitude to my supervisors, Renko de Vries, Peter A. Wierenga and Martien Cohen Stuart. Dear Renko, my special thanks for your confidence in me and dealing with this too enthusiastic guy with high language skills for almost 5 years. To be honest, I was very much convinced to coherently work with you after I had a skype meeting. During 5 years, I have been always thinking how my decision that I made to start this PhD project with you was right! Definitely, your naïve and reassuring personality encouraged me take a risk to experience in new perspective abroad. I have been so happy to have a common scientific interest. My special thanks for your understanding, your help, your encouragement, your fruitful discussion, your involvement in project, your sincerity, your supervision, your amazing communication, your democracy in giving a freedom to me, and your welcoming home parties. I think that I will never forget that you wrote very informative and honest e-mail for my long questions about everything in scientific perception when you were in USA. I really appreciate your approach to issues and feel always very lucky to work with you. I hope to continue collaborating with you in many different projects in future. Dear Peter, we had deeper discussions maybe in final phase of my PhD. I think you are the most critical and skeptical person in this project. However, your scientific approach turned out an amazing contribution for me to broaden my perspectives. I was amazed when you read almost whole thesis at your weekend. Even you kept on asking many questions by e-mail. In the end of day, I noticed to have a discussion with you and Renko by e-mails. Many thanks for your co-supervision, your honesty, your skepticism, your unique approach, your discussions, your critical view, your enthusiasm, your positivism in communication. Dear Martien, you are definitely very important figure at Fysko. When I met with many PhD students that had many problems at their department from different universities, I noticed that how you led this department with such a nice way. Your contribution to

create a very friendly and nice atmosphere at Fysko enriched with science was enormous. Even though we did not interact very often during my PhD project, it was always very important for me to know that you were my wise promotor.

Dear Surender, I would like to thank you very much for your nice company and collaboration. I think this jointed PhD project was the most effective and enjoyable collaborative work that I have seen in my research experience. I really enjoyed having a discussion about mystery of our protein nanoparticles, sharing our experience in the project and talking about science, life, and philosophy. My special thanks for your help with running my samples by AF4 and for ordering coffee at FCH and for accepting to become a paranymp. I wish all the best for you, Surender!

I also sincerely thank FOM staff members. I have been always amazed by FOM activities and approach. So far, as a FOMer PhD student, I have always felt your amazing support for almost any situation such as a residence permit issues, scientific and social courses, networking, personal development, workshops, and project involvement. I think any organization should learn many things from you how to improve employee's skills. I also acknowledge BRM Committee B for their discussion during all my project meetings.

Dear Remco, you are my inspector gadget :) I think you have a magic hand! If you touch any device, we have always had what we need in a short time. Many thanks for helping with DLS measurements and setting my home-(Remco)-made bioreactor at Fysko. Dear Josie, many thanks for helping with finding an accommodation in Wageningen. I always remember you with a smiley face and your English accent :) Without you, Fysko will be too lonely for everyone. Dear Mara, many thanks to take care of my urgent orders and lab desk. Dear Anita, many thanks for arranging all financial issues between Fysko and FOM. Dear Anton, thanks for your instruction of DSC. Besides, I would like to thank you to invite me to join volleyball team. It was great and fun to play many games with you. Dear Ronald, thanks for your IT support and instruction for UV spectroscopy. Dear Bert, thanks for creating a bridge between Fysko and FOM for reimbursement claims.

Dear all my lovely colleagues of my generation at Fysko, Armando, Liyakat, Dmitry, Thao, Soumi, Huanhuan, Monika, Yuan, Emilia, Evan, Harke, and Lennart. There is no doubt that I had a great time at Fysko because you were great. I will never forget very nice coffee

breaks with many people making much fun. Armando, I am so happy to meet with you and to share many things. I think we spent more time outside than Fysko with house warming parties, jam sessions, concerts, drinks, festivals, holidays and conferences. This small town was kind of lively due to the parties that you organized. I think our understanding of city life let us have more fun in Wageningen. Liyakat, or called Mr. Cenabi or muscle! I thank you for those amazing Indian dinners with fruitful philosophical discussions. It was nice that you did not believe in Sami :) Dimitry, our musical experiments and philosophical discussions are memorable. As you know, I always like your bass-line and your passion on drum & bass :) Thao, you are such a cute, wise and calm person. I have never seen you in anger :) Soumi Banerjee, it is pleasure for me to meet with you. I appreciate your wise and calm personality enriched with music, literature and science. Those delicious dinners that you prepared for us and movie nights are unforgettable. By the way, when are you going to cook creepy crab for us :) Huanhuan, man you're my crazy Chinese. I will never forget your dance at bbq party and enjoyable shark fillet that you cooked for us! Monika, I will remember you as a lively person with a nice smile. Yuan, you were the most dangerous and craziest person at Fysko :) I know you were real fan of my belly and Fysko's corridor to make a noise. We missed your energy at Fysko. Sorry that I missed your wedding! Emilia, I felt that you were always at Fysko even though you did your PhD in Germany. Because, you were always friendly and ingenuous whenever you were at Fysko. Evan, it was great to spend some time at Belgium and to have an intellectual discussion about social issues :) Besides, it was enjoyable to play volleyball with you. I always appreciate your modesty. Harke, thanks for playing music with us even though it was hard for you. Lennart, I thought you were such a racist when I met with you ☺ Your first words were that "I hate Turkish and Chinese". After that, I realized it was only your humor about stranger at Fysko. Thanks for your nice comments on human alienation while we're going to USA for PhD trip.

Dear PhD trip organization committee, I would like to thank you all! In the beginning, it was very hard task to go to California, in particular, as considered that we all had different schedule in preparation. However, it turned out an amazing PhD trip to California. It was such a great time that we had in California. Sabine, thanks for your good sense,

understanding and dealing with three relaxed guys. Christian, many thanks for your nice company, nice conversation during coffee breaks and optimism. It is so nice to know you. Mr. Garcia, you are real Mexican, No doubt about it! Fortunately, we did not drink tequila during meetings ☺

My lovely officemates, Maria and Rui! It is too sad that you came very late to my office. I wish I could meet with you at the same office in the beginning of my PhD. Even for a short time, we all Mediterranean (I think Rui will say I am not ☺) were connected in a fruitful company. Before you, it was just office but with you, it was a golf course, bar, astrophysics centre and lovely place. Many thanks for your company even though I dislike Yunanli and Rui's jokes ☺

Many thanks to enthusiastic musicians who made a lot of fun at my place: Dmitry, Sara, Kris, Jacob, Raimon, Lena... Kris, I met with you as you were a stranger that had a bottle of wine in the middle of night. But I will remember you as a nice friend with a unique dance. Sara, I met with you as you were crazy. And I will remember you always as you will be crazy. Jacob, I met with you as you were too blond. But I will remember you as a person having such a nice humour (please pay attention British accent here ☺) and friendly neighbour (one more time British accent☺). Don't worry nobody will learn that you bought that guitar with FOM money ☺ Raimon, you are always more than a guest in Turkish community. Many thanks for helping us almost for everything. And special thanks for Utrecht's nights, your hospitality and your contribution to jam session.

Many thanks my lovely German company at Harweeg, Lena, Johanne, Birte! I will never forget amazing times that I spent with you in The Netherlands and Istanbul. You are such lovely friends. I hope to meet with you again somewhere on this globe.

I would like to express my adoration to Istanbul and Amsterdam due to the fact that these two cities always inspire me with two different ways in my life. Hey Amsterdam, it will be so difficult to leave you alone, my darling!

Many tanks to my colleagues in volleyball team: Frans, Martin, Anton, Cas, Guido, Gerben, Henk, Luuk, Evan. It was funny that we always managed to play at the first field but again went back to second one after the first season. Unfortunately, there was no 1.5th field.

My special gratitude to my Turkish friends, who I met with in The Netherlands. Without you all, I could feel more homesick in this adventure. I feel now very luck to meet you, special people. I always think this is not about speaking Turkish and/or coming from Turkey as a foreign to abroad, it is only about speaking the same language! Oncelikle, bana kapilarini sonuna kadar acan, yetmeyip uzerine bir de oda acan, yok oda yetmedi diyip anahtari veren ama sonra nasil boyle bir manyaklik yaptim diyerek cok dert yanan Namik Akkic efendiye sevgilerimi sunarim. Biliyorum cok basin agridi gecenin bir yarısında Amsterdam donuslerimden ama cokta sey konustuk paylastik. Sonra, Murat Kilic'a cok tessekkur ederim beni Hollanda'ya gelmem konusunda surekli cesaretlendirdigi, Istanbul'dan baslayip Amsterdam'lara uzanan uzun soluklu entellektual tartismalari icin. Aslican'a tum cilginligi ve Namik'in evini ansizin bastigi icin. Bir konser vesilesi, bir gece kahvesi, bir Duman sarkisi, bir Istanbul-Ankara arasi ile tanistigim onca guzel insanlara: Melis Or Akman and Oytun Akman'a, sonsuz ev sahipligi, harika San Francisco geceleri ve gunduzleri, Leiden kahveleri, Duman Konserleri ve Gogol Bordello esliginde yapilan danslari icin. Narin Tezcan'a, inanilmaz sakinligi, kibarligi, harika gulusu ve bitmeyen nezakati icin. Ozge Zelal Zelal Aydin'a, mis kokulu carsaflari ile yaptigi Rotterdam'daki misafirperverligi, dogal ve icten sohbetleri icin. Nihal ve Birol Malkamak'a, en icten hazirlanmis birali sohbetleri icin. Bir de Nihal'e, Bahar'in kardesi olduguna beni ikna ettigi ve asiri yuksek egitimli ailesi icin ☺ Sonra daha gec tanistigim ama bunlar da ne tatli dedigim dostlar: Nihal ve Emre Erol'a, inanilmaz raki geceleri, bardan bara bira hoplamalari, ortacag yemekleri, Egeli sakinlikleri, dogalliklari, o ne gunleri bee Utrecht'deki evi bana biraktiklari, mantilarini yedigim ve Cevriye ile arami yaptiklari icin. Nalan ve Caner'e, konserler, icmeler, guzellesmeler, konserler, muhabbetler, bir de o ne guzel bir ev partisiydi icin. Alex'e, bitmek bilmeyen enerjisi, sen sakrak muhabbetleri ve ilginc yaklasiklari icin. Merve Bedir'e, sen hep uzaklarda olup yanimizdayken sanki hic ayrilmamis gibi oldugu icin. Bir de mavi ayakkabilarin cok guzel hic soylememis ve ayaginda hic gormemistim ☺ Ilhan'a hayata karsi olan tavrı icin. Babali, sana da nasil tessekkur etsem az. Ne cok konsere gittik, ne cok muhabbet ettik, ne cok Bean&Bagel'si zengin ettik. Hatta yesil yesil ne kadar cok gulduk. Sanirim Brazzaville ile baslayan o serüven hicbir zaman hafizamdan cikmayacak. Sorgusuz sualsiz ev sahipligin icin

sukranlarimi sunarim. Umarim hersey istedigin gibi, beat’lerin Ben Mono’nun gibi olur ☺ O Yale’i sallamayan o DJ setinin olmadi davul’un uzerinde sallansin ☺ Nazli, gec oldu ama bence guc olmadi. Gerci sen cok gezmekten cok konser kacirdin ama yine de gecirdigimiz onca guzellikler icin cok tessekkurler. Simdi cok baglantisi oldu ama Alp’e gecenin bir yarisi kapaga ayar cektigi icin.

Sonra geelim koyden akan nehrin sabahlara kadar suren gecelerin faydalarına. Koyde tanistim insan evlatlari: Size sesleniyorum! Siz olmasaydiniz burasi cok eksik olurdu. Resmen ve ciddiyetle bugun bir inege sarilip uyumuyorsam bunda sizin katkiniz cok ☺ Sevgili karadenuzlu usagim Sami, o kuzeyli kanina ragmen yine de benle cok iyi mucadele ettin. Farkli dunyalarin insanlari olarak, herhalde baska birisiyle bu kadar iyi anlasamazsim. Her ne kadar bircok kez senin damarina bassam da, bazen yogurtlari basinda asagiya doksem de, gece gece bu kapilar nasil kitlenir, bu parcaciklar nasil cozulur diye sorsam da valla sesin cikmadi. Yok lann bayagi da cikti aslinda ama hic kotu cikmadi ☺ Valla 2 yil harika bi ev arkadasligi harika bir dost oldun. Sagolasin! Dilgem, koyde ilk tanistigim ve neyse en azindan Dilek var herhalde yasanir burada dedirten insan evladi. 29 yil ayni yerde yasayip Hollanda’da tanistigim ve o borekler, o tatlilar, o masalar, o ekmekler, o zuhtuler bu puhtuler, o zigzagli tekneler, o bitmez tukenmez celiskiler, parcaciklar ve parcasizliklar icin. Oylum’um, hala nasil tanistik hatirlamiyorum ama iyi ki tanisdik! Varligin cidden cok ozel ve guzel benim icin. Sen ki ufkumu acan nadir insan evlatlarindan biri sagdiclarimin en guzelisin. Foca’ya verilen sozlerin, gelmelerin gitmelerin, hayata karsi durusun, anlayisin, ictenligin, dogalligin, sohbetlerin, sorgulamalarin ve sorgulatmalar icin. Onur’um, valla iyi ki tanistik iyi ayni kaygilari tasidik ayni cozumleri sorguladik. Sana ayri olarak onca caz’irdimalar, bunca festivaller, nice icmeler, nice kalkmalar, bak oradaki sinemalar, bak suradaki turuncular, uzun soluklu yollar, uzun soluklu politik tartismalar; onca paylasim bunca yardim icin. Sametim, ne manyak kimsenin dinlemedigi hic kimsenin gitmedigi dunya uzerinde 10 kisinin bildigi konserlere ve “sanat” aktivitelere gittik beee. Bazen gruplarin sadece bize caldiginu bile dusundugum oldu ☺ Su Amsterdam’da dinlemedik grup, girilmedik kanal, konusmadik ve kufretmedik konu kalmadi. Tum paylasimlarin ve sakli gizli asciligin icin. Morteza, inanilmaz guzel aksanin, kendine has algilayalayisin, dogalligin, o ne salatadir bee arkadasligin, tirbuson ile olan diyalogun, Harweg’ten

Nobelweg'e uzanan yardimlarin icin. Mustafa'ya, Harweg'in en canlisi en kanlisi en uzun sureli bbq hazirlayacayicisi, bitmeyen King gecelerinin vazgecilmezi, kucuk odaya bizi sokan uzerine lokumla besleyen, muhabbeti hos coskusu yuksek arkadasligin icin. Sevinc'e, Ankara'nin havasini koye getirdigi icin. Basak'a hep nazik tavri hep candan ictenligi icin. Robin'e, her daim isyanlari, De Zaire biralari, Albert Heijn bulusmalari ve Irlandililara cok iyi baktigi icin. Safak'a, inanilmaz ev sahipligi, politik rakili gecesi ve Almanya rehberligi icin. Yusuf'a gonul zengiligi, insan sevgisi, hayat durusu ve dogalligi icin. Pelin'e hayatimiza oyle guzelcene girip oylece cikmadigi icin COK TESSEKKUR EDERIM!

Ayrice beni hep destekleyen Prof. Dr. Dilek Turgut Balik ve Prof. Dr. Serap Gunes'e tesekkuru bir borc bilirim.

Son olarak, dunyanin en guzel insanlari, annem ve babama, bana her anlamda hayat verdikleri, bitmez tukenmez sevgileri ve destekleri, harika ebeveyinlikleri icin cok tesekkur ederim. Evet surekli onemli gunleri unutan ama sizi cok ama cok seven bir oglunuz var. Mesefaler bunu hicbir zaman azaltmadi azaltmayacak.

About the author

Yunus Saricay was born on the 15th of June, 1980, in Izmit, Turkey. His curiosity on understanding cosmos, living organism and human being let him first study science at Yildiz Technical University, Istanbul. He obtained his BSc. diploma in physics in 2004. Then, he decided to change his scientific adventure into bio-science and attended to department of bioengineering at the same university. During his MSc. project, he studied physico-chemical mechanism of the protein-polymer complex coacervate as a carrier system under supervisions of Prof. Dr. Mamed Mustafaev and Assist. Prof. Zeynep Mustafavea. In 2005, he joined to the department of bioengineering as a research assistant. He was involved in various research projects such as (1) designing peptide-based synthetic vaccines (2) developing polymeric carrier system (3) designing artificial tissues during 4 years. In 2007, he started his PhD at the same department with Prof. Dr. Dilek Turgut-Balik. The task of his PhD thesis was to design, to optimize and to test genosensors (i.e. based on electrochemical and surface plasmon resonance spectroscopy) for the detection of different Malaria species at molecular level. In 2008, he was appointed to Art and Design faculty of Yildiz Technical University as a guest MSc. student and Definition of Art Group to study conceptual art theory. In 2008, he started to examine the boundaries of art and science in daily life. This examination let him make a decision to go abroad for doing PhD in science for further broadening his scientific and personal perspective. In 2009, he was appointed as a PhD candidate at Laboratory of Physical Chemistry and Colloid Science at Wageningen University, The Netherlands under supervision of Assoc. Prof. Renko de Vries, Assist. Prof. Peter A. Wierenga and Prof. Dr. Martien Cohen Stuart within the PhD project titled “Enzymatically Cross-linked Globular Proteins as Hierarchical Biopolymers”, supported by the Industrial Partnership Programme (IPP) Bio(-Related)Materials of the Stichting voor Fundamenteel Onderzoek der Materie (FOM), which is financially supported by the Nederlandse Organisatie voor Wetenschappelijk Onderzoek (NWO).

Overview of completed training activities

Discipline specific activities

Courses

Han-sur-lesse winter school, **2012**, Belgium.

Physical Chemistry of Biointerfaces II, **2012**, San Sebastian, Spain.

11th European School on "Scattering Methods Applied to Soft Condensed Matter, **2012**, Gironde, France.

Food Structure and Rheology, **2012** (VLAG), Wageningen, The Netherlands.

13th European School on Rheology, **2011**, Leuven, Belgium.

Conferences and Symposia

5th Delivery of Functionality in Complex Food System, **2013**, Haifa, Israel.

8th NIZO Dairy Conference, **2013**, Papendal, The Netherlands.

14th European Student Colloid Conference, **2013**, Potsdam, Germany.

3rd FOM BRM day, **2012**, Utrecht, The Netherlands.

11th International Hydrocolloids Conference, **2012**, Purdue University, USA.

14th Food Colloids, **2012**, Copenhagen, Denmark.

FOM BRM day, **2011**, Utrecht, The Netherlands

4th Delivery of Functionality in Complex Food System, 2011, Guelph, Canada.

2nd FOM BRM day, **2011**, Utrecht, The Netherlands.

European Polymer Federation (EPF), **2011**, Malaga, Spain.

8th Dutch Soft Matter Meeting, **2010**, Wageningen, The Netherlands.

1st FOM BRM day, **2010**, Utrecht, The Netherlands.

General Courses

Career Planning (FOM), **2014**, Utrecht, The Netherlands.

Business Orientation Week (FOM), **2013**, Nyenrode Business University, Utrecht, The Netherlands.

Workshop FOM Young Scientist Day, **2013**, Amsterdam, The Netherlands.

The Art of Presenting Science (FOM), **2012**, Utrecht, The Netherlands.

Write it right (FOM), **2012**, Utrecht, The Netherlands.

Workshop FOM Young Scientist Day, **2011**, Amsterdam, The Netherlands.

Taking charge of your PhD Project (FOM), **2010**, Utrecht, The Netherlands.

FOM Orientation Day, **2009**, Utrecht, The Netherlands.

Optional courses and activities

PhD Trip to California, **2013**, USA.

PhD Trip to South of Asia, **2011**, Malaysia, Singapore and Vietnam.

Advance Soft Matter, **2010**, Wageningen, The Netherlands.

Group Meetings & Colloquia, **2009-2014**, Wageningen, The Netherlands.

BRM Project Meetings, **2009-2014**, Wageningen, The Netherlands.

This work is part of the Industrial Partnership Programme (IPP) Bio(-Related)Materials of the Stichting voor Fundamenteel Onderzoek der Materie (FOM), which is financially supported by the Nederlandse Organisatie voor Wetenschappelijk Onderzoek (NWO). The IPP BRM is co-financed by the Top Institute Food and Nutrition and the Dutch Polymer Institute.

Financial support from FOM for printing this thesis is gratefully acknowledged.

Cover design by Yunus Saricay

Printed by Gildeprint drukkerijen, Enschede, The Netherlands.

Personal Note:
